# DOCTORAL THESIS

## THE MEK5/ERK5 PATHWAY IN LUNG AND OVARIAN CANCER

**Adrián Sánchez Fernández**

Instituto de Investigación Biomédica de Salamanca
Instituto de Biología Molecular y Celular del Cáncer
CSIC-Universidad de Salamanca
2021

Dña. Azucena Esparís Ogando, Investigadora del Instituto de Investigación Biomédica de Salamanca e Instituto de Biología Molecular y Celular del Cáncer de Salamanca,

CERTIFICA

Que la presente Tesis Doctoral titulada "La vía de MEK5/ERK5 en cáncer de pulmón y ovario / The MEK5/ERK5 pathway in lung and ovarian cancer" presentada por el Licenciado en Biotecnología D. Adrián Sánchez Fernández, ha sido realizada bajo su dirección en el Instituto de Investigación Biomédica de Salamanca e Instituto de Biología Molecular y Celular del Cáncer, centro mixto CSIC-Universidad de Salamanca, y reúne, a su juicio, originalidad y contenidos suficientes para que sea presentada ante el tribunal correspondiente y optar al grado de Doctor por la Universidad de Salamanca.

Y para que así conste, a efectos legales, expide el presente certificado en Salamanca a 10 de junio de 2021.

Fdo: Azucena Esparís Ogando

*A Felisa, Adrián, Piedad y Pedro.*

*Esto y todo. Siempre.*

# FINANCIAL SUPPORT

This doctoral thesis has been carried out with the financial support of the Scientific Foundation of the Spanish Association Against Cancer (AECC), grantor of the Predoctoral Oncology Fellowship - 2017 call - of which Mr. Adrián Sánchez Fernández was beneficiary. Mr. Adrián Sánchez Fernández was also supported by the Cancer Center Network Program from the ISCIII (RD12/0036/0003).

The work carried out in this thesis project has been supported by grants from the Instituto de Salud Carlos III (ISCIII) (PS09/00868, PI15/01180, and PI19/00840) to Dr. Azucena Esparís Ogando.

Our Cancer Research Institute and the work carried out at our laboratory receive support from the European Community through the regional development funding programme (FEDER).

*“The aim of science is not to open*
*the door to infinite wisdom,*
*but to set a limit to infinite error”.*

*Galileo Galilei*

# Index

# *ABBREVIATIONS*

| | |
|---|---|
| **ADC** | Adenocarcinoma |
| **AGE** | Advanced Glycation Endstage products |
| **AIS** | Adenocarcinoma in situ |
| **AMCHA** | Trans-4-(aminomethyl)cyclohexanecarboxylic acid |
| **ARMS** | Amplification Refractory Mutation System |
| **ATP** | Adenosine Triphosphate |
| **BCA** | Bicinchoninic acid |
| **BLAST** | Basic Local Alignment Search Tool |
| **BMK1** | Big MAPK 1 |
| **BrdU** | 5-Bromo 2'-Deoxy-Uridine |
| **BRCA** | Breast Cancer Type Susceptibility Protein |
| **BSA** | Bovine Serum Albumin |
| **CAR-T** | Chimeric Antigen Receptor Therapy |
| **CCC** | Clear Cell Carcinoma |
| **CCLE** | Cancer Cell Line Encyclopedia |
| **CDK** | Cyclin-Dependent Kinase |
| **cDNA** | Complementary DNA |
| **CI** | Combination Index or Confidence Interval |
| **CNA** | Copy-Number Alterations |
| **CSC** | Cancer Stem Cell |
| **CTLA-4** | Cytotoxic T-Lymphocyte Antigen 4 |
| **DFS** | Disease Free Survival |
| **DMEM** | Dulbecco's Modified Eagle's Medium |
| **DMSO** | Dimethyl Sulfoxide |
| **DNA** | Deoxyribonucleic Acid |
| **DSBs** | Double-Strand Breaks |
| **DUSPs** | Dualspecificity Protein Phosphatases |
| **EC** | Endometrioid Carcinoma |

| | |
|---|---|
| **EDTA** | Ethylenediaminetetraacetic acid |
| **EGFR** | Epidermal Growth Factor Receptor |
| **EGF** | Epidermal Growth Factor |
| **EMA** | European Medicines Agency |
| **EMT** | Epithelial-to-Mesenchymal Transition |
| **EOC** | Epithelial Ovarian Cancer |
| **EpCAM** | Epithelial cell adhesion molecule |
| **ER** | Estrogen Receptor |
| **ERK1/2** | Extracellular Signal-Regulated Kinase 1/2 |
| **ERK5** | Extracellular Signal-Regulated Kinase 5 |
| **FAP** | Fibroblast Activation Protein |
| **FBS** | Fetal Bovine Serum |
| **FDA** | Food and Drug Administration |
| **FDR** | False Discovery Rate |
| **FIGO** | International Federation of Gynecology and Obstetrics |
| **FISH** | Fluorescence In Situ Hybridization |
| **FITC** | Fluorescein isothiocyanate |
| **FMO** | Fluorescence Minus One |
| **GAPDH** | Glyceraldehyde 3 phosphate dehydrogenase |
| **GPCR** | G-protein-coupled receptors |
| **HBOC** | Hereditary Breast and Ovarian Cancer syndrome |
| **HDR** | Homology-Directed Repair |
| **HEPES** | 2-[4-(2-hydroxyethyl)piperazin-1-yl] ethanesulfonic acid |
| **HER** | Human Epidermal Growth Factor Receptor |
| **HGSOC** | High-Grade Serous Ovarian Carcinoma |
| **HR** | Hazard Ratio |
| **HRD** | Homologous Recombination Deficiency |
| **HRP** | Horseradish peroxidase |

| | |
|---|---|
| **HUP3D** | Human Plasma Derived 3D culture |
| **H&E** | Hematoxylin and Eosin |
| **IC50** | Inhibitory Concentration50 |
| **IF** | Immunofluorescence |
| **IP** | Immunoprecipitation |
| **KO** | Knockout |
| **LCC** | Large-Cell Carcinoma |
| **LCNEC** | Large-Cell Neuroendocrine Carcinoma |
| **LGSOC** | Low-Grade Ovarian Serous Carcinoma |
| **mAb** | Monoclonal antibody |
| **MAPK** | Mitogen-Activated Protein Kinase |
| **MAPK7** | Mitogen-Activated Protein Kinase 7 |
| **MAP2K5** | Mitogen-Activated Protein Kinase Kinase 5 |
| **MEK1/2** | Mitogen-Activated Protein Kinase Kinase 1/2 |
| **MEK5** | Mitogen-Activated Protein Kinase Kinase 5 |
| **MEKK2/3** | Mitogen-Activated Protein Kinase Kinase Kinase 2/3 |
| **MFI** | Mean Fluorescence Intensity |
| **MIA** | Microinvasive Adenocarcinoma |
| **MMLV-RT** | Moloney Murine Leukemia Virus Reverse Transcriptase |
| **mRNA** | Messenger RNA |
| **MTT** | 3-(4,5-dimethylthiazol-2-yl)-2,5-diphenyltetrazolium bromide |
| **NES** | Nuclear Export Sequence |
| **NET** | Neuroendocrine Tumor |
| **NLS** | Nuclear Localization Signal |
| **NSCLC** | Non-Small Cell Lung Cancer |
| **on** | Overnight |
| **ORR** | Objective Response Rate |
| **OS** | Overall Survival |

| | |
|---|---|
| **OXPHOS** | Oxidative Phosphorylation |
| **PARP** | Poly-ADP ribose polymerase |
| **PB1** | Phox and Bem 1 |
| **PBC** | Platinum-Based Chemotherapy |
| **PBS** | Phosphate-buffered saline |
| **PBST** | 0.1% Triton X-100 supplemented PBS |
| **PCA** | Principal Component Analysis |
| **PCR** | Polymerase Chain Reaction |
| **PD-1** | Programed Death-1 |
| **PD-L1** | PD-1 Ligand |
| **PDX** | Patient Derived Xenograft |
| **PFA** | Paraformaldehyde |
| **PFS** | Progression-Free Survival |
| **PI** | Propidium Iodide |
| **PI3K** | Phosphatidyl Inositol 3-Kinase |
| **PMSF** | Phenylmethylsulfonyl fluoride |
| **PPS** | Post-Progression Survival |
| **PR** | Progesterone Receptor |
| **PTEN** | Phosphatase and Tensin Homolog |
| **PVDF** | Polyvinylidene difluoride |
| **qRT-PCR** | Quantitative Reverse Transcription Polymerase Chain Reaction |
| **RAF** | RAF-1 Proto-Oncogene |
| **RAS** | Rat Sarcoma Viral Oncogene |
| **RNA** | Ribonucleic Acid |
| **ROS** | Reactive Oxygen Species |
| **rpm** | Revolutions per minute |
| **RPMI** | Roswell Park Memorial Institute medium |
| **RTK** | Receptor Tyrosine Kinase |

| | |
|---|---|
| **SC** | Scramble |
| **SCLC** | Small-Cell Lung Cancer |
| **SD** | Standar Desviation |
| **SDS-page** | Sodium Dodecyl Sulfate polyacrylamide gel electrophoresis |
| **shRNA** | short hairpin RNA |
| **SmartAMP** | Smart Amplification Process |
| **SqCC** | Squamous Cell Carcinoma |
| **SSBs** | Single-Strand Breaks |
| **STAT** | Signal Transducer and Activator of Transcription |
| **STR** | Short Tandem Repeat |
| **TBS-T** | Tris-Buffer Saline with Tween |
| **TCGA** | The Cancer Genome Atlas Research Network |
| **TG** | Transgenic |
| **TKI** | Tyrosine Kinase Inhibitor |
| **Tris** | Tris(hydroxymethyl)aminomethan |
| **UFT** | Uracil Tegafur |
| **VEGF** | Vascular Endothelial Growth Factor |
| **WB** | Western Blot |
| **WHO** | World Health Organization |
| **WNK1** | WNK Lysine Deficient Protein Kinase 1 |
| **WT** | Wild Type |
| **5-FU** | 5-Fluorouracil |

# *INTRODUCTION*

# 1. LUNG CANCER

## 1.1 EPIDEMIOLOGY

### 1.1.1 Incidence

More than 2 million new cases of lung cancer are diagnosed globally every year, thus making lung tumors the most common cancer worldwide (Figure 1, blue bars). Lung cancer presents the second highest incidence in men after prostate cancer, with approximately 1.4 million cases. It is also the second most common cancer in women after breast cancer, with an estimate of 725,000 new diagnosed patients per year (Thandra et al., 2021). In Spain, 29,638 new cases are diagnosed every year and lung tumors are the third most common both in men (21,847 cases in 2020) and women (7,791 cases diagnosed in 2020).

The mean age of patients diagnosed with lung cancer is around 70 years considering both genders. More than 50% of cases occur in patients ranging from 56 to 75 years old, while 37% occur in those older than 75. Patients younger than 55 account for a small percentage of cases. The highest lung cancer rates are observed in Europe, Eastern Asia, Northern America and Australia (Torre et al., 2016).

Lung cancer incidence and mortality is directly linked to tobacco smoking habits. In almost every country around the globe, men are the first of increase their smoking rate, which is followed by women a few years or decades later. Once lung cancer incidence and mortality peaks, the implementation of tobacco control programs by the national authorities usually achieve a significant declining of cases and deaths (Thun et al., 2013). This fact has been already observed in industrialized countries, where the smoking habit peaked around the middle of the last century, and lung cancer incidence and mortality have been decreasing since then (Bosetti et al., 2012; Malvezzi et al., 2013). In Spain, the tobacco epidemic peaked later, particularly in women. As a consequence, the lung cancer incidence rates are decreasing in men, but not in women (Torre et al., 2014). In contrast, developing countries where the smoking habit is more recent still present an increasing number of cases, and their lung cancer incidence is estimated to continue rising for the next decades (Jha et al., 2019).

### 1.1.2 Mortality

Lung cancer is the leading cause of cancer mortality among both genders worldwide, accounting for approximately 1.8 million deaths every year (Figure 1, red bars). Internationally, this data represents an impressive 19% of all cancer deaths. Men are more than double as likely to die of lung cancer as women. The latest estimates indicate that near 1.2 million men and 600,000 women are passing away every year due to this dismal disease (Global Cancer Observatory, 2020). Lung tumors are also the leading cause of cancer-related mortality in Spain, accounting for 22,000 deaths every year.

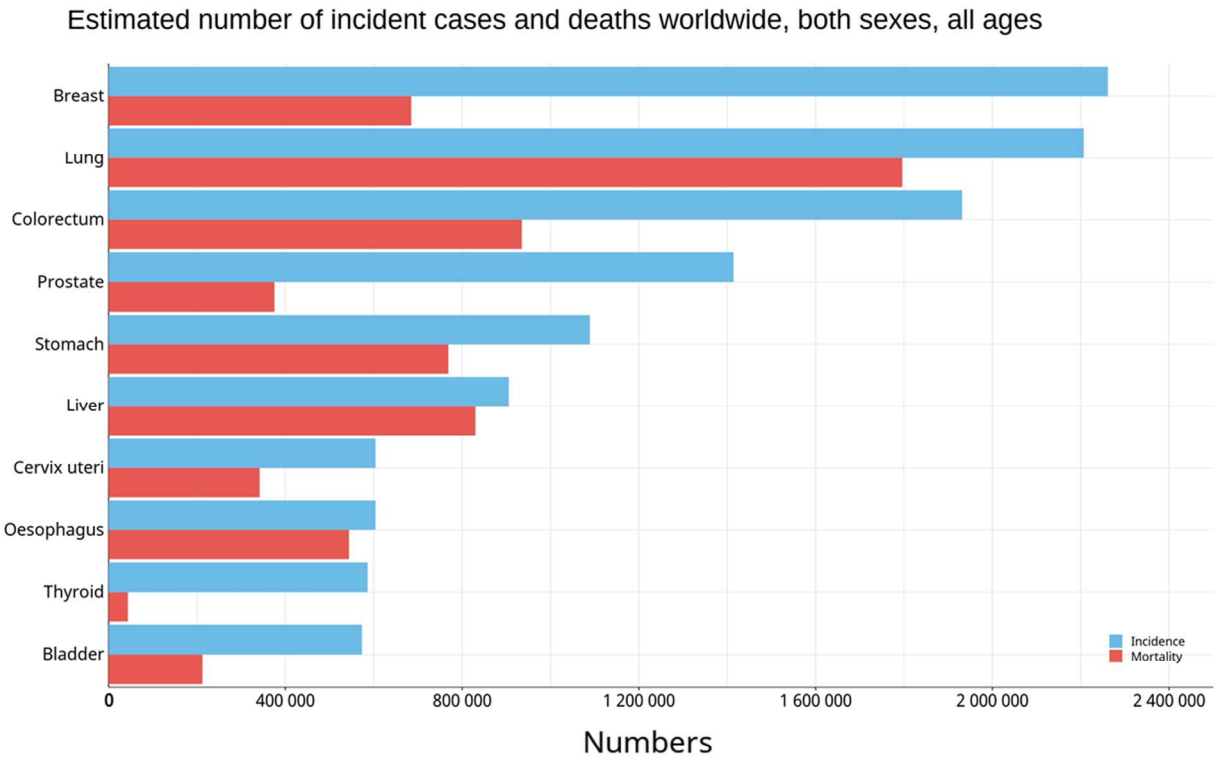


**Figure 1.** Estimated incidence and mortality global statistics of lung cancer in 2020. Blue bars = incidence. Red bars = mortality. Data source: Globocan 2020. International Agency for Cancer Research (2021). Graph production: Global Cancer Observatory (http://gco.iarc.fr/)

Given that lung cancer mortality is still rising among women in Europe and Northern America, it has recently surpassed breast cancer as the tumor with the highest mortality rates. In contrast, it remains behind breast cancer in developing countries. However, these differences in the number of lung cancer related deaths between industrialized and developing nations are not observed among men.

Regarding racial and ethnic features, non-Hispanic whites and blacks present the highest incidence and mortality rates, while Asian Americans present the lowest ones (Bray et al., 2018).

### 1.1.3 Survival

It is estimated that the 5-year survival rate for lung cancer in Western countries is approximately 21%. These statistics entail a considerable improvement when compared to the first 5-year survival rate reported in 1975 (11.5%) (Howlander et al., 2019). There is no doubt that this doubling in the survival rate is due to two main factors: an earlier detection facilitated by better screening methods; and the increased efficacy of the therapeutic regimens along with the introduction of targeted and immune therapies.

It is important to mention that incidence and mortality disparities among races or industrialized versus developing nations may be explained by unequal access to healthcare assistance, diagnosis methods and treatment options, together with environmental contamination and sociocultural issues rather than underlying genetic reasons (Goss et al., 2014). In other words, patients from Western nations have better access to early detection programs, cutting-edge diagnosis technologies and better treatment tools and therefore better lung cancer survival (Barta et al., 2019).

The 5-year survival rate greatly varies upon tumor stage at diagnosis: 59% among those with stage I-II disease at diagnosis, 31.7% at stage III, and 5.8% among those with metastatic disease (stage IV). One of the biggest challenges that must be faced in order to increase survival rates is reducing the high frequency of lung cancer cases that are diagnosed after metastasis (Howlander et al., 2019).

### 1.1.4 Risk factors

Smoking causes the vast majority of lung cancers, both in smokers and in people exposed to secondhand smoke. It is estimated that near 80% of lung tumors in the industrialized countries are attributable to cigarette smoking. Because it is not only related to lung tumor development, tobacco smoking is considered the first preventable cause of death

worldwide (Bray et al., 2018). The tobacco plant is not carcinogenic itself but combustion of tobacco, which generates more than 60 compounds known to be carcinogenic, since they induce DNA damage and mutations that favor tumorigenesis (Hecht et al., 1999). People who smoke are 15 to 30 times more likely to develop lung cancer than non-smokers. This relative risk is also dependent on the amount of cigarettes and the period of time of smoking. Quitting at any age can significantly lower the risk of developing lung cancer. But lung cancer also occurs in people who never smoked and in those who never had prolonged exposure to secondhand smoke (Boffetta et al., 1999). There are some other risk factors that can significantly increase the probability of developing lung cancer:

- **Previous radiation therapy.** Undergoing radiation therapy to the chest for another type of cancer, may increase the risk of developing lung cancer.

- **Pulmonary conditions.** Chronic Obstructive Pulmonary Disease presents a prevalence that ranges from 30 to 70% in lung cancer patients, making it the most common comorbidity (Young et al., 2009). Different studies have also reported that non-smokers that have suffered from chronic bronchitis or pneumonia present a higher risk of developing lung cancer. Respiratory infections may cause inflammation and cellular damage, which have been also involved in lung carcinogenesis. Other dismal diseases that have been reported to confer an odds ratio of lung cancer are tuberculosis (1.76 fold increase) and human immunodeficiency virus (HIV) (2.5 fold increase) (Brenner et al., 2012). More recently, it has been suggested that the long-term sequelae provoked by COVID-19 and composed of pulmonary inflammation, cytokine release storm, and acute respiratory distress may promote a higher risk of lung cancer (Lin et al., 2020).

- **Exposure to carcinogens.** Exposure to asbestos can increase the risk of developing lung cancer, especially in smokers. Induction of oxidative damage and subsequent DNA deletions, somatic gene alterations, and enhanced delivery of tobacco carcinogens to the airway epithelium are the main mechanisms by which carcinogens promote lung cancer. Indoor emission of domestic biomass fuels in developing countries, which contain high

concentrations of carcinogens such as polycyclic aromatic hydrocarbons or benzene, have been directly implicated with lung cancer appearance. The same effect has been associated to **ambient air pollution,** which is usually higher in some developing countries but has been also confirmed in several European countries. A significant relationship between radon exposure or arsenic presence in food or drinking water and lung cancer mortality has also been reported (Thandra et al., 2021).

- **Family history of lung cancer.** The existence of a previous family history of lung cancer rises the possibilities of suffering the disease by 1.7 times. Furthermore, the closer the relative the higher the likely of developing lung cancer. When those affected are first-degree relatives, the risk increases double to quadruple (Lissowska et al., 2010). From a molecular point of view, the are three different heritable genomic variants that have been reported to impact the probabilities of developing lung cancer. These comprise the chromosomal locus 5p15 (harboring the telomerase reverse transcriptase gene), the 6p21 locus (harboring regions implicated in the regulation of G-protein signaling), and the 15q25–26 loci (implicated in nicotine dependence and lung cancer susceptibility). However, these genetic factors leading to increased susceptibility to lung cancer remain poorly understood (Kanwal et al., 2017).

## 1.2 HISTOLOGICAL CLASSIFICATION

Lung cancer is a very heterogeneous disease, at a cellular and histological level. Such heterogeneity has important implications in the development of tumors, diagnosis, treatment efficacy and patient outcome (De Sousa et al., 2018). Efforts to broaden the understanding of the biological basis of these tumors are continuously being made. Consequently, the histological classification of lung tumors is periodically updated by the World Health Organization (WHO), whose next edition will be available this spring of 2021. According to this classification, lung tumors are divided into two main types: Non–Small Cell Lung Carcinoma (NSCLC, accounting for approximately 83% of cases) and Small-Cell Lung Carcinoma (SCLC, accounting for approximately 13% of cases) (Fujimoto et al., 2014). The subclassification of

NSCLC into more detailed histologic subtyping differentiates three main groups: adenocarcinoma (ADC), squamous cell carcinoma (SqCC), and large-cell lung carcinoma (LCLC). SCLC is included into a category that comprises neuroendocrine tumors. The are other NSCLC subtypes (as adenosquamous carcinoma) or neuroendocrine tumor subtypes (as typical carcinoids, atypical carcinoids or large-cell neuroendocrine carcinomas), but they represent a very small percentage of cases.

The development of lung cancer molecular profiling, together with the improvements in targeted therapies, outline the importance of a precise histological classification. To date, the diagnosis and histologic subtyping of lung tumors is generally carried out by microscopic visualization of the morphological and immunohistochemical characteristics of patient samples, which can be obtained by several different methodologies depending on the tumor features: percutaneous biopsy, bronchoscopy, mediastinoscopy, or open lung biopsy by thoracotomy (Rodriguez-Canales et al., 2016).

### 1.2.1 Non-Small Cell Lung Carcinomas (NSCLC)

#### 1.2.1.1 Adenocarcinoma (ADC)

ADC is the most prevalent lung cancer subtype, representing around 40% of all cases and near 60% among NSCLC cases. Even though ADC is commonly detected in non-smoker patients, its incidence has been incessantly increasing over the past few decades. In histological terms, ADC is an epithelial tumor with glandular differentiation which usually presents a peripherally location and central fibrosis. It is immunohistochemically identified by the expression of the pneumocyte marker napsin A and the thyroid transcription factor 1 (TTF-1), which can be found in up to 85% of cases, thus facilitating its differentiation from SqCC or LCLC (Rekhtman et al., 2011). ADC has been precisely subclassified in recent years according to refined histological growth patterns. Although there are some other rare variants, the main subtypes are lepidic, acinar, papillary, micropapillary, and solid adenocarcinoma (Travis et al., 2015).

Invasiveness is other key feature of adenocarcinomas. Adenocarcinoma in situ (AIS) is defined as a small sized tumor (3 cm) which develops along preexisting alveolar structures

without stromal, vascular, or pleural invasion. In contrast, if the tumor presents a small invasive focus (<5 mm) it is defined as microinvasive adenocarcinoma (MIA), which is characterized by generation of a desmoplastic stroma and by an absence of deep invasive patterns. Both AIS and MIA show a 5-year survival rate close to 100%. Mortality increases in the advanced invasive adenocarcinomas, which are generally characterized by appearance of tumor necrosis, lymphovascular invasion, and pleural invasion. Among them, those presenting a lepidic pattern associate with a better outcome, while micropapillary and solid patterns associate with a worse prognosis (Yanagawa et al., 2013).

#### 1.2.1.2 Squamous Cell Carcinoma (SqCC)

SqCCs account for around 20% of all lung cancer cases. The 5-year survival rate of SqCC is considerably better than ADC. Its development is highly associated to tobacco smoking and, for that reason, the decrease in the smoking behavior in many countries has led to a decreased incidence (Dela-Cruz et al., 2011). In contrast to ADC, SqCC commonly arises in the main bronchus, therefore presenting a central location in the lungs. Histologically, SqCC is an epithelial tumor characterized by the presence of keratinization or intercellular bridges. However, these features are not always present, complicating the identification of SqCC. This is of particular interest for the analyses of poorly differentiated tumors, where pathologist cannot achieve a reliable morphologic classification (Brambilla et al., 2014). In those cases, the most common identification approach is the immunohistochemical analysis of the squamous cell differentiation markers p40, p63 and cytokeratin 5/6, accompanied by a negative staining of the TTF-1 marker (Kadota et al., 2015). This allows the classification of SqCCs as keratinizing, nonkeratinizing or basaloid.

It is also important to mention that, even though the subclassification into different subtypes does not have an implication in the prognosis of the SqCC patients, it may be useful in the selection of an adequate treatment, especially considering that some targeted therapies (i.e bevacizumab) or chemotherapeutic agents present adverse side effects or resistance, respectively (Sandler et al., 2006).

#### 1.2.1.3 Large-Cell Lung Carcinoma (LCLC)

This subtype is named after the large and polygonal shaped cells composing the tumor. LCLC shows the lowest incidence among NSCLC, accounting for approximately 3% of all lung cancers cases. However, it is usually associated to a worse prognosis (Dela-Cruz et al., 2011). LCLC are histologically defined as undifferentiated carcinomas lacking glandular, squamous or small-cell differentiation morphology or immunohistochemical patterns. This is, they are usually positive for cytokeratins, negative for TTF-1 (in contrast to neuroendocrine tumors or solid ADC) and negative for p40 (in contrast to nonkeratinizing SqCC) (Rehktman et al., 2013). A reliable diagnosis is dependent on multiple sample testing to exclude any of the other NSCLC subtypes. Subsequently, biopsies or cytologies are frequently insufficient; and large tumor tissue samples must be surgically resected to perform the appropriate analyses. LCLC generally appears as a cumbersome tumor with a peripheral location on the lungs, with presence of necrotic areas but without mucin production. At the molecular level, some studies have suggested that null immunophenotype LCLC share many features with solid ADC (Travis et al., 2015).

#### 1.2.1.4 Adenosquamous Carcinoma

Adenosquamous carcinomas present a very low incidence and a worse outcome when compared to conventional NSCLC. They are histologically composed of a mixture of ADC and SqCC characteristics (Mordant et al., 2013). Since adenosquamous carcinomas share many histological features with lung sarcomas, immunohistochemical staining must show expression of cytokeratin markers to rule out an erroneous diagnosis (Travis et al., 2010).

### 1.2.2 Neuroendocrine Tumors (NETs)

NETs represent nearly 20% of lung cancer cases and they are histologically characterized by the presence of an organoid growth pattern and immunohistochemical expression of neuroendocrine markers such as chromogranin A, synaptophysin, and CD56. These features allow their differentiation from NSCLC tumors (Litzky et al., 2010). The WHO differentiates four major subtypes of neuroendocrine tumors: typical carcinoid, atypical

carcinoid, small cell carcinoma (SCLC), and large-cell neuroendocrine carcinoma (LCNEC). All of them may present different differentiation or proliferation characteristics, which entail distinct treatments and survival rates (Travis et al., 2013).

#### 1.2.2.1 Typical and atypical carcinoids

Typical and atypical carcinoids are rare tumors that nevertheless present a relatively common incidence in young patients. They are mainly characterized by an early detection and a favorable prognosis, especially in the case of typical carcinoid, whose development is not associated to tobacco smoking. A higher presence of atypia is the basic feature for distinguishing atypical carcinoids from the typical subtype (Zheng et al., 2016).

#### 1.2.2.2 Large Cell Neuroendocrine Carcinoma (LCNEC)

LCNEC is a very aggressive subtype. Patients suffering from LCNEC present a 5-year survival rate considerably worse than other lung cancer tumors (under 30%). They share many characteristics with SCLC (i.e., high number of mitoses and association with previous history of tobacco smoking) but is easily differentiated by the existence of large and polygonal-shaped cells (Battafarano et al., 2005)

#### 1.2.2.3 Small Cell Lung Carcinoma (SCLCs)

SCLC is, by far, the most common neuroendocrine subtype, accounting for nearly 13% of all lung cancers cases. A vast majority of SCLCs are associated to tobacco smoking, are detected at late stages (usually when the disease has already metastasized) and present an aggressive behavior. This entails a devastating prognosis, with rapid recurrences after treatment and extremely poor survival rates (Lewis et al., 2014). Macroscopically, it presents a central location on the lungs. Histologically, SCLCs are named after the small cells that compose the tumors, which grow forming organoid nests or diffuse sheets, and which can be reliably identified by visualization of basic H&E-stained sections. High mitotic and apoptotic rates are also common. Immunohistochemical detection of keratin, neuroendocrine and TTF-1 markers facilitate SCLC differentiation from other histologic subtypes. The latter is of special relevance, given that it is expressed in almos all cases. The high staining pattern of the

proliferation marker Ki67 is additionally used to identify SCLC and rule out low or intermediate grade neuroendocrine tumors from other histologic subtypes (Planchard et al., 2011).

## 1.3 THERAPEUTIC OPTIONS

### 1.3.1 Surgery

Surgical resection remains the most effective therapeutic option for the patients diagnosed of lung cancer. However, this option is not adequate for all patients, who must meet some specific conditions before undergoing surgery. Firstly, the overall health condition of the patient must be good enough to tolerate the intervention. More importantly, the tumor features must allow a complete resection. Achieving such total resection is the main factor for the outcome and potential cure of the patients. Unfortunately, only 25-30% of patients present with an early enough stage to be offered surgical resection (Molina et al., 2008). In any case, surgery plays an essential role for lung cancer patients not only as a curative treatment, but also in the obtaining of tumor samples for subtyping and stage identification. A precise preoperative staging and restaging of mediastinal lymph nodes is also crucial for patients with potentially resectable tumors (Little AG, 2006).

The specific standard procedure selected for resection depends on the extension of the tumor. Many small, peripheral or low-graded mases are resected using limited resections such as segmentectomy or wedge resections. However, lobectomy is the preferred intervention for NSCLC, as it shows a better long-term survival and decreased local recurrence when compared to those patients undergoing limited resections. Furthermore, the technical and medical improvements achieved in the last decades have lowered the mortality ratios of lobectomies to a 1.3% of cases (Allen et al., 2006).

Of note, the wide standardization of video-assisted lobectomies in hospitals around the globe has allowed to perform tumor resections with the same accuracy but minimizing the invasiveness (McKenna et al., 2006). This milestone has broadened the spectrum of patients

that can undergo surgical treatment to those that formerly could not tolerate a standard surgical treatment due to its morbidity.

### 1.3.2 Chemotherapy

Increased understanding of cancer biology is focusing the pharmacologic interest towards development of new targeted therapies, relegating traditional chemotherapy to the background. However, chemotherapeutic treatments are still crucial for a vast majority of patients, to the point that 80-90% of all NSCLC patients may become candidates for chemotherapy during the course of their disease. This is mainly due to the high percentage of cases that are diagnosed at locally advanced or metastatic stages and to the fact that chemotherapy may be used at different time points (Pfister et al., 2003).

**Neo-adjuvant chemotherapy** is offered to those patients presenting healthy enough status with the aim of down-staging the disease before surgery. Several studies have shown a clinical benefit in the outcome of patients with advanced tumors receiving pre-operative chemotherapy when compared to those treated with surgical intervention alone (Rosell et al., 1999). The same conclusion was observed for those patients with earlier tumor stages (Maghfoor et al., 2005).

**Adjuvant chemotherapy** is administered after the surgical intervention and is commonly indicated for patients with resected tumors at stages IIA through IIIA. Large meta-analyses conducted decades ago demonstrated that administration of platinum-based adjuvant chemotherapy significantly improved the 5-year survival rate of patients. Thus, vinorelbine or cisplatin treated patients achieved a 14-30% decrease in the mortality risk when compared to those without adjuvant chemotherapy (Douillard et al., 2005). Even though not all lung tumor subtypes, tumor stages and chemotherapy agents (i.e., carboplatin, paclitaxel or UFT [uracil tegafur]) showed the same clinical benefit; the general conclusions of many clinical trials strongly support the utilization of platinum based post-operative chemotherapy for 3 to 4 cycles as standard of care after complete tumor resection, particularly for stages IIA to IIIA.

The benefit of **chemotherapy for very advanced** (stage IIIB and IV) **and relapsed tumors** is limited to patients presenting a healthy status. Unluckily, low response rates are observed at these advanced stages, where most of the cases remain incurable. Platinum-based treatments have traditionally been considered the standard of care, achieving slight improvements of 1-year survival rates ranging from 10% to 20%. It is important to notice that these agents can also improve the patient's quality of life and therefore can be used as supportive care beyond survival responses (Maghfoor et al., 2005).

Agents such as paclitaxel, docetaxel, gemcitabine, and vinorelbine have been added to platinum-based therapy regimens proving to be similarly effective. So, it became common to administer combinations of two different drugs. In contrast, triple combinations showed augmented side effects without outcome improvements (Kelly et al., 2000). In most cases, primary oncologists are allowed to decide the selected chemotherapeutic agents and regimen duration, which usually ranges from 3 to 6 cycles. If first-line platinum-based chemotherapy shows a good effect and the patient maintains an adequate performance status, second-line chemotherapeutic agents may be offered (Fosella et al., 2000).

In conclusion, even if chemotherapy is still appropriate for a significative number of NSCLC patients, there is a global feeling that chemotherapy efficacy has gotten stuck and that major research efforts must be directed in the development of biologic therapies (Molina et al., 2008).

### 1.3.3 Immunotherapy

Immune checkpoints are key regulators of the immune system responses, that allow self-tolerance and prevent autoimmunity. However, some cancers can escape from the immune attack by stimulating immune checkpoint targets. Cytotoxic T-Lymphocyte Antigen 4 (CTLA-4) and Programed Death-1 (PD-1) receptors, which are predominantly expressed by T cells, are the most widely studied regulators of these antitumor responses.

Immunotherapy agents stimulate immune responsiveness, contribute to the recognition of cancer cells as foreign, and impede the tumor ability to inhibit the natural

immune system response. Intense efforts are being devoted to determining which tumors may show a positive response to these immunotherapies. In this regard, PD-1 ligand (PD-L1) expression is consistently considered as a biomarker that predicts which patients are more likely to be positive responders to immunotherapy (Lim et al., 2020).

Continuous advances in the knowledge of the immunotherapy field are facilitating the development of new immunotherapeutic agents. A few drugs targeting PD-1 and PD-L1 have improved the outcome of some subsets of patients with advanced lung cancer and therefore have been already approved for clinic use: pembrolizumab (anti-PD-1) is administered as first- and second-line in patients showing positive expression of PD-L1 (Herbst et al., 2016). In contrast, the anti-PDL1 agent nivolumab is used as second-line treatment regardless of PD-L1 expression. The same occurs for the anti-PD-L1 compound atezolizumab (Rittmeyer et al., 2017). Finally, the anti-PD-L1 agent durvalumab is indicated as a maintenance therapy for those patients whose tumors were not resectable but showed a good initial response to chemoradiotherapy regimens (Antonia et al., 2018). As commented above, the immunotherapy field is rapidly evolving, with some other drugs being tested under clinical trials and many issues (including patient selection, first-line or second-line drug selection and combination settings with chemotherapy or targeted therapies) still being addressed.

## 1.4 MOLECULAR ALTERATIONS AND TARGETED THERAPIES

Lung cancer is a very heterogeneous disease not only at the histological level but also at the molecular level. Extensive efforts aimed at unveiling the molecular alterations that promote this disease are continuously been made by research groups around the world. Such works are based on the certainty that a better understanding of the genetic alterations driving lung cancer will open the possibility of designing novel targeted therapies leading to important clinical benefits. In the past, treatment decisions were only based on the histologic subtype of the tumor. However, recent advances in the identification of driver alterations in oncogenes and tumor suppressor genes changed the landscape of lung cancer etiology. Many of these new molecular alterations are only (or mostly) present in a certain histologic subtype, thus allowing

to utilize them as reliable predictive biomarkers or personalized therapy targets specifically for some tumors (Fujimoto et al., 2014).

Regarding the molecular alteration patterns of different lung cancer histologic subtypes, lung adenocarcinomas are usually associated with amplification of *EGFR* and *MET;* mutation of *EGFR* and *KRAS*; and rearrangements of *ALK*, *RET* and *ROS1 (*Jang et al. 2009; Cappuzzo et al., 2009*)*. Despite the fact that squamous cell carcinomas are nowadays commonly excluded from molecular analyses, identification of its driver alterations such as *DDR2, PI3KCA*, and *AKT1* mutations or *FGFR1* amplification, may enable the future development of personalized therapies (Gold et al., 2012). Mutation of *RB* and amplification of *MYC* are commonly present in small cell lung cancer. *P53* mutation is widely present in all lung cancer subtypes. It is found in around 50% of NSCLC (46% for lung adenocarcinoma, 80% for squamous cell carcinoma) and even at higher frequencies among small cell lung cancers (Sato et al., 2008; Gray et al., 2010).

Smoking history plays an important role on the number of mutations present in the lung tumors, with non-smokers presenting 10-fold lower mutation when compared to smokers. Mutations in *BRAF, JAK2, JAK3, TP53* and mismatch repair genes are strongly associated with tobacco smoking. In contrast, *EGFR, ROS1*, and *ALK* rearrangements can be easily found in never smokers (Govindan et al., 2012).

As commented above, many of the molecular alterations driving the tumor development are only present in a specific subtype, raising the possibility of utilizing targeted therapies only in those cases presenting the alteration of interest. To achieve that goal, the identification of patients that may benefit from those therapies is of particular relevance. In this regard, commonly used detection methods include direct DNA sequencing, high-resolution melting analysis, PCR assay, or targeted methods such as ARMS (Amplification Refractory Mutation System or SmartAMP (Smart Amplification Process). Additionally, the detection of fusion gene alterations is also performed by FISH (Li et al., 2015). Considering that this thesis project is focused on NSCLC, the main molecular alterations present in this lung cancer subtype (Figure 2) are described below.

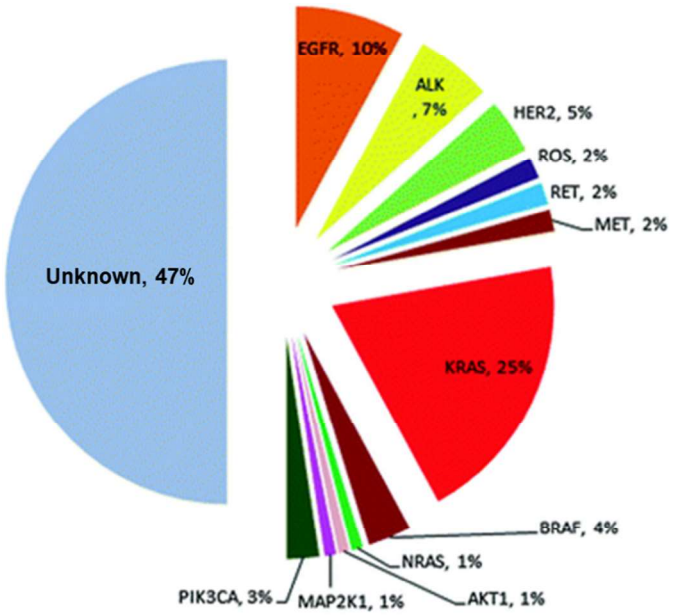


**Figure 2.** Pie chart representing the relative frequency of the main molecular driver alterations in NSCLC. Advances in the identification of new targets may offer novel therapeutic opportunities. Modified from Rodriguez-Canales et al., 2016.

### 1.4.1 Epidermal Growth Factor Receptor (EGFR)

EGFR is a transmembrane glycoprotein receptor that, upon ligand binding, triggers downstream signaling pathways leading to DNA synthesis and cell proliferation. Oncogenic *EGFR* mutations in the exons coding for the kinase domain of *EGFR* (exons 19,19,20 or 21) provoke its constitutive activation and the subsequent hyperactivation of its downstream signaling routes, thus promoting aberrant tumor growth (Scagliotti et al., 2004). 10% to 30% of NSCLC patients harbor *EGFR* mutations, with a higher incidence among adenocarcinomas of non-smoker females. Nevertheless, *EGFR* mutations are also present in smokers and patients with different lung tumor subtypes. Furthermore, *EGFR* mutations are also associated with gene amplification. This entails that, in addition to mutation incidence, more than half of the NSCLC patients harbor EGFR overexpression (Soh et al., 2009).

Those tumors harboring *EGFR* mutations are good candidates for treatment with EGFR tyrosine kinase inhibitors such as gefitinib, erlotinib, afatinib, brigatinib and dacomitinib (Ladanyi et al., 2008; Pines et al., 2010). These targeted agents inhibit EGFR phosphorylation and thus impede the constitutive activation of downstream signaling

promoted by *EGFR* mutations. Because of that, *EGFR* mutated tumors are often highly responsive to these first-line targeted therapies (response rate is near 75%). Consequently, the detection of *EGFR* mutations in the tumor is crucial to decide whether to treat or not the patient with EGFR TKIs (Maemondo et al., 2010). Unfortunately, the majority of patients develop an additional *EGFR* mutation (T790M) that confers resistance to TKIs and therefore promotes tumor relapse. Alternative resistance mechanisms include *MET* amplification and *PI3KCA* mutations. The approach commonly used to overcome such tumor relapse is based on platinum chemotherapy and second-line TKIs as osimertinib (Liao et al., 2019).

### 1.4.2 Anaplastic Lymphoma Kinase (ALK)

The oncogenic alteration of the tyrosine kinase receptor ALK is caused by the exchange of chromosomal segments with other genes. Such rearrangements cause the formation of aberrant ALK fusion proteins, which usually present a constitutive activation of ALK kinase, thus exerting oncogenic functions. The standard chimeric protein in NSCLC is EML4-ALK, which is found in up to 7% of tumors, presenting a higher incidence among adenocarcinomas. For this reason, molecular assays for the detection of EML4-ALK are commonly performed on those tumors with an adenocarcinoma component. (Cao et al., 2019). The incidence of ALK fusion proteins is considerably higher in young non-smoker patients. Other *ALK* fusions detected in NSCLC include translocations with genes such as *KLC, TFG*, and *KIF5B* (Takeuchi et al., 2009; Togashi et al., 2012). It is important to note that, in most cases, *ALK* translocations are mutually exclusive with other main oncogenic molecular alterations such as mutation of *KRAS* and *EGFR*.

Crizotinib is a small-molecule tyrosine kinase inhibitor that targets ALK and is approved for the treatment of positive EML4-ALK patients. As common for this kind of inhibitors, the development of secondary mutations or alternative signaling mechanisms habitually result in drug resistance. Next-generation TKIs directed against ALK appear as a promising treatment option to overcome crizotinib resistance. Patients with ALK mutations can be given alectinib or ceritinib (Maione et al., 2015).

### 1.4.3 Kirsten Rat Sarcoma Viral Oncogene Homolog (KRAS)

Together with HRAS and NRAS, KRAS belongs to the RAS family of oncogenes. The *KRAS* gene encodes a GTPase protein that converts GTP molecules into GDP. KRAS is an upstream effector of the RAS-RAF-MEK-ERK signaling pathway. This route is implicated in the integration of extracellular signals and their transduction to the nucleus, where subsequent changes on gene expression result in cell responses mainly involved in the regulation of cell proliferation. Because of that, mutations that provoke its constitutive activation exert an oncogenic role (Jancik et al., 2010). While mutated-*KRAS* is found in 15-20% of NSCLCs, it presents a higher incidence in lung adenocarcinomas (30-40% of cases) and is very infrequent in SqCCs. The most common oncogenic point mutations in *KRAS* affect codons 12 and 13. Other mutations affecting codons 61, 63, 117, 119, and 146 have also been reported, but in very rare cases (Tam et al., 2006). These mutations present a noticeable higher incidence among smokers (when compared to nonsmokers), particularly among Western countries (when compared to Asian countries). As commented before for ALK alterations, the mutations in *KRAS* are mutually exclusive with other key driver molecular alterations of NSCLC (Stella et al., 2013).

The molecular characteristics of KRAS is making the development of KRAS inhibitors very challenging. Fortunately, after years of extensive work, two compounds have recently showed very promising results. Adagrasib (MRTX-849), has shown in current clinical trials to effectively bind and inhibit the specific G12C mutant form of KRAS, which is commonly present in various forms of cancer (Thein et al., 2021). More importantly, a few days ago (May 28, 2021), the FDA granted an urgent approval to sotorasib (Lumakras™, Amgen, USA), which is another G12C KRAS inhibitor specifically developed for the treatment of those patients with advanced or metastatic NSCLC harboring this mutation (Skoulidis et al., 2021). Its efficacy was evaluated in 124 patients that did not respond to previous systemic therapy. Its encouraging objective response rate (ORR) was 36% (95% CI: 28%, 45%). These drugs could entail an impactful improvement in the outcome of lung cancer patients and potentially other cancers presenting KRAS mutations. Nevertheless, RAS signaling blockade using inhibitors directed

against the downstream proteins RAF-MEK-ERK are also under clinical trials or already reaching the clinic.

*NRAS* is another member of the Ras family of oncogenes, although it is found to be mutated in only 1% of lung tumor cases. Again, such incidence is diferentially higher among the adenocarcinoma subtype and among smokers (Ohashi et al., 2013).

### 1.4.4 B-RAF Proto-Oncogene Serine/Threonine Kinase (BRAF)

As mentioned above, BRAF is located downstream of RAS in the RAS/MAPK signaling pathway. Therefore, this serine/threonine kinase is involved in the transmission of the same chemical signals and regulation of the same biological processes. *BRAF* mutations, which mainly occur at codons of exon 11 and 15 within the kinase domain, have been described in 1-4% of NSCLC tumors. As usual for many oncogenic alterations, *BRAF* mutations also appear to be mutually exclusive with *EGFR* or *KRAS* alterations (Paik et al., 2011). One more time, their incidence is higher among those patients with a previous history of tobacco smoking and those presenting lung adenocarcinomas (Cardarella et al., 2013).

Targeted inhibitors such as vemurafenib, encorafenib and dabrafenib have been already developed against BRAF. Some of them are precisely designed to recognize a specific point mutation BRAF form (i.e., V600-mutant). Even though these inhibitors are mainly used for the treatment of BRAF-mutated melanomas, they have also show clinical benefit for the treatment of NSCLC patients (Gautschi et al., 2015).

### 1.4.5 Mitogen-Activated Protein Kinase 1 (MAP2K1)

The *MAP2K1* gene encodes the MEK1 threonine/tyrosine protein kinase, which is located downstream of RAF within the RAS/MAPK signaling route. Together with MEK2, MEK1 is phosphorylated by activated RAF and in turn, phosphorylate ERK1 and ERK2, leading to cell proliferation and migration. *MEK1* oncogenic mutations are found in nearly 1% of all NSCLC cases, mostly at positions 56 and 57. Such alterations present a similar pattern and behavior to other key alterations of the MAPK signaling pathway: they are more frequently

detected among smoker patients suffering from adenocarcinoma tumors, and are mutually exclusive of other driver *EGFR, KRAS* or *BRAF* mutations (Arcila et al., 2015).

Since MEK1/2 are located downstream of the MAPK pathway, MEK inhibition appears as a promising approach for the treatment of patients harboring *KRAS*, *BRAF* and *MEK* mutation. 4 different targeted therapies against MEK have already been approved for clinical use, including trametinib, binimetinib, selumetinib, and cobimetinib; with many other agents being tested in ongoing clinical trials. All of them are very selective allosteric ATP-non-competitive MEK1/2 inhibitors that hardly ever produce off target effects (Han et al., 2021). Of note, trametinib (®Mekinist) is the only agent approved for the treatment of NSCLC patients in combination with dabrafenib. The summary of the above-mentioned targeted therapies is represented below (Figure 3).

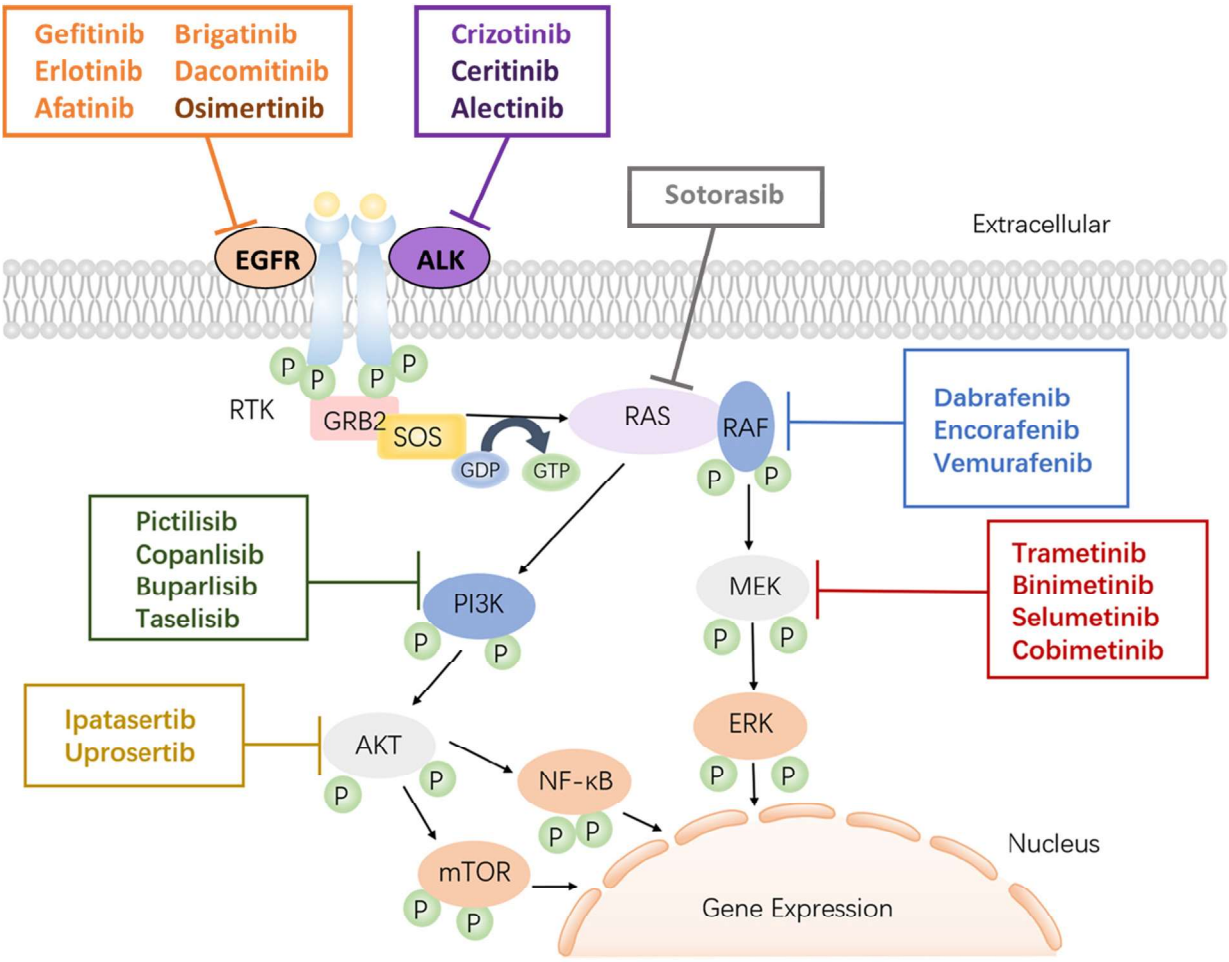


**Figure 3.** Schematic representation of the different agents targeting EGFR, ALK, RAS, RAF, MEK, PI3K, and AKT used in the therapy of NSCLC patients. Modified from Hang et al., 2021.

### 1.4.6 Other oncogenic molecular alterations

**HER2** is another tyrosine kinase receptor involved in the activation of downstream signaling pathways as MAPK and PI3K routes. Oncogenic mutations within its tyrosine kinase domain (therefore promoting aberrant constitutive activation signaling) are found in nearly 5% of NSCLC tumors, most of them corresponding to a 12-base pair insertion in exon 20 (Shigematsu et al., 2005).

The rearrangement of the receptor tyrosine kinase **ROS1** with several different gene partners provokes the appearance of chimeric fusion proteins with hyperactivated kinase activity. Such rearrangements can be found in up to 2% of NSCLC, with a higher presence among lung adenocarcinoma patients. A vast majority of these patients present no coexisting *EGFR, KRAS* nor *ALK* alterations. Notably, the ALK inhibitor crizotinib, is clinically approved for the treatment of NSCLC patients harboring ROS1 rearrangements and shows efficacy independently of the ROS1 chimeric partner (Gainor et al., 2013).

The molecular alteration of **RET** leading to oncogenic responses is the rearrangement and subsequent formation of fusion proteins with many gene partners. Such rearrangements have been found in 1-2% of NSCLC, but with a higher incidence among smokers with lung adenocarcinomas (Wang et al., 2012). RET alteration is not coexisting with other driver alterations and, for that reason, it has been postulated as a new etiological mechanism of lung tumor development. Even though there are no specific RET inhibitors, agents that target other molecules such as cabozantinib or vandetanib show clinical benefit for the treatment of patients harboring RET-rearranged lung adenocarcinomas (Drilon et al., 2016).

**MET** deregulation, which has also been described as an oncogenic driver in lung cancer, may occur through different mechanism including overexpression, overexpression of the HGF ligand, or gene amplification. MET overexpression has been found in nearly 70% of ADCs, 60% of LCLCs and SqCC and 25% of SCLCs (Sattler et al., 2011). In the case of lung adenocarcinomas, the oncogenic alteration underlying the disease is a significant amplification of the *MET* gene, that in turn provokes the overexpression of the MET protein (Kanteti et al., 2009). Of note, *MET* amplification has also been reported as a second alteration that confers

resistance to EGFR-mutated tumors treated with EGFR TKI agents (Stewart et al., 2015). Their pathological relevance is still not well understood, but its potential as a target for the treatment of NSCLC patients is fuelling clinical trials testing inhibitory agents.

Other key molecular alterations that can act as oncogenic drivers in NSCLC are the rearrangement of ***NTRK1*** (observed in approximately 1% of cases, with larotrectinib as its most promising therapeutic inhibitor) (Ekman S., 2020); the mutation of ***PIK3CA*** (which is found in 1-3% of NSCLC cases, particularly among squamous cell tumors) (Fang et al., 2015); the mutation ***AKT1*** (a downstream member of the PI3K pathway that has been found mutated in approximately 1 % of all NSCLC including ADC and SqCC ; the amplification of ***FGFR1*** (Dutt et al., 2011); and the mutation of ***DDR2*** (specifically in SqCCs) (Hammerman et al., 2011). Finally, combination of the monoclonal antibody bevacizumab, which targets ***VEGF***, with chemotherapy, have demonstrated significantly better survival rates for patients with advanced nonsquamous lung tumors (Russo et al., 2017).

# 2. OVARIAN CANCER

## 2.1 EPIDEMIOLOGY

Ovarian cancer remains the 5th cause of death in women and the first cause of death due to gynecological cancer in the western world. It is the second most common malignancy of the female reproductive system after endometrioid cancer. In 2021, it is estimated that 21,410 new cases and 13,770 deaths will occur in the United States, 29,000 deaths will occur in Europe and 1,900 in Spain (Redondo et al., 2021). Approximately 1.3% of women will be diagnosed with ovarian cancer at some point during their lifetime; and woman's risk of dying from this disease is about 0.9% (American Cancer Society, 2021).

To date, there is an obvious lack of methods for early diagnostics of ovarian tumors, which, together with the absence of early warning symptoms in this disease entails that only 15% of the cases are locally detected (confined to primary site). On the contrary, 21% of the cases are detected at regional stages (spread to lymph nodes) or advanced stages (65% of cases), therefore presenting a bad prognosis. In general terms, ovarian cancer presents a 5-year survival rate of 48%, but it varies from 92.6% in localized tumors to a poor 30.3% in metastasized cases (Torre et al., 2018).

Although there have been important improvements in the treatment of ovarian cancer over the past several decades, recurrent ovarian cancer remains incurable in most cases. This is, 3 out of every 4 ovarian cancer patients diagnosed with FIGO stage III or IV tumors will have a recurrence during the first 5 years (Kurnit et al., 2021).

This cancer mainly develops in older women. About half of the women who are diagnosed with ovarian cancer are 63 years or older. However, the rate at which women are diagnosed with ovarian cancer has been slowly falling over the past 20 years. It is more common in white women than African American women (American Cancer Society, 2021)

The causes that provoke ovarian cancer as well as their underlying tumor biology are poorly understood (Auersperg N., 2013). The most important risk factor for developing ovarian cancer is age. However, other risk factors reported to impact on the likely of suffering this

disease are obesity, never having a full-term pregnancy, undergoing hormone therapy after menopause, or having a hereditary family cancer syndrome. The latter is of special importance, given that up to 25% of ovarian cancers are due to family cancer syndromes resulting from inherited mutations in certain genes. Among them, Hereditary Breast and Ovarian Cancer syndrome (HBOC), promoted by mutations in BRCA1 and BRCA2, is responsible for most inherited ovarian cancers. On the other side, pregnancy, breastfeeding and taking oral contraceptives are the main factors that can help in the prevention of ovarian cancer (National Cancer Institute, 2021).

## 2.2 HISTOLOGICAL CLASSIFICATION

Ovarian cancers are now known to be several distinct diseases. The WHO histological classification for ovarian tumors separates ovarian neoplasms according to the type of cell they come from: epithelial, germ cell and stromal. These are the three main cell types present in the ovary. Each tumor type differs in how it spreads, how it is treated, and its prognosis. Based on atypia, they can be further divided into benign, borderline (atypical proliferation with low malignant potential) or malignant, which may be invasive or non-invasive (Stewart et al., 2014). Epithelial tumors are the most frequent type of ovarian cancer, accounting for approximately 90% of cases, whereas malignant ovarian germ cell and stromal tumors comprise less than 10% (Mangili et al., 2011). On this thesis project we will focuss on the epithelial subtypes.

### 2.2.1 Epithelial Ovarian Carcinomas (EOCs)

They can be divided into five main subtypes: High-grade serous ovarian carcinoma (HGSOC; accounting for ~70% of the cases), clear cell carcinoma (CCC; ~12%), endometrioid carcinoma (EC; ~11%), mucinous carcinoma (~3%) and low-grade serous ovarian carcinoma (LGSOC; ~3%). Malignant Brenner tumors and undifferentiated carcinomas are very rare, accounting for less than 1% of the cases (Prat J., 2012). Each histologic subtype presents different biological and clinical features (Table 1).

| Characteristics | High grade serous carcinoma | Clear cell carcinoma | Endometrioid carcinoma | Mucinous carcinoma | Low grade serous carcinoma |
|---|---|---|---|---|---|
| % of cases | 70 | 12 | 11 | 3 | 3 |
| Median age at diagnosis | 61 | 55 | 56 | 53 | 43 |
| Tumor marker(s) | CA-125 | CA-125 | CA-125 | CEA; CA19-9 | CA-125 |
| Genetic risk factors | BRCA1/2 | HNPCC | HNPCC/BRCA | Not known | Serous borderline tumor |
| Common stage at presentation | Advanced | Early | Early | Early | Advanced |
| Response to platinum based chemotherapy | Chemo-sensitive | Chemo-resistant radiosensitive | Chemo-sensitive | Chemo-resistant | Chemo-resistant |
| Common gene mutations | *P53*; *BRCA1/2*; HR defects | *PIK3CA*; *ARD1A*; *PTEN*; MSI | *CTNNB1*; *ARID1A*; *PTEN*; MSI | *KRAS*; *HER2*; *CDKN2A* | *BRAF*; *KRAS*; *NRAS*; *ERBB2*; *PIK3CA* |
| Common immune profile | P53+; WT1+; Pax8+; high Ki67 | HNF β+; WT1-; ER- | ER+; Pax8+; vimentin+ WT1-; P53 wild-type | CK20+; Cdx2+; CK7+; ER-; WT1- | WT1+; Pax8+; P53 wild-type; low Ki67 |

**Table 1.** Histological subtypes of epithelial ovarian cancers and summary of their common characteristics. Modified from Kuroki et al., 2020.

#### 2.2.1.1 High-Grade Serous Ovarian Carcinoma (HGSOC)

HGSOC is the most common type of ovarian cancer (approximately 70-75% of EOCs) (Prat J., 2014). This is basically due to the fact that the most common subtypes of high-grade serous cancers may originate in the distal fallopian tubes, with subsequent cancer in the ovaries a result of the spread from a primary tumor in the fallopian tubes. (Cole et al., 2016).

Although fallopian tube origin of HGSOC is likely and widely accepted, early serous tubal intra-epithelial lesions are only seen in about half of HGSOC cases (Lee et al., 2007) and there have been mouse models of HGSOC that seem to primarily involve precursor cells in the ovary (Kim et al., 2012).

They have an average size of 15cm at the time of diagnosis. At the time of surgery, cancer involves both ovaries in 66% of patients with HGSOC. Recent studies have found that high-grade serous cancers that begin in the distal fallopian tubes take approximately 7 years to progress to the ovaries, followed by the rapid development of metastases. (Labidi-Galy et al., 2017).

Early HGSOC tumors do not cause signs or symptoms in the majority of cases. When signs or symptoms do appear, the cancer is frequently in an advanced stage. These carcinomas typically spread to the peritoneum first, and they are believed to later metastasize by direct contact with intra-abdominal surfaces helped by the peritoneal circulation. These metastases

have a predilection for the omentum, pelvic or para-aortic lymph nodes, although brain and lung metastases can also be found (Pradeep et al., 2014).

#### 2.2.1.2 Low-Grade Serous Ovarian Carcinoma (LGSOC)

Represents 3-5% of all serous tumors and it is usually detected in patiens younger than those suffering from HGSOC (Vang et al., 2009). This subtype of tumors usually appears in both ovaries presenting a characteristic pattern of invasion and low-grade malignant atypia. In most cases (approximately 85%), LGSOC is concurrent with borderline serous tumors, given that it is very often the precursor lesion leading to the development of LGSOC (Seidman et al., 2020; Ahn et al., 2016). These tumors only develop into high grade serous carcinoma in very infrequent cases (Murali et al., 2019).

#### 2.2.1.3 Clear Cell Carcinoma (CCC)

CCC accounts for approximately 8-12% of all ovarian cancers. The mean diagnosis age is 55 years (Chan et al., 2018). They are commonly unilateral (60 to 80% of cases) with a mean size of 15cm. CCCs are named after the clear cells that conform the tumors in a tubulocystic, papillary and solid configuration.

Regarding risk factors for this specific subtype of EOC, it has been widely demonstrated that endometriosis is associated with their development in 7 out of every 10 cases (Ogawa et al., 2000). However, it is also associated with Lynch syndrome (Helder-Woolderink et al., 2016). When confined to the pelvis CCC presents a much better survival rate than HGSOC but, in contrast, when detected at advanced stages has a worse outcome (Delair et al., 2011). Interestingly, Japanese women present a differential higher incidence of CCC tumors when compared to other industrialized countries (25% of EOCs) (Aoki et al., 2014).

#### 2.2.1.4 Endometrioid Carcinoma (EC)

EC accounts for around 10% of primary EOCs (Peres et al., 2019). Its mean tumor size is 11 cm and they are characterized by a cystic and solid component with areas of hemorrhage. Most EC tumors are diagnosed at early stages (confined to the ovary) and in a single ovary

(95% of cases), commonly presenting a low grade. The mean diagnosis age is 55 years and, as previously commented for CCCS, it also seems to be associated with endometriosis (15% of the cases) or other pathologies of the endometrioid tissue including adenofibromas, synchronous adenocarcinomas or hyperplasia (15 - 30%) (Machado-Linde et al., 2015). Other known risk factors are hormone replacement therapy and first-degree family history of breast carcinoma (Wentzensen et al., 2016). Of note, those patients harboring a specific mutation in *CTNNB1* present a better outcome (Zyla et al., 2021). Regardless of disease stage, these tumors seem to respond to treatment better than serous carcinomas.

#### 2.2.1.5 Mucinous Carcinoma

Mucinous ovarian cancer accounts for 3% of EOCs. They usually appear in a single ovary of young women, at early stages, and they mostly remain confined to the ovaries (even though the mean tumor size is around 20 cm, significantly bigger than otrher EOC subtypes). For these reasons, they have a better prognosis than serous tumors. In most cases (77%), mucinous carcinomas are metastases coming from the colon/rectum, appendix, cervix or pancreas (Morice et al., 2019; Khunamornpong et al., 2006).

## 2.3 MOLECULAR ALTERATIONS

### 2.3.1 High-Grade Serous Ovarian Carcinoma

According to the data reported by the TCGA, there are 9 genes found to be diferentially mutated: *TP53, BRCA1, BRCA2, RB1, NF1, FAT3, CSMD3, GABRA6* and *CDK12*. Among them, *TP53* mutation is the most frequent molecular alteration (96% of HGSOC patients) (Ahmed et al., 2010). While *BRCA1/2* mutations are found in up to 21% of tumors, the incedence of mutations in the other genes is significantly lower (ranging from 2% to 6%). It is important to bear in mind that, since *TP53* mutations cause chromosomal instability, a high percentage of HGSOC patients present CNAs. Thus, near 50% of HGSOC cases present defects in the homologous recombination molecular machinery, which in addition to *BRCA1/2* include a set of Fanconi Anaemia genes, *EMSY*, *RAD51, PTEN* and also DNA damage sensing genes such as

*ATM* and *ATR (*Oaknin et al., 2019). Nevertheless, *CCNE1* is the gene most commonly amplified (around 20% of the cases). On the other hand, while shallow deletions are numerous, the most important deep deletions involve the tumor suppressor genes *PTEN, RB1* and *NF1* (Pennington et al., 2014). The above-mentioned molecular alterations are summarized below (Figure 4).

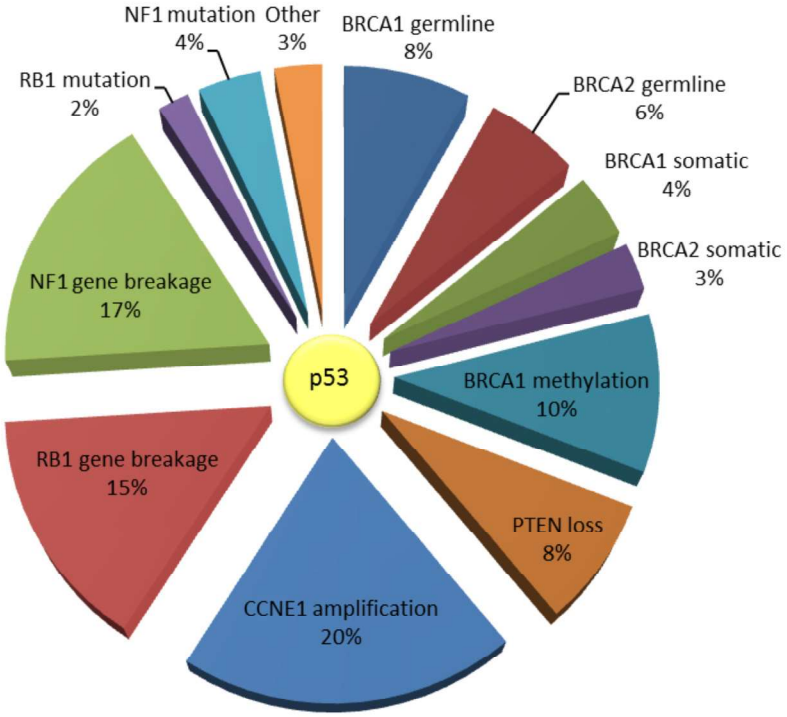


**Figure 4.** Pie chart representing the molecular alteration landscape of High Grade Serous Ovarian Cancer. Adapted from Patch et al., 2015 and Cancer Genome Atlas Research, 2011.

Recent genomic studies have identified four gene expression clusters in high grade serous cancer which have been termed immunoreactive, immunomodulatory, proliferative, and mesenchymal. These molecular subtypes vary in their prognoses, with the immunoreactive subtype identified as having the best outcome (Cancer Genome Research Network, 2011).

Remarkably, the profound CNAs of HGSOC tumors have been described to facilitate the appearance of aberrant structural variants and rearrangements that affect a considerable portion of the genome, therefore altering its integrity without the presence of specific driver alterations (Patch et al., 2015). Moreover, it is important to appreciate that the alterations in HGSOC are rarely mutually exclusive. These facts make classification of HGSOC genomes particularly challenging.

### 2.3.2 Low-Grade Serous Ovarian Carcinoma

The more frequent and important molecular alterations of LGSOC affect genes belonging to the MAP Kinase family and, more specifically to those within the canonical KRAS-BRAF-MEK1/2-ERK1/2 pathway. While *KRAS* mutations are present in approximately half of the patients, *BRAF* mutations are only found in 2-6% of the cases (Kaldawy et al., 2016). Of note, such mutations are mutually exclusive in all cases and occur at early stages, favouring the development of these tumors. Compared with HGSOC, LGSOC has lower *TP53* and *BRCA1/2* mutation rates (10% and 3%, respectively) (Kurman et al., 2016).

### 2.3.3 Clear Cell Carcinoma

The most common molecular alterations in CCC are inactivating mutations in the *ARID1A* gene (46–57%), activating mutations in *PIK3CA* (40%), overexpression of *HIF-1b* and inactivating mutations in *PTEN* (8.3%). Recent studies have demonstrated that *ARID1A* inactivation alone is not enough to generate CCC. On the contrary, coocurrence of *ARID1A* and *PIK3CA* deletion are also neccesary. Interestingly, some studies reported a specific methylation profile of CCC tumors, particularly showing a higher methylation of genes within the ERα pathway, and a lower one of genes belonging to the HNF-1 pathway (Oaknin et al., 2018).

### 2.3.4 Endometrioid Carcinoma

The most typical molecular alteration of endometrioid carcinomas are mutations in *CTNNB1* (20 to 40% of cases, which commonly correlate with a promotion of squamous differentiation and a favourable outcome) (Moreno-Bueno et al., 2001); mutations in *ARID1A* (30%), *PTEN* (15–20%) and *PIK3CA* (near 20% of cases); microsatellite instability (around 15%); and mutations in *KRAS* and *BRAF* (less than 7% of EC tumors) (McConechy et al., 2014).

### 2.3.5 Mucinous Carcinoma

The most typical molecular alterations in mucinous carcinomas are somatic mutations in *KRAS* and *HER2* amplification (15–20%). In the endocervical variant, 30% of cases have *ARID1A* mutations (Cancer Genome Research Network, 2011).

## 2.4 THERAPEUTIC OPTIONS

Ovarian cancer is incurable in most cases due to its late diagnosis at advanced stages. Advances in surgical proceedings, improvement of chemotherapy regimes, as well as the incorporation of new targeted compounds into the pharmacologic armamentarium have exerted a positive impact in the outcome of patients. Treatment options and recomendations vary depending on several factors, including tumor subtype and stage, patient overall health, side effects, personal preferences and whether the patient plans to have children. Age alone is not a determining factor since several studies have shown that older women tolerate ovarian cancer treatments well (National Cancer Institute, 2021). Without a doubt, targeted therapies are the most promising strategies to find the disease. However, it is important to bear in mind that even though many driver alterations and specific drugs are continuously identified and tested under clinical trials, very few finally reach the clinic. Moreover, those achieving clinical approval have not shown to cure this disease but allowing a delay of recurrence or stabilization of the disease.

### 2.4.1 Surgery

Surgery is the main treatment for most ovarian cancers. The extend of surgery depends on how far the cancer has spread and on general health of the patient. So, surgery is not only important from a therapeutic point of view, but also as an efficient way to precisely define the stage of the cancer. Staging is crucial because ovarian cancers at different stages are treated differently (Santaballa et al., 2016). If the tumors are diagnosed at eary stages or confined to the ovaries, the most common approaches are the hysterectomy (removing the uterus), along with bilateral salpingo-oophorectomy (both ovaries and fallopian tubes). In addition, if the cancer has spread to the omentum (a layer of fatty tissue that covers the abdominal area) an omentectomy is usually performed. Biopsies of the pelvic and abdominal peritoneum and the pelvic and para-aortic lymph nodes are also performed. Peritoneal washings are routinely obtained (Nickles et al., 2013). For women of childbearing age who have certain kinds of tumors and whose cancer is in the earliest stage, it may be possible to treat the disease without removing both ovaries and the uterus (Zanetta et al., 1997).

Debulking (removing as much of the tumor as posible) is the other main objective of ovarian cancer surgery. It is extremely important when ovarian cancer has already spread throughout the abdomen at the time of surgery. In some cases, other organs might be affected by debulking (often including resection of the bowel or adjacent organs as needed) to reduce tumor to microscopic, if it can safely be performed. The aim of debulking surgery is to completely remove all visible tumors. Patients undergoing an accurate and successful debulking process show a better outcome than those sub-optimally debulked (Trimbos et al., 2003; Colombo et al., 2003), to the point that patients with optimal cytoreduction had a median survival doubling that of patients with suboptimal residual disease (Nickles et al., 2013).

In the case of patients harboring stage IV tumors, the efficacy of surgery is very low. Since the bulk of the tumoral masses are intra-abdominal, the surgical procedures applied are similar to those used in the management of patients with stage II and III tumors.

### 2.4.2 Chemotherapy

Chemotherapy is the most frequent treatment for ovarian cancer together with surgery. It can be useful to kill very small amounts of cancer cells that may still be around after surgery, for cancers that have metastasized, or to shrink very large tumors to make surgery easier (Santaballa et al., 2016). Most of the time, chemotherapy is administered by intravenous injection or orally. In some cases, chemotherapy may also be intraperitoneally injected through a catheter directly into the abdominal cavity. The typical course of chemotherapy for epithelial ovarian cancer involves 3 to 6 cycles of treatment, depending on the stage and type of ovarian cancer.

**Adjuvant chemotherapy** is administered after surgery and usually involves getting a combination of drugs instead of just one drug alone, as it seems to work better as a first treatment for ovarian cancer. Based on the evidence, the initial standard treatment for patients with ovarian cancer is the combination of a platinum compound (usually cisplatin or carboplatin), and a taxane, such as paclitaxel (Taxol®) or docetaxel (Docefrez®, Taxotere®).

This is defined as induction chemotherapy.

**Neoadjuvant chemotherapy** is administered before surgery with the aim of reducing the tumor size before the surgical intervention**.**

**Consolidation chemotherapy** is given once a remission is achieved. The goal of this therapy is to sustain a remission, avoiding or delaying cancer recurrence.

**Chemotherapy after recurrence**. Epithelial ovarian cancer often shrinks or even seems to go away with chemotherapy, but the cancer cells may eventually begin to grow again. If the first chemotherapy administered seemed to work well and the cancer stayed away for at least 6 to 12 months, it can be treated with the same chemotherapy used the first time. If the tumor responds to platinum, the common treatment will include a combiantion of carboplatin and doxorubicin (Doxil®), paclitaxel (Taxol®) or gemcitabine (Gemzar®). If that is not the case, chemotherapy options may include monotherapy administration of doxorubicin (Doxil®), paclitaxel (Taxol®), docetaxel (Taxotere®), nab-paclitaxel (Abraxane®), gemcitabine (Gemzar®), etoposide (Toposar®, VePesid®), pemetrexed (Alimta®), cyclophosphamide (Cytoxan®), topotecan (Hycamtin®), vinorelbine (Navelbine®), Altretamine (Hexalen®), Capecitabine (Xeloda®) or irinotecan (Camptosar®) (American Cancer Society, 2021).

### 2.4.3 Immunotheraphy

The interaction between PD-1 and its ligand PD-L1 promotes the progression of ovarian cancer through inducing host immunosuppresion of peripheral cytotoxic T lymphocytes (Blank et al., 2005). In addition, the high expression of PD-L1 in ovarian cancer was reported to be associated with poor survival of patients (Hamanishi et al., 2007).

Immunotherapy emerged as a potential novel approach in the therapy of recurrent EOC. Different clinical trials have shown mixed results about the efficacy of these strategies: both anti-PD-1 and anti-PD-L1 antibody monotherapies demonstrated promising benefit and tolerability in platinum-resistant ovarian cancer patients (Hamanishi et al., 2015). Ipilimumab

(MDX-CTLA-4), a monoclonal antibody that impairs the activity of CTLA-4, showed significant antitumor effect in a minority of the previously immunized ovarian cancer patients (Hodi et al., 2008). Pembrolizumam also showed consistent antitumoral actions and low toxicity in a subset of PDL-1 positive patients with EOC (Varga et al., 2019. In addition, preclinical evidence suggested that PARP and VEGF/VEGFR inhibitors could improve the effect of immune PD-1 or CTLA-4 checkpoint blockade (Wang et al., 2019).

### 2.4.4 Targeted therapies

Given the fact that ovarian cancer remains as a dismal disease, there has been a recent surge in research efforts to explore new avenues and methods for treating ovarian cancer. Further, demonstration of the fact that a single short-term treatment of ovarian cancer cells with chemotherapy could result in a cancer stem cell (CSC)-like enriched residual population that may possess selective advantages and significant increased growing capacity, has fostered the search for better therapeutic manoeuvres for ovarian tumors (Abubaker et al., 2014).

There has also been a surge in clinical trials with drugs that specifically target altered molecular drivers, induce apoptosis, and inhibit angiogenesis in site specific ovarian cancer cells, thus, utilizing the molecular profile of each cancer patient to design a more precise therapeutic strategy for fighting the disease (Guan et al., 2018).

#### 2.4.4.1 ERBB receptors inhibitors

Aberrant EGFR expression is detected in up to 60% of ovarian cancers, occurs in all histologic subtypes and is associated with poor outcome of ovarian cancer patients (Siwak et al., 2010). Agents against this receptor have demonstrated antitumor activity in preclinical models. However, the clinical results of the use of drugs directed against EGFR in ovarian cancer have not yielded good results (Yap et al., 2009). Similarly, anti-HER2 therapy, with both trastuzumab and pertuzumab, has not been of clinical benefit in unselected cases of ovarian carcinoma (Gordon et al., 2006). In this sense, the appropriate selection of patients could predict the sensitivity to drugs against HER2. Those patients with activation of HER2,

assessed by phosphorylation, or with overexpression or amplification of the receptor (as occurs in 18% of mucinous ovarian carcinomas) could benefit from these treatments.

On the other hand, HER3 targeting appears as a promising strategy. In preclinical studies, treatment with an antibody raised against HER3 has shown to reduce tumor growth in mice with human ovarian cancer cell xenografts (Sheng et al., 2010). HER3 has also been reported to play a relevant role in the hematogenous spread of ovarian cancer (Pradeep et al., 2014).

### 2.4.4.2 PARP inhibitors

PARP plays an essential part in the repair of DNA single-strand breaks (SSBs). Once PARP is inhibited, the SSBs will not be repaired, leading to the appearance of doble-strand breaks (DSBs) and consequently inducing cell death (Murai et al., 2012).

PARP inhibitors were first approved for use as single agents in patients with recurrent EOC with deficient *BRCA1/2* and not responders to previous chemotherapeutic treatments. However, the noticeable improvement exerted on the PFS of patients after platinum-based chemotherapy (PBC) has postulated PARP inhibitors as the preferred therapeutic strategy in many EOC, particularly among patients harboring impaired BRCA function.

Both the FDA and EMA have approved three different PARP inhibitors (olaparaib, rucaparib and niraparib) to expand the armamentarium of targeted therapeutics for patients with EOC. Olaparib monotherapy demonstrated a good efficacy (tumor response rate of 31.1%) for platinum-resistant recurrent ovarian cancer patients with germline *BRCA1/2* mutations (gBRCAm) and was thereby approved by the FDA (Kaufman et al., 2015).

Niraparib also achieved a significant prolongation of the PFS in platinum-sensitive patients and is accepted as maintenance therapy independently of the presence or absence of gBRCAm or HRD status (Mirza et al., 2016).

Similar with niraparib, rucaparib maintenance treatment for platinum-sensitive ovarian cancer patients showed PFS benefit with manageable toxicity in several specific cohorts (Coleman et al., 2017). Based on this, rucaparib was approved by FDA as maintenance

therapy for recurrent epithelial ovarian cancer patients who have complete or partial response to platinum-based chemotherapy.

### 2.4.4.3 Angiogenesis inhibitors

Angiogenesis plays an important role in the growth, metastasis, and ascites formation of cancer. Overexpression of angiogenic factors such as VEGF, FGF, PDGF, and angiopoietin was reported to be associated with malignant progression and poor prognosis of ovarian cancer patients (Schmitt and Matei, 2012), among which the activation of VEGF/VEGFR signal pathway presented as a dominant mechanism. Drugs targeting this pathway are mainly divided into two categories:

1) Anti-VEGF monoclonal antibody

Bevacizumab (Avastin®) monotherapy showed clinical benefit with a favorable tolerance as second- and third-line treatment in recurrent or persistent epithelial ovarian cancer. It is administered in combination with different chemotherapeutic agents both on platinum-resistant (Burger et al., 2011) and platinum-sensitive patients (Coleman et al., 2017b).

2) Tyrosine kinase inhibitors (TKIs)

Most components that participate in angiogenesis are tyrosine kinases (e.g., VEGFR, PDGFR). Targeting tyrosine kinase is an important anti-angiogenesis strategy especially for patients that developed resistance to bevacizumab. Among them, pazopanib, combined with paclitaxel in patients with platinum-resistant or platinum-refractory ovarian cancer (Pignata et al., 2015), and nintedanib (Du Bois et al., 2016) significantly improved the patient's median PFS.

Considering TKIs are commonly multi-target inhibitors, the balance between increased toxicity and benefits needs to be noted in future trials.

### 2.4.4.4 MAPK inhibitors

In contrast to HGSOC, LGSOC showed a low response rate to cytotoxic chemotherapy and a relatively stable genome which was characterized by *BRAF* and *KRAS* mutations

(Gershenson et al., 2009). Therefore, drugs targeting the RAS/RAF/MEK pathway are reasonable to treat patients with LGSOC. A phase II clinical trial (GOG-239) demonstrated that recurrent LGSOC patients treated with selumetinib (an inhibitor of MEK1/2) had an ORR of 15.4%, which was 4 times that of cytotoxic chemotherapy in the setting of recurrent LGSOC. Besides, selumetinib was well-tolerated. However, the response to selumetinib did not appear to be related with RAS/RAF mutational status, which might result from tumor heterogeneity (Farley et al., 2013).

Trametinib (®Mekinist) is another promising oral MEK1/2 inhibitor (Cappuccio et al., 2020). Besides its clinical approval for the treatment of melanoma and NSCLC, it is currently concluding a phase III clinical trial for the treatment of patients with recurrent or progressive low-grade serous ovarian or peritoneal cancer (latest updates were made in May 2021) (Gershenson et al., 2020). Provisional results show that the trametinib treated arm presents a 52% reduction in the risk of disease progression or mortality. The median progression-free survival (PFS) was 13.0 months (95% CI, 9.9-15.0) with trametinib versus 7.2 months (95% CI, 5.6-9.9) in the control arm (patients treated with different standard of care agents) (HR, 0.48; 95% CI, 0.36-0.64; 1-sided P <.0001). Additionally, median OS was 37.0 months (95% CI, 30.3-not estimable) with trametinib compared with 29.2 months (95% CI, 23.5-51.6) with standard of care. This represents a remarkably 25% decrease in the mortality risk.

#### 2.4.4.5 PI3K/AKT inhibitors

Activation of the PI3K/AKT pathway (mediated by *PI3KCA* or *AKT* mutations or inactivation of *PTEN*) is common in EC and CCC ovarian cancer subtypes and correlates with with poor prognosis (Hanrahan et al., 2012). Although preclinical studies about PI3K/AKT pathway inhibitors were promising, the results of early clinical trials were disappointing (Cleary et al., 2010; Lee et al., 2020).

Preclinical data suggested that concurrent blockade of RAS/RAF/MEK and PI3K/AKT pathways might be synergistic (Kinross et al., 2011). A phase Ib study demonstrated that the combination of pan-PI3K inhibitor buparlisib and MEK1/2 inhibitor trametinib in RAS/BRAF

mutant patients showed a promising antitumor activity, but frequent dose interruptions and reductions for toxicity made this combination unlikely to be tolerable for long-term therapy (Bedard et al., 2015).

### 2.4.4.6 Other therapies and final considerations

Three additional therapies have recently emerged as promising novel ways to fight ovarian cancer:

**Chimeric antigen receptor therapy (CAR-T).** CAR-T treatment involves extraction and gene editing of host T cells to induce expression of chimeric antibodies on the cell surface that, after reintroduction in the patient, attach and attack cancer cells. This process, based on MUC16 overexpression in ovarian cancer cells, has shown potential benefit in the management of metastatic ovarian tumors (Koneru et al., 2015). Although promising, these results utilizing CAR-T are still very preliminary.

**Mismatch repair and microsatellite instability.** Given that defects in mismatch repair considerably increase the risk of developing ovarian cancer, its testing is increasingly being used to identify point mutations that may offer targeted therapies in ovarian cancer. Identification of these defects in ovarian cancer patients is important both for genetic testing of family members and for the use of novel therapies. For instance, some studies have suggested that mismatch repair deficient and microsatellite instability-H ovarian cancer tumors may predict responsiveness to anti-PDL-1 immunotherapy agents such as pembrolizumab (Caliman et al., 2012).

**Folate receptor antibody drug conjugates.** Folate is an essential component in the synthesis, methylation, and repair of DNA that are necessary for rapidly growing cancer cells. Since folate receptor alpha (FRα) is highly expressed in ovarian cancer and considering that it recycles to the cell surface rapidly, it can be efficiently detected, and it can be chemically conjugate with other agents, alltogether makes FRα a very good candidate for the development of new targeted therapies (Luyckx et al., 2014). In fact, clinical trials of fully humanized antibodies as farletuzumab; and folate receptor antibody drug conjugates targeting FRα such

as mirvetuxumab soravtansine, *v*intafolide or IMGN853, have reported some promising results.

In the last two decades, we have assisted to relevant achievements in ovarian cancer regarding the knowledge of molecular biology, surgical outcome, chemotherapy administration, and implementation of therapies that have ultimately translated into clinically significant improvements (Redondo et al., 2021). However, the landscape of ovarian cancer treatment is complicated by the heterogeneity of these tumors. Different histological types of epithelial ovarian cancer have distinct cellular origin, diverse molecular alterations, and thus, different prognosis (Kurman et al., 2011). To address these issues there is a need to better characterize such differences, find reliable biomarkers and develop appropriate targeted therapies.

# 3. THE MEK5/ERK5 SIGNALING PATHWAY

## 3.1. OVERVIEW OF MAPK SIGNALING PATHWAYS

The MEK5/ERK5 signaling pathway belongs to the mitogen-activated protein kinases (MAPKs) superfamily of serine / threonine kinases. This family of signaling proteins is highly conserved among eukaryotes, and their members regulate signal transduction cascades that mediate a wide range of intracellular processes in response to extracellular stimuli (Widmann et al., 1999).

Growth factors, hormones, cytokines, cell-cell or cell-matrix interactions, metabolic stress and also environmental stress (osmotic shock, heat shock, hypoxia, UV light and ionizing radiation) have been described among the external signals that trigger stimulation of MAPK routes (Kyriakis and Avruch., 2012; Cargnello and Roux., 2011; Howe et al., 1992; Lange-Carter et al., 1993). The upstream stimuli are generally transduced by receptor proteins, such as the G-protein-coupled receptors (GPCRs) (Naor et al., 2000) or the receptor tyrosine kinases (RTKs) (Katz et al., 2007), and transmitted by small GTPases to the MAPK network.

Upon activation, the conventional signaling of MAPKs comprise a cascade of three-tiered hierarchical modules that sequentially activate each other by phosphorylation: the extracellular stimuli activate a MAPKKK (MAP3K or MAPKK kinase) that in turn promotes the activation of a MAPKK (MAP2K or MAPK kinase) by specific dual phosphorylation of its serine-threonine motif. Then, at the third level, the MAPKK activates a MAPK by dual phosphorylation of the conserved Thr-X-Tyr motif within the activation loop of the kinase domain (Zhang and Dong., 2007). Finally, MAPK activation provokes the phosphorylation of a great variety of substrates (transcription factors, structural proteins, cytoplasmic enzymes and phospholipases) (Yoon and Seger, 2006) that induce changes in gene expression and/or mediate the specific biological responses. (Canagarajah et al., 1997; Schaeffer et al., 1999). (Krishna and Narang., 2008). The main cellular functions regulated by MAPKs include differentiation, migration, proliferation, cell cycle progression and apoptosis (Herskowitz, 1995; Pearson et al., 2001). However, these routes have also been reported to play a role in

immunological processes (Huang et al., 2009), synaptic plasticity (Thomas and Huganir., 2004), insulin resistance, and cardiovascular disease (Liu and Cao., 2009).

In humans, four conventional MAPK signaling pathways have been described so far: extracellular signal-regulated kinases 1 and 2 (ERK1/2), c-Jun amino (N) - terminal kinases 1/2/3 (JNK1/2/3), p38 isoforms (α, β, γ and δ) and extracellular signal-regulated kinase 5 (ERK5). (Payne et al., 1991; Cuenda and Rousseau., 2007; Nakamura and Johnson., 2007; Zhou et al., 1995) (Figure 5).

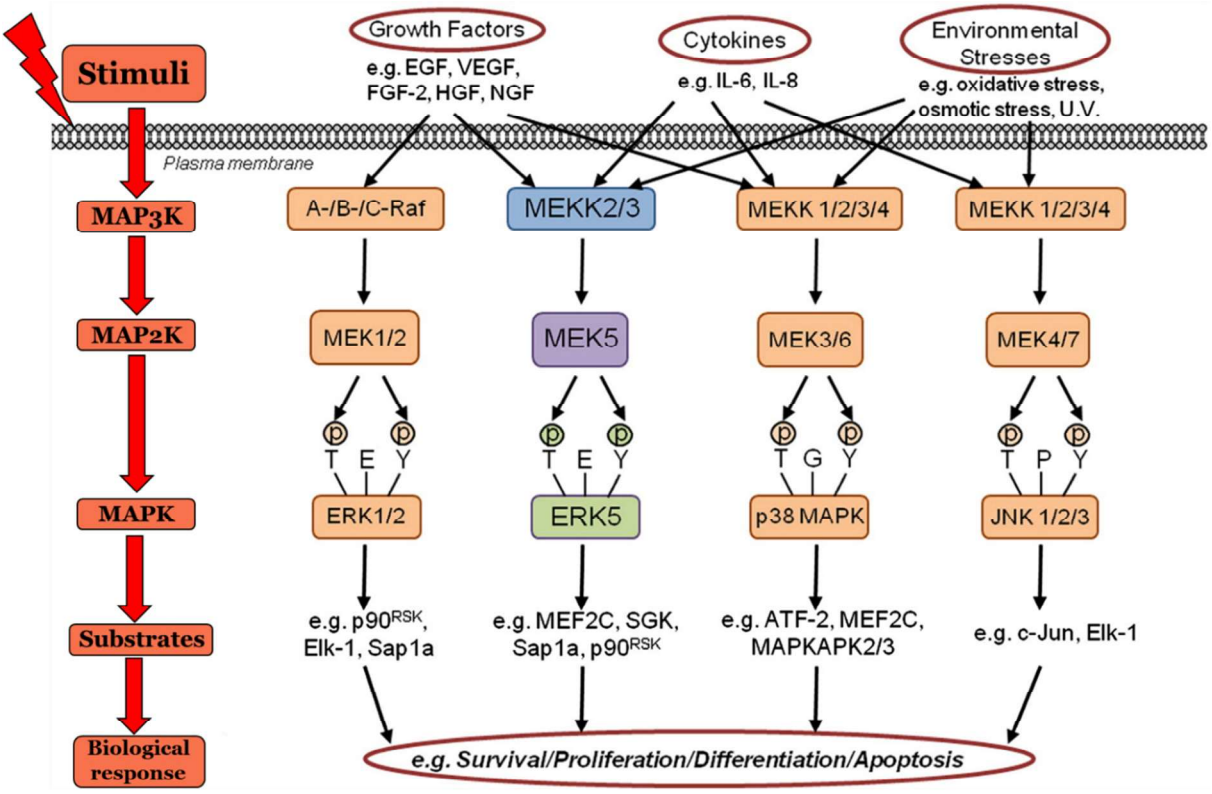


**Figure 5.** Signaling cascades of classical MAPK routes. The conventional three module system is initially activated by an extracellular stimulus (environmental stress, growth factor or cytokines) that is transduced by a receptor with kinase activity or a receptor associated with a MAP4K that in turn promotes the sequential activation of MAP3K, MAPKK and MAPK. The final activation of transcription factors or other MAPK substrates drives the functional response of the cell. Adapted from Nithianandarajah-Jones et al. 2012.

**Atypical subfamilies of MAPKs include** ERK3/4, ERK7/8 and NLK, which are considered unconventional for not following the three-tiered kinase system and lacking the T-X-Y motif, with the exemption of ERK7/8, which presents a T-G-Y activation motif that, in contrast to conventional MAPKs, is not phosphorylated by a MAPKK (Cargnello and Roux., 2011).

The great variety of stimuli, upstream effectors and downstream substrates make MAPK signaling very complex. Moreover, similar extracellular signals can activate different MAPKKK members and MAPKK can be activated by more than one MAPKKK. (Chang and Karin., 2001). Nevertheless, these cascades are tightly regulated so the specificity of signal transfer to MAPK results in an adequate cellular response (Tanoue and Nishida., 2003; Raman et al., 2007): the specificity of the biological response is based on the specificity of the downstream targets activated by the MAPK, which at the same time depend on the specific cell type and extracellular stimuli. Of note, the activation of the appropriate substrate/s by each MAPK is either achieved through direct interaction between their docking domains (Bardwell et al., 2009) or mediated by scaffold proteins (Dhanasekaran et al., 2007). Diversity and complexity of MAPK signaling increases as new factors, such as scaffold proteins or dual specificity protein phosphatases (DUSPs), responsible for inactivation of MAPKs through dephosphorylation of their Threonine-X-Tyrosine motif, are being described to come into play. (Keyse., 2008; Haneda et al., 1999; Pearson et al., 2001; Pouyssegur et al., 2002).

The crucial role of MAPK routes in several biological processes entails that, when aberrant expression or activating mutations occur, altered signaling may cause uncontrolled cell proliferation or cell survival leading to disease development and resistance to various therapies (Knight and Irving., 2014).

## 3.2. IDENTIFICATION OF THE MEK5/ERK5 SIGNAL TRANSDUCTION PATHWAY

Mitogen-Activated Protein Kinase Kinase 5 (also termed MAPKK5 or MEK5) was first discovered in 1995 by Zhou et. al., making it the most recently identified MAPKK. Its cDNA, isolated by degenerate PCR and screening of a human fetal brain cDNA library, showed all 11 conserved kinase subdomains and around 40% homology to other known MEKs (Zhou et al., 1995). However, MEK5 differs from other MAPKKs by having a long N-terminal sequence.

ERK5 was identified immediately after by the same research group through its interaction with MEK5 using a yeast two-hybrid assay (Zhou et al., 1995). At the same time,

Lee et al. also discovered the cDNA of a novel MAPK when *screening a cDNA library from placenta tissue* by PCR assays. (Lee et al., 1995). The encoded protein was very similar to other MAPKs at the N-terminal region, showing the conventional Thr-X-Tyr phosphorylation motif present in other ERK proteins and required for their activation. However, it was almost twice the size of other MAPK members due to the presence of a long C-terminal tail. For that reason, it was termed Big-MAPK1 (BMK1). After contrasting their findings, both research groups finally concluded that ERK5 and BMK1 were encoded by the same gene, so they were the same protein indeed.

## 3.3 MEK5 AND ERK5 GENES AND TRANSCRIPTS

The human MEK5 gene (MAP2K5) consists of 264 Kb and is genomically located at the cytogenetic band 15q23. The canonical protein encoded by this gene contains 448 amino acids (UniProt identifier Q13163), which corresponds to a molecular weight of 50.1 kDa. Four different isoforms produced by alternative splicing have been described, however, the most studied are MEK5α (canonical, isoform B) and MEK5β (also called isoform A). The latter lacks 89 amino acids at the N-Terminal domain and therefore consists of a shorter protein (40 kDa).

MEK5β is ubiquitously expressed, although its expression is more prominent in highly differentiated tissues, mainly showing a cytosolic location in cells. In contrast, MEK5α presents a more restricted distribution, particularly higher in brain and mitotically active tissues such as the liver (English et al., 1995; Cameron et al., 2004).

The human ERK5 gene consists of 5824 bases, with 6 exons, and presents an open reading frame of 2451 base pairs. It is genomically located at the cytogenetic band 17p11.2, encoding a protein of 816 amino acids with a molecular weight of 98 kDa (UniProt identifier Q13164) (Yan et al., 2001). 11 different transcripts variants have been reported, however not all of them are protein coding (Inesta-Vaquera and Cuenda., 2010). Four different human ERK5 isoforms have been described by alternative splicing. In isoform 2, amino acids 1-139 from the canonical isoform 1 are missing, constituting a shorter protein (677 amino acids). Isoforms 3 and 4 lack ample regions of the canonical sequence and are even shorter, consisting

of 533 and 431 amino acids, respectively. In the case of mouse ERK5 protein (UniProt identifier Q9WVS8), it presents a 90.81% identity to the human sequence, accounting for several amino acidic substitutions or missing residues to make a final protein of 806 amino acids. Five splicing variants have been identified. Isoforms 2 and 3 (also called ERK5b and c) lack the first 77 and 139 N-terminal amino acids, respectively. This fact impedes their kinase activity and activation of the substrate MEF2C and, for that reason, it has been postulated that they may function as dominant negative inhibitors of the canonical ERK5 signaling pathway (Yan et al., 2001). While isoform 4 (also called ERK5-T) presents a premature stop codon that eliminates key domains of the protein and make it unable to translocate from the cytoplasm to the nucleus (McCaw et al., 2005).; isoform 5 lacks the last 50 amino acids of the C-terminal region.

ERK5 is expressed ubiquitously in mammals, but shows a higher presence in heart, placenta, skeletal muscle, lungs, and kidney (Lee et al., 1995; Zhou et al., 1995). It has also been found widely expressed in many different cell lines, although its subcellular distribution may be diffuse or concentrated in certain subcellular compartments (Buschbeck and Ulrich.,2005; Borges et al., 2007). Based on these findings, MEK5-ERK5 signaling pathway is not expected to exert very specific functions in highly specialized cells, but to mediate in the regulation of various biological functions which may depend on the cellular context (Buschbeck and Ulrich., 2005).

## 3.4 FUNCTIONAL DOMAINS

There are two main domains along the 448 amino acidic residues that form the MEK5 protein: the Phox and Bem1 (PB-1) domain, which comprises positions 18-109; and the protein kinase domain, which consists of amino acids 166-409. The PB1 domain allows MEK5 binding to its downstream target ERK5 and to the upstream effectors MAP3K2/MAP3K3 via non-overlapping residues. This is, interacts with ERK5 through amino acids 18-25 and with MAP3K2/MAP3K3 through positions 64-68. It also mediates its interaction with other proteins such as SQSTM1 or PARD6A. On the other hand, the phosphorylation motif of MEK5

is located at serine 311 and threonine 315 within the kinase domain. Phosphorylation of these residues by the upstream members of the pathway cause MEK5 activation.

The unique structure of ERK5 can be divided into a N-terminal and a large and unique C-terminal regions, each of them containing several domains that entail specific functions of the protein (Figure 6).

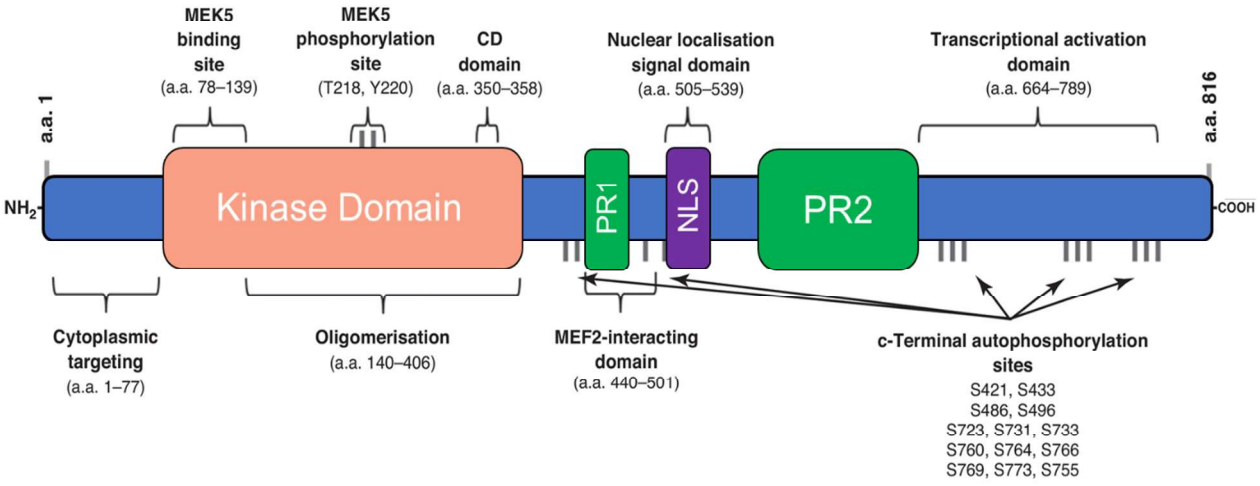


**Figure 6.** Schematic representation of ERK5 protein structure and the functional domains contained within its 816 amino acid residues. Adapted from A. E. Simões et al., 2016.

### N-terminal region

The first domain present at the N-terminal region of ERK5 is the cytoplasmic targeting domain (amino acids 1-77). It is followed by a big kinase domain (amino acids 78-406) that, as previously commented, is highly homologous to ERK1/2, sharing a 66% sequence homology. Importantly, it contains three specific domains: the MEK5 binding domain (amino acids 78-139), the oligomerization domain (amino acids 140-406), and a common docking (CD) domain (amino acids 350-358) responsible for the interaction between ERK5 and its substrates. Of note, residues 218-220 correspond to the Thr-Glu-Tyr (TEY) phosphorylation motif within the activation loop. These residues are similar to the Thr-X-Tyr motifs of other MAPK proteins, whose phosphorylation is required for activation. In the case of ERK5, the dual phosphorylation of the TEY motif is specifically mediated by MEK5. (Kasler et al., 2000; Yan et al., 2001; Tanoue and Nishida., 2003).

**C-terminal region**

The large and unique C-terminal domain is what makes ERK5 to double the size of other MAPKs members. (Buschbeck and Ullrich., 2005). This characteristic 396 amino acid-long tail is thought to be responsible for driving ERK5 specific signaling events (Lee et al., 1995) and allowing ERK5 to be regulated in a more complex way (Nithianandarajah-Jones et al., 2012). From left to right, this extended C-terminal tail is composed of several domains: a proline-rich (PR) domain 1 (PR1, amino acids 434-485), a myocyte enhancer factor-2 (MEF2) interacting region (amino acids 440-501), a nuclear location signal (NLS, amino acids 505-539), a second proline-rich domain (PR2, amino acids 578-701), a transcriptional activation domain (amino acids 664-789), and a nuclear export signal (NES, amino acids 771-816). (Zhou et al., 1995; Yan et al., 2001).

The two proline-rich domains serve as binding for proteins containing the SH3 domain (Borges et al., 2007). As its names imply, NLS and NES play a key role in the nuclear shuttling and the cytoplasmic retention of ERK5, respectively (Kondoh et al., 2006). Furthermore, the MEF2 interacting region is regulated via auto-phosphorylation by the transcriptional activation domain. This allows ERK5 to act as a transcription factor itself by regulating the activity of the MEF2 transcription factor (Kasler et al., 2000).

There are numerous phosphorylation sites scattered along the C-terminal region, which are responsible for different physiological outcomes. Of note, truncation of the C-terminal region of ERK5 provokes an increased kinase activity, suggesting that it could exert an auto-inhibitory role (Buschbeck and Ullrich., 2005).

## 3.5 MEK5/ERK5 PATHWAY ACTIVATION

### 3.5.1 Activation stimuli

The MEK5/ERK5 route can be activated by a wide range of stimuli. Soon after its discovery, ERK5 was reported to be activated by serum (Kato et al., 1997). Following studies demonstrated that, as its name suggests, this MAPK pathway can be activated by several mitogens, including EGF (Kato et al., 1998), NRG (Esparis-Ogando et al., 2002), FGF-2

(Kesavan et al., 2004), VEGF (Hayashi et al., 2004), PDGF (Rovida et al., 2008; Izawa et al., 2007), and neurotrophins (trophic factors in neurons) including BDNF, NT-3, NT-4 (Cavanaugh et al., 2001; Watson et al., 2001*)*, and NGF (Finegan et al., 2009). Interestingly, ERK5 was the first MAPK reported to be activated by neurotrophins but not by neuronal activity.

Beside the osmotic and oxidative stresses, which were the first stimuli reported as ERK5 activators back in 1996 (Abe et al., 1996), cellular stimulation of ERK5 is also induced in response to physiological stresses such as hyperosmolar conditions or laminar shear stress in endothelial cells (Yan et al., 1999). Furthermore, pathological stresses such as ischemia (Takeishi et al., 1999), hypoxia (Sohn et al., 2002) or certain inflammatory cytokines during inflammation like IL-6 and IL-8, have been identified to phosphorylate and stimulate the ERK5 pathway (Carvajal-Vergara et al. 2005). Other cytokines such as LIF have the ability to activate ERK5 (Nicol et al., 2001).

### 3.5.2 Upstream pathway members

Once the activation stimuli occur, the pathway activation implies a sequential cascade of kinase-mediated phosphorylation. The two protein members located upstream of MEK5 in the signaling cascade are MEKK2 and MEKK3 (Chao et al., 1999; Sun et al., 2001). Upon activation, MEKK2/3 can both activate MEK5 by phosphorylation of residues Ser311 and Thr315 within MEK5 kinase domain. MEKK2 and MEKK3 share a 94% sequence homology but present differences in their N-terminal regulatory domains so that they can carry out a differential regulation of the pathway activity. In addition, like MEK5 they contain PB1 domains in their N-terminal regions (Blank et al., 1996) which are responsible for MEKK2-MEK5 and MEKK3-MEK5 interactions, allowing signal transduction specificity by different hetero-dimerization adjusts (Nakamura and Johnson, 2003). Although alternative anchorage domains have been described for the MEK5-ERK5 interaction, (Seyfried et al., 2005), the conventional regulation process entails that MEKK2 and ERK5 compete for the same MEK5 PB1 binding domain. This establishes a sequential binding order in which firstly MEKK2 and

MEK5 form a complex that results in MEK5 phosphorylation, followed by its dissociation and subsequent MEK5 binding to ERK5 that results in ERK5 activation of (Wang et al., 2006).

Importantly, MEKK2 shows a higher binding affinity to MEK5 than MEKK3. For this reason, MEKK2 is capable to achieve a greater phosphorylation of MEK5 and is considered a more prominent activator of the MEK5/ERK5 pathway (Sun et al., 2001). It is also important to mention that MEK5β, which lacks an ample N-terminal region, does not contain this PB1 domain. Even though it can bind ERK5, it is thought to impede MEK5α-ERK5 interaction, therefore acting as a dominant negative isoform that can block ERK5 signaling (Cameron et al., 2004).

In the case of mitogenic factors, the binding to their corresponding RTK (i.e., EGF/EGFR, NRG/HER2 or VEGF/VEGR) triggers the downstream stimuli signal transduction by tyrosine kinases that end up activating MEKK2/3 (Figure 7). Proteins such as SRC (Abe et al., 1997) and RAS (Kamakura et al., 1999) can mediate in the activation of the MEK5/MEK5 pathway, often with the support of adaptor proteins. For instance, EGF activates ERK5 by a mechanism that involves SRC kinase activity and MEKK2 association to the SH2 domain containing scaffold protein LAD (Sun et al., 2003).

In contrast, there are several examples demonstrating that the pathway activation mechanism is substantially different upon cytokine and stress-induced stimulation: the phosphorylation events provoked by hydrogen peroxide and sorbitol treatment cause MEKK2/3 activation by RAS-independent mechanisms (Nakamura et al., 2003). In addition, both MEKK2 and MEKK3 can independently activate MEK5 through GAB1 and SHP2 (Hagiwara et al., 2007; Nakaoka et al., 2003).

CDKs during the G2–M phase transition, as well as the protein kinase COT and STAT3 have also been described as potential ERK5 stimulators (Alvarez-Fernandez et al., 2013; Iniesta-Vaquera et al., 2010; Chiarello et al., 2000; Song et al., 2004).

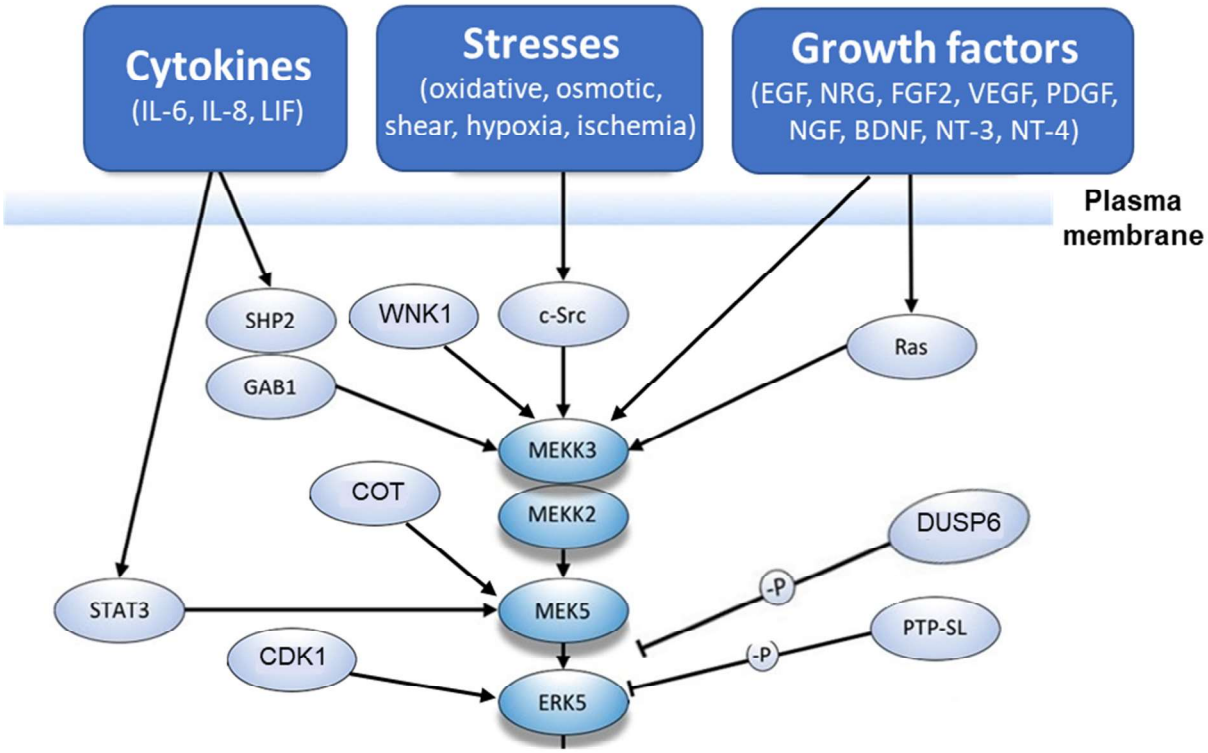


**Figure 7.** Schematic representation of the main activation stimuli and upstream members of the MEK5/ERK5 signaling pathway. Adapted from Hoang et al., 2017.

It is important to highlight that WNK1 (With-no-lysine kinase 1) protein has been identified as a new MAP4K member, upstream of MEKK2/3 in the MEK5/ERK5 signaling pathway (Xu et al., 2004). This protein, discovered in 2000, belongs to WNK subfamily of serine/threonine protein kinases (Xu et al., 2000), and it is mainly involved in the regulation of blood pressure through the control of electrolyte homeostasis by activating sodium-coupled chloride cotransporters and inhibiting potassium-coupled ones (Marx et al., 2001; Wilson et al., 2001). Nevertheless, it has also been implicated in cell signaling (Serysheva et al., 2013), autophagy inhibition (Gallolu et al., 2017), angiogenesis (Sie et al., 2020), cell adhesion and migration (Köchl et al., 2017), survival, and proliferation functions (Jiang et al., 2005a; Lee et al., 2007). There is evidence supporting that WNK1 is implicated in the EGF-mediated activation of the ERK5 pathway by directly interacting with MEKK2/3. In fact, both MEKK2 and MEKK3 coimmunoprecipitated with endogenous WNK1 from cell lysates, which was able to phosphorylate them *in vitro*. Further experiments demonstrated that, while abrogation of WNK1 using siRNA sequences diminished ERK5 activation, WNK1 overexpression promoted

an increase of ERK5 activity in HEK293 cells. Additional studies have recently described the implication of WNK1 in the signaling of the MEK5/ERK5 route (Fulford et al., 2016; Adams et al., 2017; Wu et al., 2020), reinforcing the consideration of WNK1 as the upstream kinase member of this pathway.

### 3.5.3 ERK5 molecular changes upon activation

As previously described, several stimulation signals cause phosphorylation of MEKK2/3 through different mechanisms. Such MEKK2 and/or MEKK3 activation triggers MEK5 phosphorylation on its serine 311 and threonine 315 residues which, in turn, phosphorylates Thr218 and Tyr220 residues of the phosphorylation motif within the activation loop of ERK5 (English et al., 1995). To date, MEK5 is the only recognized MAP2K capable to directly bind and activate ERK5. It has also been reported that dual phosphorylation of both residues is required for achieving a complete activation and catalytic function of ERK5, whereas single phosphorylation of Thr218 (which appears to be preferential, occurring first and facilitating subsequent phosphorylation of Tyr220) only allows partial ERK5 activation (Mody et al., 2003).

The transcriptional activation domain of ERK5 plays an essential role on the molecular conformation that regulates activation and cellular location of the protein. In the basal inactive state, ERK5 presents a closed conformation where the N-terminal domain is folded over the C-terminal region (Figure 8). This folding establishes a structural conformation that exposes both the NES and the NLS domain. However, the strength of the interaction between the CRM1 system and NES is greater than that of importin α/β with NLS, therefore maintaining the folded state that retains ERK5 in the cytoplasm (Plotnikov et al., 2011).

However, MEK5 dual phosphorylation of the TEY motif within the N-terminal region of ERK5 induces its activation, phosphorylation of downstream effectors as well as autophosphorylation at several residues located in its C-terminal tail, including Ser421, Ser433, Ser496, Ser731, Thr733 (Mody et al.,2003), Thr723 and serines located at positions 760, 764 and 766 (Morimoto et al., 2007).

The autophosphorylation of this carboxyl-terminal region interrupts its binding to the N-Terminal domain and provokes a structural change to an open conformation that therefore causes the exposition of the NLS domain. This event promotes the translocation of ERK5 from the cytosol to the nucleus. (Kondoh et al., 2006) together with an increase in the transcriptional activity of this MAPK (Morimoto et al., 2007) (Figure 8).

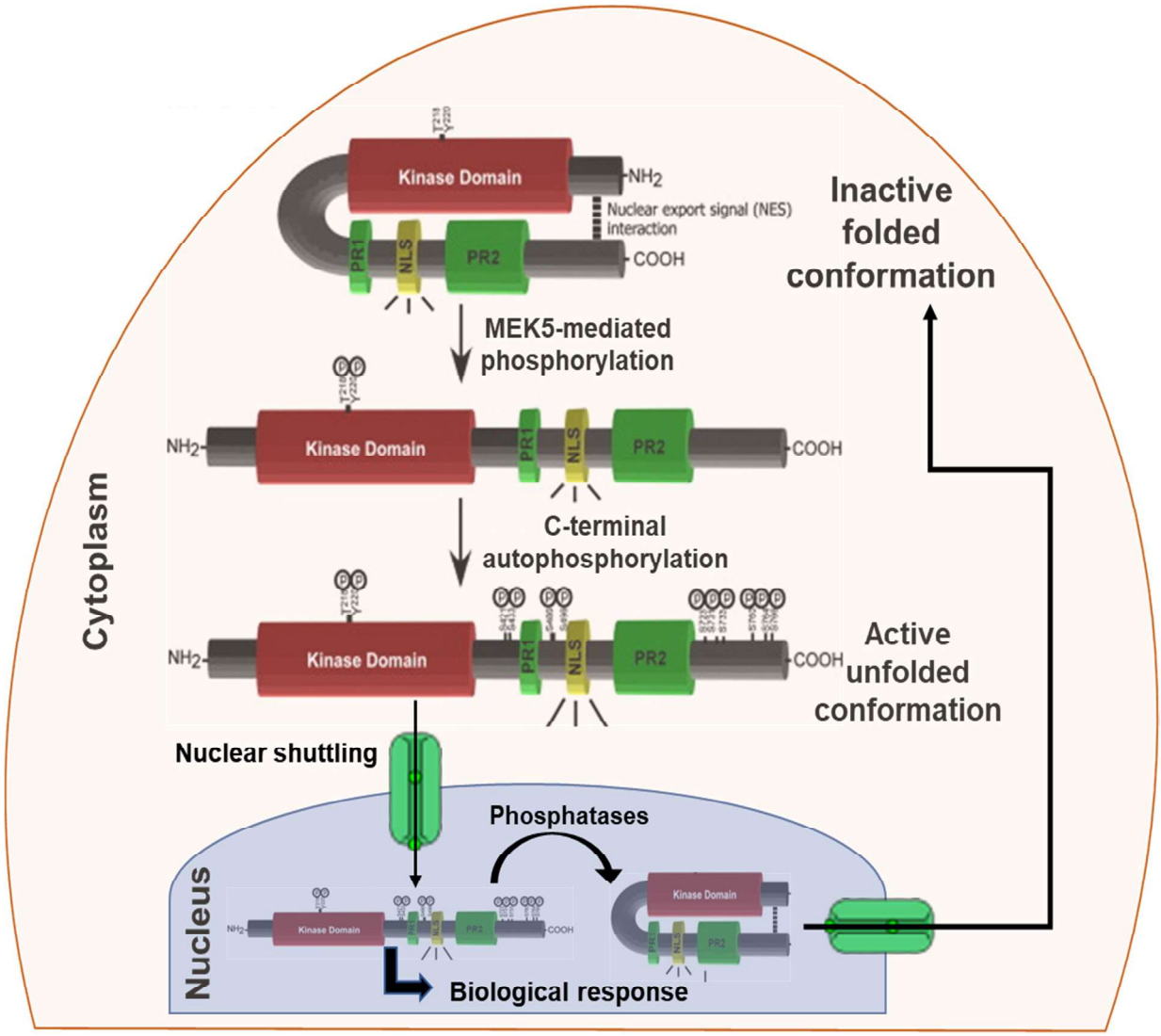


**Figure 8.** Schematic representation of the ERK5 conformational changes induced by MEK5 phosphorylation of the TEY activation motif leading to ERK5 C-terminal autophosphorylation and nuclear shuttling. ERK5 dephosphorylation, which is mediated by MAPK phosphatases, facilitates its refolding and subsequent cytoplasmic shuttling. Adapted from Nithianandarajah-Jones et al., 2012.

In fact, while overexpressed ERK5 is found at a cytoplasmatic location, the coexpression with a constitutively active mutant form of MEK5 promotes an ERK5 nuclear shuttling (Kato et al., 1997). Thus, while cytoplasmic ERK5 utilizes the canonical

NLS/importin-α/β for its translocation, in those cells where MEK5 and ERK5 present a constitutively nuclear location, their activation is promoted by translocation of active MEKK2/3 (Raviv et al., 2004). The translocation mechanism is not clear, since none of these MAPKKKs contain a canonical NLS domain (Plotnikov et al., 2011).

Once in the nucleus, the active unfolded conformation of ERK5 continues to expose its NLS domain (Kondoh et al., 2006). ERK5 only returns to a resting folded conformation when dephosphorylation of its residues allows the exposure of the NES domain and the re-binding of the N-terminal and C-terminal regions, which finally results in the export of ERK5 to the cytoplasm (Plotnikov et al., 2011).

Different phosphatases are involved in such dephosphorylation process, playing an important role in the mechanism controlling ERK5 nucleocytoplasmic transport. For instance, ERK5 activity is diminished by the PTP-SL phosphatase (Buschbeck et al., 2002). Nevertheless, the canonical phosphatases responsible for dephosphorylating MAPK proteins are those belonging to the MAP kinase phosphatase (MKP) subfamily. They are also called dual-specificity protein phosphatases (DUSPs) since the can achieve the dual dephosphorylation of the TXY motif present in most MAPKs (Dickinson et al., 2006). To date, the only MKP enzyme reported to directly dephosphorylate ERK5 is MKP3, also known as DUSP6, which in addition to ERK5 can also dephosphorylate ERK1/2 (Razmara et al., 2012; Moncho-Amor et al., 2019).

ERK5 can also be inactivated by other molecules that downregulate its transcriptional promoter activity such as SUMO3. Upon exposure to AGE or H2O2, SUMO3 covalently binds to residues Lys6 and Ly22 promoting ERK5 sumoylation without affecting its kinase activity (Woo et al., 2008). More recently, miRNAs 143 and 145 have been identified to target ERK5 gene expression, thus exerting a reduction of its activity (Ahmad et al., 2013; Zhou et al., 2017).

In summary, the folded/inactive or unfolded/active state of ERK5 is the main mechanism regulation the cytoplasmatic or nuclear localization of ERK5. However, it should be kept in mind that such subcellular localization greatly depends on the specific cell type, which varies from predominantly cytoplasmatic in cells where ERK5 is not active (i.e., in the

MCF10A cell line) (Borges et al., 2007), to mostly nuclear in cells where ERK5 is constitutively active (i.e., BT474 cells or human lung adenocarcinoma cells) (Esparis-Ogando et al., 2002; Sanchez-Fdez et al., 2019).

### 3.5.4 Substrate activation and physiological implications

The MEK5/ERK5 pathway signaling continues downstream of ERK5 resulting in the activation of several substrates that are involved in numerous cellular functions. Among them, transcription factors are considered the predominant targets of ERK5-mediated regulation.

One of the first families to be unveiled as an ERK5 direct target was the MEF family of transcription factors, consisting of MEF2C (Kato et al., 1997), MEF2A, and MEF2D (Kato et al., 2000) with effects on proliferation, survival, and differentiation-related genes. As previously described, ERK5 sequence contains a MEF2 interacting domain that, together with the transcriptional activation domain regulates the activation of MEF2 members (Kasler et al., 2000). In fact, if the C-terminal tail of ERK5 is truncated, it is not able to further control MEF2 activity (Yan et al., 2001). While MEF2A and MEF2C can be dually regulated by ERK5 and p38 signaling pathways, MEF2D is only activated by ERK5 (Ornatsky et al., 1999; Kato et al., 2000). ERK5 activation of MEF2 is able to mediate the cellular proliferation signals generated by G-CSF and EGF, through regulating the transcriptional activity of *c-JUN* (Kato et al., 1997). (Kayahara et al., 2005; Drew et al., 2012). In addition, it has been shown that MEF2 factors also mediate the antiapoptotic action of ERK5 in BDNF-promoted survival of developing cortical neurons (Liu et al., 2003), and the myogenic differentiation (Liu et al., 2004).

Other classically recognized transcription factors regulated by ERK5 include SAP1a (Kamakura et al., 1999), c-MYC (whose stability is increased by ERK5-mediated phosphorylation) (English et al., 1998; Sears et al., 2000), c-FOS and FRA-1 (Terasawa et al., 2003), which are implicated on cell survival and proliferation responses, mostly induced by growth factors or serum.

Regarding similar cell survival effects, ERK5 also mediates this function in neuronal cells through phosphorylation of p90RSK, leading to activation of CREB and regulation of pro-

apoptotic and survival proteins (Finegan et al., 2009; Watson et al., 2002).

At the same time, a role in endothelial cell survival upon laminar shear stress has also been described for ERK5. The mechanism underlying such effect involves that activation of AKT promotes an increased expression of the BCL2 apoptosis regulator and phosphorylation of BAD, which finally cause apoptosis suppression (Pi et al., 2004; Roberts et al., 2010). Moreover, ERK5 signaling promotes fibroblast cell survival upon sorbitol treatment by downregulating FasL expression via a mechanism that implicates PKB-dependent inhibition of Foxo3a downstream of PI3K/Akt (Wang et al. 2006; Finegan et al., 2009) (Figure 9).

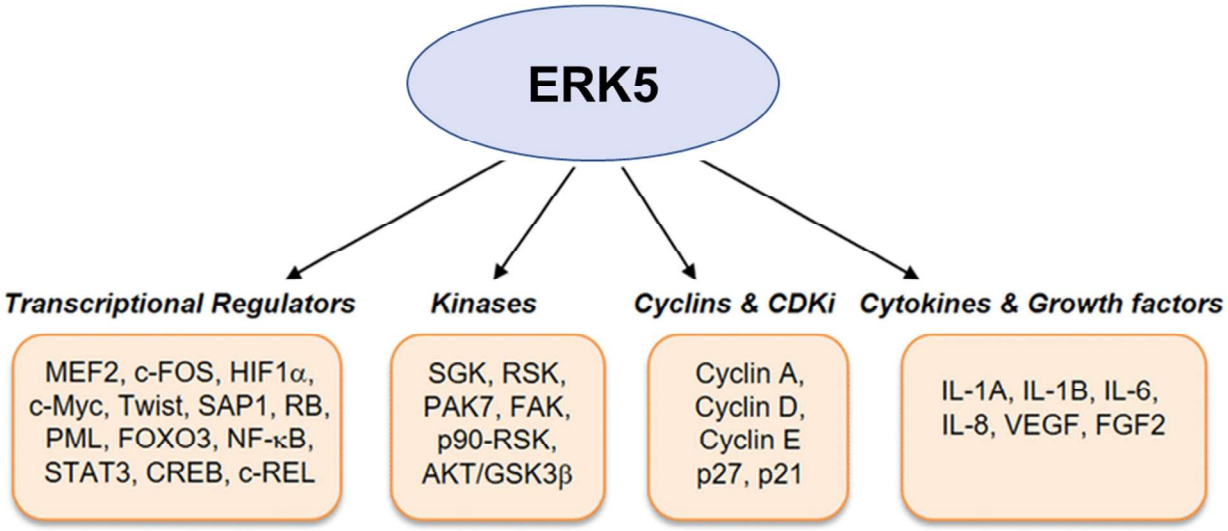


**Figure 9.** Schematic representation of the main substrates activated by ERK5, grouped by functional categories. Adapted from Stecca et al., 2019.

ERK5 activation also mediates the regulation of many other transcription factors, like phosphorylation of SGK, which promotes cell proliferation in response to growth factors (Hayashi et al., 2001; Terasawa et al., 2003); the phosphorylation of Cx43 (Cameron et al., 2004b); the inhibition of PDE3A and ICER feedback loop, thus inhibiting apoptosis signals (Yan et al., 2007), and regulation of the ZEB family of zinc proteins and the TWIST1, SNAI1 and SNAI2 transcription factors (Antoon et al., 2013), which are involved in epithelial-to-mesenchimal transition processes (EMT).

More recently, ERK5 has been unveiled as a key regulator Brk/PTK6, promoting the blockade of cell migration that facilitates tumor progression and metastasis in response to the Met / HGFR signaling (Castro et al., 2010), PML, blocking its tumor suppressor activity (Yang

et al., 2010), and transcription factors KLF2 and 4 (Sunadome et al., 2011), where ERK5 mediated activation is involved in cardiovascular development, endothelial cell migration (Komaravolu et al., 2015), and anti-inflammatory responses (Finegan et al., 2015; Kinderlerer et al., 2008; Woo et al., 2008).

## 3.6 MEK5/ERK5 PATHWAY INHIBITORS

MEK5/ERK5 pathway inhibitors are intended to block ERK5 activation with the aim of ultimately impeding its downstream regulatory functions. The ideal compounds should be designed to specifically target MEK5 or ERK5 without affecting the structure similarities shared with ERK1/2 nor other related kinases showing a great sequence homology.

The MEK5 inhibitors BIX02188 and BIX02189 were the first developed to specifically target the MEK5/ERK5 route, and therefore they have been widely used. Both of them demonstrated to inhibit the catalytic function of MEK5, thus blocking ERK5 phosphorylation and transcriptional activation of downstream targets such as MEF2C, without affecting phosphorylation of ERK1/2 (Tatake et al., 2008). Of note, one of the few off target molecules observed to be inhibited by these compounds is CSF1R kinase with $IC_{50}$ of 280 nM (BIX02188) and $IC_{50}$ of 46 (BIX02189). However, BIX02189 showed a greater selectivity and efficacy against MEK5 catalytic activity (IC50 of 1.5 nM versus 4.3 nM for BIX02188) and therefore, it has been preferentially utilized by research groups worldwide.

Nevertheless, efficient and accurate pathway inhibition by BIX02188 demonstrated key roles of ERK5 signaling in the induction of apoptosis in leukemic cell lines (Razumovskaya et al., 2011), in the atheroprotective effects of blood flow (Li et al., 2008), neural differentiation process (Obara et al., 2009), contribution to morphine physical dependence (Wang et al., 2011), diabetic renal disease (Badshah et al., 2014), and spinal cord injury (Liu et al., 2019).

As commented before, BIX02189-mediated precise inhibition of MEK5 has been reported by numerous studies, most of them related to the tumorigenic processes regulated by the MEK5/ERK5 signaling pathway (Yang et al., 2011).

Soon after BIX compounds development, a group of benzimidazole-based inhibitors

were also reported to inhibit the activation of ERK5, among which compound number 6 showed the best inhibitory results (Flaherty et al., 2010). However, their low potency excluded them from further research usage.

XMD8-92 is an ERK5 inhibitor incidentally discovered in an ample screening looking for ATP-competitive polo kinase inhibitors (Yang et al., 2010). XMD8-92 demonstrated its selectivity for ERK5 in a panel of 402 kinases and in the kinome of HeLa cells, where ERK5 appeared as the most potently inhibited target with $IC_{50}$ of 1.5 μM without affecting MEK5 nor ERK1/2. XMD8-92 efficacy against ERK5 blocked tumor cell proliferation *in vitro* and also prevented tumor growth *in vivo* without morbidity or mortality signs after animal treatment (Yang et al., 2010). Unfortunately, latter studies demonstrated that XMD8-92, in common with some other kinase inhibitors, can also inhibit bromodomain (BRD) proteins (Lin et al., 2016). Since this undesirable feature may be responsible of some of the biological effects of the compound, its usage was thereon restrained.

TG02, is an oral pyrimidine-based multi-kinase inhibitor that also demonstrated the capability to inhibit ERK5 catalytic activity with an $IC_{50}$ value of 43 nM. Even though it reached clinical trial stage, the fact that it also blocked CDKs 1, 2, 3, 5, and 9 in addition to janus kinase 2 (JAK2) and p38δ with $IC_{50}$ values below 60 nM advised the scientific community against its usage for the research specifically focused on the ERK5 route (Alvarez-Fernandez et al., 2013; Goh et al., 2012; William et al., 2012).

Further structure–activity relationship studies of the benzopyrimido-diazepine chemical core led to the discovery of ERK5-IN-1 as the most selective and potent ERK5 inhibitor reported to date with an IC50 of 162 nM (Deng et al., 2013).

During the last 5 years we have experienced a boom in the development of a new generation of MEK5/ERK5 inhibitors. Thus, in 2016 Stephanie M. Myers and colleagues (Myers et al., 2016) performed a high-throughput screening to identify potential ERK5 inhibitors from a library of 57,617 compounds. Four distinct chemical series were potentially specific, and among them, the pyrrole series of ERK5 inhibitors showed the better results. Their studies concluded 3 years later, reporting the identification of compound number 5 of

this series as the best candidate inhibitor (Myers et al., 2019), but it has not been finally validated as its potency ($IC_{50}$ value of 2 μM) is significantly lower than that achieved by previous inhibitors.

Also in 2016, a more potent and selective ERK5 inhibitor series were synthesized from derivatives of the benzopyrimidodiazepinone XMD8-92 first-generation ERK5 kinase inhibitor. Among these compounds, AX15836 was disclosed as the most useful tool for the study of ERK5 inhibition with an $IC_{50}$ value of 8 nM (Lin et al., 2016).

The development of a novel MEK5 inhibitor, SC-1-181, was reported in May 2018 after deep chemical investigations (Chakrabarty et al., 2018). This compound was able to inhibit 82.4% of ERK5 phosphorylation in MDA-MB-231 cells when compared to EGF stimulated control cells. However, it was then observed that very high concentrations of SC-1-181 (greater than 30 μM) were needed to significantly decrease the viability of TNBC cells (Wright et al., 2020), which entailed that it has not been used afterwards.

A few months later, Jinhua Wang and colleagues defined the structure-activity relationships required to achieve direct selectivity toward inhibition of ERK5 without affecting BRD4 bromodomain structures. This effort resulted in identification of one of the first reported kinase-selective chemical probes for ERK5, named JWG-071 (Wang et al., 2018).

In parallel, Vaseva A.V. and colleagues reported in November 2018 a new chemical structure from the PKIS2 library capable of selectively inhibiting MEK5 (Vaseva et al., 2018). The 4-anilinoquin(az)oline chemotype compound (named UNC10225170 or GW284543), demonstrated to dose-dependently inhibit MEK5, as determined by reductions in pERK5. Furthermore, it was able to decrease endogenous MYC protein and suppress pancreatic ductal adenocarcinoma growth when administered with concurrent inhibition of ERK1/2. This inhibitor remains comercially available.

The discovery and characterization of another potent and highly selective *in vitro* inhibitor of ERK5, termed BAY-885, took place two years ago (Nguyen et al., 2019). This chemical probe, selected by high-throughput screening and structure-based optimization, is a (Piperidin-4-yl)pyrido[3,2-d]pyrimidine based compound. Its chemical structure, together

with that of other main MEK5 or ERK5 inhibitors is shown below (Figure 10).

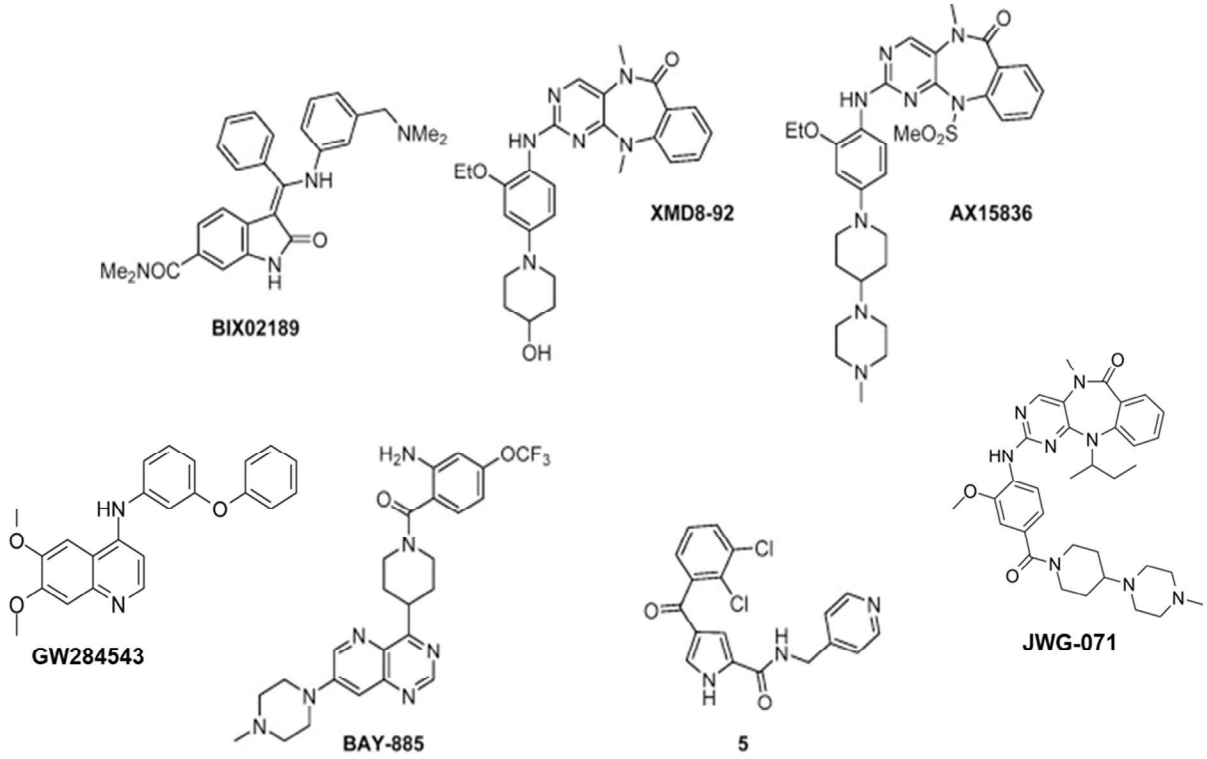


**Figure 10.** Chemical structure of the main MEK5 and ERK5 inhibitors. Modified from Myers et al., 2019; Wang et al., 2018; and Vaseva et al., 2018.

Surprisingly, inhibition of ERK5 kinase and transcriptional activity with BAY-885 did not translate into antiproliferative activity in different relevant cell models, which contrasts with the results obtained by the vast majority of research groups utilizing MEK5 or ERK5 inhibitors. Nevertheless, the fact that ERK5 kinase activity is dispensable for cellular immune response and proliferation was also previously observed (Lin et al., 2016).

It is noteworthy that recent studies have highlighted that selective ERK5 kinase inhibitors fail to recapitulate the results obtained by ERK5 genetic abrogation, therefore suggesting kinase-independent functions for ERK5. Such works have pointed out that ERK5 kinase inhibitors (i.e., AX15836) provoke a paradoxical activation of ERK5 transcriptional activity mediated through its unique C-terminal transcriptional activation domain (Lochhead et al., 2020). Direct binding of the inhibitor to the ERK5 kinase domain triggers a conformational change in this domain that, in turn promotes nuclear translocation of ERK5 and subsequent induction of transcriptional activity. Taking this into account, it has been

suggested that both the kinase and transcriptional activation domain must be considered when evaluating the effectiveness of anti-ERK5 therapeutics and elucidating the biological roles exerted by ERK5 signaling.

In the same line, it has been remarked that the different mechanisms controlling ERK5 nuclear import, which allow the pivotal functions of ERK5 in the nucleus to happen, should be considered as a new strategy for the development of novel ERK5 probes with a complete inhibitory power for the treatment of those diseases in which ERK5 plays a pathophysiological role (Tubita et al., 2020).

In summary, these data demonstrate that the recently developed inhibitors offer novel pharmacological tools to better characterize the role of the MEK5/ERK5 pathway in various biological systems as well as in pathological processes, with a particular consideration as potencial drugs for effectively suppressing tumor growth and with the final goal to develop improved MEK5/ERK5 inhibitors that could be used in the clinic.

## 3.7 IMPLICATION OF THE MEK5/ERK5 ROUTE IN CANCER

For the last 20 years, the number of research studies unveiling the implication of the MEK5/ERK5 signaling pathway in cancer has incessantly grown (Figure 11). Such works have been focused on the pathogenic role of this route in different oncogenic mechanisms of many different tumor types, to the point that these kinases are already widely recognized as key cancer players by the scientific community.

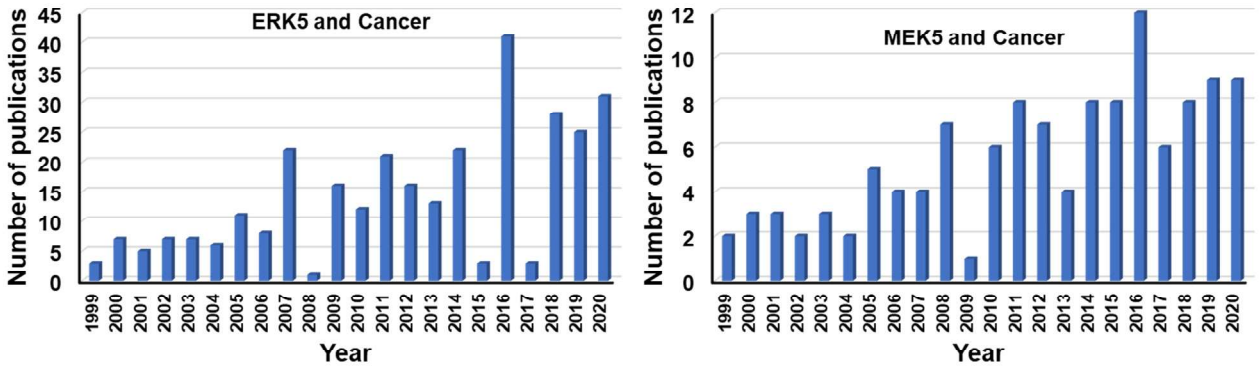


**Figure 11.** Graphics showing the timeline evolution in the number of scientific publications involving the terms "ERK5 and Cancer" (left panel) and "MEK5 and Cancer" (right panel) for the last 20 years collected in the PubMed database (National Center for Biotechnology Information, www.ncbi.nlm.nih.gov/, accessed June, 10th 2021).

Such amount of scientific evidence has been recently summarized by several review papers (Drew et al., 2012; Simões et al., 2016; Hoang et al., 2017; Stecca and Rovida., 2019).

Regarding the role of this route in the onset, progression, and therapy response of specific tumor tissues, those most extensively reported include breast cancer, prostate cancer, colon cancer, leukemia, hepatocellular carcinoma, pancreatic cancer, melanoma, osteosarcoma and lung cancer (Simões et al., 2016).

Whereas MEK5/ERK5 have been already related to most of the hallmarks of cancer, the ample spectrum of studies performed to date point to a more important role of this pathway in some specific features, namely:

**Facilitating EMT and metastatic processes.**

Aberrant MEK5 signaling has been associated with metastatic risk in prostate, breast, colon, kidney, bone, and oral cancers in addition to decreased overall survival. In the same line, migration and invasion properties were enhanced in cancer cells overexpressing MEK5/ERK5, as demonstrated by the generation of an increased number of tumor metastases. In contrast, the inhibition of ERK5 activity led to an *in vitro* diminishing in the motility and invasion capacity of liver, breast, and prostate cancer cells, as well as *in vivo* reduction of breast metastases (Baht et al., 2021).

**Promoting tumor angiogenesis and inflamation.**

The pivotal role of ERK5 signaling in endothelial functions and integrity of blood vessels was formerly established by ERK5 knock out mice, where absence of ERK5 showed to be fatal due to abnormalities in the endothelial cell structure, causing a blood vessel collapse and generalized hemorrhage (Hayashi et al., 2004; Hayashi et al., 2005). A substantial number of studies have implicated the MEK5/ERK5 route in endothelial and angiogenic processes thereafter. These studies suggested that ERK5 mediates these functions through its action on rpS6, on VEGF (Roberts et al., 2010), on bFGF (Yang et al., 2010), KLF-4 (Ohnesorge et al., 2010), KLF-2 (Komaravolu et al., 2015), and by destabilizing HIF1α (Pi et al., 2005).

ERK5 has been also postulated as a critical mediator of inflammation-driven cancer. This is evidenced by its capability to remodel the epidermal inflammatory microenviroment

through the regulation of proinflammatory cytokines (such as IL-1A, IL-1B, and COX-2) leading to the development of skin squamous cell carcinoma. Such role is further supported by the findings that ERK5 abrogation pevents inflammation-driven tumorigenesis in epidermal keratinocytes and reduces tumor growth in neoplastic ones (Finegan et al., 2015). Furthermore, it has been demonstrated ERK5 pharmacological inhibition of mesothelioma cells by XMD8-92 treatment provokes an antitumoral effect by regulating the expression of inflammatory proteins (Thompson et al., 2017). Similar results have been recently observed in melanoma and carcinoma xenograft models, where ERK5 genetic silencing in macrophages impeded STAT3 phosphorylation, promoted the transcription of proinflammatory factors and reduced tumor growth (Giurisato et al., 2018).

**Altering cellular energetics**. Global gene expression analyses have revealed that the MEK5/ERK5 route is implicated in the regulation of certain genes involved in tumor cell metabolic remodeling (Schweppe et al., 2006). Besides generating ATP less efficiently than aerobic respiration, cancer cells usually present metabolic changes that allow them to obtain energy by fermentation process. This is a faster way of generating ATP and therefore, confers a selective advantage to rapidly growing tumor cells over normal cells. It has been demonstrated that exposure of leukemia tumoral cells to external conditions forcing the aerobic oxidative phosphorylation (OXPHOS), provoke an increase of ERK5 expression and accumulation in the mitochondria that in turn, promotes MHC-I upregulation. In contrast, genetic abrogation of ERK5 reduces the cell viability upon forced OXPHOS. Thus, expression of ERK5 is linked to cell survival under these conditions and significantly silenced in metabolically adapted tumor cells (Charni et al., 2010).

Another study revealed that ERK5 expression is necessary for optimal survival of leukemic cells upon certain oxidative stresses (such as $H_2O_2$ and DMNQ treatment), and for the subsequent antioxidant responses (Lopez-Royuela et al., 2014). In the same line, recent studies have pointed out that leukemic cells can protect themselves from the damaging reactive oxygen species (ROS) generated in the mitochondria during OXPHOS through an antioxidative genetic program that involves ERK5 signaling (Khan et al., 2015).

**Generating mechanisms of resistance to cell death.** Chemotherapy is the standard treatment for many cancer subtypes. It has been observed that the the cytotoxic effect exerted by some chemotherapeutic agents is coped by a compensatory activation of the MEK5/ERK5 signaling module, which appears as a drug resistance mechanism. For instance, MEK5/ERK5 overexpression correlates with a worse patient outcome for those basal-like breast cancer patient that have undergone chemotherapy treatment when compared to those not chemotherapeutically treated (Miranda et al., 2015). Biological studies using a mutant ERK5 that accumulates in the nucleus indicated that nuclear ERK5 favours resistance to TRAIL-induced cell death in HeLa cells (Borges et al., 2007). MEK5 upregulation has also been reported in apoptotically resistant MCF7 breast cancer cells, whereas expression of a dominant negative form of ERK5 reduced their viability and sensitized them to apoptosis inducing agents (Weldon et al., 2002). In fact, the drug resistance conferred by the activation of the route can be avoided by concurrent combination of MEK5/ERK5 inhibition and chemotherapy/targeted agents. Thus, knockdown of ERK5 favored the action of drugs commonly used in the treatment of HER2+ breast cancer (Montero et al., 2009).

Another example is observed in colorectal cancer, where genetic or pharmacologic inhibition of ERK5 synergized with chemotherapy (5-FU), increasing apoptosis and significantly decreasing cell growth *in vitro* and *in vivo* when compared to individual treatments (Pereira et al., 2016). Similar effects have been observed in other tumoral models, as mesothelioma, cervical and lung cancer cells; therefore supporting the role of this pathway in the promotion of cell survival, evasion of apoptosis and ultimately chemotherapy resistance. This entails that MEK5/ERK5 expression or activation could serve as a predictive marker for patient benefit from systemic or specific treatments.

**Sustaining proliferative signals.** Besides the above-mentioned functions, ERK5/MEK5 oncogenic signaling is involved in sustaining uncontrolled proliferation and tumorigenesis above anything else. This effect can be promoted by different mechanisms that generally entail the transduction of signals generated by oncogenes (i.e., RAS, Cot or Src) (Drew et al., 2012) or the inhibition of growth suppression signals generated by several factors

(i.e., cyclin-dependent protein kinase inhibitors p27, p21 or p15; RB, p53 or ATM) (Stecca et al., 2019). Nevertheless, such uncontrolled proliferation stimuli can also be generated by altered MEK5/ERK5 expresion or activation, independently from other molecular alterations. The conclusions of the bulky number of scientific efforts directed to elucidate the role of MEK5/ERK5 in tumor cell proliferation are summarized below (Table 2).

| Disease | Cell line | Targeted approach | Effects (compared to control) | Refs. |
|---|---|---|---|---|
| **T cell leukemia** | Jurkat T | shRNA | Did not affect cell cycle progression, sensitized cells to TNF-α | Garaude et al. 2006 |
| **Breast carcinoma** | BT-549 | shRNA, TG02, U0126, DN-ERK5 | Decreased cell proliferation, delayed cell cycle progression, induced apoptosis, sensitized to targeted therapies | Esparís-Ogando et al. 2002<br>Montero et al. 2009<br>Ortiz-Ruiz et al. 2014 |
| | Hs-578T | | | |
| | HCC1187 | | | |
| | MDA-MB-231 | | | |
| | MCF7 | | | |
| | BT474 | | | |
| | SKBR3 | | | |
| **Prostate carcinoma** | LNCaP | CA-MEK5, overexpression | Increased proliferative index | Metha et al. 2003<br>McCracken et al. 2008 |
| | PC3 | | | |
| **Multiple myeloma** | MM1S | TG02 | Suppressed cell cycle progression and induced apoptosis | Álvarez-Fernández et al. 2013 |
| **Cervical adenocarcinoma** | HeLa | DN-ERK5, XMD8-92 | Inhibited proliferation | Yang et al. 2010 |
| **Lung carcinoma** | A549 | XMD8-92, shRNA | Inhibited proliferation | Gavine et al. 2015<br>Sánchez-Fdez et al. 2019 |
| | H23 | | | |
| **Esophageal carcinoma** | KYSE30 | siRNA | Decreased proliferation, increased cell death | Gavine et al. 2015 |
| **Hepatocellular carcinoma** | HepG2 | siRNA, XMD8-92, BIX02189 | Decrease in proliferation, reduction of cells in S phase and increased percentage of cells in G0/G1, no indications of apoptosis | Rovida et al. 2015<br>Lochhead et al. 2016<br>Zen et al. 2009 |
| | Huh-7 | | | |
| | SNU449 | | | |
| **Colon carcinoma** | HCT116 | siRNA, BIX02189, DN-MEK5, CA-MEK5 | Inhibited proliferation at high doses (>10 μM), did not affect proliferation in 3D culture. In HCT116 did not affect proliferation, however ERK5 overactivation by CA-MEK5 increased cell proliferation. In SW620, accelerated cell cycle progression in CA-MEK5 cells, which was abolished by XMD8-92 treatment | Pereira et al. 2016<br>Simões et al. 2015 |
| | HT29 | | | |
| | SW620 | | | |

| Disease | Cell line | Targeted approach | Effects (compared to control) | Refs. |
|---|---|---|---|---|
| **Lung carcinoma** | LL/2 | Deletion of host gene, XMD8-92 | Genetic approach delayed tumor development, reduced tumor vasculature. Pharmacologic treatment suppressed tumor growth, blocked tumor cell proliferation | Yang et al. 2010 Hayashi et al. 2005 |
| | A549 | | | |
| **Melanoma** | B16F10 | Deletion of host gene | Delayed tumor development, reduced tumor vasculature. | Hayashi et al. 2005 |
| **Prostate carcinoma** | PC3 | Overexpression | Enhanced tumor formation | McCracken et al. 2008 |
| **Breast carcinoma** | MCF7 | CA-MEK5, shRNA, TG02 | CA-MEK5 enhanced tumor growth independent of estrogen. shRNA-downregulation of ERK5 decreased MCF7 tumor growth, TG02 delayed tumor growth | Antoon et al. 2013 Ortiz-Ruiz et al 2014 |
| | MDA-MB-231 | | | |
| **Multiple myeloma** | MM1S | TG02 | Inhibited tumor growth | Álvarez-Fernández et al. 2013 |
| | OPM2 | | | |
| **Malignant mesothelioma** | HMESO | shRNA | Impaired tumor formation | Shukla et al. 2013 |
| | H2373 | | | |
| **T cell leukemia** | EL-4 | shRNA | Impaired tumor formation | Garaude et al. 2006 |
| **Hepatocellular carcinoma** | Huh-7 | shRNA, XMD8-92 | Suppressed tumor growth due to reduction in cell proliferation, no change in levels of apoptosis | Rovida et al. 2015 |
| **Colon carcinoma** | HCT116 | XMD8-92 | Inhibited tumor growth by 46% | Pereira et al. 2016 |
| **Pancreatic adenocarcinoma** | AsPC-1 | XMD8-92 | Inhibited tumor growth and decreased tumor volume | Sureban et al. 2014 |
| **Cervical adenocarcinoma** | HeLa | XMD8-92 | Suppressed tumor growth, blocked tumor cell proliferation | Yang et al. 2010 |

**Table 2.** Summary of the *in vitro* (green) and *in vivo* (blue) evidence of the implication of the MEK5/ERK5 pathway in the proliferation and tumorigenesis of different tumor subtypes. The cell lines and targeted approaches used, as well as the effects observed, and bibliographic references are indicated. Adapted from Hoang et al., 2017.

# *OBJECTIVES*

There is an obvious clinical need for unveiling novel pathophysiological mechanisms underlying lung and ovarian tumors that could foster the development of new targeted therapies and which, in turn, may positively impact the outcome of patients suffering from these severe diseases.

Considering all the bibliographic precedents and the previous expertise of our laboratory on the study of the MEK5/ERK5 signaling pathway, the main objectives of this doctoral thesis project were:

- To develop a mouse model genetically engineered to express a constitutively active form of MEK5 to answer the question whether the sole activation of this signaling route promotes tumorigenesis.

- To study the functional relevance of the MEK5/ERK5 route in ovarian cancer.

# *MATERIALS AND METHODS*

# 1. REAGENTS AND ANTIBODIES

## 1.1 REAGENTS

The pharmacological inhibitors BIX02189, crizotinib and WNK463 were obtained from Selleckchem (Houston, TX, USA), XMD8-92 was from Tocris (Bristol, UK), cisplatin and carboplatin from Pharmacia (Peapack, NJ, USA), pemetrexedfrom Eli Lilly (Indianapolis, IN, USA), docetaxel from Hospira (Lake Forest, IL, USA), trametinib and gefitinib from LC Laboratories (Woburn, MA, USA), and JWG-071 was initially provided by Dr. Nathanael S. Gray (Dana-Farber Cancer Institute, Boston, MA, USA) and later purchased from Glixx Laboratories (Hopkinton, MA, USA).

Protein A and Gammabind G-Sepharose were from GE Healthcare (Uppsala, Sweden). Puromycin, polybrene and MTT were from Sigma-Aldrich (St Louis, MO, USA). Annexin V/fluorescein isothiocyanate (FITC) was purchased from BD Biosciences (San Jose, CA, USA). The DNA polymerase and its reaction buffer were from Biotools Biotechnological & Medical Laboratories (Madrid, Spain). The dNTPs were obtained from Fermentas Life Sciences (Burlington, Canada). The PCR reagents were obtained from Invitrogen (Carlsbad, CA, USA) and Promega (Madison, WI, USA). The cell transfection reagent jetPEI was purchased from Polyplus Transfection (Sélestat, France) and the lentiviral vectors were obtained from Thermo Fisher Scientific (Waltham, MA, USA).

Other general chemical reagents were purchased from Sigma-Aldrich, BD Biosciences, Roche Applied Science (Penzberg, Germany) or Merck (Darmstadt, Germany).

## 1.2 ANTIBODIES

The antibodies were obtained as follows: anti-MEK5 antibody was from Enzo Life Sciences (Farmingdale, NY, USA); anti-GAPDH, anti-ERK1/2, anti-PARP, anti-pCDK1 and anti-Wee1 from Santa Cruz Biotechnology (Santa Cruz, CA, USA); anti-pERK1/2, anti-MEK1/2, anti-pMEK1/2, anti-WNK1, anti-MEKK2, anti-MEKK3, anti-cleaved Caspase-3, anti-pS6, and anti-p27 from Cell Signaling Technology (Danvers, MA, USA); anti-Calnexin

from Stressgen Bioreagents (Victoria, BC, Canada); anti-Ki-67 (clone SP6) from Vitro Master Diagnostica (Granada, Spain); anti-CK 7, anti-napsin-A and anti-TTF-1 were purchased from Leica Biosystems (Wetzlar, Germany); anti-pWNK1 from R&D Systems (Minneapolis, MN, USA); anti-caspase-8, anti-caspase-3, anti-cyclin A, anti-BubR1, anti-Rb, and anti-pRb$^{Ser807/811}$ were from BD Biosciences (San Jose, CA, USA);anti-pH3 from Millipore (Billerica, MA, USA); anti-Flag from Sigma-Aldrich (St Louis, MO, USA); and horseradish peroxidase-conjugated secondary antibodies were from Bio-Rad Laboratories (Hercules, CA, USA).

The anti-pMEK5 antibody was developed in rabbit in our laboratory against an epitope containing pSer$^{311}$ and pThr$^{315}$. Antibodies raised against ERK5 and pERK5 were developed in our laboratory as previously described (Esparís-Ogando et al., 2002; Borges et al., 2007).

# 2. CELL CULTURE

## 2.1 CELL LINES

A549, H23, H1975 and HCC4006 (lung adenocarcinoma); H441, H820 and H1404 (papillary lung adenocarcinoma); H322 and SW1573 (minimally invasive lung adenocarcinoma); H1703 and H520 (squamous cell lung carcinoma); H1299 and H460 (large cell lung carcinoma) and H727 (lung carcinoid tumor) Non-Small Cell Lung Cancer cell lines, HBEC3-KT human bronchial epithelium cell line (used as non-tumoral control), HEK-293T cell line (used for the production of lentiviruses) and HeLa cell line were obtained from the ATCC (Manassas, VA, USA)

SKOV-3 serous ovarian adenocarcinoma cell line, OVCAR-8 high-grade serous ovarian adenocarcinoma cell line, A2780 and IGROV-1 endometrioid adenocarcinoma ovarian cancer cell lines were kindly supplied by Pharmamar (Madrid, Spain).

## 2.2 CULTURE CONDITIONS

All cell lines were cultured at 37°C in a humidified atmosphere in the presence of 5% CO2 and 95% air using a HERAcell 150 incubator (Heraeus, Hanau, Germany). Cells were

grown in DMEM containing high glucose (4.5 g/L), L-glutamine 4 mM and L-pyruvate 5 mM or RPMI-1640 medium containing L-glutamine 4 mM. The medium was supplemented with 10% FBS and antibiotics (penicillin 100 U/mL and streptomycin 100 µg/mL). Cell culture media, FBS and penicillin-streptomycin were purchased from GIBCO BRL (Gaithersburg, MD, USA). HBEC3-KT cells were cultured in Keratinocyte-SFM Medium with L-glutamine, EGF and Bovine Pituitary Extract (Fisher Scientific, Madrid, Spain). General cell culture plasticware and glassware were obtained from BD Biosciences and Corning Inc (Corning, NY, USA).

Cells were generally subcultured when confluence reached a 70-90%, approximately. To that end, cells were washed with sterile PBS (2.7 mM KCl; 1.5 mM KH2PO4; 137 mM NaCl; 8 mM Na2HPO4) to remove residual growth medium and individualized by incubation with Trypsin-EDTA Solution 1X (0.25% trypsin, 0.02% EDTA) for 3-5 minutes. Cells were then resuspended in the appropriate medium and transferred to new culture dishes at the adequate subculture dilution for each cell line.

## 2.3 PRESERVATION AND CHECKING OF CELL LINES

Cells were maintained in culture no longer than 4 months. Mycoplasma testing was periodically performed, and their authenticity was checked by STR profiling. Whenever it was necessary to preserve the cell lines, they were frozen in liquid nitrogen at -180 C$^{0}$. To that end, cells in an exponential growing phase were trypsinized, collected and centrifuged at 1200 rpm/3min. Cells were then resuspended in 1mL of the appropriate culture medium supplemented with 10% DMSO and transferred to cryogenic vials (Sarsdedt, Nümbrecht, Germany) that were storage for 24-48 hours at -80°C. After that, the cryovials were transferred to the liquid nitrogen tanks for long term storage.

## 2.4 GENETIC MODIFICATIONS

### 2.4.1 Plasmid transfection

Transfection experiments were performed using the jetPEI transfection reagent following provider's instructions (Polyplus Transfection, Sélestat, France). Two tubes were

prepared: in tube A 250 µl of NaCl 150 mMwere added to 10 µg of the plasmid of interest; in tube B 250 µl of NaCl 150 mM were added to 20 µl of jetPEI. Next, tube B solution was transferred to tuve A, gently mixed and incubated at room temperature for 30 minutes. Then, the mixed solutionwas added drop wise to the culture dish with the target cells at a low confluence (around 50%). 24 hours later, the culture medium was aspired and replaced by fresh medium. After another 24-48 hours, target cells were finally used for the appropriate experiments.

### 2.4.2 Genetic knockdown by shRNA

The knockdown of MEK5, ERK5, MEKK2, and WNK1 was carried out by lentiviral infections with TRC lentiviral pLKO vectors containing human WNK1 (gene set RHS4533-EG65125), MAP3K2 (gene set RHS4533-EG10746), MAP2K5 (gene set RHS4533-EG5607) or MAPK7 (gene set RHS4533-EG5598) sequences; purchased from Thermo Fischer Scientific (Waltham, MA, USA) or Dharmacon (Lafayette, CO, USA).

For the production of lentiviruses, host HEK293T cells were co-transfected with four different plasmids obtained from Addgene (Cambridge, MA, USA) using the jetPEI reagent, namely:

A) 4 µg of the pMDLg/pRRE plasmid, which contains the *gag* gene coding for viral structural proteins, the *pol* gene coding for retroviral enzymes involved in the packaging of the genomic RNA, and the RRE region, which serves as binding site for the Rev protein.

B) 4 µg of the pRSV-Rev plasmid, which codes for the Rev protein that allows exportation of mRNA from nucleus to citoplasm.

C) 4 µg of the pMD2.G virus envelope expression plasmid.

D) 8 µg of the pLKO lentiviral plasmid containing an shRNA control sequence (sh-Control, not directed against any human gene); an shRNA sequence against the target gene of interest; or a GFPsequence used as positive control of transfection.

All these plasmids were mixed, incubated, and added dropwise to the HEK293T cells as described in the previous section. 24 hours later, the HEK293T medium containing the recently produced lentiviruses was collected, filtered with 0,45 μm PVDF Millex-HV filters (purchased from Merck) and added to the target cells of interest.24 h prior transduction, such target cells had beenseeded andallowed to grow to 60-70% confluency. In the moment of transduction, the culture medium of target cells was aspirated and replaced by the HEK293T lentivirus-containing filtered medium mentioned above. 6 μg/mL of Polibrene (purchased from Sigma Aldrich) was added to the target cells in order to increase the transduction efficiency. 8 to 12 hours later, the medium was replaced by fresh medium to avoid polybrene toxic effects. Cells were then maintained in culture for 48 hours to allow the gene silencing process. After that, positive transduced (knockdown) cells, which should harbor the puromycin resistance gene contained in the pLKO.1plasmid, were selected by adding 3 μg/mL of puromycin (purchased from Sigma-Aldrich) to the culture medium for 48 hours. In general terms, 2 to 5 different shRNA sequences against the target gene were tested, and the ones provoking a higher knockdown (tested by Western Blotting) were used for subsequent experiments.

### 2.4.3 Genetic knockout by CRISPR/Cas9

H460 cells were knocked out for ERK5 expression using a *MAPK7* human gene CRISPR/Cas9 knockout kit (reference KN200655) from Origene (Rockville, MD, USA) or MEK5 expression using a MEK5 CRISPR/Cas9 knockout system (references sc-401688 and sc-401688-HDR), with a control CRISPR/Cas9 plasmid (reference sc-418922) from Santa Cruz Biotechnology, following manufacturer's instructions. OVCAR-8 cells were knocked out for MEK5 expression using a *MAP2K5* human gene CRISPR/Cas9 knockout kit (reference KN203171) from Origene.The donor plasmid containing the puromycin resistance cassette and the left and right homologous, as well as the three guide RNA plasmids (2 of them recognize a fragment of the target gene while the other one is a scramble control that is not directed against any human genomic sequence) were previously amplified by transformation of DH5 alpha cells

and purified utilizing a Midi or Maxi kit (Qiagen, Hilden, Germany). 3 x $10^5$ cells were seeded in 2 mL culture medium of a 6 well plate 1 day before transfection to obtain a 60% confluence on the following day. Donor plasmid and guideRNA plasmids (1 ug each) were co-transfected by adding 6 ul of Turbofectin 8.0 transfection reagent (Origene). After that, cells were maintained in culture for 7 passages in order to dilute cells with the episomal donor vector. Approximately 3 weeks after transfection, cells were split at a 1:50 dilution in a 100mm plate and selected by adding puromycin.

Finally, cells from single colonies were isolated and cultured separately. ERK5 and MEK5 levels were tested by Western blotting to identify the positive CRISPRed clones. The proliferation of positive knockout clones was compared to scramble control cells by cell counting pr by MTT assay; and some of them (#20 and #57 for ERK5 and #17 for MEK5 in the case of H460 cells; #16 and #19 for MEK5 in the case of OVCAR-8 cells) were further used for the *in vivo* experiments.

## 2.5 CELL PROLIFERATION ASSAYS

For determining cell proliferation, to different approaches were utilized. On the one hand, the MTT metabolization assay was performed. To that end, cells were plated in 24-well culture plates in quadruplicatesat the adequate density (depending on each cell line) and incubated until the time of proliferation measurement. For those experiments testing the effect of a specific drug on cell proliferation, the treatment was added 24 hours after plating and maintained in culture for the indicated times. At that point, the MTT reagent (purchased from Sigma Aldrich) was disolved in PBS and added to the culture medium to a final concentration of 0.5 mg/mL. Cells were then incubated at 37 °C for 1 hour in the dark to allow MTT metabolization. This metabolization process is based on the capacity of living cells to reduce the MTT compound (water-soluble) into purple insoluble formazan crystals, so that the amount of living cells is directly proportional to amount of formazan produced (Mosmann., 1983). After that period of time, the medium was aspirated. 500 µL of DMSO were immediately added to each well and plates were incubated in an orbital shaker for 10 minutes in the dark to

facilitate the dissolution of the formazan crystals. Finally, the absorbance was read at 570 nm using an ULTRA Tecan plate reader (Tecan; Männedorf, Switzerland). The results were represented either as mean absorbance ± SD of the quadruplicates or relativized as percentage from mean absorbance of the control (untreated or scramble) condition.

On the other hand, direct cell counting was also performed to analyze cell proliferation. In this case, cells were similarly cultured in duplicates in 6-well plates. At the indicated times, cells were trypsinized and diluted in a 1/10 or 1/20 solution of ISOTON (Beckman Coulter, Brea, CA, USA). Finally, the solution containing the individualized cells was counted using a Z1 Coulter Particle Counter (Beckman Coulter).

Again, the results were represented either as mean count ± SD of the triplicates or relativized as percentage from the mean cell count of the control (untreated or scramble) condition.

## 2.6 SYNERGISM STUDIES

NSCLC cells were treated for 60 h with combinations of suboptimal doses of BIX02189 and antitumoral agents used in the lung cancer clinic. The effect of these combinations on cell growth was analyzed by the MTT assay. The effect of each combination was measured with the CalcuSyn 2.11 software (Biosoft, Ferguson, MO, USA) which allows the evaluation of constant-ratio or non-constant-ratio combinations of drugs and calculates a combination index (CI) based on the Chou-Talalay method (CI: 0-0.9 synergistic effect, CI: 0.9-1.1 additive effect, CI>1.1 antagonistic effect).

## 2.7 CELL VISUALIZATION AND IMAGE ACQUISITION

Cell morphology, status and growth was daily monitored by visualization using a Zeiss Axiovert 25 microscopy (Zeiss, Jena, Germany). 10x or 20x image acquisition was carried out by bright field microscopy with an EVOS Floid Cell Imaging Station (Invitrogen)or by using a contrast phase Axiovert 135 microscopy (Zeiss) equipped with a Hamamatsu camera (Hamamatsu Photonics; Tokyo, Japan).

# 3. FLOW CITOMETRY

## 3.1 CELL CYCLE PROFILING

For determining the effect of BIX02189 on the cell cycle, H460 cells were treated or not with 5 μM BIX02189 for the indicated times. Treatment was performed in asynchronous as well as in mitosis synchronized cultures, obtained by treatment with nocodazole (121 ng/mL, 18 h). Cells were trypsinized, collected, gently washed with PBS, resuspended in ice-cold 70% ethanol and incubated at -20°C overnight for permeabilization. The processed cells were washed again and resuspended in 1 mL of PBS containing 50 μg of PI (Propidium Iodide) and 200 μg of DNase-free RNase A (Sigma Aldrich). After incubation at room temperature in the dark for 1 to 2 hours, DNA content was measured using an Accuri C6 flow cytometer (BD Biosciences). The appropriate gating, debris exclusion and analyses of the percentage of cells in the different phases of the cell cycle were performed using the C6 software (BD Biosciences).

## 3.2 BrdU INCORPORATION ASSAY

The BrdU incorporation assay was carried out todetermine the cells undergoing DNA synthesis. To that end, 10 μM BrdU was directly added into cell culture media and incubated for 45 minutes. After that, cells were fixed, permeabilized, treated with DNase and stained using a FITC BrdU Flow Kit according to provider's instructions (BD Biosciences). 20 μL of 7-AAD were added to stain total DNA and the fluorescence was read in an Accuri C6 flow cytometer.

## 3.3 APOPTOSIS ASSAYS

For apoptosis analysis, H460 cells were treated with 5 μM BIX02189 for the indicated times, trypsinized, collected, washed twice with cold PBS and resuspended in 20 μL of cold binding buffer (10 mM HEPES, 140 mM NaCl and 2.5 mM CaCl2, pH 7.4). Cells were then incubated with 5 μL of Annexin V/FITC and 5 μL propidium iodide staining solution (50 mg/mL) for 15 min in the dark. After that, another 400μL of binding buffer were added to labeled cells, which were immediately read in an Accuri C6 flow cytometer. Results were

analyzed with the C6 software.

Alternatively, caspase activity assays were performed. Cells were treated with the appropriate drug and lysed in lysis buffer. 50 μg of cell lysates were placed in three different wells (triplicates) of 96-well plates. The final volume of the lysates was taken to 100 μL by 1X Caspase Buffer (25 mM HEPES pH 7.4, 150 mM NaCl, 1 mM EDTA, 0.1% CHAPS, 10% sucrose). 100 μL of 2X Caspase Reaction Buffer supplemented with 20 mM DTT and 10 μM fluorescent labeled caspase substrate Ac-IETD-AFC (caspase 8) or Ac-DEVD-AFC (caspase 3) were added to each well containing cell lysates. The plate was shaken to mix the solution and incubated at 37°C in the dark for 1 h. The signals were measured at 400/505 nm in a multi-well fluorescent reader from BioTek (Winooski, VT, USA).

# 4. RNA AND DNA METHODS

## 4.1 RNA EXTRACTION AND PURIFICATION

For RNA extraction, 100mm culture plates containing 5 to 10 million cells depending on the cell line were trypsinized, collected and centrifuged at 1200rpm for 4 minutes. The supernatants were aspirated and 1 mL of Trizol (Invitrogen) was added to the cell pellets. The samples were gently mixed by up and down pipetting, transferred to DNase and RNase-free 1.5mL tubes (Eppendorf) and kept at room temperature for 5 minutes. Next, 200μL of chloroform (Merck) were added to the samples, which were then vigorously shaken for 10-20 seconds, incubated for another 3 minutes at room temperature, and centrifuged at 12,000 g for 15 minutes at 4°C. The upper colorless aqueous phase containing the RNA was transferred into a new DNase and RNase-free tube. Total RNA was precipitated by adding 500μL of isopropanol (Honeywell, Morris Plains, NJ, USA) and washed by adding 1 mL of 75% ethanol (Merck). The RNA pellet was air-dried and dissolved in 50 μL of DEPC $H_2O$ (Thermo Fischer Scientific).

If RNA was further needed for microarray analyses, it was cleaned by using the purification columns of the RNeasy Mini kit (Qiagen; Hilden, Germany), following manufacturer's instructions. The RNA concentration and purity were determined using a

NanoDrop1000 apparatus (Thermo Fischer Scientific) by the OD260/OD280 ratio; where a ratio value ≥1.8 indicates "pure" DNA and an OD ratio of ~2.0 indicates "pure" RNA. This RNA could be subsequently used for further experimentation or frozen at -80°C for long term storage.

## 4.2 REVERSE TRANSCRIPTION

Reverse transcription reaction was performed with the aim of synthetizing complementary DNA (cDNA) to the originally extracted RNA. To that end, 2 μg of such purified RNA was mixed in 200 μL PCR microtubes (Thermo Fischer Scientific) with 0.5 μg of oligo-dT (Invitrogen) and 1 μL of 10 mM dNTP mix (Biotools). These procedures were carried out under sterile conditions using a Telstar AV-100 laminar flow hood (Azbil Telstar Technologies). The resulting volume was made up to 12 μL by adding nuclease-free water. The microtubes were heated at 65°C for 5 minutes in a PCR thermal cycler (GeneAmp PCR System 2400 from Perkin Elmer, Waltham, MA, USA) to melt secondary structures and immediately chilled on ice. Samples were briefly spun down and 4μL of 5x First-Strand Buffer, 2μL of 0.1M DTT and 1 μL of RNaseIn Ribonuclease Inhibitor (Promega, Madison, WI, USA) were sequentially added to the microtubes. The resulting samples were mixed and incubated at 37°C for 2 minutes. Finally, 1 μL (200 units) of M-MLV Reverse Transcriptase (Invitrogen) were added and the solution was mixed by up and down pipetting. The final reaction was carried out at 37°C for 50 minutes and then inactivated by heating at 70°C for 15 minutes. The synthesized first strand cDNA was ready for use and could also be stored at -20°C.

## 4.3 qRT-PCR

Once the first strand cDNA has been synthetized, the quantitation of *MEK5* gene expression was carried out by the quantitative reverse transcriptase polimerase chain reaction. The reaction was set in an iCycler iQ 96-well plate (Bio-Rad Laboratories) by mixing 1μL of the cDNA with 12.5 μL ofiQTM SYBR Green Supermix (Bio-Rad Laboratories), 0.4μL of 10 μM *MEK5* Forward Primer (5'-ACGTGAAGCCCTCCAATATG-3') and 0.4μL of 10 μM *MEK5* Reverse Primer (5'-ACTGCTCCCCTGAAATCCTT-3') reaching the final volume to 25 μL by

addition of nuclease free water. The *MEK5* primer oligonucleotides were previously designed in our laboratory by selecting the mRNA sequence of the gene from the Ensembl database and by customizing their length (<250 pb) and melting temperature using the Primer3 software publicly available at http://primer3.ut.ee. The PCR reaction was performed in duplicates on an iCycler iQ5 PCR Thermal Cycler (Bio-Rad Laboratories) with the following phases and conditions: initial step of 15 minutes at 95ºC; denaturing step of 40 cycles of 30 seconds at 95ºC; annealing step of 30 seconds at 60ºC, extension step of 30 seconds at 72ºC; and a final extension step of 5 minutes at 72ºC. Negative controls containing all the mixture components with the exemption of the CDNA were also included. Increased fluorescence was measured and recorded using the Bio-Rad iQ5 software. A melting curve was obtained according to the cycler's instructions to ensure specificity of the primer pairs. The results were normalized to the reference gene, *GAPDH* utilizing the Forward Primer (5'-TGCACCACCAACTGCTTAGC-3') and Reverse Primer (5'-GGCATGGACTGTGGTCATGAG-3'). The relative quantitation of gene expression was performed through the cycle threshold (CT) increment method (Livak and Schmittgen, 2001).

## 4.4 GENE EXPRESSION MICROARRAYS

The analyses of gene expression were performed on three replicates of 3 μg for each condition/sample under evaluation. Preparation and hybridization of RNA was performed by the Genomic Service of the Cancer Research Center of Salamanca. Briefly, RNA integrity and concentration were measured with the Agilent 2100 Bioanalyzer (Agilent Technologies; Santa Clara, CA, USA) utilizing de OD260/OD280 ratio previously mentioned. Biotinylated single strand cDNA was synthetized using the GeneChip WT PLUS Reagent kit (Affymetrix), which provides a complete transcriptome coverage and is optimized for the utilization of an ample spectrum of total RNA samples (including those coming from cell lines) without making necessary to eliminate ribosomal or globin RNA. Labeled RNA was then hybridizated with human Clariom S Array Affymetrix (Thermo Fischer Scientific) by incubation for 16-18 hours at 45ºC in a GeneChip Hybridization Oven 645 (Thermo Fischer Scientific). Finally, the

fluorescence intensity of each array probe was captured using the GeneChip Scanner 3000 7G System (Thermo Fischer Scientific) and subsequently quantified and converted into resulting raw data files (CEL. files) through the Affymetrix GeneChip Commnad Console 3.2 (AGCC).

The CEL. files containing the information of more than 20,800 genes were first utilized for quality control checking of the results utilizing the Expression Console Software. Batch effect correction and analyses of differential gene expression between samples were performed with the Transcriptome Analysis Console 4.0 Software (Affymetrix). The criteria followed for considering genes as differentially expressed between different samples were presenting a p-value ≤ 0.05 and a fold change ≥ 2 or ≤-2.

## 4.5 GENE SEQUENCING

The *MEK5* forward and reverse oligonucleotides needed for carrying out the sequencing methodology were designed to recognize the cDNA coding isoforms of the gene as described in the previous section 4.3. Once designed, the selected sequences were sent to the Custom DNA Oligos Synthesis Services from Invitrogen.

After RNA extraction, purification and reverse transcription, 500 ng of cDNA from each cell line were diluted in 5µl of nuclease free water, followed by addition of 3 picomoles of each oligonucleotide diluted in 3µl of nuclease free water. The resulting samples were sequenced in the Genomic Service of the Cancer Research Center of Salamanca by utilizing a 3130xl Genetic Analyzer sequencer (Applied Biosystems, Waltham, Massachusetts, USA).

Sequencing data were provided as “ab1.” files, which were subsequently analyzed with the Chromas 2.6.6 software (Technelysium Pty Ltd, South Brisbane, Australia). The results are presented as chromatograms, where each differently colored peak corresponds to the signal emited by a single nucleotide. Finally, the Basic Local Alignment Search Tool (BLAST) (National Center for Biotechnology Information, Beteshda, MD, USA) bioinformatic tool was used to align and compare the obtained sequences with the canonical MEK5 cDNA sequence (NCBI Reference Sequence: NM_145160.3).

# 5. PROTEIN IMMUNOASSAYS

## 5.1 WESTERN BLOTTING

### 5.1.1 Cell lysates from cell lines

Protein extraction was performed by chemical lyse of the cells, maintaining the samples on ice to ensure protein stability and avoid protein degradation or dephosphorylation. Firstly, cell culture medium was discarded and the 100mm culture plates with the attached cells were washed twice with phosphate□buffered saline. After that, cells were lysed with 0.5 – 1mL (depending on confluency) of ice-cold lysis buffer (140 mM NaCl, 50 mM EDTA, 10% glycerol, 1% Nonidet P-40, 20 mM Tris-HCl, pH 7.0, 1 mM PMSF, 1 mM $Na_3O_4V$, 10 μM pepstatin, 10 μg/mL aprotinin, 10 μg/mL leupeptin, 25 mM β-glycerolphosphate, 10 mM NaF) that was homogeneously distributed in the plate and incubated for 10 min. Cell lysates were then collected using a cell scraper (Sarsdedt; Nümbrecht, Germany), pipetted up and down to facilitate cell clump lyses, placed in 1.5mL eppendorf tubes and centrifuged at 4°C /17,000 x *g*/10 min. Supernatants were then transferred to new tubes and protein concentration measured by the BCA Assay (Thermo Fisher Scientific) or the Bradford assay as explained below.

### 5.1.2 Cell lysates from human and mice tissue samples

Mice organs and lung tumors were obtained after sacrifice of the animals and immediately frozen in liquid nitrogen. Frozen human lung and ovarian samples were selected by H&E staining to contain more than 90% of tumoral cells. The day of the experiment, samples were washed twice with PBS and centrifuged at 4°C/1500 x *g* to remove the blood. Samples were then homogenized at a ratio of 1.6 mL of ice-cold lysis buffer (supplemented with 1% Triton X-100, 10 μM pepstatin, 10 μg/mL aprotinin and 10 μg/mL leupeptin) per 100 mg of tissue using a Dispomix apparatus (L&M Biotech). After centrifugation at 4°C /15000 x *g*/20 min, the supernatants were transferred to new tubes. Protein concentration measurement, immunoprecipitation and immunodetectionof samples were carried out as described below.

### 5.1.3 Measurement of protein concentration

The concentration of protein extracts was quantitated by the Pierce BCA Protein Assay (Thermo Fisher Scientific), following manufacturer's instructions. Samples were measured in duplicates in a 96-well plate (Corning). 20 µL of Milli-Q H2O, 5 µL of each cell lysate and 200 µL of the mixed comercial solutions (1:51 dilution of reagents A and B) were added to each well. The plate was gently shaken for 1 minute in a Boeco OS20 orbital shaker (Boeckel, Hamburg, Germany) and incubated at 37 °C for 30 minutes in the dark. After that, sample absorbance was read at 570 nm using anUltra Evolution 1536 spectrophotometer (Tecan, Männedorf, Switzerland). Mean absorbance values were extrapolated using a previously calculated calibration curve to obtain the protein concentration values.

In some cases, cell lysates were quantitated by the colorimetric Bradford method (Bradford, 1976). 4 µL of each cell lysate sample were diluted with 16 µL of distilled water and mixed with 1 mL of 1:5 diluted Bradford reagent (Bio-Rad Laboratories) in a 1.5 mL tube. Samples were gently mixed, and the reaction was allowed to proceed for 5 min at room temperature. The OD595 of the samples was then measured using a SmartSpec™ Plus Spectrophotometer (Bio-Rad Laboratories). The protein concentration of the samples was calculated using a calibration curve derived from bovine serum albumin standards.

### 5.1.4 Immunoprecipitation

Immunoprecipitation was performed by incubating 0.5 to 3 mg of cell lysate (depending on the specific protein of interest) with the corresponding capture antibody and 60 µLof Protein-A SepharoseCL-4B beads (GE Healthcare, Little Chalfont, England). In the specific case of Flag antibody, it was coupled to 60 µl of GammaBind Sepharose. The incubation was carried out in 1.5 mL or 5 mL tubes shaked on a Speci-Mix M26120-26 rocker (Barnstead Thermolyne, Dubuque, IA, USA) for a minimum of 2 hours at 4ºC. After that, immunocomplexes were pulled down by a quick spin of 15 seconds at 10,000 x g. The supernatant was then aspirated, and the samples washed by adding 1 mL of ice-cold lysis buffer to each sample. This spin and washing proceedings were repeated three times.

Immunocomplexes were finally mixed with 40μL of 2x Sample Buffer (0.05 % w/v bromophenol blue; 4 % SDS; 20 % glycerol; 2.5 % β-mercaptoethanol; 100 mM Tris-HCl, pH 6.8) and storage at -20ºC or immediately used.

### 5.1.5 Electrophoresis and detection

Protein detection wasperformed by Western Blotting of immunoprecipited samples or direct cell lysates (20 to 80μg, generally) mixed with an equal volume of 2x Sample Buffer. As a first step, protein denaturalization was ensured by boiling the samples for 5-7 minutes at 105ºC using an AccuBlock™ D1200 (Labnet International, Woodbridge, VA, USA). Samples were then loaded on a 6-12% polyacrylamide gel assembled on a PROTEAN 3 Cell (Bio-Rad Laboratories) or a homemade Sturdier-type gel caster. The polyacrylamide percentage was selected taking into account the size of the protein of interest. In addition, an appropriate molecular weight marker (Precision Plus Protein™ Dual Color Standard, Bio-Rad Laboratories) was loaded as a control. Gel caster trays were filled with Running Buffer (SDS 0.1 %; 192 mM glycine; 25 mM Tris) and proteins separated by applying a constant voltage of 120 V for small gels or 200 V for Sturdier-type gels. The electrophoresis was stopped when the bromophenol blue from the samples reached the bottom of the gel. After that, Inmobilon PVDF membranes (Merck Millipore) and four pieces of blotting paper were cut slightly larger than the gel(s) and sequentially immersed in 100% methanol (20 seconds) and Transfer Buffer (192 mM glycine; 25 mM Tris; pH 8.1-8.5). The blot was assembled on the transfer apparatus (Trans-Blot Cell system, Bio-Rad Laboratories) in the following order: sponge, 4 pieces of blotting paper, PVDF membrane, electrophoresis gel, 4 pieces of blotting paper and sponge. Transfer was set at a constant voltage of 20 V for 14 hours or at a constant amperage of 500 mA for 1 to 3 hours (depending on size and polyacrylamide percentage of gels). Once the transfer was completed, the apparatus was disassembled and the membranes were next blocked by incubation at room temperature for a minimum of 2 hours with a TBS-T solution (Tris buffered saline with 0.1 % Tween 20; 150 mM NaCl; 20 mM Tris-HCl, pH 7.5) containing 1 % BSA or 5% non-fat dried milk to avoid the unspecific binding of antibodies to the

membrane. After this step, blots were probed with the appropriate dilution of the primary antibodies for a minimum of 2 hours on a rocking platform, washed three times with TBS-T in an orbital shaker (7 minutes/wash), probed with the adequate HRP-conjugated secondary antibodies for 30 minutes. After carrying out another 3 washing steps with TBS-T, the membranes were developed with the Clarity or Clarity Max Western ECL substrate (Bio-Rad Laboratories) or a homemade enhanced chemiluminescence solution (0.08 % luminol; 0.02 % p-iodophenol; 0.1 M Tris-HCl, pH 9.35) plus 1µL of 0.44 M H2O2 that was added right before incubation. The luminescent signal was visualized by exposing the membranes onto an Agfa CP-BU NEW autoradiograph film (Agfa-Gevaert, Mortsel, Belgium).

### 5.1.6 Computational quantification of results

Quantitative measurements of Western blot bands density were carried out using the Image Lab Software 6.0 (Bio Rad Laboratories) or the ImageJ software (1.61 version, U. S. National Institutes of Health (Schneider et al. 2012). Densitometric normalization of cell line samples were generally performed using calnexin or GAPDH, which were evaluated as loading controls. Densitometric normalization of human samples was performed using OVCAR-8 (in the case of ovarian samples) or H460 (in the case of lung samples) signal as internal control among different blots. Box-plot representations and Kaplan-Meier survival curves of ovarian cancer patients were generated using the GraphpadPrism 6.0 software (La Jolla, CA, USA). The threshold for including patients into the low/high expression cohorts was set at 10 a.u for pWNK1 and 4 a.u. for pERK1/2.

### 5.1.7 Commercial antibody arrays

Commercial antibody arrays were used with the aim of simultaneously evaluating and ample spectrum of human tyrosine-protein kinases. Specifically, we used the proteome profiler human phospho-kinase array kit and the proteome profiler human phospho-RTK array kit, (R&D Systems). The first one allows to detect the relative levels of phosphorylation of 43 kinase phosphorylation sites and 2 related total proteins. The second one was designed to simultaneously detect the relative phosphorylation of 49 different tyrosine-kinase receptors.

Following the protocol indications, 300 μg of cell lysates were hybridized to the nitrocellulose membranes provided by the kit, where the capture antibodies have been previously spotted. After 14 hours of incubation, the arrays were washed to remove the unbound proteins, followed by incubation with the cocktail of biotinylated antibodies provided. After chemiluminescent detection that corresponds to the amount of phosphorylated protein bound, the quantitation of the pixel intensity of each antibody spot was analyzed with theImage Studio V5.2 software (LI-COR).

### 5.1.8 *In vitro* kinase assay

OVCAR-8 cells were either untreated or treated with increasing doses of trametinib for 2 hours. Cells were then lysed, and protein extracts were immunoprecipitated with the ERK5 antibody and 60 μL of Protein-A Sepharose. Immunocomplexes attached to the beads were recovered by a short centrifugation and washed 3 times with 1 mL of Lysis Buffer and twice with 1 mL of Kinase Buffer (20 mM HEPES, pH 7.6,20 mM $MgCl_2$, 25 mM β-glycerophosphate, 0.1 mM orthovanadate). After that, immunocomplexes were incubated at 30°C for 30 min in 40 μL of Kinase Buffer along with 1 μL of 4 mM adenosine triphosphate (ATP). The *in vitro* kinase reaction was stopped by adding 25μL of Sample Buffer 4x to each sample, that were then analyzed by Wester Blotting.

## 5.2 IMMUNOFLUORESCENCE

Coverslips were placed on the culture plates and cells were allowed to grow attached to the coverslips surface. When cells reached an adequate confluency, the culture medium was removed, and coverslips were washed twice with PBS supplemented with 1 mM $CaCl_2$ and 0.5 mM $MgCl_2$ (PBS/CaMg) and fixed with a solution of 2% paraformaldehyde (PFA) in PBS/CaMg for 30 minutes. PFA was removed and the coverslips washed twice (10 minutes/wash) with PBS/CaMg and after that, the quenching process to diminish cell autofluorescence intensity was performed by incubation with $NH_4Cl$ in PBS/CaMg for 10 minutes. Cells were permeabilized with 0.1% Triton-X100 in PBS / CaMg for 10 minutes and non-specific binding sites were blocked by incubation with blocking buffer (0.2% BSA in

PBS/CaMg) for 1 hour. Subsequently, the coverslips were incubated with the primary antibodies diluted (generally ranging from 1:50 to 1:500) in the blocking buffer for 1-2 hours in a humidified atmosphere. As a background control, one of the coverslips was not incubated with primary antibody. After three washes of 10 minutes each in blocking solution, cells were incubated with the corresponding secondary antibody conjugated to fluorochromes. Again, as a background control, another coverslip was not incubated with the secondary antibody. After three additional washes (10 minutes/wash) with blocking buffer, the nuclei of the labeled cells were contrasted with 1 μg / ml DAPI diluted in milliQ H2O. The coverslips were finally mounted onto glass microscope slides with Gelvatol (12% mowiol; 30% glycerol; 0.12 M Tris pH 8.5). Images were collected with an Axioplan 2 epifluorescence microscope (Zeiss) using a 4X, 20X or 40X objective magnification. The images were captured and analyzed with the Leica Application Suite Advanced Fluorescence software platform, LAS AF version 2.6.3.8173 (Leica Microsystems; Wetzlar, Germany).

# 6. IN VIVO STUDIES USING MICE MODELS

All animals were manipulated by authorized personal at the animal facility following legal and institutional guidelines. Experimentation was approved by the University of Salamanca Bioethics Committee.

## 6.1 MEK5DD TRANSGENIC MICE

To obtain a constitutively active form of human MEK5 (UniprotKB accession number Q13163), site-directed mutagenesis of the MEK5 Ser311 and Thr315 residues to aspartic acid (MEK5DD) was performed on pCDNA3-MEK5 by using the QuikChange II Site-Directed Mutagenesis kit (Stratagene, Madrid, Spain) following provider's instructions. MEK5DD was subcloned into the pCEFL mammalian expression vector, that includes a Flag tag after which the MEK5DD cDNA was located. SmaI and XhoI sites were incorporated by PCR and Flag-MEK5DD was then inserted into the multiple cloning site of the pMSG vector. The constructs were verified by DNA sequencing and validated *in vitro* using HeLa cells.

After plasmid digestion, the cassette MMTV-Flag-MEK5DD-SV40 polyA was obtained, purified and given to the Animal Experimentation Service of the University of Salamanca to generate founder lineages by microinjecting this construct into fertilized eggs from FVB mice (The Jackson Laboratory, Bar Harbor, ME, USA). Founder animals and offspring identification was performed by PCR genotyping of genomic DNA from tail crops with specific primers corresponding to MEK5DD (Forward: 5'-GGTGAATGACATAGCCAAGGA-3'. Reverse: 5'-ATTGAACTGCACGATGAACG-3') and MMTV (Forward: 5'-CCCCTTTCGTGAAAGACTCG-3'. Reverse: 5'-CCCCTCCTTGGTATGGAAAA-3'). Analyses of the genetic material amplified by PCR was evaluated by electrophoresis in 2% agarose gels diluted in TAE Buffer (2 M Tris; 0.05 M EDTA), with 2 μg/ml ethidium bromide. A 100 bp DNA ladder (Invitrogen) was also loaded on the gels to precisely define the size of the fragments. The bands corresponding to the amplified fragments were visualized using a UV/White light GELDoc 2000 transilluminator (Bio-Rad).

## 6.2 XENOGRAFT MODELS

### 6.2.1 Xenoinjection

The xenograft experiments were performed on 5-6 weeks old female BALB/c nude mice (Charles River, Wilmington, MA, USA), whose weight ranged from 16 to 20 gr.

For the *in vivo* studies using H460 ERK5 or MEK5 knockout cells, 25 mice were randomly divided into 5 groups of 5 mice each (H460 scramble, #20 or #57 ERK5 CRISPR cells for the ERK5 knockout studies, and H460 scramble or #17 MEK5 CRISPR cells for the MEK5 knockout studies). To assess the effect of the MEK5 or ERK5 knockdown on *in vivo* tumorigenesis, 10 mice for each cell line (A549, H1299 or H727) were randomly divided into 3 groups (4 mice injected with shControl, 3 mice with shMEK5 and 3 mice with shERK5 cells). $1x10^6$ H460 cells, $2.5x10^6$ A549 cells, $2.5x10^6$ H1299 cells or $3x10^6$ H727 cells were injected following standard procedures into the left and right flanks of these mice. Cells were trypsinized, collected, counted, and transferred to 5 mL Eppendorf tubes, where they were resuspendend in an equal volume of cell culture medium and Matrigel (BD Biosciences). A

total volume of 100 µL containing the appropriate number of cells was injected per tumor. Masses were allowed to engraft for one week and measured using a caliper daily (H460 tumors), three times a week (H1299 and H727 tumors) or twice a week (A549 tumors) until the end of the experiment. Volume progression was measured and calculated by the formula: $V(mm3) = Length\ x Width^2 x 0.5$. After experimentation, animals were humanely sacrificed.

For the *in vivo* studies with ovarian cell lines, 18 mice were divided into 3 groups of 6 mice with a similar mean weight. Mice were subcutaneously xenografted with 1x106 OVCAR-8 scramble, #16 or #19 MEK5 CRISPR cells following standard procedures into both flanks (n=12 tumors per group). Tumors were allowed to engraft for one week and measured once a week until the end point of the experiment.

### 6.2.2 Pharmacologic treatments

For conducting the lung cancer pharmacological *in vivo* experiments, 60 female BALB/c nude mice were xenografted with 1 x $10^6$ H460 cells into the left and right flanks. One week after implantation, mice were divided into 12 groups of 5 mice each, with a mean group tumor volume of 125 $mm^3$. BIX02189 and JWG-071 (30 mg/Kg dissolved in 30% 2-hydroxypropyl beta-cyclodextrin, i.p.), and crizotinib (30 mg/Kg in sterile water, p.o, using an oral gavage) were administered daily. Cisplatin (3 mg/Kg in physiological saline, i.p.) was given twice per week and pemetrexed (250 mg/Kg in physiological saline, i.p.) once a week. All treatments were administered for two weeks. The control group received 30% 2-hydroxypropyl beta-cyclodextrin, intraperitoneally as vehicle. Standard of care drugs were obtained from the inpatient pharmacy of the University Hospital of Salamanca.

The start point of the ovarian cancer *in vivo* pharmacological experiments was stablished when the mean tumor volume of each group reached 470 mm3. Mice xenografted with OVCAR-8 scramble or MEK5 KO cells were divided into two groups: each of them received 100 µL of trametinib (0.5 mg/Kg dissolved in 30% PEG, 5% Tween-80 and 2% DMSO) or vehicle, administered i.p. daily for four weeks. Tumor progression of SC and CRISPR groups

were measured weekly. For the analysis of treatment efficacy, the tumor volume of the trametinib treated mice were relativized to their corresponding untreated (vehicle) groups.

### 6.2.3 Tumor processing for biochemistry or immnohistochemistry

After animal sacrifice, tumors were resected and divided in two halves. One half was formalin-fixed for histochemical analyses while the other one was immediately frozen in liquid nitrogen and afterwards used for biochemical analyses. The day of the experiment samples were washed twice with PBS to remove blood. Samples were then homogenized at a ratio of 1.6 mL of ice-cold lysis buffer (supplemented with 1% Triton X-100 and 10-fold pepstatin, aprotinin and leupeptin) per 100 mg of tissue using a Dispomix apparatus (L&M Biotech). After centrifugation at 4°C /15000 x g/20 min, the supernatants were transferred to new tubes and protein concentration was measured by the BCA assay. After processing of the samples, immunoprecipitation, Western blotting and quantitative measurements of bands density were carried out as described above. For the MEK5DD mice tumors, lung tissue derived from non-transgenic littermate mice was used as control.

For immunohistochemical analyses, mice tumors were formalin fixed, paraffin embedded, sectioned, and stained either with hematoxylin and eosin following standard procedures; with the ERK5 antibody; with the CK-7, Napsin-A and TTF-1 adenocarcinoma markers, or with the Ki-67 proliferation marker using the Bond Polymer Refine Detection kit (Leica Biosystems). Image analyses for the quantitation of Ki67 positive cells were performed using the Leica LAS V3.7 software.

# 7. HUMAN SAMPLES

## 7.1 LUNG AND OVARIAN SAMPLES FOR BIOCHEMISTRY OR SURVIVAL ANALYSES

Frozen human lung samples (23 adenocarcinomas and 11 nontumoral lung samples, 9 of them corresponding to counterparts of the same lung adenocarcinoma patient) and 63 ovarian tumoral samples (32 high-grade serous carcinomas, 8 low-grade serous carcinomas, 3

moderately differentiated serous carcinomas, 13 borderline serous carcinomas and 7 endometrioid carcinomas, obtained from a total of 58 patients) were randomly obtained from the University Hospital of Salamanca, following the Declaration of Helsinki on ethical principles for medical research involving human subjects. Patients provided written informed consent for the usage of the samples and their respective clinical data (histologic subtype, grade, size, age, surgery date and survival status) which was approved by the Institutional Review Board Ethics Committee on Human Research of the hospital. Of note, survival data was only available for 52 of the 58 patients. Frozen human lung samples were selected by H&E staining to contain more than 90% of tumoral cells. The day of the experiment samples were washed, homogenized, and biochemically / immunohistochemically analyzed following the same protocol utilized with mice tissues (described above). The anonymous clinical data needed for elaborating de survival curves (birth date, surgery date, passing date or last contact date) was provided by the Pathology Service of the University Hospital of Salamanca.

## 7.2 HUMAN PLASMA DERIVED 3D CULTURES (HUP3D) OF PRIMARY OVARIAN TUMOR BIOPSIES

Human ovarian patient tumor biopsies and matched plasma samples were obtained from the Sanford Biobank. Informed consent was obtained from all subjects with approval from the Sanford Health Institutional Review Board and in accordance with the Declaration of Helsinki. Tumor biopsies were harvested to collect tumor cells using a commercially available tumor dissociation kit (Catalog # 130-095-929, Miltenyi Biotec, Bergisch Gladbach, Germany), as per manufacturer's instructions. Primary ovarian isolated cells were embedded in a human plasma derived 3D culture (HuP3D) made with the plasma from the same ovarian cancer patient. HuP3D cultures were engineered through the cross-linking of the corresponding patient's fibrinogen into fibrin as previously described (Calar et al., 2020). Briefly, plasma was first mixed with tumor cell suspension (to yield $3x10^4$ cells/per scaffold) prepared in DMEM complete media followed by encapsulation into matrices that were established using calcium

chloride ($CaCl_2$) as a cross-linker and trans-4-(aminomethyl)cyclohexanecarboxylic acid (AMCHA) as a stabilizer, in a 4:4:1:1 ratio, respectively.

## 7.3 DRUG SCREENING IN HUP3D CULTURES BY FLOW CYTOMETRY

HuP3D cultures were allowed to stabilize and at the end of Day 0, primary ovarian tumor cells seeded within the HuP3D matrix were subjected to DMSO control treatment; trametinib (0.25 μM) treatment for 72 hours, where trametinib was refreshed after the initial 24 hours; BIX02189 (25 μM) treatment from 24 hours to 72 hours, or initial 24 hours trametinib treatment followed by an additional 48-hour treatment with a combined dose of trametinib (0.25 μM) and BIX02189 (25 μM). After 72 hours, HuP3D cultures were enzymatically digested with collagenase (20 mg/ml for 2 - 3 hours at 37°C) and cells were retrieved as previously described (Calar et al., 2020; Bhattacharya et al., 2020). Cells retrieved from the digested HuP3D cultures were probed with anti-EpCAM antibody conjugated to PE-Cy7 fluorophore (324222, Biolegend, San Diego, CA, USA) to help selectively identify the epithelial-tumor cells, with anti-Fibroblast Activation Protein (FAP) antibody conjugated to AF700 fluorophore (FAB3715N, R&D Systems) and anti-CD45 antibody conjugated to BV510 fluorophore (304036, Biolegend) to help remove stromal and immune cells, respectively. Cell viability was evaluated by using a Live/Dead Blue cell stain (L34962, Thermo Fischer Scientific).

Tumor cells were isolated and identified by gating cells demonstrating high EPCAM/low FAP signal after dead and immune cell removal as illustrated in Figure 12. In order to determine pERK1/2 and pERK5 expressions, an activated control was included where retrieved cells were activated for at least 6 hours using a commercially available cell stimulation Cocktail (Catalog # 50-930-5, Invitrogen), as per manufacturer's recommendations.

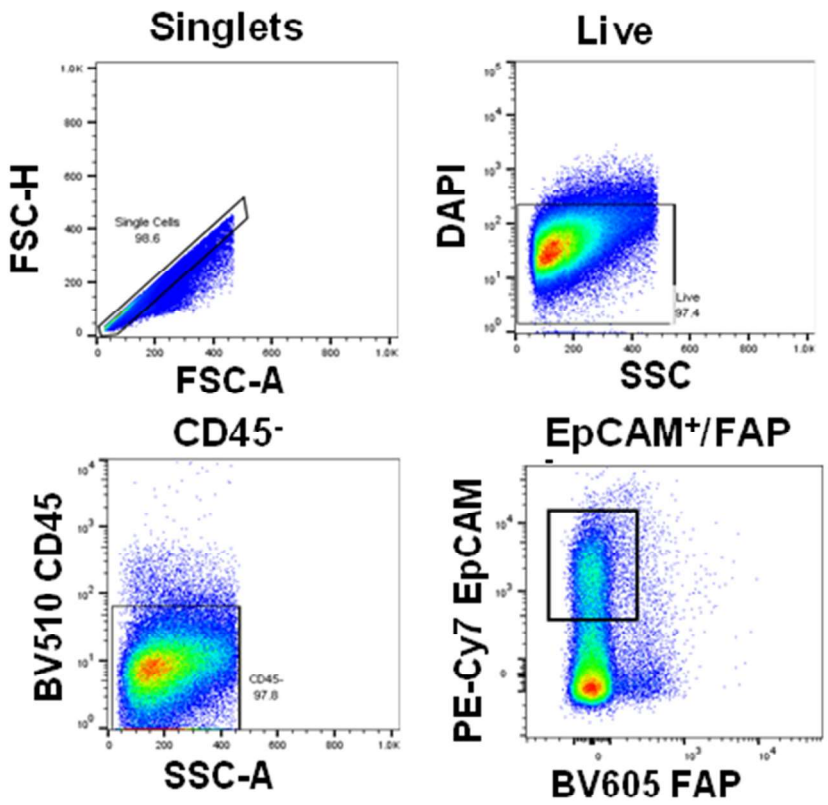


**Figure 12.** Gating strategy for analysis of patient biopsy material grown in HuP3D cultures. Data acquisition was completed by collecting information for a specified number of events determined by counting beads. Firstly, cellular populations were isolated from beads and then singlets were gated. After that, the live cell population was identified by live/dead viability marker. Following this, CD45- BV510 cells were identified from the live cell population. Finally, EpCAM+ (CD326+) PE-Cy7 cells and FAP- AF700 cells were identified from the CD45- population. Fluorescence minus one (FMO) controls were used to set the gating for each population BV510 (CD45), PE-Cy7 (EpCAM), and AF700 (FAP).

This was followed by Fix-Perm treatment and incubation with anti-pERK1/2 conjugated to PE fluorophore (369506, Biolegend) and anti-pERK5 conjugated to AF488 (sc-135760, Santa Cruz Biotechnology) or their respective Fluoresence Minus One (FMO) control. For all analyses, a minimum of 10,000 events were acquired using BD FACS Fortessa and FACSDiva v6.1.2 software. The EpCAM+ expressing ovarian tumor cell counts were always normalized to a predetermined number of counting beads (424902, Biolegend, CA, USA), where survival (% of untreated-DMSO control) was calculated and the mean fluorescence intensity (MFI) ratios for pERK1/2 and pERK5 were assessed with respect to the corresponding FMO control in the EpCAM+ cells. The data was analyzed using FlowJo program v10 (Ashland, OR, USA).

# 8. IN SILICO STUDIES

## 8.1 KM-PLOTTER DATABASE ANALYSES

Analyses of the relationship between, ERK5, MEK5, MEKK2 or WNK1 mRNA expression and outcome (overall survival, post progression survival or progression free survival) of lung and ovarian cancer patients were carried out using the open access database Kaplan-Meier plotter (Győrffy et al., 2013), available at http://www.kmplot.com. The gene expression values of MEK5 and ERK5 were computed together in the lung cancer studies, which were performed using the multigene classifier tool by selecting the mean expression values for both MEK5 (Affymetrix probe id 211370_s_at) and ERK5 (Affymetrix probe id 35617_at).

On the other hand, ovarian cancer studies were performed using the same ERK5 and MEK5 probes, as well as WNK1 (Affymetrix probe id 211994_at) and MEKK2 (Affymetrix probe id 226441_at) probes. The cut off values used to split patients into low or high expression groups were automatically selected by the database for each cohort of patients. These cut off values were those bringing the most significant *p*-value between the two groups, which were scored computing one by one all the possible percentiles between the lower and upper quartiles. False discovery rates are indicated.

Alternatively, association between WNK1 MRNA expression and overall survival was also evaluated by utilizing the Pan-cancer RNA-seq section of the database, splitting patients into the high or low expression cohorts by selecting the T1 vs T3 trichotomization tool. Analyses were not filtered by tumor grade, tumor stage, gender, surgery's success nor chemotherapy/radiotherapy treatments. The array quality controls excluded biased arrays. Cox regression was used to compute the Hazard Ratio and *p*-value.

## 8.2. cBIOPORTAL DATABASE ANALYSES

The analyses of Copy Number Alterations (CNA) of MEK5, ERK5 and WNK1 in tumors from lung cancer and ovarian serous carcinoma patients were carried out using the cBioPortal

genomic database and their available bioinformatic tools (http://cbioportal.org) (Cerami et al., 2012; Gao et al., 2013). Analyses were performed on the data collected by The Cancer Genome Atlas studies (TCGA, PanCancer Atlas), which usually presented the largest number of patients: Lung Adenocarcinoma (n=566), Lung Squamous Cell Carcinoma (n=487), and Ovarian Serous Cystoadenocarcinoma (n=585). These studies also allowed the evaluation of MEK5, ERK5 or WNK1 mRNA expression levels in correlation with the CNA status of the tumors. In addition, the information corresponding to patient outcome was used to perform the overall survival curves. Patients were stratified into two groups depending on one of the following criteria:

-The CNA status: patients harboring gene amplification/gain compared to those without such alterations; or patients harboring gene shallow/deep deletions compared to those without such alterations.

-The mRNA level: the altered group comprises those patients with mRNA levels > 2 (mRNA expression z-scores>2 relative to diploid samples, measured by RNA Seq V2 RSEM) and the unaltered group those with mRNA levels < 2.

## 8.3. FIREBROWSE BIOINFORMATIC TOOL ANALYSES

Analyses of the significant copy number variations of 73 focal events of ovarian cancer patients was carried out by using the Firebrowse bioinformatic tool (©2019 Broad Institute of MIT & Harvard, Version: 1.1.40) available at www.firebrowse.org. The analyses were preformed on the Ovarian Serous Cystadenocarcinoma dataset (TCGA, n=573), whose available data was obtained by pipelines from Firehose run. Core samples were used to select differentially expressed marker focal events for each subtype by comparing the subclass versus the other subclasses, using Student's t-test. Raw results were obtained from the Broad Institute TCGA Genome Data Analysis Center (2016): Analysis Overview for Ovarian Serous Cystadenocarcinoma (Primary solid tumor cohort) - 28 January 2016. Broad Institute of MIT and Harvard (doi:10.7908/C1VQ324T).

# 9. STATISTICAL ANALYSES

For *in vitro* studies, the analyses of variance between variables were calculated for each experiment according to the Fisher's exact test. Unless otherwise indicated, comparison of continuous variables between groups were carried out using a two-sided Student's *t*-test. For the *in vivo* tumor growth experiments, normality of data distribution was analyzed by the Kolmogorov-Smirnov test. One□way ANOVA followed by Bonferroni multiple comparison test was used to compare control group versus treatment groups. Wilcoxon-Mann-Whitney test was used to compare two groups when the distribution was not assumed to be normal. Mean differences between groups were considered statistically significant at $p$-value ≤ 0.05 (*), p≤0.01 (**) or p≤0.001 (***). Statistical analyses were performed using SPSS 19.0 software (SPSS Inc., Chicago, IL, USA). Additional information is described in the appropriate figure legends.

# *RESULTS AND DISCUSSION*

# CHAPTER 1

# IMPLICATION OF THE MEK5/ERK5 PATHWAY IN LUNG CANCER

## 1.1 Mice expressing constitutively active MEK5 develop lung carcinomas

To activate the MEK5/ERK5 route, we used a mutant form of MEK5 in which $Ser^{311}$ and $Thr^{315}$, located in the MEK5 activation domain, were changed to aspartic acid (MEK5DD, Figure 13A). These acidic changes result in a MEK5 form in which the aspartic acid substitutions function as phosphomimetic residues (English et al., 1999; Nicol et al., 2001). As a consequence, MEK5DD acts as a constitutively active kinase that sustains ERK5 in an activated status. The MEK5DD cDNA was subcloned into the pCEFL mammalian expression vector, which contains an N-terminal Flag tag sequence that serves to differentiate MEK5DD from endogenous MEK5 (Figure 13B). Increasing amounts of the cDNA coding for Flag-tagged MEK5DD were transfected in HeLa cells and its expression was analyzed by Western blotting with an anti-Flag antibody. The activation of the MEK5/ERK5 route was assessed using an antibody that recognizes ERK5. As shown in Figure 13C, expression of Flag-MEK5DD caused the appearance of pERK5, indicative of such activating phosphorylations.

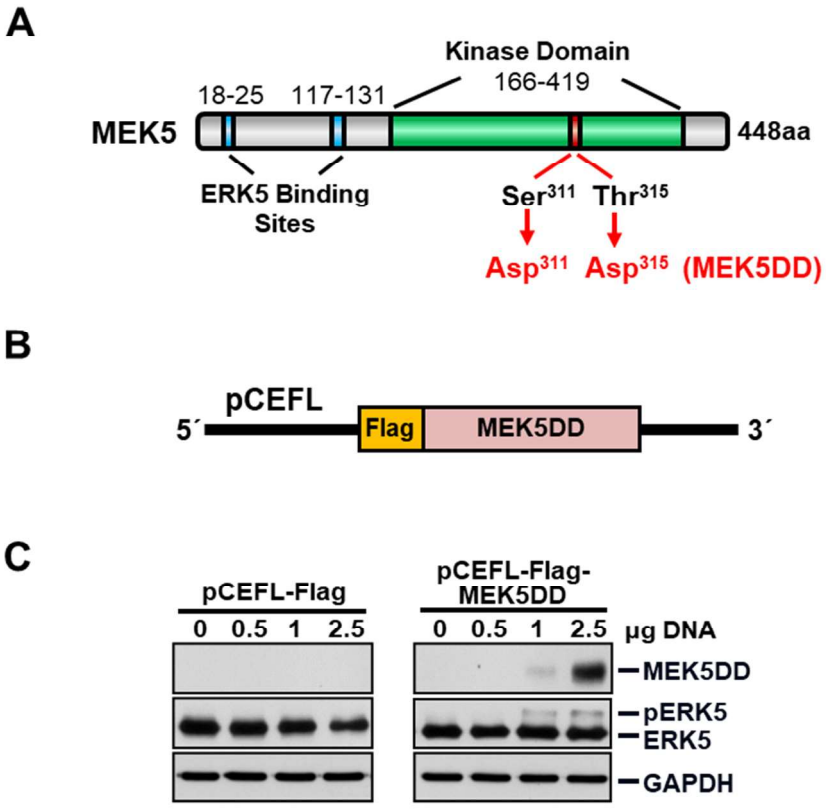


**Figure 13.** A) Schematic representation of MEK5 and the sites mutated to create constitutively active MEK5 (MEK5DD). B) Schematic representation of MEK5DD within the pCEFL vector with the Flag tag that allows to distinguish between the exogenous transgene and the endogenous MEK5. C) The indicated amounts of pCEFL-Flag-MEK5DD were transfected into HeLa cells. ERK5 and MEK5DD were immunoprecipitated from cell lysates with the anti-ERK5 or anti-Flag antibodies and analyzed with the C-terminal ERK5 or MEK5 antibodies, respectively. GAPDH was used as loading control.

After that, SmaI and XhoI sites were incorporated by PCR to the Flag-MEK5DD cassete, which was then inserted into the multiple cloning site of the pMSG vector, downstream of the MMTV long terminal repeat and upstream of the SV40 polyadenylation site (Figure 14A). That promoter was selected because of its capability to drive expression of transgenes in several tissues, primarily epithelial (Vargo-Gogola et al., 2007). In order to validate the MEK5DD construct functionality *in vitro* before its *in vivo* utilization, HeLa cells were transfected with 5ug of the empty pMSG or PMSG-Flag-MEK5DD vectors. Cells were either untreated or treated with Dexametasone (DXM), which is a potent synthetic glucocorticoid with actions resembling those of steroid hormones and which induces the MMTV promoter. As seen in Figure 14B, no effect was observed in HeLa cells transfected with the empty pMSG vector. In contrast, DXM was able to induce the expression of the MEK5DD transgene in those cells transfected with the full construct, that consequently triggered ERK5 activation.

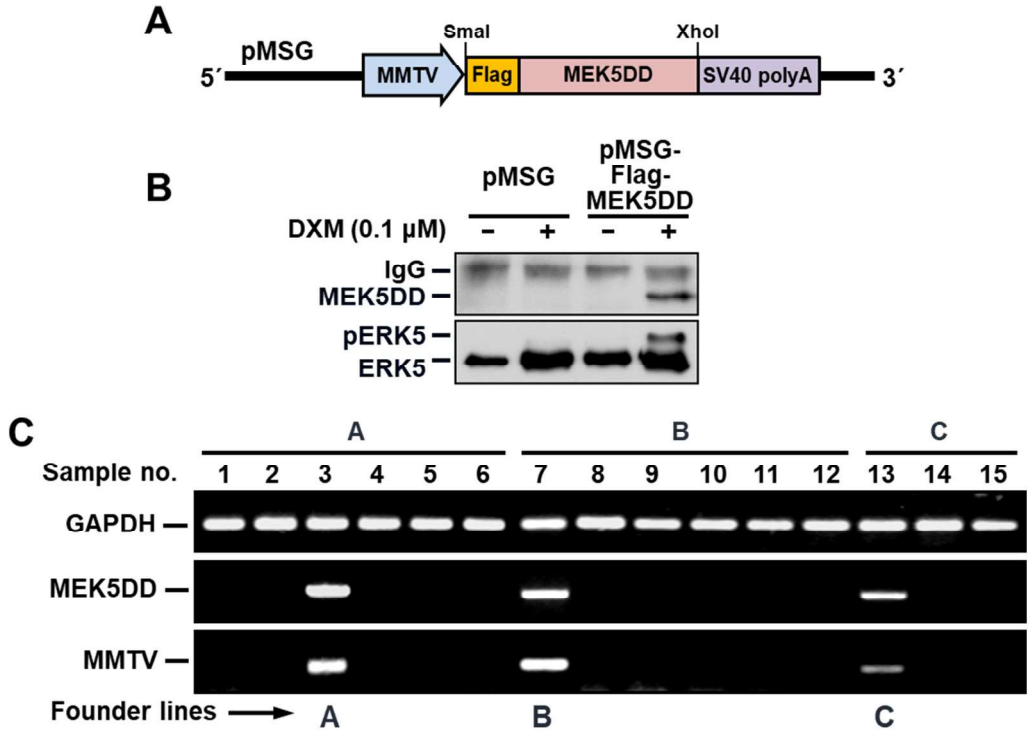


**Figure 14.** A) Schematic representation of the final Flag-MEK5DD construct under the MMTV promoter within the pMSG vector that was utilized for the generation of the MEK5DD transgenic mice. B) In order to validate the MEK5DD construct functionality *in vitro* before its *in vivo* utilization, HeLa cells were transfected with 5ug of the empty pMSG or PMSG-Flag-MEK5DD vectors using the fransfection reagent JetPEI. 0.1 μM Dexametasone was added 48 hours after transfection and added again 36 hours later. After another 36 hours, HeLa cells were lysed and the protein extracts immunoprecipitated and analyzed for MEK5DD and ERK5 expression by Western blotting. C) Identification of transgenic founders by PCR of genomic DNA from tail snip with specific primers corresponding to MEK5DD and MMTV.

After this validation, the generation of the transgenic mice was carried out in the USAL transgenesis service by microinjection of the construct in the pronucleus of fertilized ovules of the FVB strain. This strain was chosen due to its good reproductive characteristics, the resistance of its zygotes during manipulation and the large size of its male pronucleus, which greatly facilitates the microinjection of the DNA fragment to be inserted. After repeating the microinjection procedure several times, 15 neonates were born. PCR genotyping of genomic DNA from tail crops with specific primers corresponding to MEK5DD and MMTV revealed that only 3 of them expressed the transgene (mice A, B and C, Figure 14C). Of these, only the founders of lineages A and B were able to stably transmit the transgene to the offspring and were therefore used for colony expansion.

In order to evaluate whether the transgene was being expressed at the protein level and where, we processed different organs of the transgenic animals and analyzed them by carrying out immunoprecipitation with an anti-flag antibody followed by western blotting with anti-MEK5 antibody to recognize to exogenous MEK5DD. These analyses revealed expression of MEK5DD in the lung, spleen, kidney, brain, and breast (Figure 15).

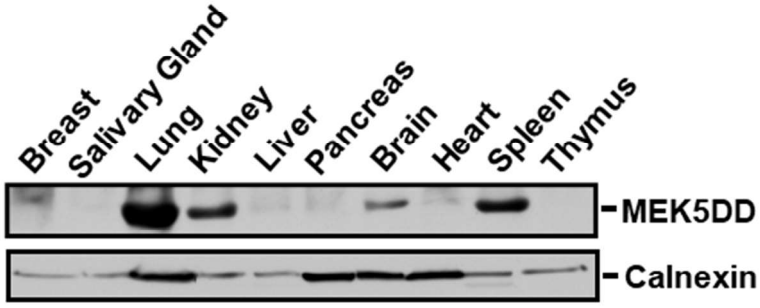


**Figure 15.** Expression of MEK5DD in different transgenic mice tissues. 2 mg of protein from different organs were immunoprecipitated with the anti-Flag antibody followed by Western blotting with the anti-MEK5 antibody. Calnexin was used as loading control. Note: A lane between lung and kidney was cut out from the Western blots.

Animals were periodically monitored at the animal facility, and no signs of disease were observed during the first months. Some animals were randomly picked for necroptic analyses. After several months, a first lung tumor was macroscopically observed in a 10-month-old mouse. From that moment on and considering that the transgene was expressed mainly in the

lung, we turned to pay special attention to the lungs. Necropsies of mice ranging from 12 to 22-months-old mice showed lung masses in many of the MEK5DD transgenic animals. From a total population of 71 transgenic mice, lung tumor incidence was 46.47%. (Figure 16A). Among them, a majority developed a single tumor, although up to three lung masses could be observed in the same animal (Figure 16B). Since we did not have image detection techniques available and, given that we could only detect tumors perceptible to the naked eye when we performed the necropsy of the animals, we cannot rule out that we have not identified the smaller tumors and that the tumor incidence is actually higher. For the same reason, it was not possible to control when they could arise. Consequently, these tumors showed variability in their size, ranging from big tumors that colonized most of the lung tissue (Figure 16C) to very small tumors (Figure 16D) that, in some cases required ink staining to be visualized (Figure 16E).

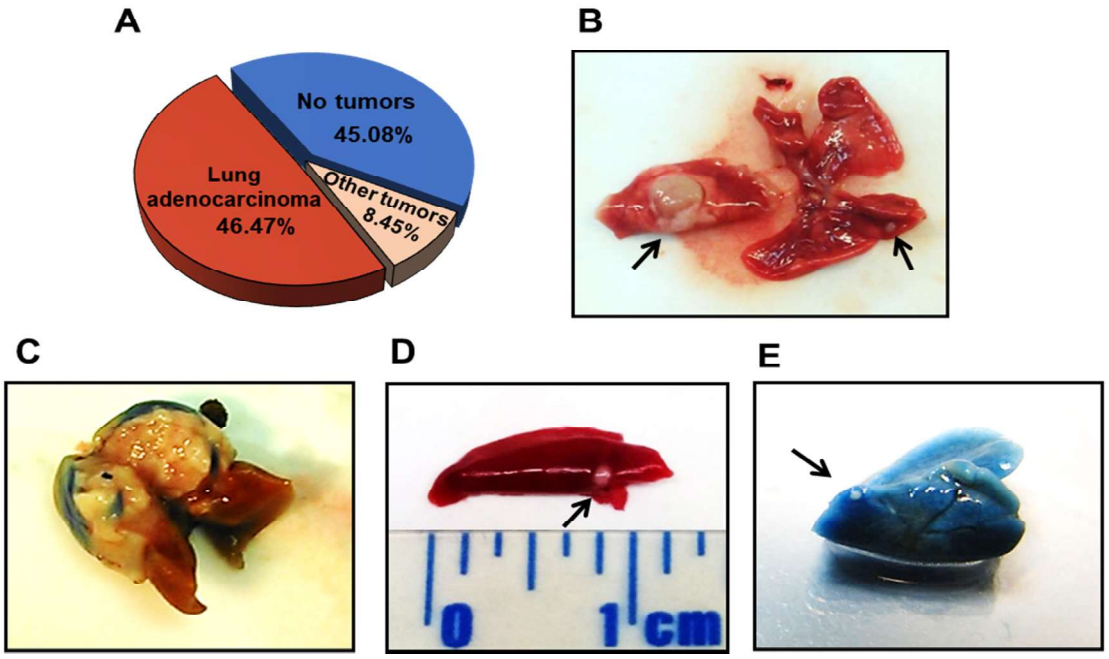


**Figure 16.** A) Pie chart of the tumoral incidence in the MEK5DD transgenic mice. B) Representative macroscopic image of a MEK5DD transgenic tumoral lung (tumors are indicated by arrows). C-E) Representative images of the size variability observed in lung tumors from MEK5DD transgenic mice.

Other types of tumors were observed in some animals, although to a much lower incidence (8.45%). Tumors were found in the spleen (N=3, 4.2%), breast (N=3, 4.2%), skin (N=5, 7.04%) and the suprarenal gland (N=1, 1.4%). Some animals bore more than one tumor type. Other non-malignant pathologies found in these animals were hyperplasia of the splenic

white pulp, neuroendocrine hyperplasia of the pancreas and type II pneumocyte hyperplasia. Of note, lung tumors were observed in males and females from both transgenic lineages (40.85% incidence in lineage A and 57.14% in lineage B. Histopathological analyses defined the lung masses as malignant grade I-II adenocarcinomas (Figure 17).

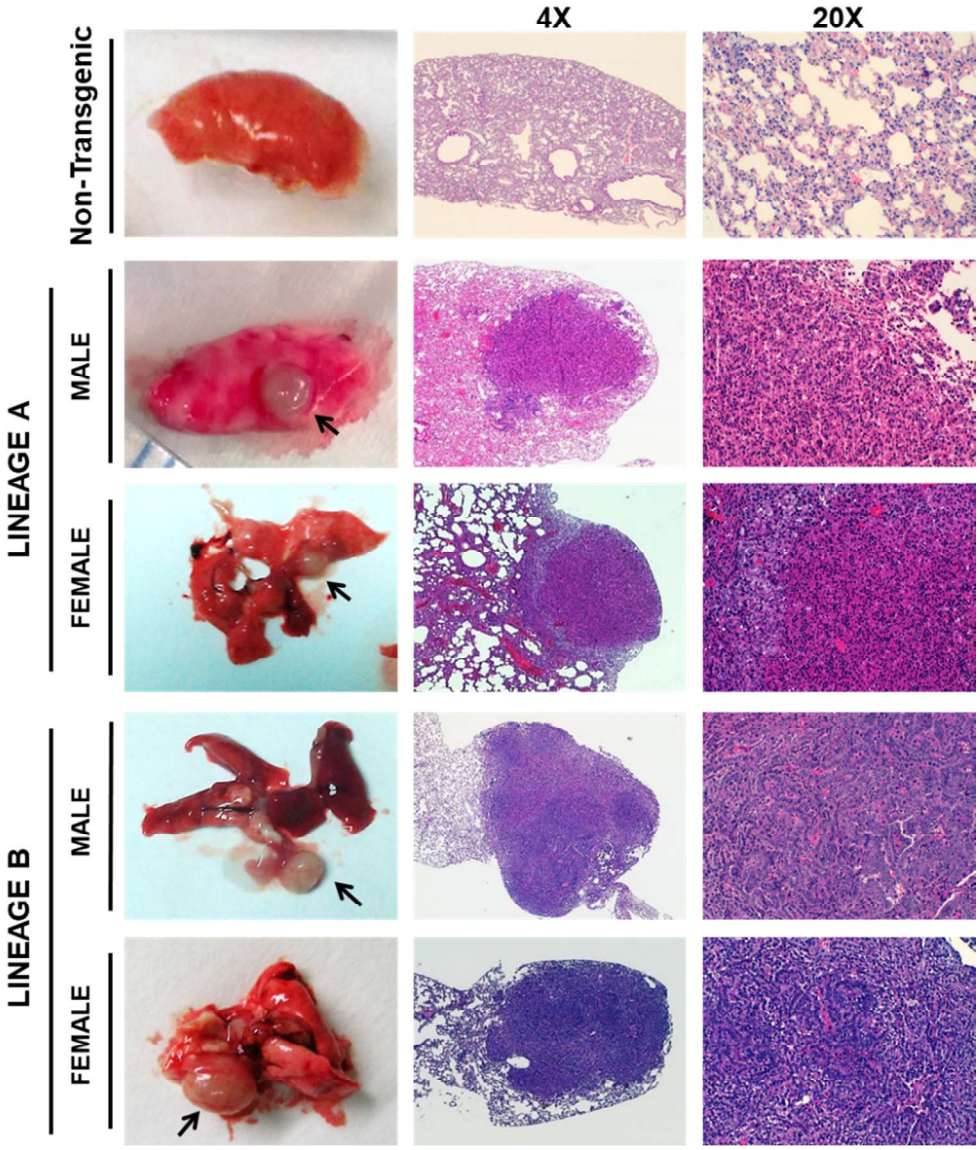


**Figure 17.** Representative macroscopic images of tumoral lungs from males and females from both MEK5DD transgenic lineages, including their corresponding histologic hematoxylin-eosin staining. Lung from non-transgenic littermate is shown.

This malignant diagnosis was determined by the histologic appearance and the infiltration of tumoral cells into the parenchymal lung tissue. Morphological inspection of the tumors showed resemblance to human lung ADC, since they were peripheral, well delimited,

and non-encapsulated. In fact, they presented immunoreactivity to napsin-A, CK7, and TTF-1, the immunohistochemical markers commonly used to identify this ADC tumors (Figure 18).

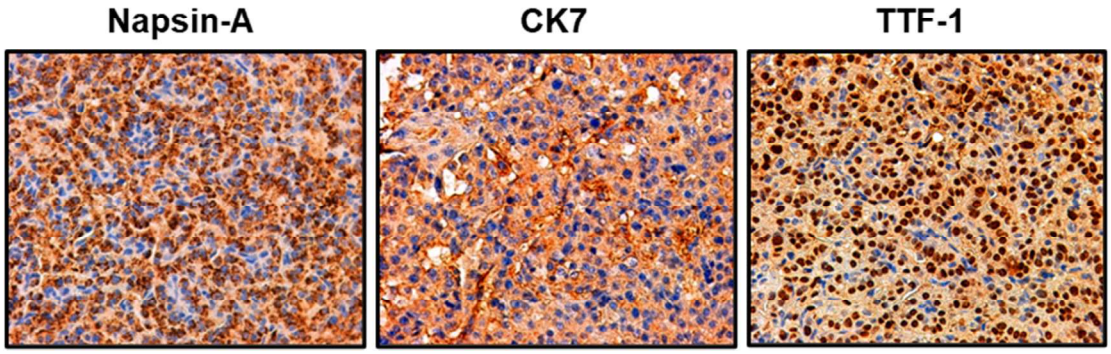


**Figure 18.** 40x representative immunohistochemical images of Napsin-A, CK-7 and TTF-1 of a lung adenocarcinoma from MEK5DD mouse.

Transgenic lung tumors from both lineages expressed Flag-MEK5DD, which was accompanied by activation of ERK5. In contrast, analyses of lungs from non-transgenic (WT) littermate mice, which appeared negative for the transgene, did not show ERK5 activation (Figure 19A). Quantitative analyses of eight TG tumoral lungs confirmed a statistically significant higher ERK5 activation (Figure 19B) and expression (Figure 19C) when compared to eight normal lungs from wild-type littermates.

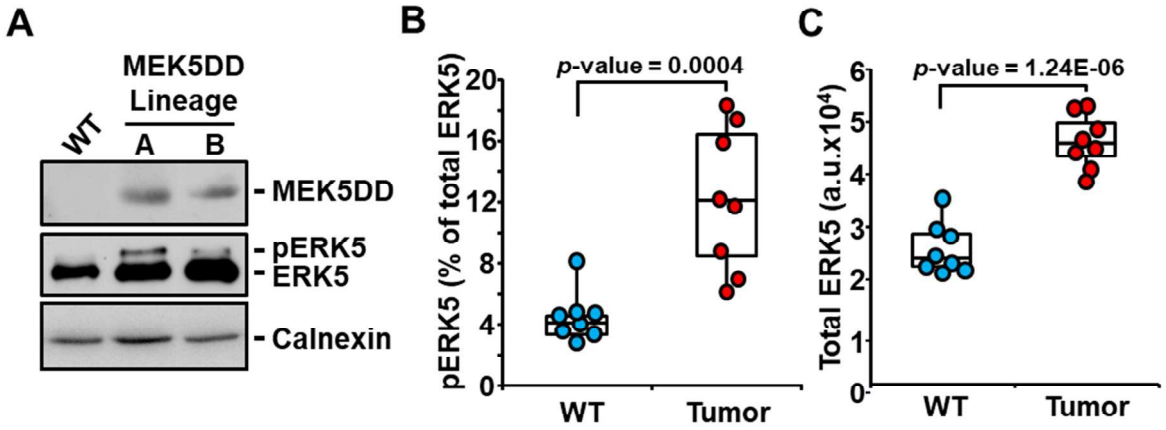


**Figure 19.** A) Western blot analysis of MEK5DD and ERK5 expression in the transgenic lung tumors from both lineages compared to normal lung tissue from a non-transgenic (WT) littermate mouse. Protein extracts were immunoprecipitated with the anti-Flag or anti-ERK5 antibodies, and blots were probed with the anti-MEK5 or anti-ERK5 antibodies, respectively. Calnexin levels were analyzed as loading controls. B) pERK5 and C) total ERK5 levels from NT lungs (n=8) versus TG tumoral lungs (n=8) were quantitated from Western blot analysis using ImageJ software and represented in a box plot. The median value for each group is represented as the central line of the box. Black dots represent the outlier values. Statistical comparisons were performed by calculating the p-value according to a two-sided Student's t-test. pERK5 levels were represented as percentage from total ERK5 expression.

## 1.2 Activation and expression of MEK5/ERK5 in human lung samples

The preclinical precedents linking the MEK5/ERK5 pathway to promotion of lung carcinogenesis in mice led us to explore the relevance of this kinases in human lung cancer. To that end, MEK5 and ERK5 protein activation and expression were evaluated in tumor samples from patients diagnosed with lung adenocarcinoma. 23 samples from lung ADC patients and 11 samples from non tumoral lung tissue (9 of them corresponding to the counterpart of the same ADC patient) were analyzed by Western blotting. Figure 20A shows a representative immunoblot of normal lung tissue compared to lung adenocarcinoma samples. Interestingly, constitutively active MEK5, identified using an anti-pMEK5 antibody, was present in tumor samples whereas no pMEK5 was detected in normal lung tissue. Consequently, pERK5 was observed in the ADC samples but not in their non-tumoral counterparts (Figure 20B).

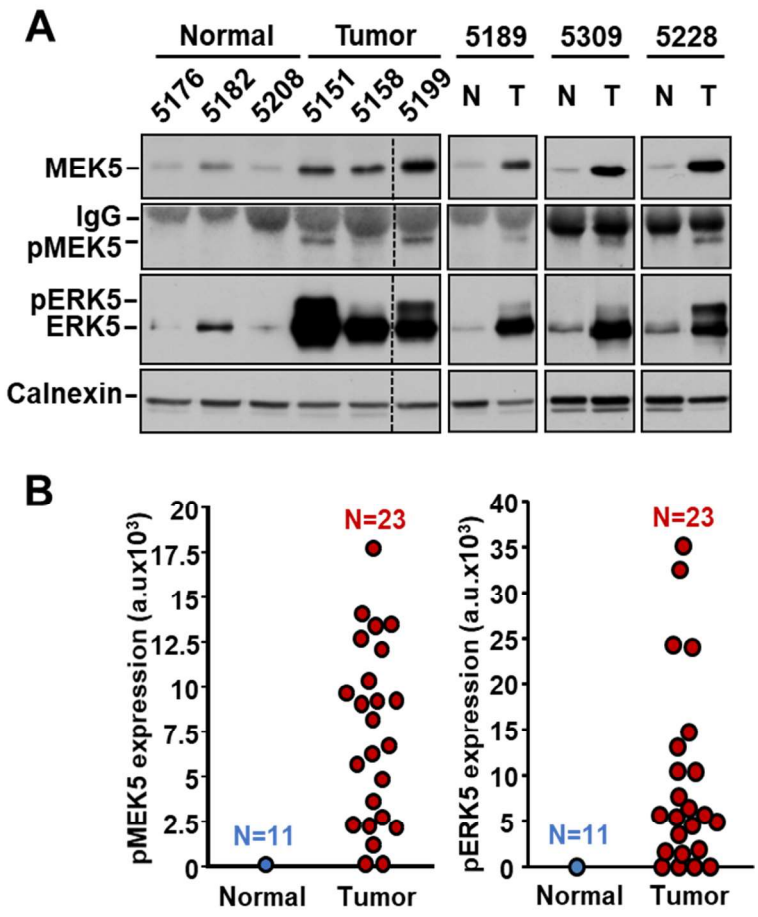


**Figure 20.** A) Representative Western blot analyses of MEK5, pMEK5, and ERK5 expression in human lung adenocarcinomas compared to healthy lung tissue from a total of 34 samples from patients of the University Hospital of Salamanca (numbers correspond to the tissue bank classification of each patient; N: Normal, T: tumor). 2 mg of protein were immunoprecipitated with the anti-MEK5 antibody followed by Western blotting with the pMEK5 or MEK5 antibodies. In parallel, ERK5 expression was also evaluated. Calnexin was used as loading control. Note: A lane between lung adenocarcinoma samples 5158 and 5199 was cut out from the Western blots. B) Plots representing the levels of pMEK5 (left) and pERK5 (right) in patient tumoral lungs (N=23) and healthy samples (N=11), which were quantitated from Western blot analysis using the ImageJ software. Note that no statistical analysis could be performed since pMEK5 and pERK5 are undetectable (value = 0) in normal lung tissue.

Moreover, MEK5 and ERK5 expression levels were higher in tumoral samples than in normal lung tissue. Quantitative analysis of the protein levels from all patient samples evidenced a MEK5 6.2-fold increase and an ERK5 5.5-fold increase in tumoral samples when compared to normal tissue (Figure 21A). These differences were highly significative with a $p$=2.7e-08 and $p$=2.2e-09 for MEK5 and ERK5, respectively. Moreover, a positive linear correlation between MEK5 and ERK5 expression was statistically evidenced when analyzed by the Pearson correlation coefficient (r=0.779, $p$=5.9e-08) (Figure 21B). These results are in line with those observed in transgenic mice, which also showed higher levels of ERK5 expression and activation than the healthy lungs of non-transgenic mice.

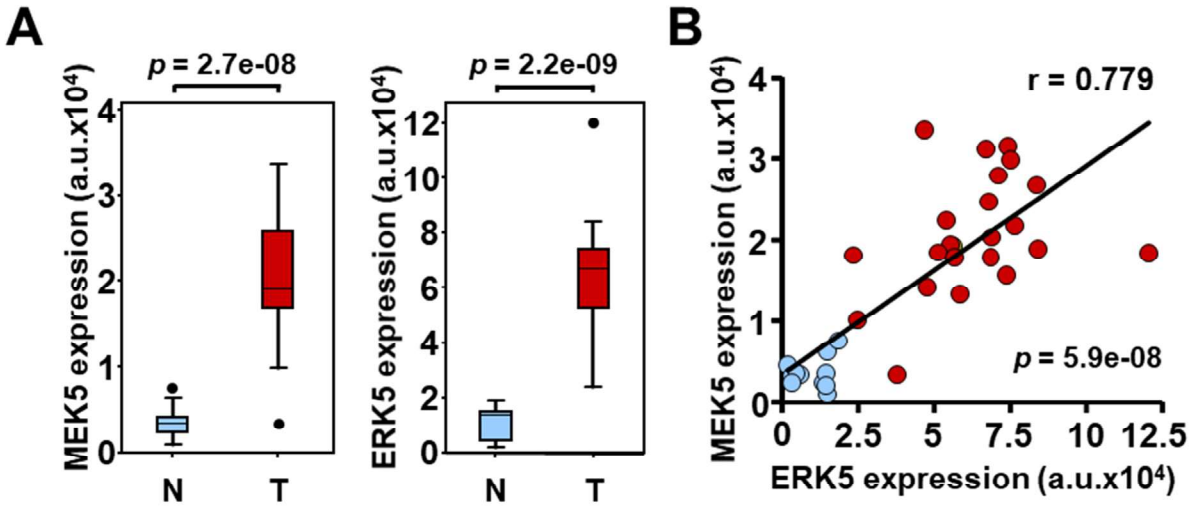


**Figure 21.** A) Comparison between MEK5 levels (left panel) from the total 34 samples (23 lung adenocarcinoma and 11 healthy human lung samples). MEK5 expression was quantitated from Western blot analysis using ImageJ software and represented in a box plot. The median value for each group is represented as the central line of the box. Black dots represent the outlier values. Statistical comparisons were performed by calculating the $p$-value according to a two-sided Student's $t$-test. ERK5 levels (right panel) were similarly evaluated and compared. B) Pearson correlation analysis of MEK5 versus ERK5 protein expression in the total 34 samples from human lung adenocarcinoma (green, 23 samples) and healthy lung tissue (blue, 11 samples) (Pearson r = 0.779; $p$ =5.9e-08). Line represents linear regression of data (y=0.2572x + 3392; $R^2$ = 0.606).

Of note, ERK5 immunochemistry detection in the lung adenocarcinoma samples revealed a mainly nuclear localization, which is though to be the preferential cellular localization of ERK5 in activated status (Figure 22).

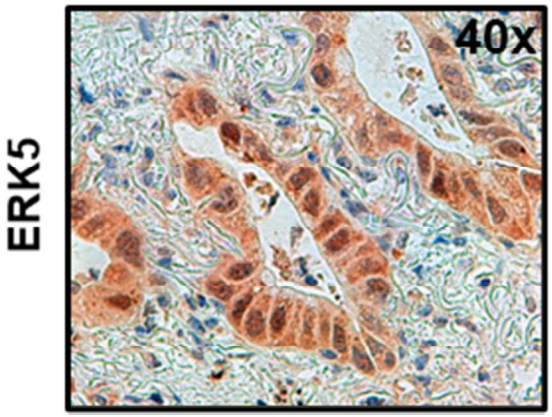


**Figure 22.** Representative 40x immunohistochemical analysis of the cellular location of ERK5 in human lung ADC tissue using an N-terminal ERK5 antibody.

By exploring the publicly available Kaplan-Meier plotter database (Győrffy et al., 2013), which allows *in silico* analysis of the transcriptomic expression levels in tumoral versus non-tumoral human lung tissue, we also found that MEK5 and ERK5 presented a statistically significant higher expression in lung tumors when compared to healthy tissue ($p$=3.38e-06 and $p$=0.0074, respectively) (Figure 23).

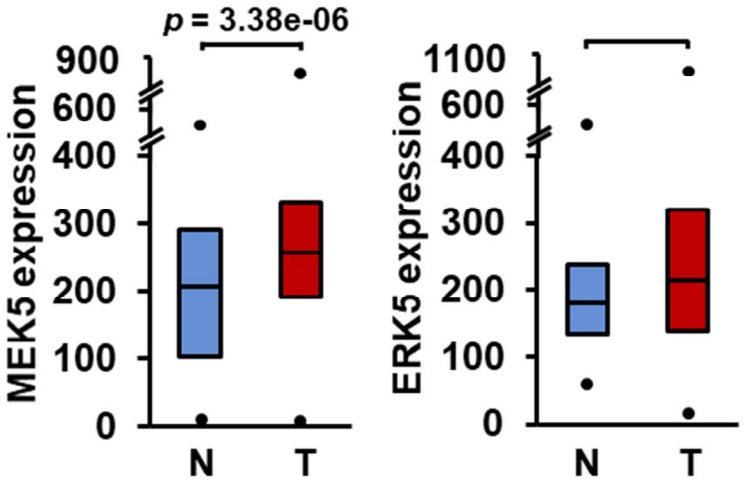


**Figure 23.** Comparison between MEK5 levels (left panel) of 2437 lung tumors and 86 healthy lung samples plotted from patient data collected in the Kaplan-Meier plotter database. Data were first MAS5 normalized, and then a scaling normalization was performed to set the mean expression across all genes to 1000, as described in Győrffy et al., 2013. ERK5 levels (right panel) were similarly represented and compared. Black dots correspond to the minimum and maximum values. *p*-values were calculated according to the Mann-Whitney U-test.

### 1.3 MEK5/ERK5 expression linked to lung cancer patient outcome

After observing that MEK5 or ERK5 expression were higher in tumoral samples than in normal tissue, we next explored the potential relationship between their expression levels and patient outcome. mRNA analyses of pooled data from the whole lung cancer patient population present in the database (n=1925) were performed. These studies showed that high levels of MEK5 and ERK5 expression associate with worse prognosis (*p*-value=0.0032, HR=1.22 (1.07-1.39), FDR=0.50) (Figure 24A), with a median survival of 63 months (high expression cohort), compared to 81 months (low expression cohort). Statistically, this association was more robust when selecting for analysis the adenocarcinoma cohort (*p*-value=3e-5, HR=1.65 (1.3-2.1), FDR=0.01) (Figure 24B). When the squamous carcinoma cohort was selected, such association did not reach statistical significance (*p*-value=0.07, HR=0.78 (0.6-1.02), FDR=1) (Figure 24C).

The negative association between high levels of MEK5/ERK5 expression and worse prognosis was observed irrespectively of whether lung cancer patients did not have previous history of tobacco smoking (n=204, p-value=1.7e-05, HR=3.22 (1.83-5.66), FDR=0.01) (Figure 24D), or were smokers (n=820, p-value=6.9e-06, HR=1.66 (1.33-2.08), FDR=0.01) (Figure 24E). Complementary studies indicated that MEK5 and ERK5 high expression was also associated with a poor post progression survival prognosis (Figure 24F) whose median survival was reduced by more than half in the never-smoking cohort of patients (p-value=0.029, HR=1.98 (1.06-3.7), FDR=0.50). Similar results were obtained by utilizing RNA-seq data both from the KMplotter and the Lung Cancer Explorer databases (data not shown).

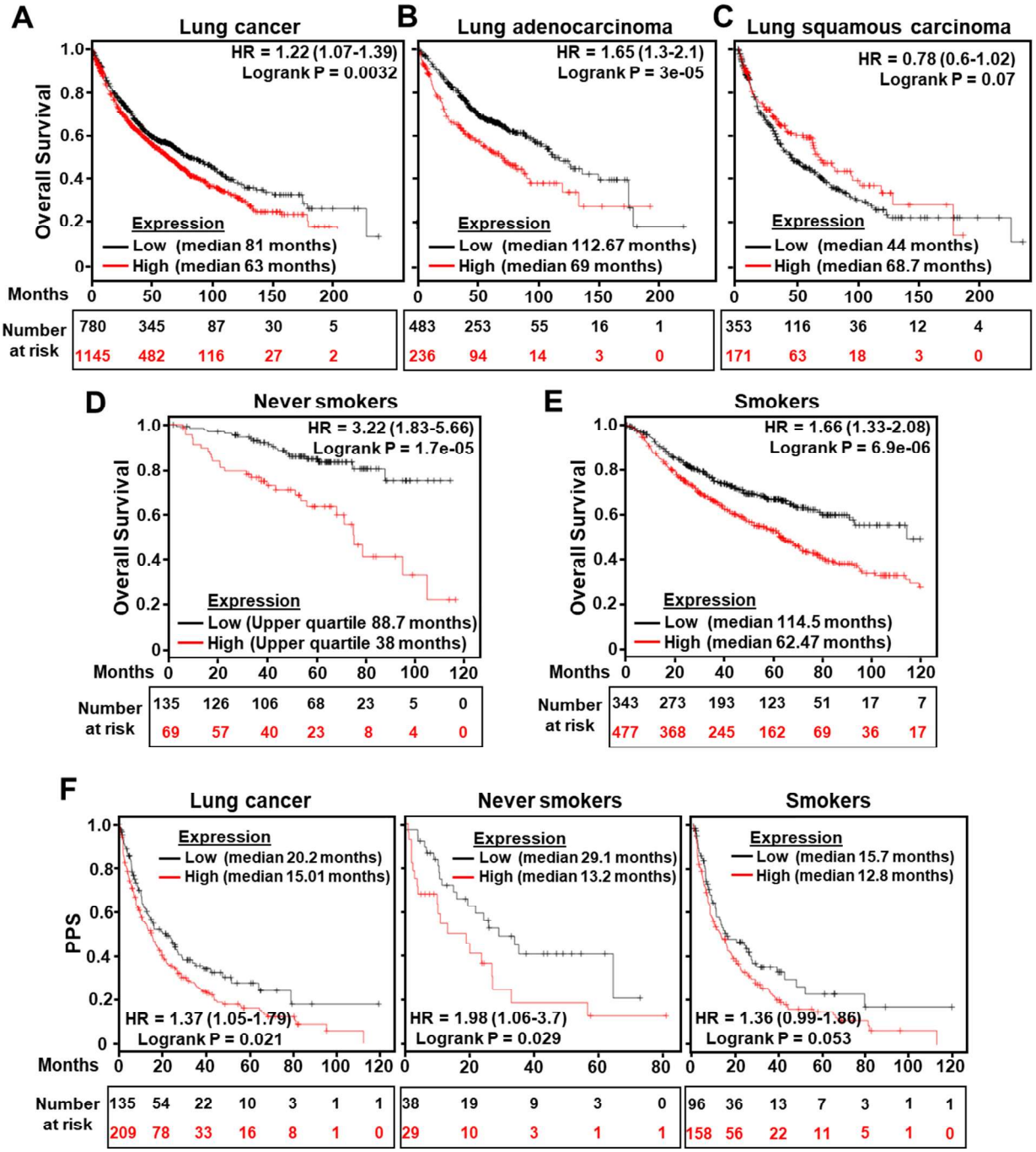


**Figure 24.** 240 months follow-up Kaplan-Meier analysis of the relationship between combined MEK5/ERK5 expression and overall survival in lung cancer patients (A) (n=1925), lung adenocarcinoma patients (B) (n=719), or squamous cell carcinoma patients (C) (n=524) collected in the public Kaplan-Meier plotter database. Patients were stratified according to low or high MEK5/ERK5 expression as indicated in the materials and methods section. The *p*-value, hazard ratio, median survival and number of patients at risk in the low and high expression groups are indicated. FDR values for the analyses of the lung cancer, lung adenocarcinoma and lung squamous carcinoma cohorts are 0.05, 0.01 and 1, respectively. D) 120 months follow up Kaplan-Meier analysis in never-smoking lung cancer patients (n=204) and E) the lung cancer patient population excluding never-smokers (n=820) similarly calculated. F) Kaplan-Meier analyses of the relationship between MEK5/ERK5 expression and Post Progression Survival (PPS) in lung cancer (n=344, left panel), never-smoker (n=67, central panel) and those excluding never-smoker (n=254, right panel) patients. FDR values for the analyses of the whole lung cancer, never smoker and smoker cohorts are 0.50, 0.50, and 1, respectively.

The potential correlation between MEK5 and ERK5 expression and patient outcome was also explored using the cBioPortal for Cancer Genomics database available at http://cbioportal.org (Cerami et al., 2012; Gao et al., 2013) which, in addition to mRNA expression levels, allows analysis of other molecular alterations such as gene copy number alterations (CNA) and mutations. Gain or amplification of MEK5 were present in 8.7% of adenocarcinomas and 25.8% of squamous carcinomas, while in the case of ERK5 such molecular alterations were present in 18.9% of adenocarcinomas and 13.5% of squamous carcinomas (Figure 25A). Lung adenocarcinoma patients presenting amplifications or gains in MEK5 or ERK5 showed a worse clinical outcome when compared to those without such alterations (p-value= 5.181e-3) (Figure 25B). However, no significant differences were observed in the clinical outcome of lung squamous carcinoma patients.

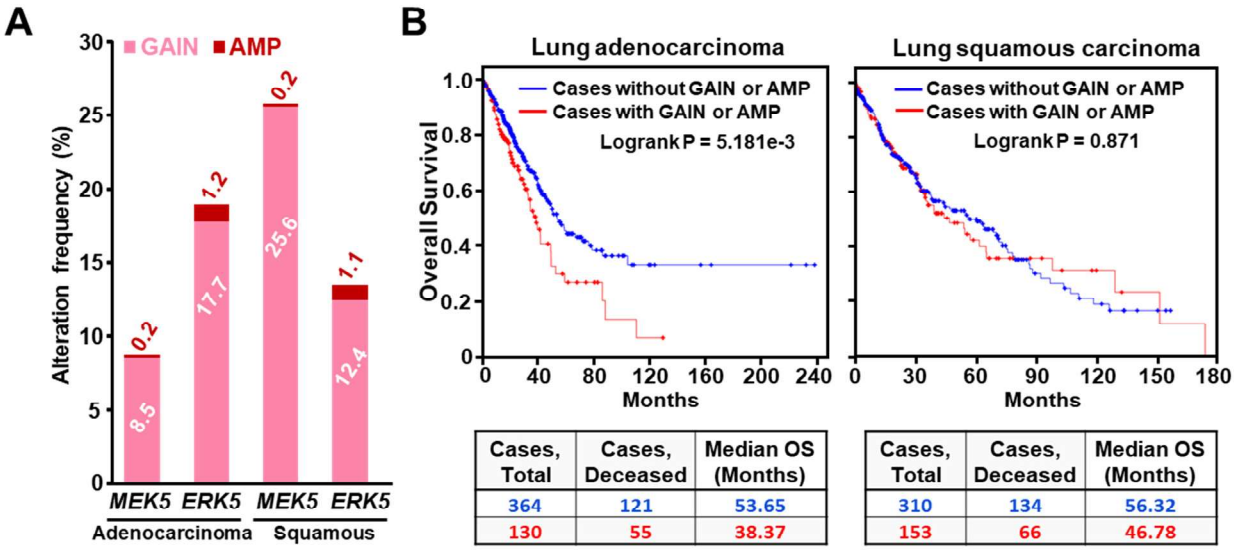


| Cases, Total | Cases, Deceased | Median OS (Months) |
|---|---|---|
| 364 | 121 | 53.65 |
| 130 | 55 | 38.37 |

| Cases, Total | Cases, Deceased | Median OS (Months) |
|---|---|---|
| 310 | 134 | 56.32 |
| 153 | 66 | 46.78 |

**Figure 25.** A) The cBioPortal database was explored in order to determine the gains and amplifications present in *MEK5* and *ERK5* genes of lung adenocarcinoma (n=503) and lung squamous cell carcinoma (n=469) patients. Copy-number alteration data was obtained from the TCGA. Patients with gains and high-level amplifications were quantified and represented as percentage from the total patients included in the study. B) Overall survival curves of lung adenocarcinoma (n=494) and lung squamous carcinoma (n=463) patients with available clinical data from (A). Patients harboring gain or amplification in MEK5 or ERK5 (red line) were compared to those without such alterations (blue line). The *p*-value of the studies, follow-up (months) and median overall survival are indicated.

As expected, the cases with gains or amplifications presented the highest mRNA levels in lung adenocarcinomas as well as squamous cell tumors, that are the main lung cancer subtypes (Figure 26A). Similar analyses of MEK5 or ERK5 gene deletions failed to show

association between these molecular alterations and patient outcome (Figure 26B and C). Together, these clinic-genomic studies linked high expression levels of MEK5 or ERK5 to worse patient outcome in lung cancer, especially in lung adenocarcinoma patients.

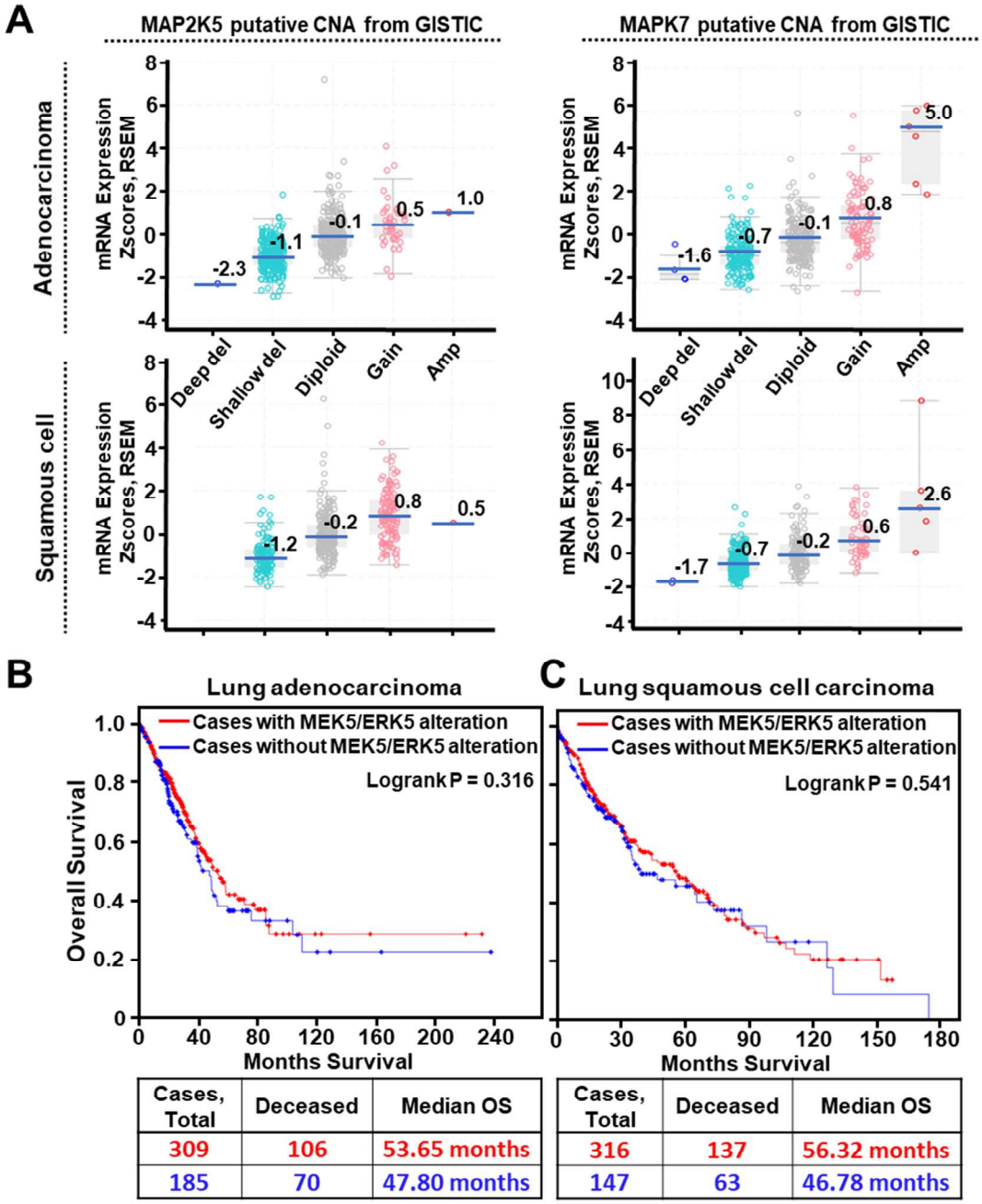


**Figure 26.** A) Relationship between Copy Number Alterations (CNA) of *MEK5* or *ERK5* genes and the mRNA expression of patients collected in the lung adenocarcinoma or lung squamous cell carcinoma studies from cBioPortal (TCGA Pan-Lung cancer Study). The blue lines correspond to the median mRNA expression value of each CNA subgroup. The copy number data sets were generated by the GISTIC algorithm. B) Overall survival curves of lung adenocarcinoma (n=494) and C) lung squamous carcinoma (n=463) patients with available clinical data from patients harboring shallow or deep deletion in *MEK5* or *ERK5* (red line), compared to those without such alterations (blue line). The *p*-value of the studies, follow-up (months) and median overall survival are indicated.

It is also relevant to mention that analyses of the TCGA PanCancer Atlas study (n=1144) revealed mutation frequencies of 0.6% and 0.9% in MEK5 and ERK5, respectively, in lung cancer patients, which were scattered along the length of these proteins (Figure 27). The relevance of those mutations on patient outcome or their impact on the function of these kinases remains to be established.

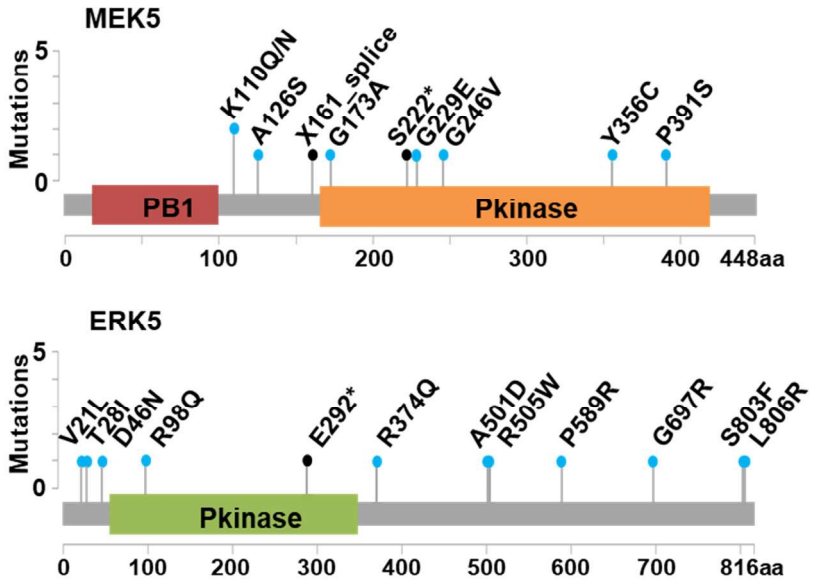


**Figure 27.** cBioportal data (TCGA, PanCancer Atlas study, n=1144) was explored in order to determine the missense (blue) and truncating (black) mutations present in MEK5 or ERK5 proteins from lung adenocarcinoma and lung squamous cell carcinoma patients. Data was collected and mutations represented across the protein length. The aminoacidic change is indicated. Blue dots = missense mutation. Black dot = truncating mutation.

## 1.4 Genetic targeting of MEK5 and ERK5 regulates the proliferation of lung cancer cells

The link between MEK5/ERK5 expression levels and patient outcome led us to explore the value of targeting such route as a potential therapeutic strategy using non-small cell lung cancer (NSCLC) cell lines. To that end, we aimed at selecting *in vitro* cellular models that in addition to expressing ERK5, would also show evidence of MEK5/ERK5 pathway activation. Of a panel of 14 NSCLC cell lines, all expressing ERK5, we selected the four ones (A549, H1299, H460 and H727) that constitutively expressed pERK5 (Figure 28). The latter represents a readout of MEK5/ERK5 pathway activation status (Kato et al., 1998; Esparís-Ogando et al., 2002; Rovida et al., 2015).

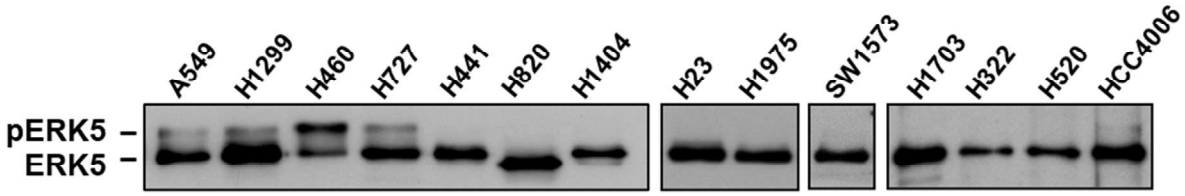


**Figure 28.** Expression of ERK5 and pERK5 in a panel of 14 NSCLC cell lines. Cell extracts were prepared and 1 mg immunoprecipitated with the anti-ERK5 antibody and Western blots probed with the same antibody.

Even though the presence of MEK5 mutations in the lung cancer patients was less than 1% (Figure 27), we thus decided to sequence the MEK5 gene in the four NSCLC cell lines expressing pERK5 to check whether they present any mutation causing a constitutive activation of ERK5.

Such sequencing process was carried out in the genomics service of the CIC-IBMCC, following the methodology described in the Materials and Methods section 4.5. After obtaining the resulting chromatograms, we compared the MEK5 sequence of these cell lines with that of the canonical MEK cDNA sequence deposited in bioinformatic databases by performing a BLAST analysis. However, none of them harbored MEK5 mutations (Figure 29).

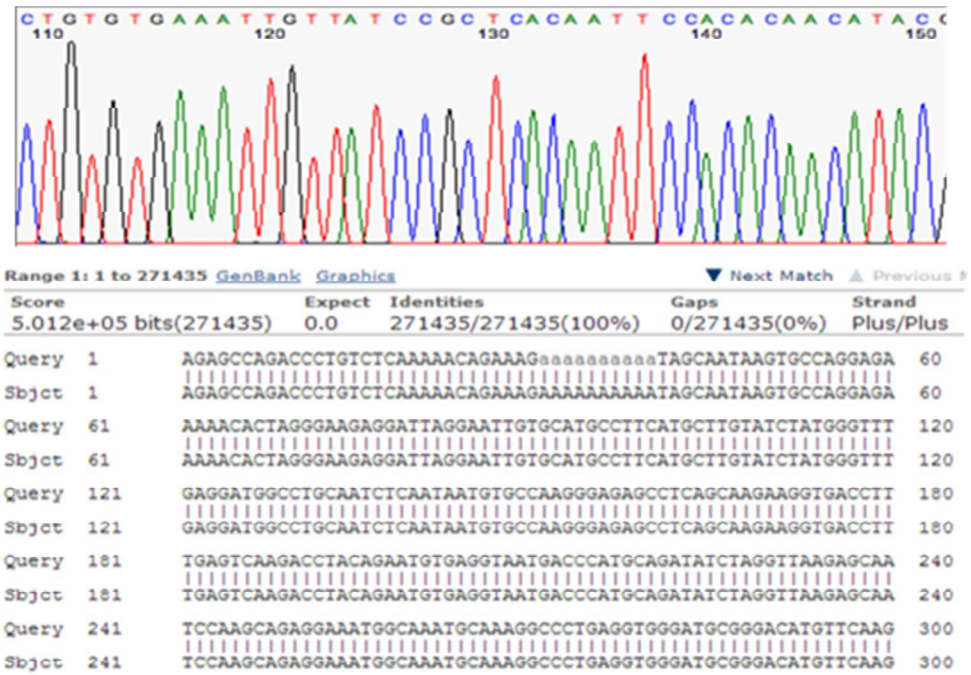


**Figure 29.** Fragment of a chromatogram obtained from the sequencing of MEK5 in one of the NSCLC lines (upper panel) and its corresponding BLAST alignment (lower panel) between the canonical sequence of MEK5 and that inferred from the chromatogram, exemplifying that no mutations were observed in the NSCLC cell lines.

Quantitative PCR demonstrated expression of MEK5 mRNA in A549, H1299, H460 and H727 NSCLC cell lines (Figure 30A). Western blot analyses of MEK5 and pMEK5 (the latter using an antibody that was developed in our laboratory against residues pSer$^{311}$ and pThr$^{315}$ present in the MEK5 activation domain) showed expression and activation of MEK5 in these cell lines, although at different levels (Figure 30B).

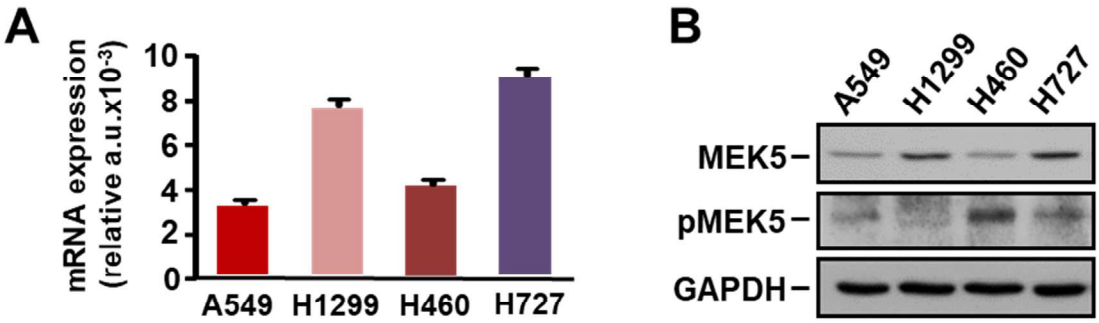


**Figure 30.** A) MEK5 mRNA expression was determined by quantitative RT-PCR in NSCLC cell lines. GAPDH was used as control for differences in cDNA input. Data shows the mean expression ± SD of an experiment that was repeated twice, calculated according to the ΔΔCt relative quantitation method. B) Expression of MEK5 and pMEK5 in NSCLC cell lines. 50 μg of whole-cell lysates were used to detect MEK5 by Western blotting. For pMEK5 detection, 2 mg of protein were immunoprecipitated with the anti-MEK5 antibody followed by Western blotting with the anti-pMEK5 antibody. GAPDH was used as loading control.

The first approach towards establishing the potential role of that kinase in lung cancer cell proliferation was utilizing lentiviral vectors including shRNA sequences expected to interfere with MEK5 expression. The four sequences explored were able to reduce MEK5 expression in the H460 cell line (Figure 31A). Since the largest interference was observed in cells infected with vectors including sequences sh66 and sh68, they were subsequently used for MEK5 silencing in the other cell lines. Both sh66 and sh68 diminished MEK5 expression in the four lung cancer cell lines, which resulted in significant reduction of their proliferation (Figure 31B). Of note, the level of MEK5 knockdown correlated with the inhibition of proliferation: the greater the silencing, the greater the antiproliferative effect. In addition, the reduction of MEK5 levels caused a reduction of ERK5 activity, as demonstrated by the decrease of pERK5 levels (Figure 31C).

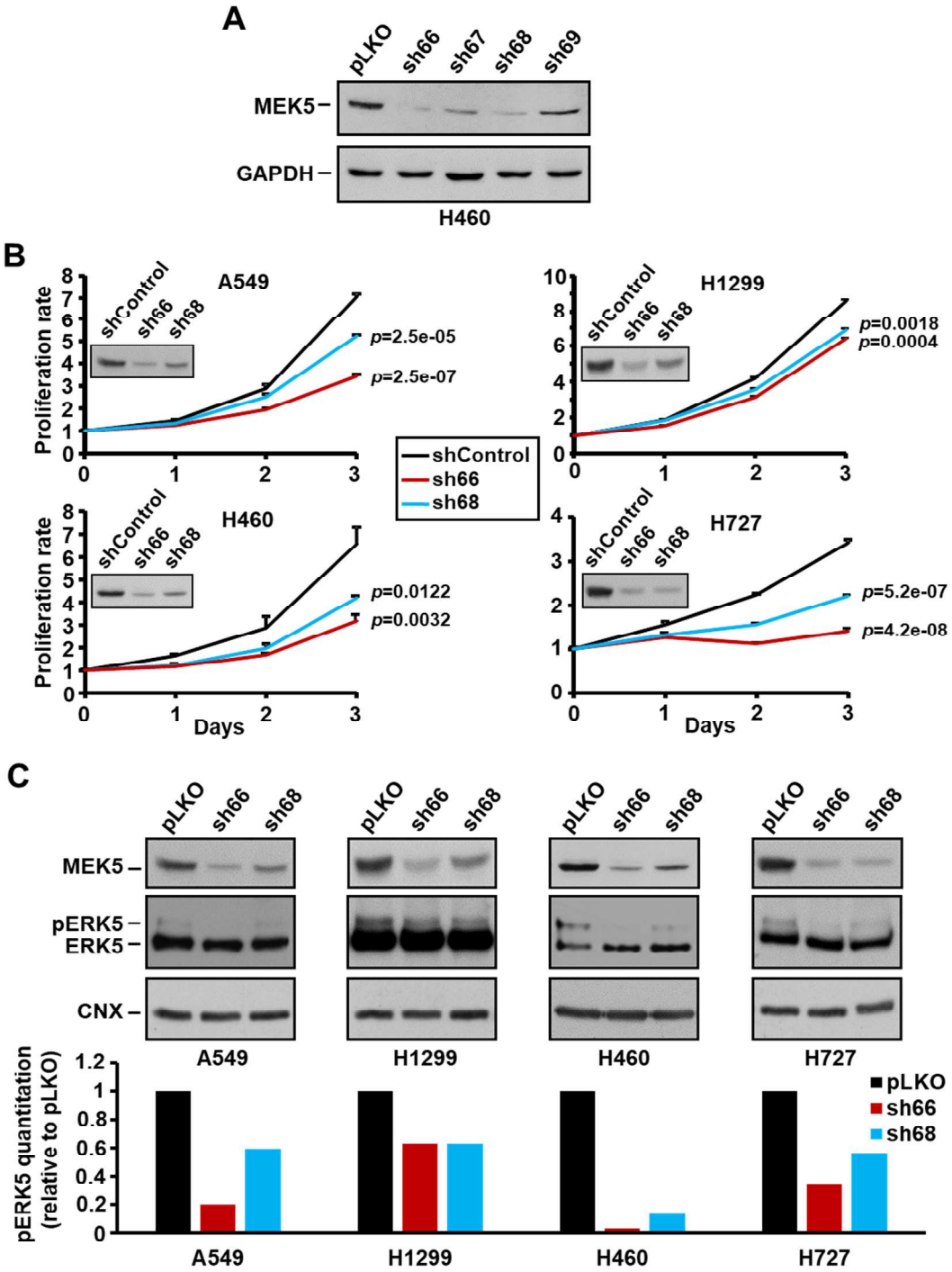


**Figure 31.** A) H460 cells were infected with a pLKO shControl sequence or 4 different MEK5 specific shRNA sequences. Cells were lysed and 70 µg of cell extracts were used to determine the MEK5 knockdown by Western blotting with the anti-MEK5 antibody. GAPDH was used as loading control. B) Knockdown of MEK5 was carried out by lentiviral infection of NSCLC cells with a scrambled control sequence or MEK5 specific shRNAs (sh66 and sh68) and levels of MEK5 were evaluated by Western blotting. The effect of MEK5 knockdown on cell proliferation was measured by MTT assay at the indicated times. Data is presented as the mean ± SD of an experiment that was repeated three times. *p*-values were calculated according to a two-sided Student's t-test. C) Cells infected with pLKO shControl, sh68 and sh66 were lysed and MEK5 levels were evaluated on 70 micrograms of cell extracts by Western blotting with the anti-MEK5 antibody. The effect of MEK5 knockdown on ERK5 activation was analyzed by immunoprecipitating 1 mg of protein followed by Western blotting with the anti-ERK5 antibody. The bar graph shows the quantitation of the pERK5 levels, relativized to the levels present in the pLKO shControl-infected cells.

The relevance of ERK5 in lung cancer cells was explored. 5 different Western blotting studies were performed and quantitated, revealing that all cell lines studied expressed pERK5, with H460 cells showing the highest pERK5/ERK5 ratio (Figure 32).

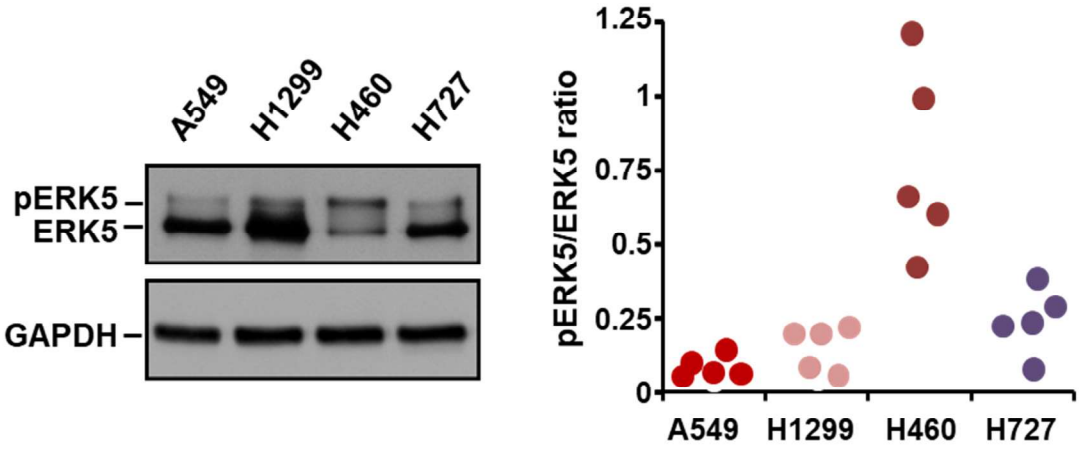


**Figure 32.** Expression of total ERK5 in NSCLC cell lines. pERK5 and total ERK5 were evaluated by immunoprecipitating 1 mg of protein with the anti-ERK5 antibody and blots probed with the C-terminal anti-ERK5 antibody. GAPDH was used as loading control (left panel). pERK5 (upper band) and ERK5 (lower band) levels from five independent Western blot studies were quantified with the ImageJ software and the pERK5/ERK5 ratio represented (right panel).

The cellular localization of ERK5 in the four NSCLC cells was analyzed by immunofluorescence staining with an N-terminal ERK5 antibody. The results reported a strong nuclear pattern, whereas cytoplasmic and cell membrane staining were diffuse an undetectable, respectively (Figure 33).

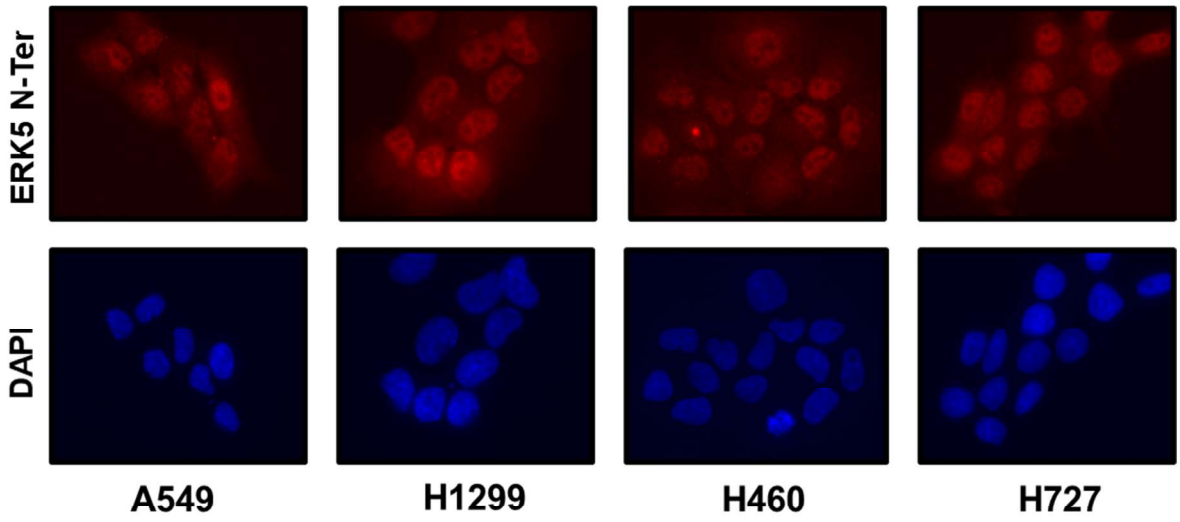


**Figure 33.** Representative 20x immunofluorescence analysis of the cellular location of ERK5 in the four NSCLC cell lines using an N-terminal ERK5 antibody.

The value of targeting the MEK5/ERK5 route in lung cancer was also evaluated by genetic manipulation of ERK5 using lentiviral vectors including a shRNA sequence directed against this kinase. Knockdown of ERK5 reduced the amounts of both ERK5 and pERK5 (Figure 34, upper panel). Such protein silencing correlated with a significantly decreased in the growth of the four cell lines (Figure 34, lower panel) suggesting an important role of this pathway in the control of cell proliferation.

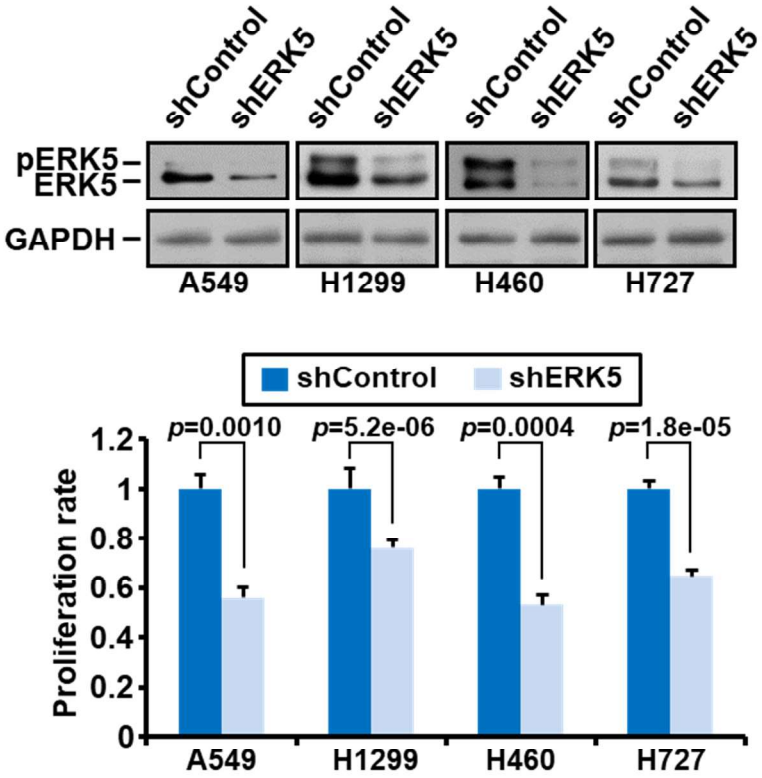


**Figure 34.** Silencing of ERK5 in NSCLC cells by shRNA was confirmed by Western blotting with the anti-ERK5 antibody. GAPDH was used as loading control (left panel). Proliferation effect of ERK5 knockdown (right panel) was evaluated at three days as in Figure 31B.

The participation of the MEK5/ERK5 route in the proliferation of non-transformed immortalized human bronchial epithelial cells (HBEC) was also evaluated. MEK5 or ERK5 knockdown decreased proliferation of HBEC (Figure 35A and B, respectively). As it can be observed, those shRNA sequences achieving a higher protein expression silencing exerted a higher antiproliferative effect, hence suggesting that this pathway has also an important role in the control of the proliferation of non-transformed lung epithelial cells.

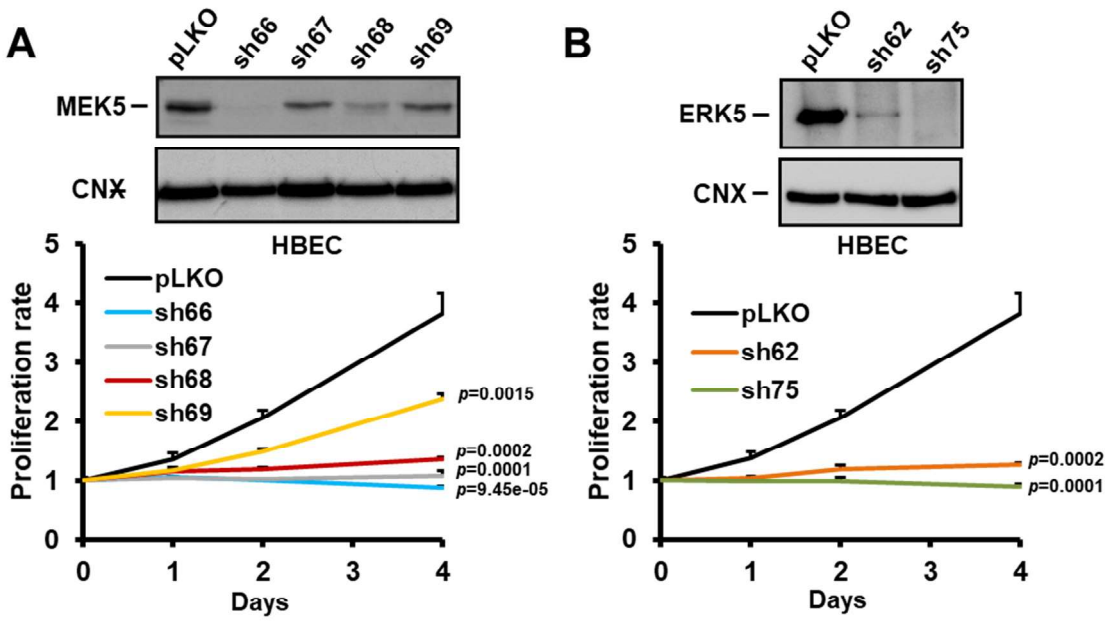


**Figure 35.** A) Effect of sh66 and sh68 MEK5 targeting shRNA sequences on HBEC proliferation. 4500 cells were plated and proliferation was measured at the indicated times by MTT proliferation assays. The Western blot at the top shows the effect of different knockdown sequences on the levels of MEK5. B) Effect of sh62 and sh75 ERK5 targeting shRNA sequences on HBEC proliferation. The Western blot at the top shows the effect of these knockdown sequences on the levels of ERK5. Note that the proliferation of pLKO shControl is the same in panels A) and B) since the results plotted come from the same experiment.

In order to complement the knockdown studies on the relevance of MEK5 and ERK5 in lung cancer cell proliferation, we next used the CRISPR/Cas9 technique to completely abrogate MEK5 and ERK5 levels. For these studies we selected the H460 cell line which, as shown above, presented the highest ratio of ERK5 activation. From a total of 47 H460 CRISPR clones obtained and analyzed by western blotting, only four of them lacked ERK5 expression (Figure 36A) and were therefore used for further experimentation. RNA from these clones were extracted and utilized for carrying out Clariom S Human gene expression microarrays, as described in the Materials and Methods section. Transcriptomic analyses made it clear that the different clones separate from the WT or SC cells (Figure 36B). The PCA analysis also indicated that the clones were different from each other, as desired, because in case different clones would have appeared too close, that would raise the possibility that they represent the same clone from the genetic point of view and then there would be no point as to analyze brother

clones. The PCA analyses also revealed that the clones separate more from the WT or SC than from each other. Despite these genomic differences, the biological behaviour of these clones was similar. Thus, *in vitro* cell proliferation studies demonstrated that CRISPR-mediated ERK5 elimination significantly affected the proliferation of all H460 knockout clones (Figure 36C).

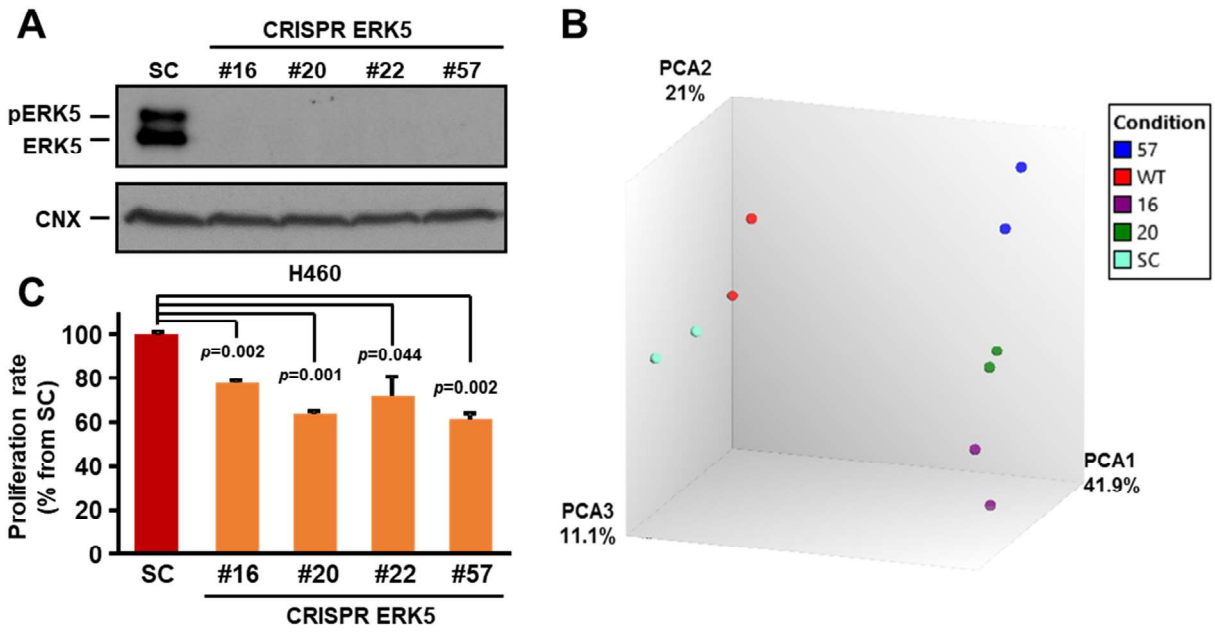


**Figure 36.** A) Western blot showing lack of ERK5 expression in the different H460 ERK5 CRISPR clones when compared to the control H460 scramble cells (SC). B) Principal Component Analysis (PCA) resulting from the microarray of gene expression of H460 Wild Type (WT), scramble (SC) and ERK5 knockout clones (#16, #20 and #57). C) Effect of ERK5 knockout on the cell proliferation of H460 cells. 35000 cells of H460 SC cells or H460 CRISPR ERK5 clones were plated in p6 wells and cultured for 3 days. The proliferation rate was measured by cell counting and represented as percentage from control H460 scramble cells. Data is presented as the mean ± SD of an experiment that was repeated three times. *p*-values were calculated according to a two-sided Student's t-test.

To additionally exclude the possibility that their proliferation characteristics were due to a clonal effect, four ERK5 non-knockout clones were also analyzed. In contrast to the knockout clones, they presented a similar proliferation rate to the SC cells (Figure 37A). Furthermore, biochemical and morphology experiments showed no differences between SC, knockout, and non-knockout cells (Figures 37B and C, respectively). Taken together, these results firmly ruled out that the impact of ERK5 abolishing on cell proliferation was due to a clonal effect.

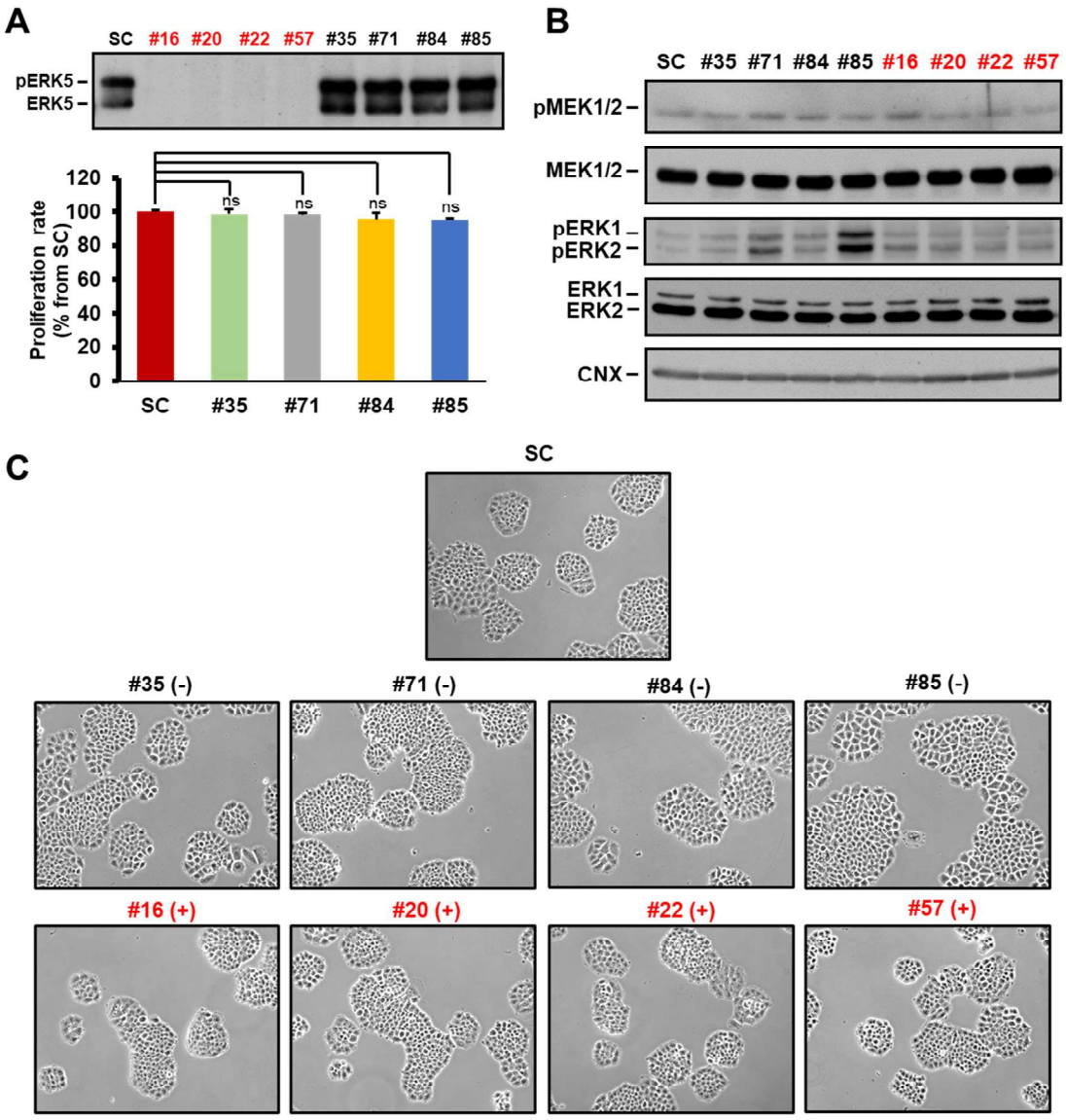


**Figure 37.** A) Immunoblot showing the ERK5/pERK5 levels of H460 clones that were not knocked out for ERK5 expression (upper panel) and their corresponding proliferation rates (lower panel). As observed, the growth behavior of scramble and non-knockout clones are similar. B) Western blot analyses comparing the expression and activation of the related MEK1/2 and ERK1/2 kinases between knockout and non-knockout ERK5 clones. C) Representative pictures of ERK5 knockout and ERK5 non-knockout clones showing that their basic morphologies are undistinguishable from that of the control (H460 scramble) cells.

The antiproliferative action of ERK5 deletion was also explored in a more physiological context. To that end, H460 ERK5-KO cells from two different clones (#20 and #57) were injected into mice, and the growth of tumors generated by those cells compared to the growth of tumors created by injecting H460 scramble cells. As shown in Figure 38A, tumors in mice injected with ERK5 knockout cells grew slower than those created by injecting H460 scramble cells. Such differences on tumor growth reached statistical significance ($p<0.001$). In fact, 16

days after injection, #20 and #57 tumors presented a mean volume of 37.69% and 26.36% when compared to scramble tumors. This can also be observed in the tumor representative pictures shown below. In addition, western blot analyses of the tumors dissected from these animals demonstrated the lack of expression of ERK5 in the knockout clones, this is, the cells did not recover ERK5 expression after implantation on the mice. Moreover, tumoral tissue immunostaining with the proliferation marker Ki67 indicated that the proliferation rate was notably lower in H460 ERK5-KO than in scramble H460 tumors (Figure 38B). Computational quantitation of the percentage of positive ki67 cells revealed that such differences (2.8-fold decrease for #20 tumors and 8.9-fold decrease for #57 tumors) reached statistical significance.

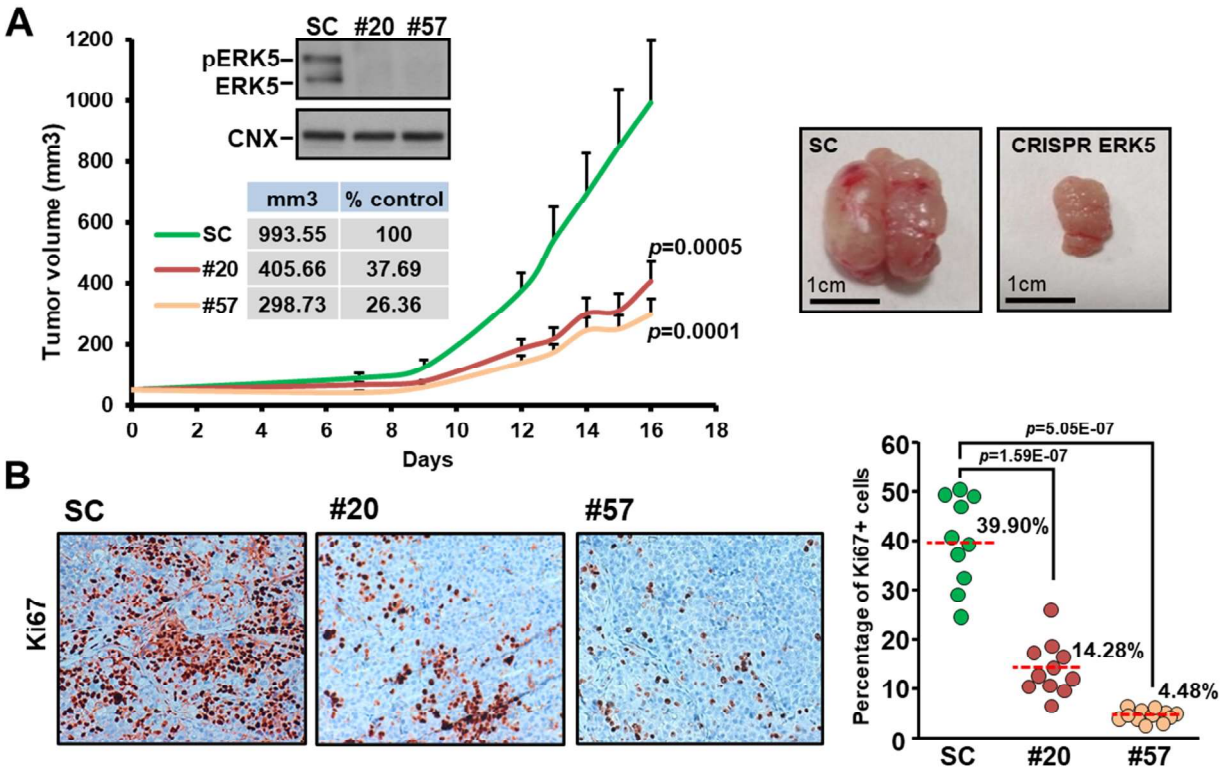


**Figure 38.** A) Tumor growth evolution of the mice xenoinjerted with the H460 SC cells or ERK5 CRISPR cells (#20 and #57 clones) (n=10 tumors, per group). The mean tumor volume and SEM error bars of each group are represented. Due to the rapid growth of the H460 cell line, the experiment was stopped at day 16, once one of the mice tumors reached a volume of 1500 $mm^3$. The significative *p*-values between groups are indicated. Data in the inset table indicates the volume percentage of ERK5 CRISPR tumors when compared to scramble tumors. Representative pictures of an ERK5 CRISPR tumor and a scramble tumor are displayed. Inset Western blot showing that ERK5 expression was not recovered in the H460 ERK5 CRISPR cells after the *in vivo* experiment is included. B) Ki67 immunostaining was quantified from 10 to 12 different pictures of each condition (scramble and ERK5 CRISPR clones) using a Leica LAS V3.7 software. Left panels show representative pictures of each condition. Right panel represents the percentage of Ki67 positive cells from total. The average percentage value (red line) and *p*-value for each ERK5 CRISPR clone are indicated.

As a complement to these studies, we also aimed to eliminate MEK5 expression using CRISPR/Cas9 technology to further elucidate the relevance of MEK5/ERK5 signaling pathway blockade on the proliferation and tumorigenic properties of H460 cells. After several attemps, only one MEK5 knockout clone (#17) derived from H460 cells was obtained (Figure 39A). Elimination of MEK5 resulted in disappearance of pERK5. As observed before in the ERK5 knockout clones, the MEK5 knocked out clone grew less than the SC H460 isogenic control cells, which expressed MEK5 (Figure 39B). Moreover, *in vivo* experiments showed that mice tumors caused by the injection of cells from the MEK5 knockout clone grew substantially less than tumors created by injection of control SC cells (Figure 39C and D). Again, this antiproliferative effect (#17 mean tumor volume was 31.23% with respect to scramble tumors) reached statistical significance (p=0.05). Furthermore, ki67 immunostaining pattern also reinforced these findings, since H460 MEK5-KO tumors presented a proliferation rate notably lower than SC H460 tumor tissues (Figure 39E). Therefore, the data obtained with the CRISPR knockout clones add support to the other genetic evidence shown by shRNA-mediated protein knockdown, indicating that the MEK5/ERK5 route is relevant in lung cancer proliferation.

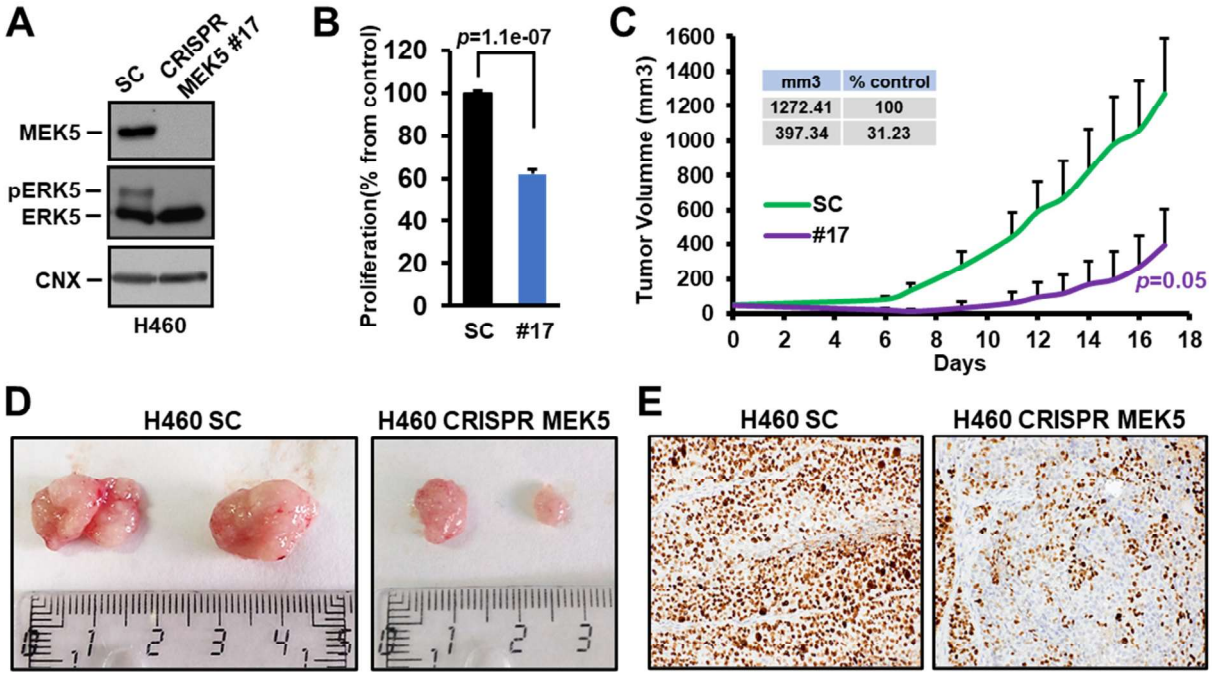


**Figure 39.** A) Western blot analyses of MEK5, ERK5 and pERK5 in a clone (#17) of H460 cells selected for its CRISPR/Cas9-mediated deletion of *MEK5*. B) *In vitro* and C) *in vivo* effect of the *MEK5* knockout on the proliferation and tumorigenesis of H460 cells (n=7 tumors per group). The procedures for evaluation of these effects were as described above for Figure 38A. D) Representative pictures comparing the size and E) Ki67 immunostaining of scrable tumors to that of MEK5 CRISPR tumors.

Finally, with the intention of extending these studies to the other NSCLC cell lines, we tested the effect of knocking down MEK5 or ERK5 on the growth of tumors derived from injection of A549, H1299, and H727 cells. As shown in Figures 40A-D, injection of cells in which MEK5 or ERK5 were knocked down by using lentiviral shRNA resulted in all cases in a noticeable slower growth of the tumors, as compared to tumors created by cells infected with a lentiviral pLKO shControl plasmid.

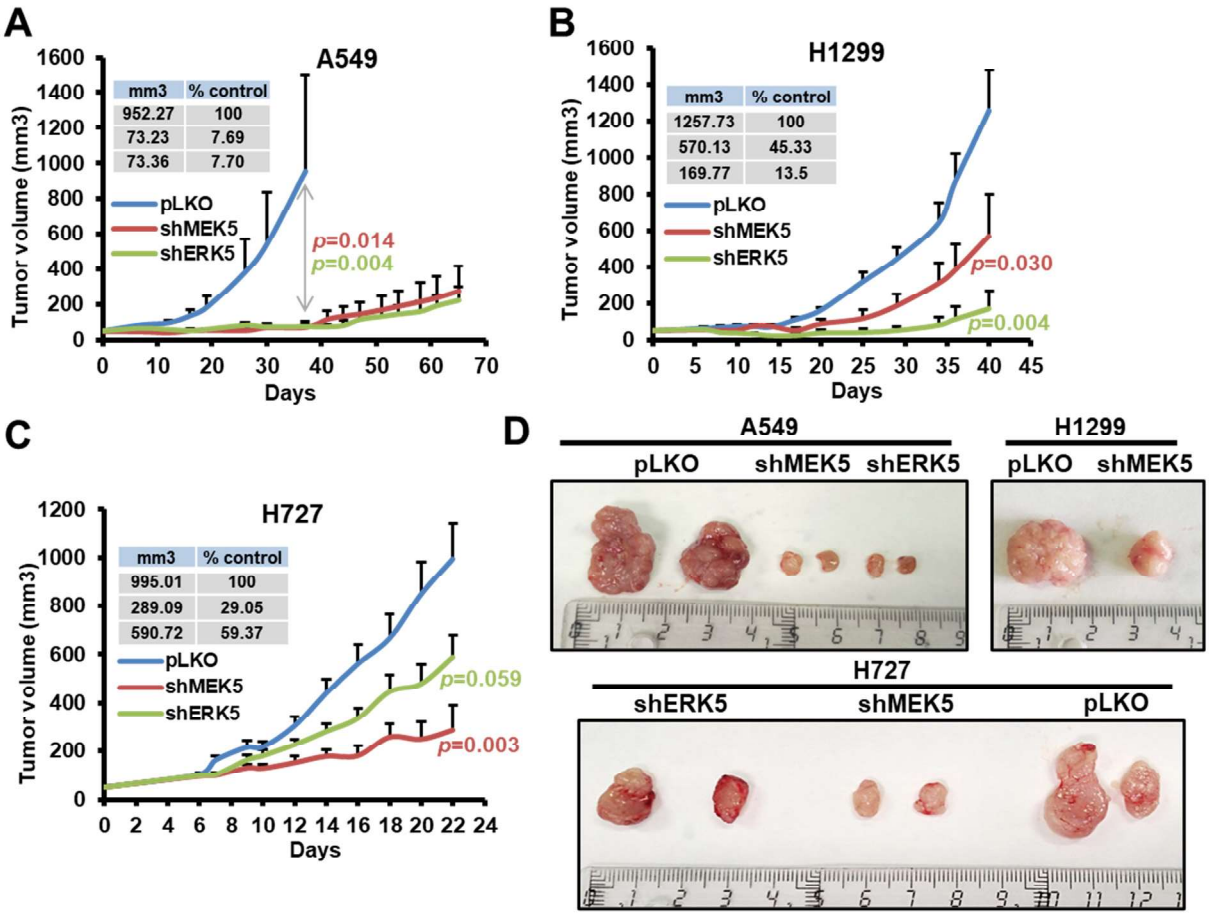


**Figure 40.** A) Effect of MEK5 or ERK5 knockdown on the *in vivo* tumorigenesis of A549 cells (n=6-8 tumors per group) B) H1299 cells (n=5-6 tumors per group) and C) H727 cells (n=6-8 tumors per group). Equal number of pLKO shControl, shMEK5 (sh66) or shERK5 cells were injected subcutaneously, and tumor sizes periodically measured. The mean tumor volume and SEM error bars of each group are represented. *p*-values between groups are indicated. Data in the inset table indicates the volume percentage of MEK5 or ERK5 knocked down tumors compared to pLKO tumors. Additional information is provided in materials and methods section. D) Representative pictures comparing the size of pLKO shControl tumors to that of shMEK5 or shERK5 tumors in these cell lines.

A similar reduced proliferation rate was observed after ki67 immunostaining of these MEK5 and ERK5 knockdown tumor tissues (Figure 41).

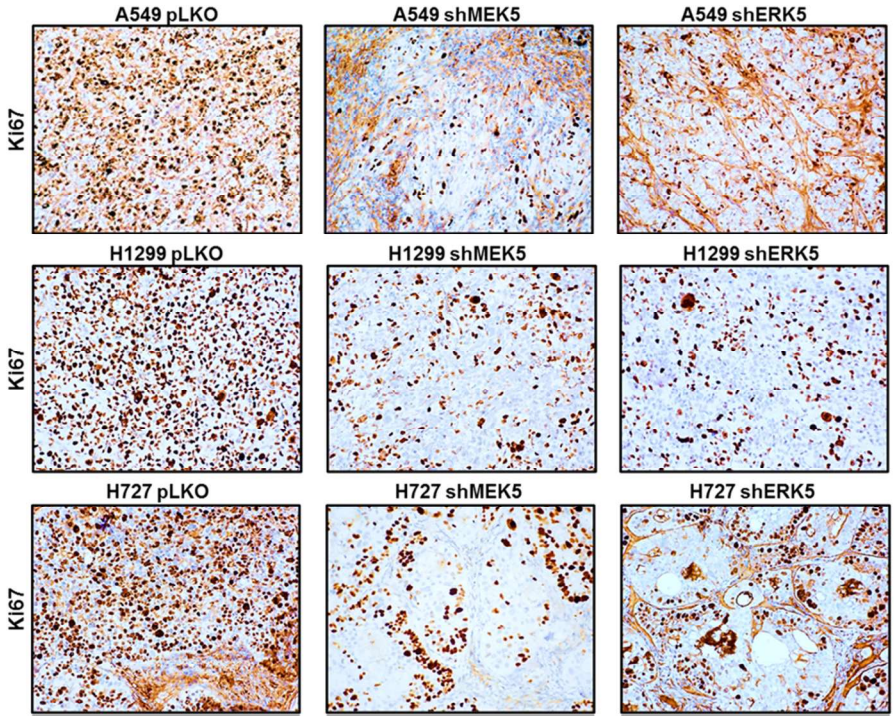


**Figure 41.** Representative pictures comparing the Ki67 immunostaining pattern of pLKO shControl tumors to that of shMEK5 and shERK5 tumors in these NSCLC cell lines.

## 1.5 Pharmacological inhibition of MEK5 and ERK5 in lung cancer cells

With the aim of exploring the therapeutic relevance of MEK5 pharmacological targeting in lung cancer, we evaluated the antitumoral action of BIX02189, a small molecule kinase inhibitor of MEK5 (Tatake et al., 2008). First, we analyzed the biochemical effect of that inhibitor on ERK5 phosphorylation (as a read out of MEK5 activity inhibition) by using the H460 cell line, which presents high basal activation of ERK5. BIX02189 caused a dose-dependent inhibition of ERK5 phosphorylation, demonstrating that the agent effectively neutralized the upstream kinase MEK5 (Figure 42A and B). That fact was corroborated by Western analysis using the anti-pERK5 antibody that detects ERK5 phosphorylation at its TEY microdomain, caused by MEK5. In contrast, the drug did not affect the phosphorylation levels of the related kinase pERK2 or pS6, that act as surrogate markers for activation of the RAS-RAF and PI3K/AKT routes, supporting that the drug did not affect the kinase pathways controlling phosphorylation of these signaling mediators. Additional immunoblots demonstrated that BIX02189 was able to impede ERK5 activation in the four cell lines (Figure 42C and D) and dose-dependently decrease MTT metabolism (Figure 42E).

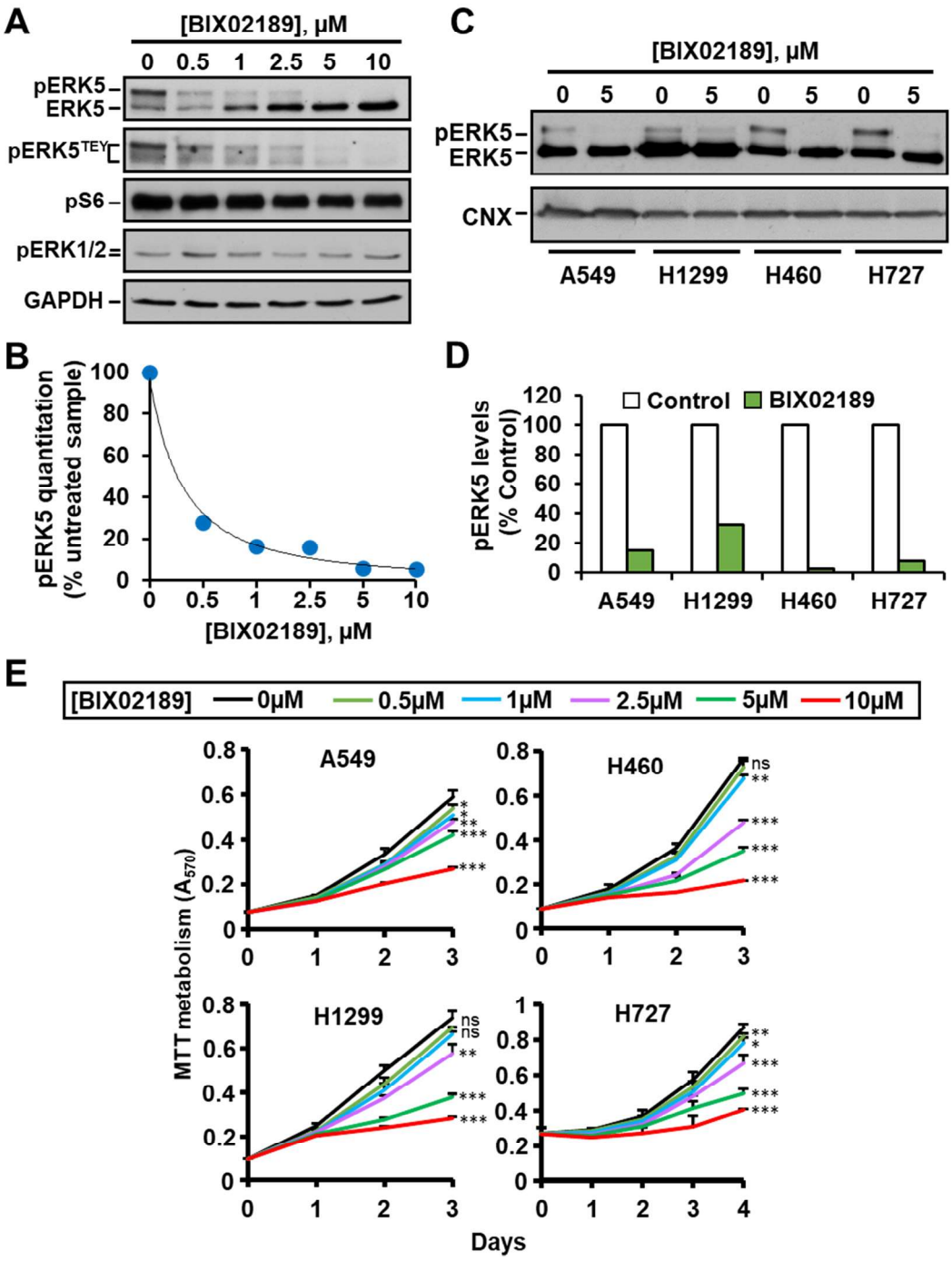


**Figure 42.** A) H460 cells were treated with increasing doses of BIX02189 for 72 hours and the effect of the drug on ERK5 activation was evaluated by immunoprecipitation of 1 mg of whole-cell lysates and Western blotting with the ERK5 or pERK5$^{TEY}$ antibodies. pS6 and pERK1/2 were used as controls to assure that BIX02189 did not affect the PI3K and ERK1/2 routes. B) Quantitation of pERK5 band in H460 cells from (A) using the ImageJ software. Data represents the percentage of the upper pERK5 band after BIX02189 treatment with respect to such band in control H460 untreated cells. C) NSCLC cell lines were treated with BIX02189 5 μM for 7 hours and the status of ERK5 phosphorylation analyzed by immunoprecipitation and Western blotting with the anti-ERK5 antibody. D) pERK5 levels (upper band) from (C) were quantified using the ImageJ software and represented as percentage from control untreated cells. E) NSCLC cells were plated in 24-well dishes and treated with increasing doses of BIX02189. Cell proliferation was measured at the indicated times by MTT. Results are expressed as mean ± SD of an experiment that was repeated three times. *, p≤0.05; **, p≤0.01; ***, p≤0.001.

The value of targeting the kinase activity of ERK5 using the inhibitor JWG-071 (Wang et al., 2018) was also explored. Western blotting analysis with the anti-ERK5 or anti-pERK5TEY antibodies showed that treatment of H460 cells with JWG-071 dose-dependently decreased the mobility of ERK5 towards a faster migrating form, indicating that the drug inhibited hyperphosphorylation of ERK5 (Figure 43A and B). Of note, such inhibition of phosphorylation did not appear to affect the phosphorylation of the TEY microdomain, since the anti-pERK5TEY antibody was still able to detect the faster migrating ERK5 forms. These results demonstrate that the drug was able to *in vivo* neutralize ERK5 autophosphorylation but did not affect the phosphorylation of ERK5 at the TEY microdomain, which is due to the activity of MEK5. Moreover, the data also demonstrate that the gel shift of ERK5 towards a lower mobility is not solely caused by phosphorylation of ERK5 at the TEY microdomain, since the faster migrating ERK5 is still recognized by the antibody. did not affect the phosphorylation levels of the related kinases pERK1/2 or pS6. As observed with BIX02189, JWG-071 was also able to impede ERK5 activation in the four cell lines (Figure 43C and D). Biologically, JWG-071 decreased, in a dose and time-dependent fashion, the proliferation of the four lung cancer cell lines (Figure 43E).

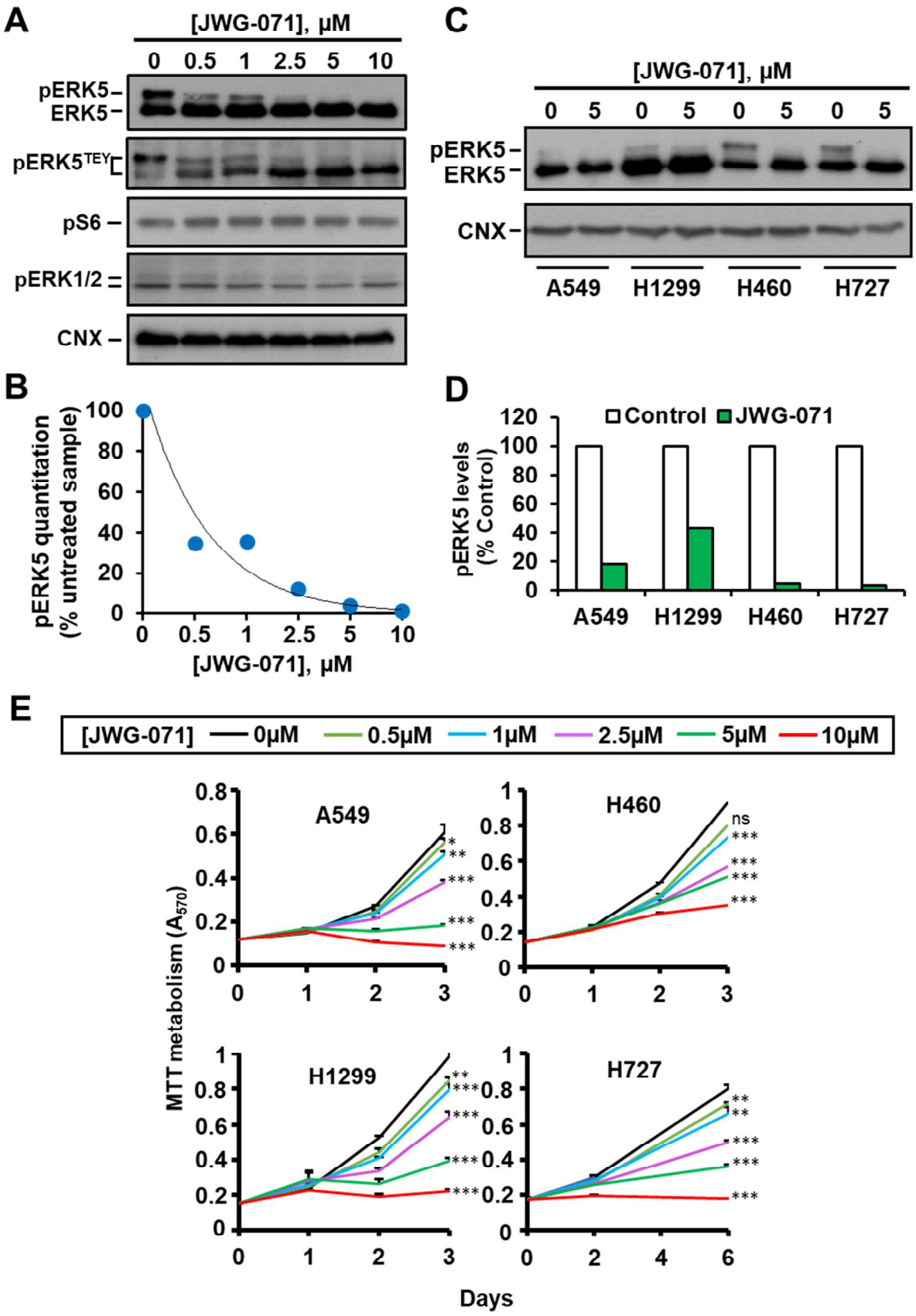


**Figure 43.** A-E) Biochemical and proliferation analyses of H460 cells treated with JWG-071 were performed as describe above for BIX02189 in Figure 42.

To reinforce these findings, the experiments were repeated with the alternative ERK5 inhibitor XMD8-92 (Yang et al.,2010). Similar biochemical and biological results were obtained by using this compound (Figure 44).

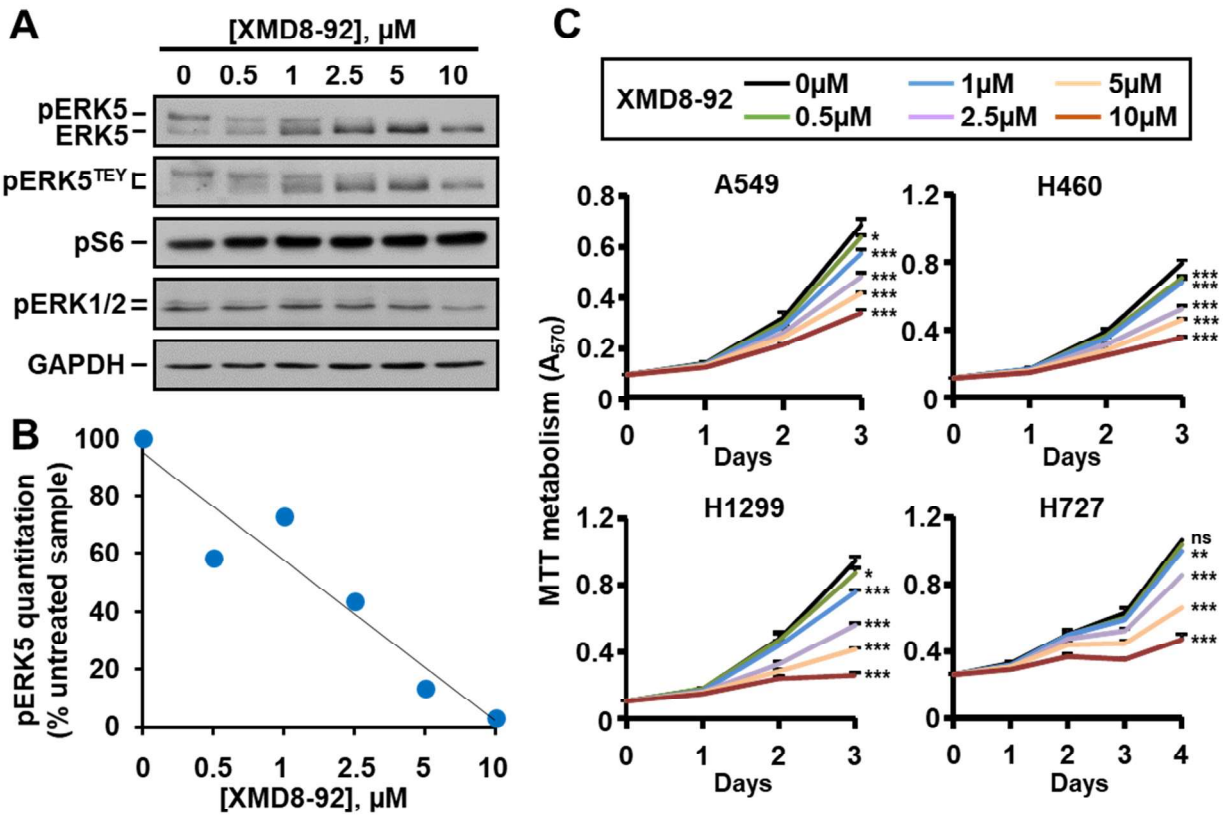


**Figure 44.** A-C) Biochemical and proliferation analyses of H460 cells treated with XMD8-92 were performed as describe above for BIX02189 in Figure 42.

Unlike the results previously observed in NSCLC cells, BIX02189 treatment of non tumoral human epithelial lung cells, which do not have a constitutive activation of the MEK5/ERK5 pathway, exerted a low antiproliferative action (Figure 45). The fact that non tumoral cells are more resistant to the action of BIX02189 than the lung cancer cell lines (Figure 42) offers clues about the existence of a therapeutic index.

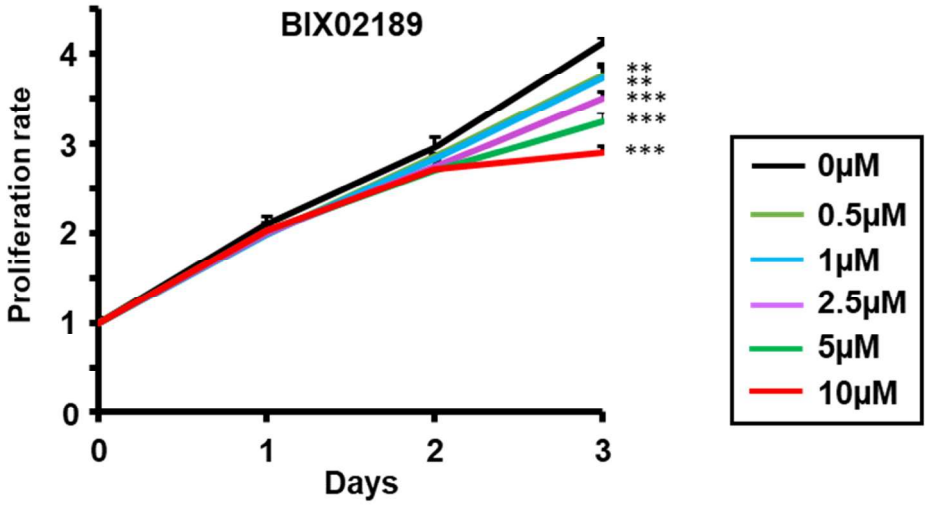


**Figure 45.** Effect of BIX02189 on the proliferation rate of HBEC cells at the indicates doses. Proliferation was measured at the indicated times using MTT metabolization assays. Data are plotted as mean and error bars represent the standard deviation. *, p≤0.05; **, p≤0.01; ***, p≤0.001.

## 1.6 MEK5 inhibition slows cell cycle progression

The decrease in MTT metabolism values caused by BIX02189 could be due to decreased proliferation, increased cell death, or both. To explore whether increased cell death contributed to the mechanism of the antiproliferative action of BIX02189, H460 cells were treated with the drug and Annexin V/propidium iodide staining performed. Treatment for up to three days with the drug did not increase Annexin V-positive staining (Figure 46A). Biochemical analyses of indicators of apoptotic cell death also failed to show an appreciable effect of the drug on their levels (Figure 46B) or caspase 8 and caspase 3 activities (Figure 46C). These data suggested that stimulation of cell death did not participate in the antitumoral action of the drug.

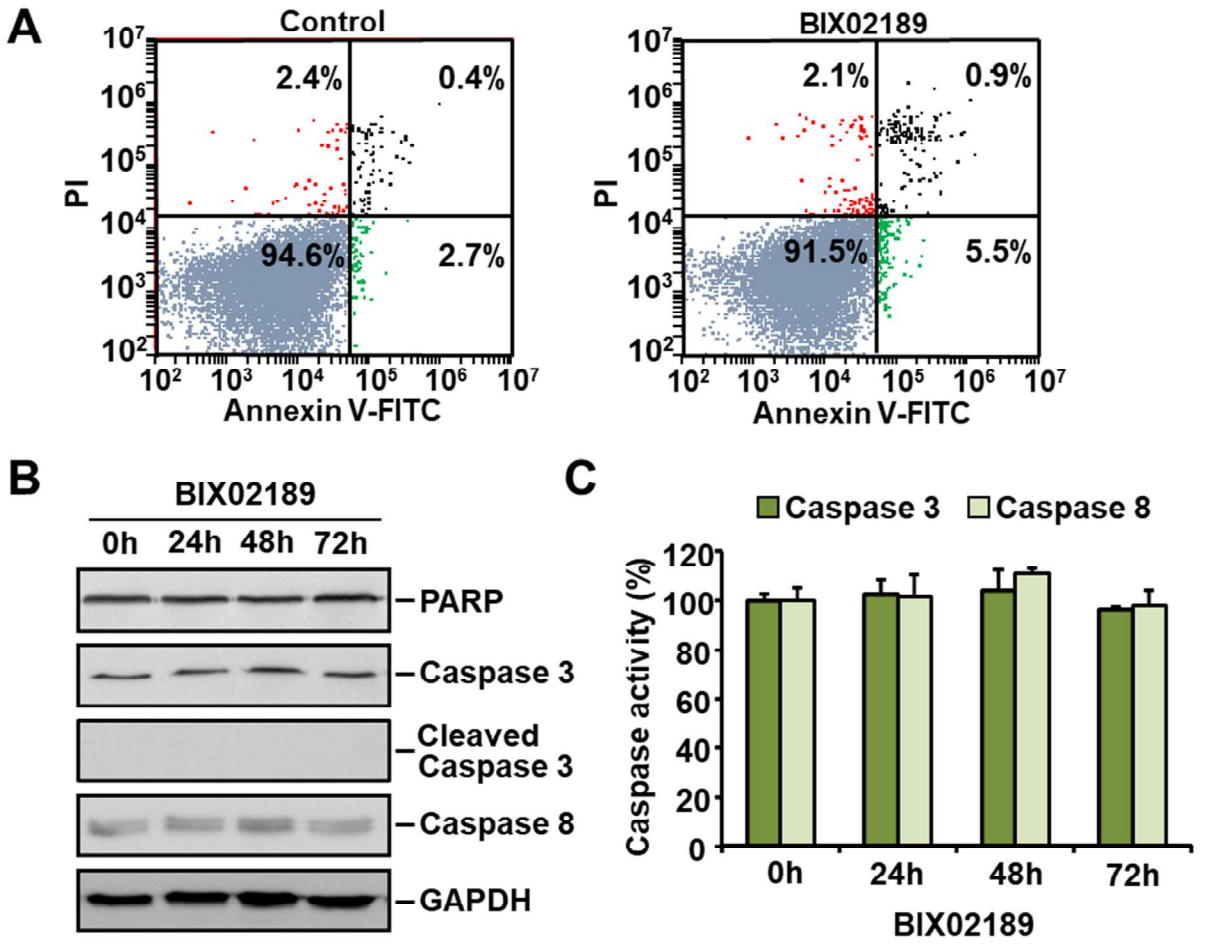


**Figure 46.** A) H460 cells were either untreated or treated with 5 μM BIX02189 for 72 hours and apoptosis was analyzed by Annexin V-FITC assay. B) Biochemical analyses of PARP, caspase 3, cleaved caspase 3 and caspase 8 by Western blotting after 0, 24, 48 or 72 hours of BIX02189 5 μM treatment in the H460 cell line. C) Caspase 3 and caspase 8 activity assays performed at the indicated times after BIX02189 5 μM treatment. Histograms show the mean ± SD of an experiment that was repeated twice.

Propidium iodide staining showed that treatment with BIX02189 significantly increased the number of cells present in the G1 phase of the cell cycle (Figure 47A). The drug decreased DNA synthesis of asynchronous H460 cells, as demonstrated by pulse labeling with BrdU followed by cytometric analysis (Figure 47B). The delay in cell cycle progression was confirmed in cell cycle synchronization experiments. H460 cells were synchronized in mitosis by incubation with nocodazole, and then released in the absence or presence of BIX02189. Parallel cultures of cells were analyzed cytometrically (Figure 47C) and by Western blotting (Figure 47D).

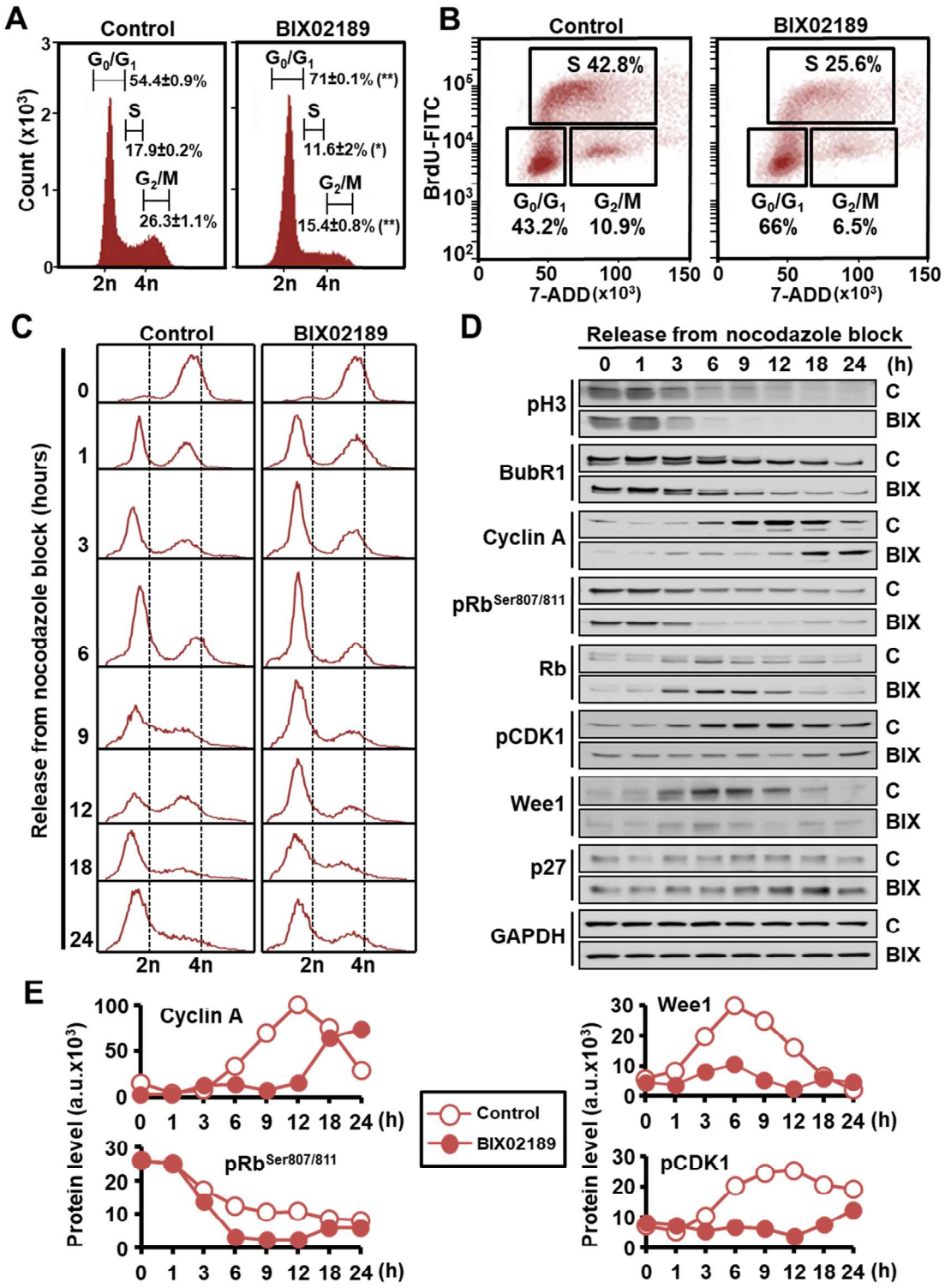


**Figure 47.** A) Cell cycle profile of H460 cells treated with 5 μM BIX02189 and analyzed by FACS at 24 hours. Results are expressed as mean percentage of each cell cycle phase ± SD of an experiment that was repeated three times. *, p≤0.05; **, p≤0.01 for the statistical comparison between the cell cycle phases of control or BIX02189-treated samples. B) BrdU incorporation was coupled to 7-ADD staining and measured at 24 hours using the FITC BrdU Flow Kit to precisely define the percentage of cells undergoing DNA synthesis. C) H460 cells were synchronized in mitosis by nocodazole and then released in the absence or presence of 5 μM BIX02189 for the indicated times and the effect of the drug on the different phases of cell cycle was analyzed by FACS, and D) proteins implicated in cell cycle progression were evaluated by Western blotting. GAPDH was used as loading control. E) Cyclin A, pRB, Wee1 and pCDK1 levels from the previous immunoblots were quantitated and represented.

H460 cells were arrested in M upon incubation with nocodazole as demonstrated by accumulation of phosphorylated histone H3 as well as phosphorylated BubR1, two proteins whose phosphorylation is used as readout for cells in mitosis (Figure 47D). One hour after release from the nocodazole block, a substantial amount of cells had progressed into G1, and such progression was unaffected by BIX02189 (Figure 47C), suggesting that exit from mitosis is unaffected by the drug. The histograms obtained at 9 and 12 hours after release showed that BIX02189-treated cultures accumulated in the G1 phase and did not efficiently progress along the S phase when compared to untreated cells. Biochemically, BIX02189 inhibited phosphorylation of Rb at serines 807/811 (Figure 47D and E). Such phosphorylations are required for adequate progression through G1 (Zarkowska and Mittnacht, 1997). As a result of such inhibition, the levels of total underphosphorylated Rb were higher in cells treated with the drug. p27 levels were also increased in cells incubated with BIX02189. In addition, cyclin A levels increased at earlier times in control cells than in BIX02189-treated cells. The levels of Wee1 and pCDK1, two proteins used as markers of G2/M transition (Den Haese et al., 1995), were also down regulated by treatment with the drug, reflecting the defective progression of cells along the cell cycle, which decreased the reaching of H460-treated cells to the G2 phase of the cell cycle (Figure 47D and E).

## 1.7 Effect of MEK5/ERK5 targeting on the action of standard of care drugs

Since most therapeutic regimens in oncology include combinations of drugs to increase antitumoral responses, we next explored whether neutralization of the MEK5/ERK5 route could increase the action of standard of care drugs used in the lung cancer clinic. In addition to the common platinum (cisplatin and carboplatin) or taxane (pemetrexed and docetaxel) chemotherapeutic agents, we aimed to select the appropriate targeted therapies to use in the combination experiments. To that end, active RTK profiling arrays including most of the receptors whose molecular alteration drive lung cancer were performed on the four lung cancer

cell lines (Figure 48). Among the receptors analyzed EGFR, AXL, ALK, DTK, RYK, Insulin R and IGF-1R showed the highest kinase activation status.

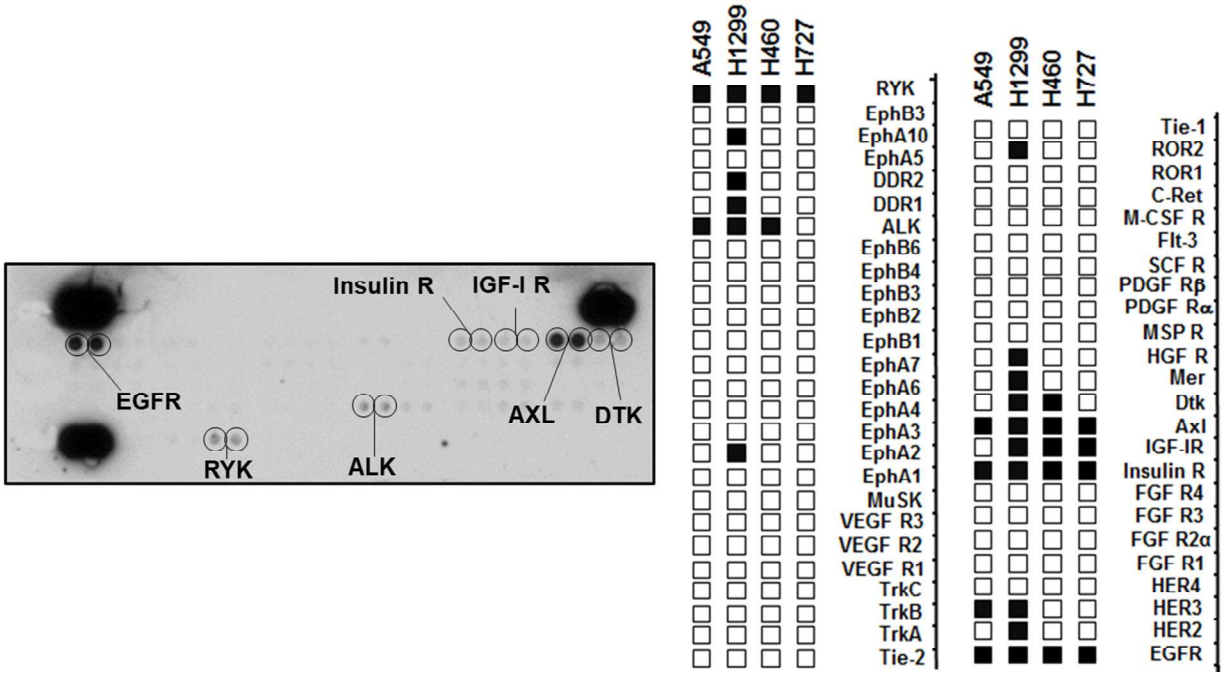


**Figure 48.** Analysis of the activation level of receptor tyrosine kinases in NSCLC cell lines by Human Phospho-RTK Array. Left panel corresponds to the results obtained in the H1299 cell line. Right panel shows a representative diagram of the activation level of each RTK with respect to each cell line, where the black boxes correspond to RTKs considered as over-activated. The evaluation was carried out visually on a scale from 0 to 3 according to the intensity of each immunodetection signal in the development films, considering an RTK as over-activated when its value was equal or higher than 2.

Before performing the proposed combination experiments, the four lung cancer cell lines were individually treated with increasing doses of platinum (cisplatin and carboplatin) or taxane (pemetrexed and docetaxel) chemotherapeutic agents, or targeted therapies (the EGFR TKI gefitinib and the ALK TKI crizotinib). The latter inhibitors were chosen based on the previous active RTK profiling arrays, since both receptors appeared to be constitutively active regardless of their mutational status. Other active RTKs were not selected because the available targeted TKIs blocking their activity have not reached clinical approval for lung cancer therapy. These dose-response experiments using individual treatments allowed to establish the appropriate doses to be used in the combination experiments (Figure 49).

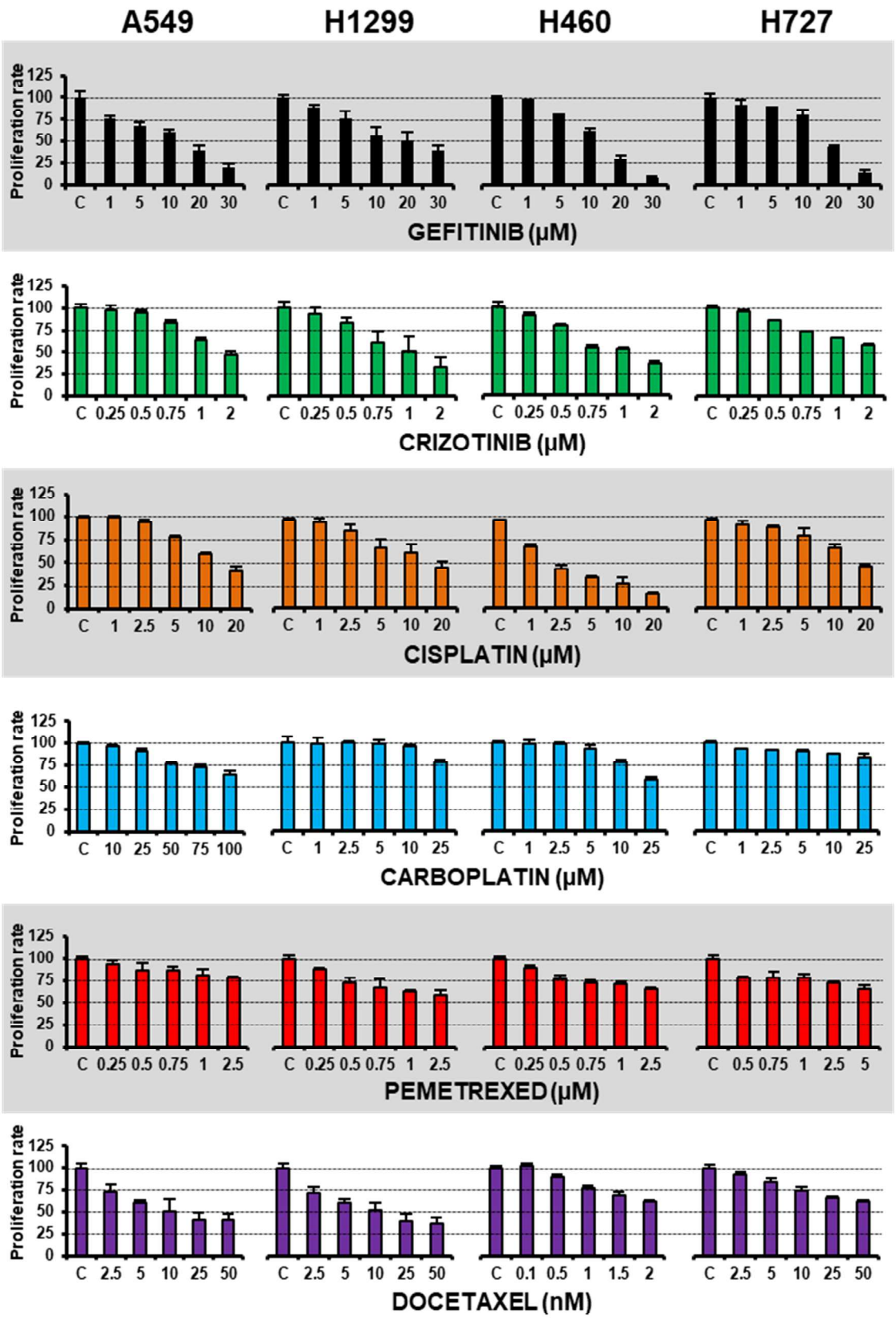


**Figure 49.** Dose-response analyses of the effect on proliferation of NSCLC cell lines of standard of care drugs commonly used in lung cancer clinic. Cell proliferation was measured by the MTT assay, and the results are expressed as mean ± SD of quadruplicates of an experiment that was repeated three times.

Next, suboptimal doses of these standard of care drugs were combined with different doses of BIX02189. The inhibition of proliferation achieved by each combination was measured by the MTT assay and the results were analyzed by the Calcusyn software to evaluate their synergism potential. Figure 50 shows for each cell line the best Combination Index (CI) values of each pharmacological combination, which mostly appeared within the synergistic or additive part of the CI plots.

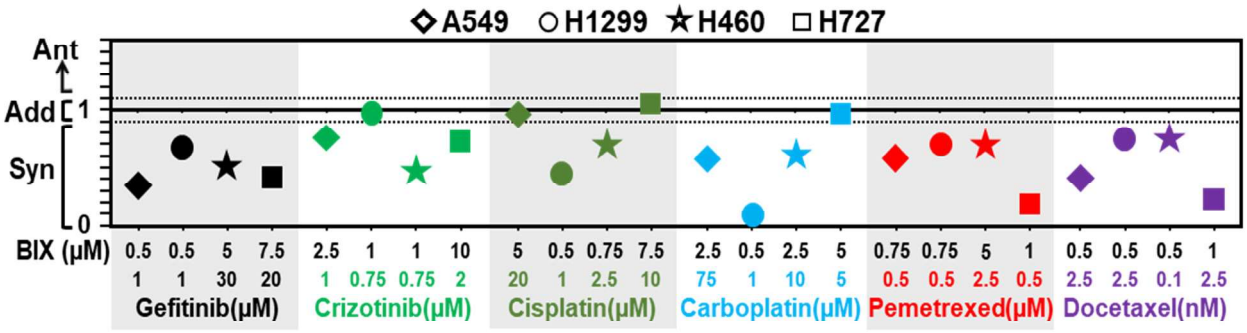


**Figure 50.** NSCLC cells were treated with combinations of indicated doses of BIX02189 and standard of care agents. Cell viability was measured by an MTT assay and the synergistic (CI: 0-0.9), additive (CI: 0.9-1.1) or antagonist effects (CI >1.1) were evaluated using the Calcusyn Software.

Furthermore, the potential synergistic increase of antiproliferative effect of standard of care agents caused by ERK5 abrogation was also explored. To this end, the impact of ERK5 loss of function on drug antitumoral efficacy was analyzed comparing the response of H460 ERK5-KO cells to the response of H460 cells expressing the kinase. H460 SC or H460 ERK5-KO cells were treated with different doses of the previously tested standard of care drugs. Deletion of ERK5 led to an increase in the efficacy of most treatments, especially in the case of cisplatin (Figure 51). Except for gefitinib, the IC50 values of the different treatments were reduced to the half or even more in the H460 ERK5-KO clones when compared to the H460 control cells.

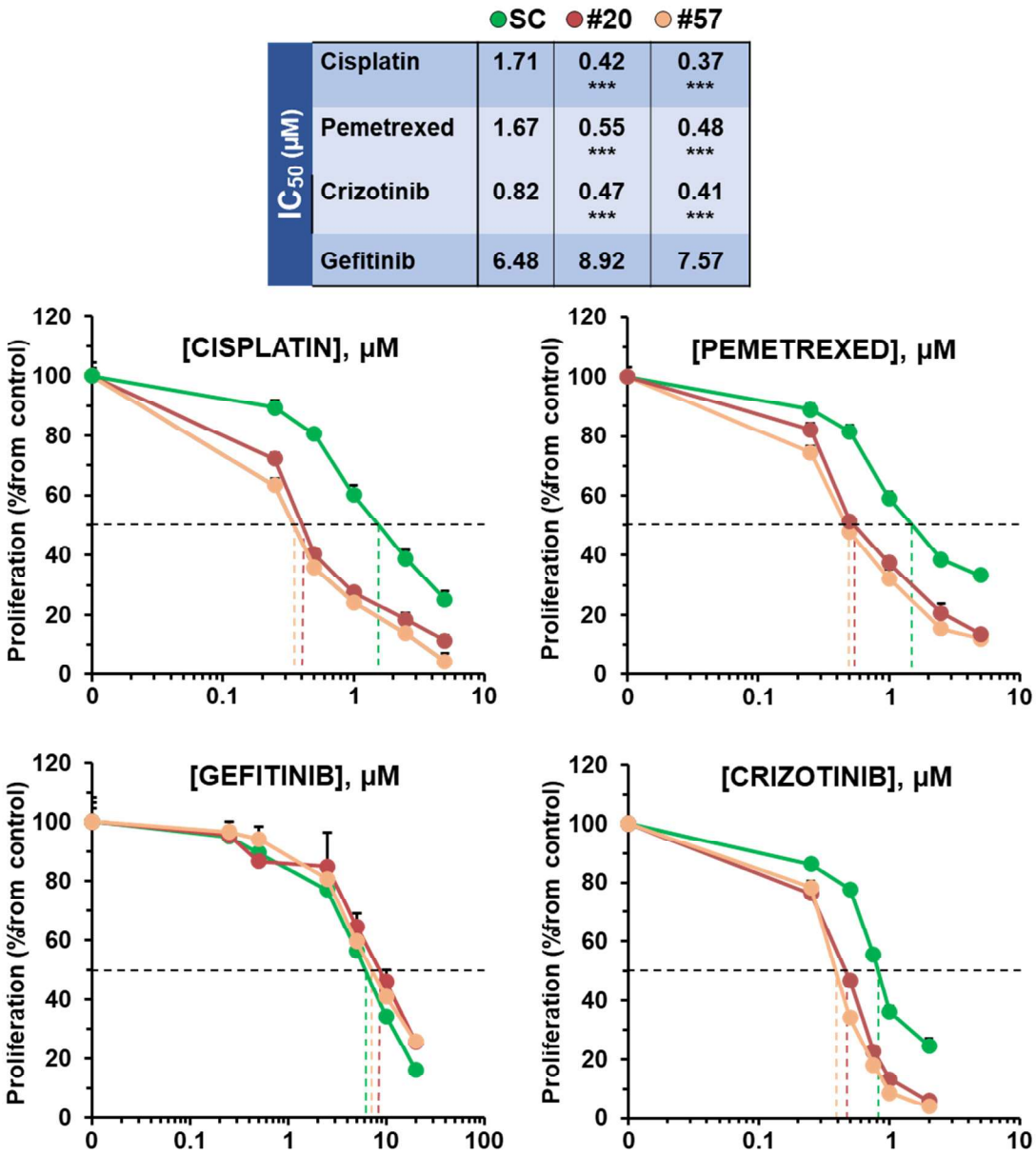


**Figure 51.** H460 scramble cells and H460 ERK5 CRISPR clones (#20 and #57) were plated in 24-well dishes, and 24 hours later treated with the indicated doses of standard of care agents for 48 hours. Cell viability was measured by an MTT assay and each condition (scramble, #20 and #57) was represented as percentage from their respective untreated cells. Results are expressed as mean ± SD of an experiment that was repeated twice. Error bars are shown. The IC50 values and *p*-values for each drug and condition are also indicated (*** p≤0.001).

Our next objective was to explore the therapeutic potential of these treatments *in vivo*. Firstly, the individual effect of MEK5 and ERK5 inhibitors and standard of care drugs were evaluated in mice injected with H460 cells. Gefitinib was excluded from these analyses since the ERK5 abrogation did not showed a noticeable potentiation of its antiproliferative action in the previous experiments. Importantly, treatment with BIX02189 or JWG-071 provoked a

considerable reduction in tumor burden (53.19% and 48.72%, respectively), whose inhibitory effect was similar to that achieved by the standard of care drugs currently used in the clinic (Figure 52). Of note, this antitumoral effect was statistically significant for the MEK5 and ERK5 inhibitors (p-value = 0.007 and 0.019, respectively) and all the other drugs except for the chemotherapeutic agent pemetrexed (p-value = 0.0935).

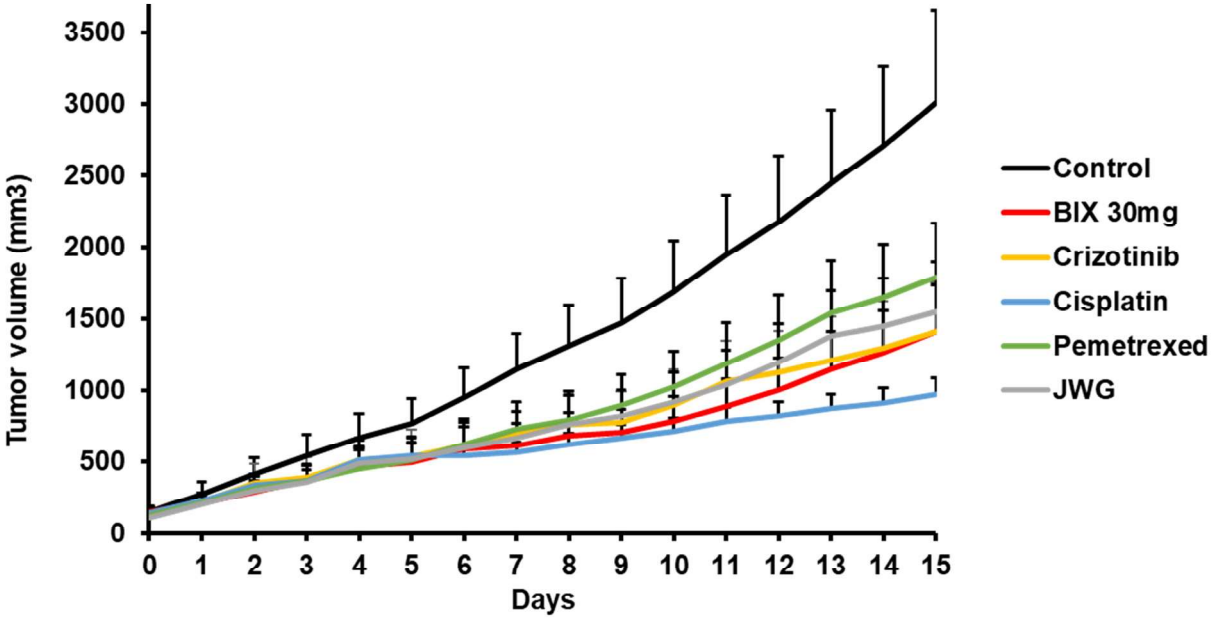


| Tumor growth inhibition (% of Control) | | | | |
|---|---|---|---|---|
| BIX | JWG | Crizo | Cis | Peme |
| 53.19 | 48.72 | 53.20 | 67.67 | 40.62 |

| P-value | BIX | JWG | Crizo | Cis | Peme |
|---|---|---|---|---|---|
| Control | 0.0072 | 0.019 | 0.0072 | 0.0002 | 0.0935 |

**Figure 52.** *In vivo* analyses of the effect of BIX02189, JWG-071, pemetrexed, cisplatin and crizotinib on the growth of H460 cells subcutaneously implanted in mice. Dosages and administration regimes are described in the materials and methods section. Tumor masses (n=8-10 tumors per group) were measured daily for two weeks. The mean tumor volume and SEM error bars of each group are represented. Tumor growth inhibition and exact *p*-values of comparisons between control untreated and treated groups are indicated in the tables shown below.

It is important to highlight that BIX02189 and JWG-071 decreased the pERK5/ERK5 ratio of the tumors from mice treated with these compounds, indicating that they were also able to inhibit MEK5/ERK5 pathway activation *in vivo* (Figure 53).

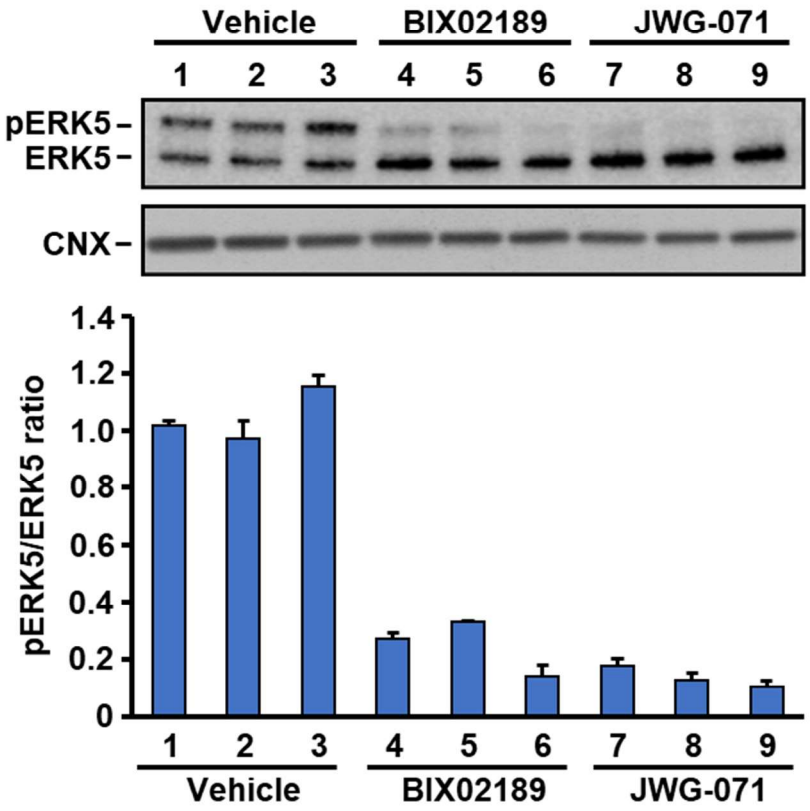


**Figure 53.** pERK5 and ERK5 levels in tumors (n=3 per condition) from mice treated with vehicle, BIX02189 or JWG-071. Samples were analyzed by immunoprecipitating 1 mg of protein followed by Western blotting with the anti-ERK5 antibody. Calnexin was used as loading control (upper panel). Quantitative analysis of pERK5/ERK5 ratios in tumors from mice xenografted with H460 cells and treated as indicated. Westerns (n=2) were quantitated using the Image Lab software, and the results represented mean ± SD (lower panel).

Finally, the effect of BIX02189 or JWG-071 in combination with the standard of care agents was tested *in vivo*. As observed in Figure 54A and B, the combination of BIX02189 or JWG-071 with these standard of care drugs exerted a noticeable antitumoral effect that was statistically significant in all cases (Figure 54C). However, while combination of BIX02189 or JWG-071 with pemetrexed or crizotinib did not reach a higher effect than individual treatments, combination of MEK5 or ERK5 inhibitors with cisplatin exerted an antiproliferative effect on the growth of the H460 xenografted tumors (90.37% for BIX02189+Cis and 82.85% for JWG-071+Cis, Figure 54D) markedly higher than the effect of the individual treatments (ranging from 48% to 53%, Figure 52). In addition, both combinations reached statistical significance when compared to individual treatments (Figure 54E).

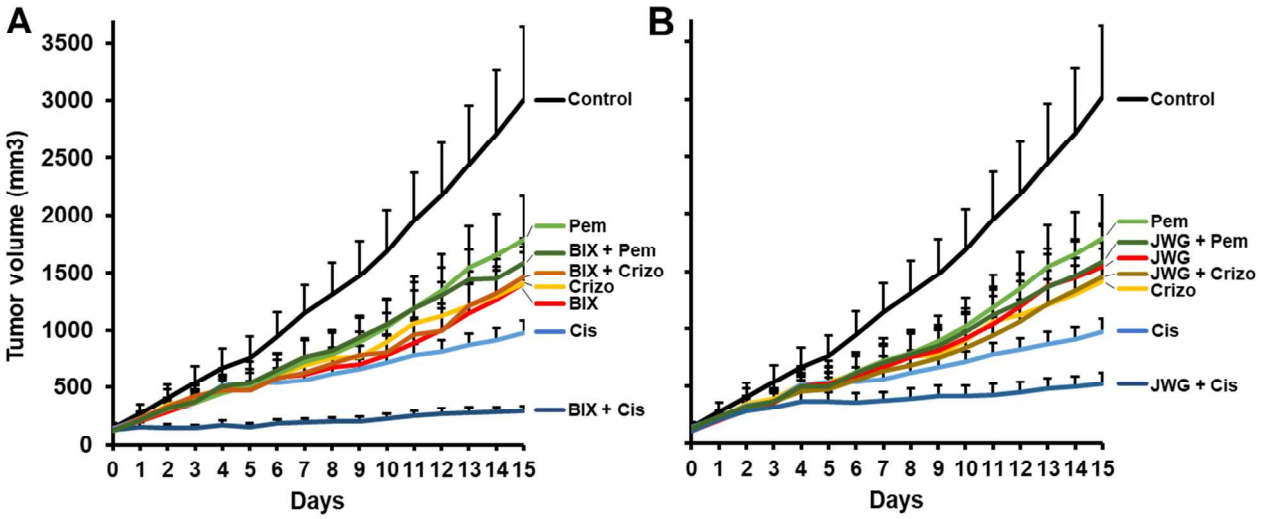


C

| Tumor growth inhibition (% of Control) | | | | | |
|---|---|---|---|---|---|
| Bix-Crizo | Bix-Cis | Bix-Peme | JWG-Crizo | JWG-Cis | JWG-Peme |
| 51.46 | 90.37 | 47.22 | 51.63 | 82.85 | 47.37 |

D

| P-value | BIX-Crizo | BIX-Cis | BIX-Peme | JWG-Crizo | JWG-Cis | JWG-Peme |
|---|---|---|---|---|---|---|
| Control | 0.0106 | <0.0001 | 0.0259 | 0.0102 | <0.0001 | 0.0251 |

E

| P-value | BIX-Crizo | Bix-Cis | Bix-Peme | JWG-Crizo | JWG-Cis | JWG-Peme |
|---|---|---|---|---|---|---|
| BIX | 0.7394 | 0.0009 | 0.2799 | | | |
| JWG | | | | 0.9705 | 0.0021 | 0.7959 |
| Crizo | 0.5787 | | | 0.5787 | | |
| Cis | | <0.0001 | | | 0.0052 | |
| Peme | | | 0.9118 | | | 0.6305 |

**Figure 54.** A) *In vivo* analyses of the effect of BIX02189 and B) JWG-071 in combination with standard of care drugs, on the growth of H460 cells subcutaneously implanted in mice and treated with the indicated drugs as described under the materials and methods section. Tumor masses (n=8-10 tumors per group) were measured daily for two weeks. The mean tumor volume and SEM error bars of each group are represented. To avoid excessive overlapping of the curves, the data of the drug combination with BIX02189 or JWG-071 were split in panels A) and B). Therefore, please notice that the curves for control, pemetrexed, crizotinib or cisplatin are the same in both A) and B). C) Table summarizing the tumor growth inhibition achieved by each combination, calculated as percentage from growth of control untreated tumors. D) Exact *p*-values of comparisons between control and combination treated groups. E) Exact *p*-values of comparisons between the growth of groups individually treated or treated with a combination of drugs.

## 1.8 DISCUSSION

Lung cancer represents the leading cause of cancer death worldwide (Travis et al., 2015). Not only because of its frequency, but also considering its dismal prognosis in advanced stages, intense efforts are being devoted to the development of novel therapeutic strategies to fight the disease (Bunn et al., 2012). In this respect, identification of new oncogenic drivers offers therapeutic opportunities in tumors in which those drivers play a pathophysiological role.

In this thesis project, we show that the MEK5/ERK5 pathway contributes to the pathogenesis of lung cancer, opening the possibility of its targeting with therapeutic purposes. We initiated this study with the aim of evaluating the oncogenic potential of that MAPK route. In fact, and despite accumulation of reports suggesting that the MEK5/ERK5 pathway may have a role in tumor progression, whether such route directly promotes tumor development has not previously been addressed. Using a transgenic mouse model, we observed that expression of a constitutively active form of MEK5 provoked lung ADCs. This is conceptually relevant as demonstrates that the sole activation of the MEK5/ERK5 route causes tumorigenesis. Moreover, the fact that incidence of lung adenocarcinomas is much higher than tumors in other MEK5DD-expressing organs underscores the role of MEK5 in lung cancer.

The appearance of lung carcinomas in the MEK5 transgenic mice fostered additional studies aimed at deciphering the relevance of the MEK5/ERK5 pathway in human lung cancer. Biochemical analyses of MEK5 and ERK5 in lung adenocarcinoma patient samples revealed an activation of both proteins when compared to their normal lung counterparts. Moreover, these studies also demonstrated higher expression of MEK5 and ERK5 in the human tumoral samples. Importantly, analyses of public databases highlighted the clinical relevance of the latter finding, since they pointed out that increased levels of MEK5/ERK5 are associated with worse outcome. It is of interest to note that this association reduced approximately by half the median survival of the high MEK5/ERK5 expression subset of lung adenocarcinoma patients, irrespective of their smoking history.

Several circumstances may explain the activation/overexpression of MEK5/ERK5 pathway in lung cancer. Fluorescence in situ hybridization analyses identified ERK5 gene amplification in 4% of non-small cell lung cancers (Gavine et al., 2015). Gene amplification provokes increased expression that in turn may favor pathway activation. In fact, overexpression of ERK5 has also been reported in triple negative breast tumors and is associated with increased activity of the pathway (Ortiz-Ruiz et al., 2014). An amplification of the region where ERK5 is located has been detected in approximately 50% of primary hepatocellular adenocarcinoma tumors (Zen et al., 2009) and, in addition, it has been shown that ERK5 modulates tumor development in this type of carcinoma (Rovida et al., 2015). Other genetic studies have linked the MEK5/ERK5 route to lung cancer. Thus, genome-wide association studies (GWAS) revealed that the chromosomal regions in which the MEK5 (15q23) and ERK5 (17p11.2) genes are located are potentially susceptible regions of lung cancer risk (Repapi et al., 2010) In addition, a recent study demonstrated that an atypical allele polymorphism in the ERK5 gene in the Chinese population was associated with increased lung cancer risk in smokers (Qiu et al., 2013). It is noteworthy to comment that exposure to cigarette smoke, a common risk factor for lung cancer, leads to ERK5 activation (Zhong et al., 2005). Moreover, certain EGFR mutants such as the G719S and L858R found in lung cancer have been reported to activate the MEK5/ERK5 route (Jiang et al., 2005b). While our study did not focus on the analysis of a potential link between oncogene-driven lung cancer and the MEK5/ERK5 route, the fact that RAS (English et al., 1998), EGFR (Kato et al., 1998) or ALK (Umapathy et al., 2014) have been reported to activate that pathway raises the interesting possibility that prooncogenic signaling by those upstream drivers may use the MEK5/ERK5 route. This deserves careful study, especially considering potential therapeutic implications. On the other hand, the downstream signaling consequences of the constitutive activation of this pathway in lung cancer remain unknown. But it would come at no surprise that the implication of this pathway in the pathogenesis of lung tumors was based on the dysregulation of key transcription factors located downstream of ERK5. For instance, alteration of the transcription factor Twist1, which is known to be regulated by ERK5 singnaling (Antoon et al., 2013), has

already been reported to promote lung tumorigenesis (Tran et al., 2012). Another possibility would point to dysregulation of specific ERK5 phosphatases such as MKP-1 (Sarközi et al., 2007), which has also been involved in lung cancer promotion (Vicent et al., 2004), as the potential mechanism mediating the prooncogenic constitutive activated status of the pathway in the human disease. The above-mentioned hypotheses are also supported by the discovery that none of the NSCLC cell lines studied presented MEK5 activating mutations, which points to altered signaling mechanisms as the most likely cause of the constitutive activation of this pathway in lung cancer. It is also relevant to mention that, while gains or amplifications of MEK5/ERK5 are present in a relevant percentage of lung cancer patients, analyses of the TCGA data revealed a low incidence of MEK5 or ERK5 mutations, therefore indicating that the latter cannot be the principal mechanism of pathway activation nor the alteration responsible of the pathogenic role of this pathway in a vast majority of patients. Nevertheless, the relevance of those mutations on patient outcome or their impact on the function of these kinases remains to be established.

Considering the medical need that lung cancer represents, the finding that the MEK5/ERK5 route has a pathophysiological role in lung cancer opens the possibility of its targeting for therapeutic purposes. To explore such possibility, genetic and pharmacologic strategies were used. *In vitro* studies using different NSCLC cell lines showed that these cells expressed MEK5 and ERK5, with pERK5 present under resting conditions, therefore indicating that the MEK5/ERK5 route is constitutively active.

Knockdown experiments revealed that MEK5 or ERK5 were required for the proliferation of lung cancer cells *in vitro* and for their tumorigenic potential *in vivo*. In addition, knockout of ERK5 or MEK5 also resulted in decreased cell proliferation *in vitro* and *in vivo*. In the latter models, the lack of ERK5 or MEK5 profoundly influenced tumor growth and had a significant effect on the proliferation marker Ki67. Of note, in those *in vivo* models, the antitumoral effect of ERK5 or MEK5 deletions was severe, underlining the relevance of the MEK5/ERK5 route in the pathophysiology of these tumors. In fact, ERK5 has been reported to

facilitate *in vivo* angiogenesis (Hayashi et al., 2005), which is expected to contribute to the increase in size of tumors.

In line with the genetic data were the findings obtained with drugs that target MEK5 or ERK5. Thus, *in vitro* pharmacologic studies carried out with MEK5 or ERK5 inhibitors indicated that these drugs inhibited pathway activity and also inhibited proliferation of lung cancer cell lines. Moreover, *in vitro* genetic-pharmacologic studies showed that deletion of ERK5 augmented the antitumoral effect of therapy currently used in the lung cancer clinic. Such effect was especially relevant in the case of cisplatin, whose antitumoral action was also potentiated *in vivo* by pharmacological targeting of MEK5 or ERK5. The latter is particularly important, since increases in the action of standard of care drugs is desirable for the clinical development of novel drugs.

Mechanistic studies indicated that the MEK5 inhibitor exerted its antiproliferative effect by slowing progression of cells along the G1 phase into S. Such delay in progression was confirmed in cell cycle synchronization experiments. In cells treated with BIX02189, the increase in cyclin A was substantially delayed with respect to control untreated cells. In addition, phosphorylation of Rb at serines 807/811, which is controlled by CDKs 2, 3, 4 and 6 and is required for adequate cell cycle progression (Brantley et al., 2000; Brugarolas et al., 1999; Ren and Rollins., 2004), was inhibited by the drug. These data indicate that progression of lung cancer cells along the cell cycle requires integrity of the MEK5/ERK5 pathway.

In conclusion, we show here that the sole activation of MEK5 provokes lung tumorigenesis. Our transgenic mice study not only demonstrated the oncogenic potential of the MEK5 route but combined with the clinical data and the functional studies supports that targeting the MEK5/ERK5 route may represent a novel therapeutically relevant strategy worth being explored in lung cancer, particularly in combination with standard of care drugs. Such strategy requires identification of patients which may benefit from therapies that target this pathway. In this regard, the studies presented here show a relation between high levels of MEK5/ERK5 and patient outcome. Therefore, analyses of those levels could be used as an

initial step to select patients for a potential therapy targeting this pathway. This criterion could be complemented with an analysis of MEK5/ERK5 pathway activation. At present, the best redout of pathway activation is the analysis of pERK5. However, measurement of pERK5 in patient samples is limited by two factors. First, routine studies of pERK5 by Western blotting in patient samples appears more complicated than immunohistochemical analyses, as it requires fresh samples and a procedure not well standardized across pathology laboratories. On the other hand, one of the limitations of the use of anti-pERK5 antibodies in immunohistochemistry is their cross-reactivity with pERK1/2. A possible alternative to these methods could be the identification of genes or genesets whose expression would indicate a pathophysiological role of MEK5/ERK5 in tumor progression. In this direction, gene expression microarrays have been recently performed in our laboratory to unveil the genes diferentially expressed upon pathway blockade (control NSCLC cells versus MEK5 and ERK5 knockout clones) or pathway activation (normal lung tissue from wild-type mice versus tumoral lung tissue from MEK5DD mice). Such studies may allow the identification of an adequate way of biomarking this route with the purpose of patient selection. Besides definition of patients that may benefit from targeting the MEK5/ERK5 pathway, efforts directed at developing clinical stage drugs that specifically target this pathway should offer novel therapeutic opportunities to fight lung cancer and potentially other tumors in which this pathway plays a pathophysiological role.

# *BIBLIOGRAPHY*

Abe J, Kusuhara M, Ulevitch RJ, Berk BC, Lee JD. Big mitogen-activated protein kinase 1 (BMK1) is a redox-sensitive kinase. *J Biol Chem*. 1996;271(28):16586-16590. doi:10.1074/jbc.271.28.16586
Abe Ji, Takahashi M, Ishida M, Lee JD, Berk BC. c-Src is required for oxidative stress-mediated activation of big mitogen-activated protein kinase 1. *J Biol Chem*. 1997;272(33):20389-20394. doi:10.1074/jbc.272.33.20389
Abubaker K, Luwor RB, Zhu H, et al. Inhibition of the JAK2/STAT3 pathway in ovarian cancer results in the loss of cancer stem cell-like characteristics and a reduced tumor burden. *BMC Cancer*. 2014;14:317. Published 2014 May 6. doi:10.1186/1471-2407-14-317
Adams NR, Vasquez YM, Mo Q, Gibbons W, Kovanci E, DeMayo FJ. WNK lysine deficient protein kinase 1 regulates human endometrial stromal cell decidualization, proliferation, and migration in part through mitogen-activated protein kinase 7. *Biol Reprod*. 2017;97(3):400-412. doi:10.1093/biolre/iox108
Ahmad I, Singh LB, Yang ZH, et al. Mir143 expression inversely correlates with nuclear ERK5 immunoreactivity in clinical prostate cancer. *Br J Cancer*. 2013;108(1):149-154. doi:10.1038/bjc.2012.510
Ahmed AA, Etemadmoghadam D, Temple J, et al. Driver mutations in TP53 are ubiquitous in high grade serous carcinoma of the ovary. *J Pathol*. 2010;221(1):49-56. doi:10.1002/path.2696
Ahn G, Folkins AK, McKenney JK, Longacre TA. Low-grade Serous Carcinoma of the Ovary: Clinicopathologic Analysis of 52 Invasive Cases and Identification of a Possible Noninvasive Intermediate Lesion. *Am J Surg Pathol*. 2016;40(9):1165-1176. doi:10.1097/PAS.0000000000000693
Allen MS, Darling GE, Pechet TT, et al. Morbidity and mortality of major pulmonary resections in patients with early-stage lung cancer: initial results of the randomized, prospective ACOSOG Z0030 trial. *Ann Thorac Surg*. 2006;81(3):1013-1020. doi:10.1016/j.athoracsur.2005.06.066
Álvarez-Fernández S, Ortiz-Ruiz MJ, Parrott T, et al. Potent antimyeloma activity of a novel ERK5/CDK inhibitor. *Clin Cancer Res*. 2013;19(10):2677-2687. doi:10.1158/1078-0432.CCR-12-2118
American Cancer Society. Cancer Facts & Figures 2021. Atlanta, Ga: American Cancer Society; 2021.
Antonia SJ, Villegas A, Daniel D, et al. Overall Survival with Durvalumab after Chemoradiotherapy in Stage III NSCLC. *N Engl J Med*. 2018;379(24):2342-2350. doi:10.1056/NEJMoa1809697
Antoon JW, Martin EC, Lai R, et al. MEK5/ERK5 signaling suppresses estrogen receptor expression and promotes hormone-independent tumorigenesis. *PLoS One*. 2013;8(8):e69291. Published 2013 Aug 9. doi:10.1371/journal.pone.0069291
Aoki D. Annual report of Gynecologic Oncology Committee, Japan Society of Obstetrics and Gynecology, 2013. *J Obstet Gynaecol Res*. 2014;40(2):338-348. doi:10.1111/jog.12360
Arcila ME, Drilon A, Sylvester BE, et al. MAP2K1 (MEK1) Mutations Define a Distinct Subset of Lung Adenocarcinoma Associated with Smoking. *Clin Cancer Res*. 2015;21(8):1935-1943. doi:10.1158/1078-0432.CCR-14-2124
Auersperg N. The origin of ovarian cancers--hypotheses and controversies. *Front Biosci (Schol Ed)*. 2013;5:709-719. Published 2013 Jan 1. doi:10.2741/s401
Badshah II, Baines DL, Dockrell ME. Erk5 is a mediator to TGFβ1-induced loss of phenotype and function in human podocytes. *Front Pharmacol*. 2014;5:71. Published 2014 Apr 21. doi:10.3389/fphar.2014.00071
Bardwell AJ, Frankson E, Bardwell L. Selectivity of docking sites in MAPK kinases. *J Biol Chem*. 2009;284(19):13165-13173. doi:10.1074/jbc.M900080200
Barta JA, Powell CA, Wisnivesky JP. Global Epidemiology of Lung Cancer. *Ann Glob Health*. 2019;85(1):8. Published 2019 Jan 22. doi:10.5334/aogh.2419
Bhattacharya S, Calar K, Evans C, Petrasko M, de la Puente P. Bioengineering the Oxygen-Deprived Tumor Microenvironment Within a Three-Dimensional Platform for Studying Tumor-Immune Interactions. *Front Bioeng Biotechnol*. 2020;8:1040. Published 2020 Sep 4. doi:10.3389/fbioe.2020.01040 **(a)**
Bhattacharya S, Calar K, de la Puente P. Mimicking tumor hypoxia and tumor-immune interactions employing three-dimensional in vitro models. *J Exp Clin Cancer Res*. 2020;39(1):75. Published 2020 May 1. doi:10.1186/s13046-020-01583-1 **(b)**
Battafarano RJ, Fernandez FG, Ritter J, et al. Large cell neuroendocrine carcinoma: an aggressive form of non-small cell lung cancer. *J Thorac Cardiovasc Surg*. 2005;130(1):166-172. doi:10.1016/j.jtcvs.2005.02.064
Bedard PL, Tabernero J, Janku F, et al. A phase Ib dose-escalation study of the oral pan-PI3K inhibitor buparlisib (BKM120) in combination with the oral MEK1/2 inhibitor trametinib (GSK1120212) in patients with selected advanced solid tumors. *Clin Cancer Res*. 2015;21(4):730-738. doi:10.1158/1078-0432.CCR-14-1814
Benito-Jardón L, Díaz-Martínez M, Arellano-Sánchez N, Vaquero-Morales P, Esparís-Ogando A, Teixidó J. Resistance to MAPK Inhibitors in Melanoma Involves Activation of the IGF1R-MEK5-Erk5 Pathway. *Cancer Res*. 2019;79(9):2244-2256. doi:10.1158/0008-5472.CAN-18-2762
Bhatt AB, Patel S, Matossian MD, et al. Molecular Mechanisms of Epithelial to Mesenchymal Transition Regulated by ERK5 Signaling. *Biomolecules*. 2021;11(2):183. Published 2021 Jan 29. doi:10.3390/biom11020183
Blank JL, Gerwins P, Elliott EM, Sather S, Johnson GL. Molecular cloning of mitogen-activated protein/ERK kinase kinases (MEKK) 2 and 3. Regulation of sequential phosphorylation pathways involving mitogen-activated protein kinase and c-Jun kinase. *J Biol Chem*. 1996;271(10):5361-5368. doi:10.1074/jbc.271.10.5361
Blank C, Gajewski TF, Mackensen A. Interaction of PD-L1 on tumor cells with PD-1 on tumor-specific T cells as a mechanism of immune evasion: implications for tumor immunotherapy. *Cancer Immunol Immunother*. 2005;54(4):307-314. doi:10.1007/s00262-004-0593-x
Boffetta P, Pershagen G, Jöckel KH, et al. Cigar and pipe smoking and lung cancer risk: a multicenter study from Europe. *J Natl Cancer Inst*. 1999;91(8):697-701. doi:10.1093/jnci/91.8.697
Borges J, Pandiella A, Esparís-Ogando A. Erk5 nuclear location is independent on dual phosphorylation, and favours resistance to TRAIL-induced apoptosis. *Cell Signal*. 2007;19(7):1473-1487. doi:10.1016/j.cellsig.2007.01.023
Bosetti C, Malvezzi M, Rosso T, et al. Lung cancer mortality in European women: trends and predictions. *Lung Cancer*. 2012;78(3):171-178. doi:10.1016/j.lungcan.2012.08.008
Brambilla C, Laffaire J, Lantuejoul S, et al. Lung squamous cell carcinomas with basaloid histology represent a specific molecular entity. *Clin Cancer Res*. 2014;20(22):5777-5786. doi:10.1158/1078-0432.CCR-14-0459
Brantley MA Jr, Harbour JW. Inactivation of retinoblastoma protein in uveal melanoma by phosphorylation of sites in the COOH-terminal region. *Cancer Res*. 2000;60(16):4320-4323.
Bray F, Ferlay J, Soerjomataram I, Siegel RL, Torre LA, Jemal A. Global cancer statistics 2018: GLOBOCAN estimates of incidence and mortality worldwide for 36 cancers in 185 countries [published correction appears in CA Cancer J Clin. 2020 Jul;70(4):313]. *CA Cancer J Clin*. 2018;68(6):394-424. doi:10.3322/caac.21492
Brenner DR, Boffetta P, Duell EJ, et al. Previous lung diseases and lung cancer risk: a pooled analysis from the International Lung Cancer Consortium. *Am J Epidemiol*. 2012;176(7):573-585. doi:10.1093/aje/kws151

Brugarolas J, Moberg K, Boyd SD, Taya Y, Jacks T, Lees JA. Inhibition of cyclin-dependent kinase 2 by p21 is necessary for retinoblastoma protein-mediated G1 arrest after gamma-irradiation. *Proc Natl Acad Sci U S A*. 1999;96(3):1002-1007. doi:10.1073/pnas.96.3.1002

Bunn PA Jr. Worldwide overview of the current status of lung cancer diagnosis and treatment. *Arch Pathol Lab Med*. 2012;136(12):1478-1481. doi:10.5858/arpa.2012-0295-SA

Burger RA, Brady MF, Bookman MA, et al. Incorporation of bevacizumab in the primary treatment of ovarian cancer. *N Engl J Med*. 2011;365(26):2473-2483. doi:10.1056/NEJMoa1104390

Buschbeck M, Eickhoff J, Sommer MN, Ullrich A. Phosphotyrosine-specific phosphatase PTP-SL regulates the ERK5 signaling pathway. *J Biol Chem*. 2002;277(33):29503-29509. doi:10.1074/jbc.M202149200

Buschbeck M, Ullrich A. The unique C-terminal tail of the mitogen-activated protein kinase ERK5 regulates its activation and nuclear shuttling. *J Biol Chem*. 2005;280(4):2659-2667. doi:10.1074/jbc.M412599200

Calar K, Plesselova S, Bhattacharya S, Jorgensen M, de la Puente P. Human Plasma-Derived 3D Cultures Model Breast Cancer Treatment Responses and Predict Clinically Effective Drug Treatment Concentrations. *Cancers (Basel)*. 2020;12(7):1722. Published 2020 Jun 29. doi:10.3390/cancers12071722

Caliman LP, Tavares RL, Piedade JB, et al. Evaluation of microsatellite instability in women with epithelial ovarian cancer. *Oncol Lett*. 2012;4(3):556-560. doi:10.3892/ol.2012.776

Cameron SJ, Abe J, Malik S, Che W, Yang J. Differential role of MEK5alpha and MEK5beta in BMK1/ERK5 activation. *J Biol Chem*. 2004;279(2):1506-1512. doi:10.1074/jbc.M308755200 (a)

Cameron SJ, Itoh S, Baines CP, et al. Activation of big MAP kinase 1 (BMK1/ERK5) inhibits cardiac injury after myocardial ischemia and reperfusion. *FEBS Lett*. 2004;566(1-3):255-260. doi:10.1016/j.febslet.2004.03.120 (b)

Canagarajah BJ, Khokhlatchev A, Cobb MH, Goldsmith EJ. Activation mechanism of the MAP kinase ERK2 by dual phosphorylation. *Cell*. 1997;90(5):859-869. doi:10.1016/s0092-8674(00)80351-7

Cancer Genome Atlas Research Network. Integrated genomic analyses of ovarian carcinoma. Nature. 2011;474:609–15.

Cao Z, Gao Q, Fu M, Ni N, Pei Y, Ou WB. Anaplastic lymphoma kinase fusions: Roles in cancer and therapeutic perspectives. *Oncol Lett*. 2019;17(2):2020-2030. doi:10.3892/ol.2018.9856

Cappuzzo F, Jänne PA, Skokan M, et al. MET increased gene copy number and primary resistance to gefitinib therapy in non-small-cell lung cancer patients. *Ann Oncol*. 2009;20(2):298-304. doi:10.1093/annonc/mdn635

Cappuccio S, Distefano MG, Ghizzoni V, Fagotti A, Scambia G. Trametinib response in heavily pretreated high-grade ovarian cancer: One step towards precision medicine. *Gynecol Oncol Rep*. 2020;32:100547. Published 2020 Feb 13. doi:10.1016/j.gore.2020.100547

Cardarella S, Ogino A, Nishino M, et al. Clinical, pathologic, and biologic features associated with BRAF mutations in non-small cell lung cancer. *Clin Cancer Res*. 2013;19(16):4532-4540. doi:10.1158/1078-0432.CCR-13-0657

Cargnello M, Roux PP. Activation and function of the MAPKs and their substrates, the MAPK-activated protein kinases [published correction appears in Microbiol Mol Biol Rev. 2012 Jun;76(2):496]. *Microbiol Mol Biol Rev*. 2011;75(1):50-83. doi:10.1128/MMBR.00031-10

Carvajal-Vergara X, Tabera S, Montero JC, et al. Multifunctional role of Erk5 in multiple myeloma. *Blood*. 2005;105(11):4492-4499. doi:10.1182/blood-2004-08-2985

Castro NE, Lange CA. Breast tumor kinase and extracellular signal-regulated kinase 5 mediate Met receptor signaling to cell migration in breast cancer cells. *Breast Cancer Res*. 2010;12(4):R60. doi:10.1186/bcr2622

Cavanaugh JE, Ham J, Hetman M, Poser S, Yan C, Xia Z. Differential regulation of mitogen-activated protein kinases ERK1/2 and ERK5 by neurotrophins, neuronal activity, and cAMP in neurons. *J Neurosci*. 2001;21(2):434-443. doi:10.1523/JNEUROSCI.21-02-00434.2001

Cerami E, Gao J, Dogrusoz U, et al. The cBio cancer genomics portal: an open platform for exploring multidimensional cancer genomics data [published correction appears in Cancer Discov. 2012 Oct;2(10):960]. *Cancer Discov*. 2012;2(5):401-404. doi:10.1158/2159-8290.CD-12-0095

Chakrabarty S, Monlish DA, Gupta M, et al. Structure activity relationships of anthranilic acid-based compounds on cellular and in vivo mitogen activated protein kinase-5 signaling pathways. *Bioorg Med Chem Lett*. 2018;28(13):2294-2301. doi:10.1016/j.bmcl.2018.05.029

Chan JK, Teoh D, Hu JM, Shin JY, Osann K, Kapp DS. Do clear cell ovarian carcinomas have poorer prognosis compared to other epithelial cell types? A study of 1411 clear cell ovarian cancers. *Gynecol Oncol*. 2008;109(3):370-376. doi:10.1016/j.ygyno.2008.02.006

Chang L, Karin M. Mammalian MAP kinase signalling cascades. *Nature*. 2001;410(6824):37-40. doi:10.1038/35065000

Chao TH, Hayashi M, Tapping RI, Kato Y, Lee JD. MEKK3 directly regulates MEK5 activity as part of the big mitogen-activated protein kinase 1 (BMK1) signaling pathway. *J Biol Chem*. 1999;274(51):36035-36038. doi:10.1074/jbc.274.51.36035

Charni S, de Bettignies G, Rathore MG, et al. Oxidative phosphorylation induces de novo expression of the MHC class I in tumor cells through the ERK5 pathway. *J Immunol*. 2010;185(6):3498-3503. doi:10.4049/jimmunol.1001250

Chiariello M, Marinissen MJ, Gutkind JS. Multiple mitogen-activated protein kinase signaling pathways connect the cot oncoprotein to the c-jun promoter and to cellular transformation. *Mol Cell Biol*. 2000;20(5):1747-1758. doi:10.1128/MCB.20.5.1747-1758.2000

Cleary JM, Shapiro GI. Development of phosphoinositide-3 kinase pathway inhibitors for advanced cancer. *Curr Oncol Rep*. 2010;12(2):87-94. doi:10.1007/s11912-010-0091-6

Cole AJ, Dwight T, Gill AJ, et al. Assessing mutant p53 in primary high-grade serous ovarian cancer using immunohistochemistry and massively parallel sequencing. *Sci Rep*. 2016;6:26191. Published 2016 May 18. doi:10.1038/srep26191

Coleman RL, Oza AM, Lorusso D, et al. Rucaparib maintenance treatment for recurrent ovarian carcinoma after response to platinum therapy (ARIEL3): a randomised, double-blind, placebo-controlled, phase 3 trial [published correction appears in Lancet. 2017 Oct 28;390(10106):1948]. *Lancet*. 2017;390(10106):1949-1961. doi:10.1016/S0140-6736(17)32440-6

Coleman RL, Brady MF, Herzog TJ, et al. Bevacizumab and paclitaxel-carboplatin chemotherapy and secondary cytoreduction in recurrent, platinum-sensitive ovarian cancer (NRG Oncology/Gynecologic Oncology Group study GOG-0213): a multicentre, open-label, randomised, phase 3 trial. *Lancet Oncol*. 2017;18(6):779-791. doi:10.1016/S1470-2045(17)30279-6

Colombo N, Guthrie D, Chiari S, et al. International Collaborative Ovarian Neoplasm trial 1: a randomized trial of adjuvant chemotherapy in women with early-stage ovarian cancer. *J Natl Cancer Inst*. 2003;95(2):125-132. doi:10.1093/jnci/95.2.125

Cuenda A, Rousseau S. p38 MAP-kinases pathway regulation, function and role in human diseases. *Biochim Biophys Acta*. 2007;1773(8):1358-1375. doi:10.1016/j.bbamcr.2007.03.010
de Jong PR, Taniguchi K, Harris AR, et al. ERK5 signalling rescues intestinal epithelial turnover and tumour cell proliferation upon ERK1/2 abrogation. *Nat Commun*. 2016;7:11551. Published 2016 May 17. doi:10.1038/ncomms11551
Dela Cruz CS, Tanoue LT, Matthay RA. Lung cancer: epidemiology, etiology, and prevention. *Clin Chest Med*. 2011;32(4):605-644. doi:10.1016/j.ccm.2011.09.001
DeLair D, Oliva E, Köbel M, Macias A, Gilks CB, Soslow RA. Morphologic spectrum of immunohistochemically characterized clear cell carcinoma of the ovary: a study of 155 cases. *Am J Surg Pathol*. 2011;35(1):36-44. doi:10.1097/PAS.0b013e3181ff400e
Den Haese GJ, Walworth N, Carr AM, Gould KL. The Wee1 protein kinase regulates T14 phosphorylation of fission yeast Cdc2. *Mol Biol Cell*. 1995;6(4):371-385. doi:10.1091/mbc.6.4.371
Deng X, Elkins JM, Zhang J, et al. Structural determinants for ERK5 (MAPK7) and leucine rich repeat kinase 2 activities of benzo[e]pyrimido-[5,4-b]diazepine-6(11H)-ones. *Eur J Med Chem*. 2013;70:758-767. doi:10.1016/j.ejmech.2013.10.052
de Sousa VML, Carvalho L. Heterogeneity in Lung Cancer. *Pathobiology*. 2018;85(1-2):96-107. doi:10.1159/000487440
Dhanasekaran DN, Kashef K, Lee CM, Xu H, Reddy EP. Scaffold proteins of MAP-kinase modules. *Oncogene*. 2007;26(22):3185-3202. doi:10.1038/sj.onc.1210411
Dickinson RJ, Keyse SM. Diverse physiological functions for dual-specificity MAP kinase phosphatases. *J Cell Sci*. 2006;119(Pt 22):4607-4615. doi:10.1242/jcs.03266
Douillard J-Y, Rosell R, Delena M, et al. Adjuvant Navelbine International Trialist Association. ANITA: phase III adjuvant vinorelbine (N) and cisplatin (P) versus observation (OBS) in completely resected (stage I-III) non-small-cell lung cancer (NSCLC) patients (pts): final results after 70-month median follow-up [abstract 7013] J Clin Oncol. 2005;23(16s pt 1) June 1 suppl:624s.
Drew BA, Burow ME, Beckman BS. MEK5/ERK5 pathway: the first fifteen years. *Biochim Biophys Acta*. 2012;1825(1):37-48. doi:10.1016/j.bbcan.2011.10.002
Drilon A, Rekhtman N, Arcila M, et al. Cabozantinib in patients with advanced RET-rearranged non-small-cell lung cancer: an open-label, single-centre, phase 2, single-arm trial. *Lancet Oncol*. 2016;17(12):1653-1660. doi:10.1016/S1470-2045(16)30562-9
du Bois A, Kristensen G, Ray-Coquard I, et al. Standard first-line chemotherapy with or without nintedanib for advanced ovarian cancer (AGO-OVAR 12): a randomised, double-blind, placebo-controlled phase 3 trial. *Lancet Oncol*. 2016;17(1):78-89. doi:10.1016/S1470-2045(15)00366-6
Dutt A, Ramos AH, Hammerman PS, et al. Inhibitor-sensitive FGFR1 amplification in human non-small cell lung cancer. *PLoS One*. 2011;6(6):e20351. doi:10.1371/journal.pone.0020351
Ekman S. How selecting best therapy for metastatic *NTRK* fusion-positive non-small cell lung cancer?. *Transl Lung Cancer Res*. 2020;9(6):2535-2544. doi:10.21037/tlcr-20-434
English JM, Vanderbilt CA, Xu S, Marcus S, Cobb MH. Isolation of MEK5 and differential expression of alternatively spliced forms. *J Biol Chem*. 1995;270(48):28897-28902. doi:10.1074/jbc.270.48.28897
English JM, Pearson G, Baer R, Cobb MH. Identification of substrates and regulators of the mitogen-activated protein kinase ERK5 using chimeric protein kinases. *J Biol Chem*. 1998;273(7):3854-3860. doi:10.1074/jbc.273.7.3854
English JM, Pearson G, Hockenberry T, Shivakumar L, White MA, Cobb MH. Contribution of the ERK5/MEK5 pathway to Ras/Raf signaling and growth control. *J Biol Chem*. 1999;274(44):31588-31592. doi:10.1074/jbc.274.44.31588
Esparís-Ogando A, Díaz-Rodríguez E, Montero JC, Yuste L, Crespo P, Pandiella A. Erk5 participates in neuregulin signal transduction and is constitutively active in breast cancer cells overexpressing ErbB2. *Mol Cell Biol*. 2002;22(1):270-285. doi:10.1128/MCB.22.1.270-285.2002
Fang B, Mehran RJ, Heymach JV, Swisher SG. Predictive biomarkers in precision medicine and drug development against lung cancer. *Chin J Cancer*. 2015;34(7):295-309. Published 2015 Jul 2. doi:10.1186/s40880-015-0028-4
Farley J, Brady WE, Vathipadiekal V, et al. Selumetinib in women with recurrent low-grade serous carcinoma of the ovary or peritoneum: an open-label, single-arm, phase 2 study. *Lancet Oncol*. 2013;14(2):134-140. doi:10.1016/S1470-2045(12)70572-7
Finegan KG, Wang X, Lee EJ, Robinson AC, Tournier C. Regulation of neuronal survival by the extracellular signal-regulated protein kinase 5. *Cell Death Differ*. 2009;16(5):674-683. doi:10.1038/cdd.2008.193
Finegan KG, Perez-Madrigal D, Hitchin JR, Davies CC, Jordan AM, Tournier C. ERK5 is a critical mediator of inflammation-driven cancer. *Cancer Res*. 2015;75(4):742-753. doi:10.1158/0008-5472.CAN-13-3043
Flaherty PT, Chopra I, Jain P, Yi S, Allen E, Cavanaugh J. Identification of benzimidazole-based inhibitors of the mitogen activated kinase-5 signaling pathway. *Bioorg Med Chem Lett*. 2010;20(9):2892-2896. doi:10.1016/j.bmcl.2010.03.033
Fossella FV, DeVore R, Kerr RN, et al. Randomized phase III trial of docetaxel versus vinorelbine or ifosfamide in patients with advanced non-small-cell lung cancer previously treated with platinum-containing chemotherapy regimens. The TAX 320 Non-Small Cell Lung Cancer Study Group [published correction appears in J Clin Oncol. 2004 Jan 1;22(1):209]. *J Clin Oncol*. 2000;18(12):2354-2362. doi:10.1200/JCO.2000.18.12.2354
Fujimoto J, Wistuba II. Current concepts on the molecular pathology of non-small cell lung carcinoma. *Semin Diagn Pathol*. 2014;31(4):306-313. doi:10.1053/j.semdp.2014.06.008
Fulford L, Milewski D, Ustiyan V, et al. The transcription factor FOXF1 promotes prostate cancer by stimulating the mitogen-activated protein kinase ERK5. *Sci Signal*. 2016;9(427):ra48. Published 2016 May 10. doi:10.1126/scisignal.aad5582
Gainor JF, Shaw AT. Novel targets in non-small cell lung cancer: ROS1 and RET fusions. *Oncologist*. 2013;18(7):865-875. doi:10.1634/theoncologist.2013-0095
Gallolu Kankanamalage S, Lee AY, Wichaidit C, et al. WNK1 is an unexpected autophagy inhibitor. *Autophagy*. 2017;13(5):969-970. doi:10.1080/15548627.2017.1286431
Gallolu Kankanamalage S, Karra AS, Cobb MH. WNK pathways in cancer signaling networks. *Cell Commun Signal*. 2018;16(1):72. Published 2018 Nov 3. doi:10.1186/s12964-018-0287-1
Gao J, Aksoy BA, Dogrusoz U, et al. Integrative analysis of complex cancer genomics and clinical profiles using the cBioPortal. *Sci Signal*. 2013;6(269):pl1. Published 2013 Apr 2. doi:10.1126/scisignal.2004088
Garaude J, Cherni S, Kaminski S, et al. ERK5 activates NF-kappaB in leukemic T cells and is essential for their growth in vivo. *J Immunol*. 2006;177(11):7607-7617. doi:10.4049/jimmunol.177.11.7607

Gautschi O, Milia J, Cabarrou B, et al. Targeted Therapy for Patients with BRAF-Mutant Lung Cancer: Results from the European EURAF Cohort. *J Thorac Oncol*. 2015;10(10):1451-1457. doi:10.1097/JTO.0000000000000625
Gavine PR, Wang M, Yu D, et al. Identification and validation of dysregulated MAPK7 (ERK5) as a novel oncogenic target in squamous cell lung and esophageal carcinoma. *BMC Cancer*. 2015;15:454. Published 2015 Jun 4. doi:10.1186/s12885-015-1455-y
Gershenson DM, Sun CC, Bodurka D, et al. Recurrent low-grade serous ovarian carcinoma is relatively chemoresistant. *Gynecol Oncol*. 2009;114(1):48-52. doi:10.1016/j.ygyno.2009.03.001
Gershenson DM, Miller A, Brady W, et al. A randomized phase II/III study to assess the efficacy of trametinib in patients with recurrent or progressive low-grade serous ovarian or peritoneal cancer. Presented at: 2020 Society of Gynecologic Oncology Annual Meeting; March 28-31, 2020; Toronto, Canada. Abstract 42. bit.ly/2XFKxdP
Goh KC, Novotny-Diermayr V, Hart S, et al. TG02, a novel oral multi-kinase inhibitor of CDKs, JAK2 and FLT3 with potent anti-leukemic properties. *Leukemia*. 2012;26(2):236-243. doi:10.1038/leu.2011.218
Ghoneum A, Said N. PI3K-AKT-mTOR and NFκB Pathways in Ovarian Cancer: Implications for Targeted Therapeutics. *Cancers (Basel)*. 2019;11(7):949. Published 2019 Jul 5. doi:10.3390/cancers11070949
Giurisato E, Xu Q, Lonardi S, et al. Myeloid ERK5 deficiency suppresses tumor growth by blocking protumor macrophage polarization via STAT3 inhibition. *Proc Natl Acad Sci U S A*. 2018;115(12):E2801-E2810. doi:10.1073/pnas.1707929115
Global Cancer Observatory: Cancer Today. International Agency for Research on Cancer. Lyon, France. Available at: https://gco.iarc.fr/today
Gordon MS, Matei D, Aghajanian C, et al. Clinical activity of pertuzumab (rhuMAb 2C4), a HER dimerization inhibitor, in advanced ovarian cancer: potential predictive relationship with tumor HER2 activation status [published correction appears in J Clin Oncol. 2008 Jun 1;26(16):2793]. *J Clin Oncol*. 2006;24(26):4324-4332. doi:10.1200/JCO.2005.05.4221
Goss PE, Strasser-Weippl K, Lee-Bychkovsky BL, et al. Challenges to effective cancer control in China, India, and Russia. *Lancet Oncol*. 2014;15(5):489-538. doi:10.1016/S1470-2045(14)70029-4
Govindan R, Ding L, Griffith M, et al. Genomic landscape of non-small cell lung cancer in smokers and never-smokers. *Cell*. 2012;150(6):1121-1134. doi:10.1016/j.cell.2012.08.024
Gray MJG, Gallick GE: The role of oncogene activation in tumor progression; in Coppola D (ed): Mechanisms of Oncogenesis: An Update on Tumorigenesis. Heidelberg, Springer, 2010, pp 19–41.
Guan LY, Lu Y. New developments in molecular targeted therapy of ovarian cancer. *Discov Med*. 2018;26(144):219-229.
Győrffy B, Surowiak P, Budczies J, Lánczky A. Online survival analysis software to assess the prognostic value of biomarkers using transcriptomic data in non-small-cell lung cancer [published correction appears in PLoS One. 2014;9(10):e111842]. *PLoS One*. 2013;8(12):e82241. Published 2013 Dec 18. doi:10.1371/journal.pone.0082241
Hagiwara Y, Miyoshi S, Fukuda K, et al. SHP2-mediated signaling cascade through gp130 is essential for LIF-dependent I CaL, [Ca2+]i transient, and APD increase in cardiomyocytes. *J Mol Cell Cardiol*. 2007;43(6):710-716. doi:10.1016/j.yjmcc.2007.09.004
Hamanishi J, Mandai M, Iwasaki M, et al. Programmed cell death 1 ligand 1 and tumor-infiltrating CD8+ T lymphocytes are prognostic factors of human ovarian cancer. *Proc Natl Acad Sci U S A*. 2007;104(9):3360-3365. doi:10.1073/pnas.0611533104
Hamanishi J, Mandai M, Ikeda T, et al. Safety and Antitumor Activity of Anti-PD-1 Antibody, Nivolumab, in Patients With Platinum-Resistant Ovarian Cancer. *J Clin Oncol*. 2015;33(34):4015-4022. doi:10.1200/JCO.2015.62.3397
Hammerman PS, Sos ML, Ramos AH, et al. Mutations in the DDR2 kinase gene identify a novel therapeutic target in squamous cell lung cancer. *Cancer Discov*. 2011;1(1):78-89. doi:10.1158/2159-8274.CD-11-0005
Han J, Liu Y, Yang S, Wu X, Li H, Wang Q. MEK inhibitors for the treatment of non-small cell lung cancer. *J Hematol Oncol*. 2021;14(1):1. Published 2021 Jan 5. doi:10.1186/s13045-020-01025-7
Haneda M, Sugimoto T, Kikkawa R. Mitogen-activated protein kinase phosphatase: a negative regulator of the mitogen-activated protein kinase cascade. *Eur J Pharmacol*. 1999;365(1):1-7. doi:10.1016/s0014-2999(98)00857-7
Hanrahan AJ, Schultz N, Westfal ML, et al. Genomic complexity and AKT dependence in serous ovarian cancer [published correction appears in Cancer Discov. 2012 Apr;2(4):376. Janikariman, Manickam [corrected to Janakiraman, Manickam]]. *Cancer Discov*. 2012;2(1):56-67. doi:10.1158/2159-8290.CD-11-0170
Hayashi M, Tapping RI, Chao TH, et al. BMK1 mediates growth factor-induced cell proliferation through direct cellular activation of serum and glucocorticoid-inducible kinase. *J Biol Chem*. 2001;276(12):8631-8634. doi:10.1074/jbc.C000838200
Hayashi M, Kim SW, Imanaka-Yoshida K, et al. Targeted deletion of BMK1/ERK5 in adult mice perturbs vascular integrity and leads to endothelial failure. *J Clin Invest*. 2004;113(8):1138-1148. doi:10.1172/JCI19890
Hayashi M, Lee JD. Role of the BMK1/ERK5 signaling pathway: lessons from knockout mice. *J Mol Med (Berl)*. 2004;82(12):800-808. doi:10.1007/s00109-004-0602-8
Hayashi M, Fearns C, Eliceiri B, Yang Y, Lee JD. Big mitogen-activated protein kinase 1/extracellular signal-regulated kinase 5 signaling pathway is essential for tumor-associated angiogenesis. *Cancer Res*. 2005;65(17):7699-7706. doi:10.1158/0008-5472.CAN-04-4540
He S, Deng Y, Liao Y, Li X, Liu J, Yao S. CREB5 promotes tumor cell invasion and correlates with poor prognosis in epithelial ovarian cancer. *Oncol Lett*. 2017;14(6):8156-8161. doi:10.3892/ol.2017.7234
Hecht SS. Tobacco smoke carcinogens and lung cancer. *J Natl Cancer Inst*. 1999;91(14):1194-1210. doi:10.1093/jnci/91.14.1194
Helder-Woolderink JM, Blok EA, Vasen HF, Hollema H, Mourits MJ, De Bock GH. Ovarian cancer in Lynch syndrome; a systematic review. *Eur J Cancer*. 2016;55:65-73. doi:10.1016/j.ejca.2015.12.005
Herbst RS, Baas P, Kim DW, et al. Pembrolizumab versus docetaxel for previously treated, PD-L1-positive, advanced non-small-cell lung cancer (KEYNOTE-010): a randomised controlled trial. *Lancet*. 2016;387(10027):1540-1550. doi:10.1016/S0140-6736(15)01281-7
Herschkowitz JI, Simin K, Weigman VJ, et al. Identification of conserved gene expression features between murine mammary carcinoma models and human breast tumors. *Genome Biol*. 2007;8(5):R76. doi:10.1186/gb-2007-8-5-r76
Hoang VT, Yan TJ, Cavanaugh JE, Flaherty PT, Beckman BS, Burow ME. Oncogenic signaling of MEK5-ERK5. *Cancer Lett*. 2017;392:51-59. doi:10.1016/j.canlet.2017.01.034
Hodi FS, Butler M, Oble DA, et al. Immunologic and clinical effects of antibody blockade of cytotoxic T lymphocyte-associated antigen 4 in previously vaccinated cancer patients. *Proc Natl Acad Sci U S A*. 2008;105(8):3005-3010. doi:10.1073/pnas.0712237105

Hongisto V, Jernström S, Fey V, et al. High-throughput 3D screening reveals differences in drug sensitivities between culture models of JIMT1 breast cancer cells. *PLoS One*. 2013;8(10):e77232. Published 2013 Oct 23. doi:10.1371/journal.pone.0077232
Howe LR, Leevers SJ, Gómez N, Nakielny S, Cohen P, Marshall CJ. Activation of the MAP kinase pathway by the protein kinase raf. *Cell*. 1992;71(2):335-342. doi:10.1016/0092-8674(92)90361-f
Howlander N, Noone AM, Krapcho M, et al. . SEER cancer statistics review 1975–2016. National Cancer Institute, 2019.
Huang G, Shi LZ, Chi H. Regulation of JNK and p38 MAPK in the immune system: signal integration, propagation and termination. *Cytokine*. 2009;48(3):161-169. doi:10.1016/j.cyto.2009.08.002
Huang KL, Wu Y, Primeau T, et al. Regulated Phosphosignaling Associated with Breast Cancer Subtypes and Druggability. *Mol Cell Proteomics*. 2019;18(8):1630-1650. doi:10.1074/mcp.RA118.001243
Iniesta-Vaquera FA, Campbell DG, Tournier C, Gómez N, Lizcano JM, Cuenda A. Alternative ERK5 regulation by phosphorylation during the cell cycle. *Cell Signal*. 2010;22(12):1829-1837. doi:10.1016/j.cellsig.2010.07.010
Izawa Y, Yoshizumi M, Ishizawa K, et al. Big mitogen-activated protein kinase 1 (BMK1)/extracellular signal regulated kinase 5 (ERK5) is involved in platelet-derived growth factor (PDGF)-induced vascular smooth muscle cell migration. *Hypertens Res*. 2007;30(11):1107-1117. doi:10.1291/hypres.30.1107
Jancík S, Drábek J, Radzioch D, Hajdúch M. Clinical relevance of KRAS in human cancers. *J Biomed Biotechnol*. 2010;2010:150960. doi:10.1155/2010/150960
Jang TW, Oak CH, Chang HK, Suo SJ, Jung MH. EGFR and KRAS mutations in patients with adenocarcinoma of the lung. *Korean J Intern Med*. 2009;24(1):48-54. doi:10.3904/kjim.2009.24.1.43
Jha P. Avoidable global cancer deaths and total deaths from smoking. *Nat Rev Cancer*. 2009;9(9):655-664. doi:10.1038/nrc2703
Jiang ZY, Zhou QL, Holik J, et al. Identification of WNK1 as a substrate of Akt/protein kinase B and a negative regulator of insulin-stimulated mitogenesis in 3T3-L1 cells. *J Biol Chem*. 2005;280(22):21622-21628. doi:10.1074/jbc.M414464200 **(a)**
Jiang J, Greulich H, Jänne PA, Sellers WR, Meyerson M, Griffin JD. Epidermal growth factor-independent transformation of Ba/F3 cells with cancer-derived epidermal growth factor receptor mutants induces gefitinib-sensitive cell cycle progression. *Cancer Res*. 2005;65(19):8968-8974. doi:10.1158/0008-5472.CAN-05-1829 **(b)**
Jinawath N, Vasoontara C, Jinawath A, et al. Oncoproteomic analysis reveals co-upregulation of RELA and STAT5 in carboplatin resistant ovarian carcinoma. *PLoS One*. 2010;5(6):e11198. Published 2010 Jun 18. doi:10.1371/journal.pone.0011198
Kadota K, Nitadori J, Rekhtman N, Jones DR, Adusumilli PS, Travis WD. Reevaluation and reclassification of resected lung carcinomas originally diagnosed as squamous cell carcinoma using immunohistochemical analysis. *Am J Surg Pathol*. 2015;39(9):1170-1180. doi:10.1097/PAS.0000000000000439
Kaldawy A, Segev Y, Lavie O, Auslender R, Sopik V, Narod SA. Low-grade serous ovarian cancer: A review. *Gynecol Oncol*. 2016;143(2):433-438. doi:10.1016/j.ygyno.2016.08.320
Kamakura S, Moriguchi T, Nishida E. Activation of the protein kinase ERK5/BMK1 by receptor tyrosine kinases. Identification and characterization of a signaling pathway to the nucleus. *J Biol Chem*. 1999;274(37):26563-26571. doi:10.1074/jbc.274.37.26563
Kanteti R, Yala S, Ferguson MK, Salgia R. MET, HGF, EGFR, and PXN gene copy number in lung cancer using DNA extracts from FFPE archival samples and prognostic significance. *J Environ Pathol Toxicol Oncol*. 2009;28(2):89-98. doi:10.1615/jenvironpatholtoxicoloncol.v28.i2.10
Kanwal M, Ding XJ, Cao Y. Familial risk for lung cancer. *Oncol Lett*. 2017;13(2):535-542. doi:10.3892/ol.2016.5518
Kasler HG, Victoria J, Duramad O, Winoto A. ERK5 is a novel type of mitogen-activated protein kinase containing a transcriptional activation domain. *Mol Cell Biol*. 2000;20(22):8382-8389. doi:10.1128/MCB.20.22.8382-8389.2000
Kato Y, Kravchenko VV, Tapping RI, Han J, Ulevitch RJ, Lee JD. BMK1/ERK5 regulates serum-induced early gene expression through transcription factor MEF2C. *EMBO J*. 1997;16(23):7054-7066. doi:10.1093/emboj/16.23.7054
Kato Y, Tapping RI, Huang S, Watson MH, Ulevitch RJ, Lee JD. Bmk1/Erk5 is required for cell proliferation induced by epidermal growth factor. *Nature*. 1998;395(6703):713-716. doi:10.1038/27234
Kato Y, Zhao M, Morikawa A, et al. Big mitogen-activated kinase regulates multiple members of the MEF2 protein family. *J Biol Chem*. 2000;275(24):18534-18540. doi:10.1074/jbc.M001573200
Katz M, Amit I, Yarden Y. Regulation of MAPKs by growth factors and receptor tyrosine kinases. *Biochim Biophys Acta*. 2007;1773(8):1161-1176. doi:10.1016/j.bbamcr.2007.01.002
Kaufman B, Shapira-Frommer R, Schmutzler RK, et al. Olaparib monotherapy in patients with advanced cancer and a germline BRCA1/2 mutation. *J Clin Oncol*. 2015;33(3):244-250. doi:10.1200/JCO.2014.56.2728
Kelly K, Mikhaeel-Kamel N, Pan Z, Murphy J, Prindiville S, Bunn PA Jr. A phase I/II trial of paclitaxel, carboplatin, and gemcitabine in untreated patients with advanced non-small cell lung cancer. *Clin Cancer Res*. 2000;6(9):3474-3479.
Kesavan K, Lobel-Rice K, Sun W, et al. MEKK2 regulates the coordinate activation of ERK5 and JNK in response to FGF-2 in fibroblasts. *J Cell Physiol*. 2004;199(1):140-148. doi:10.1002/jcp.10457
Keyse SM. Dual-specificity MAP kinase phosphatases (MKPs) and cancer. *Cancer Metastasis Rev*. 2008;27(2):253-261. doi:10.1007/s10555-008-9123-1
Khan AUH, Rathore MG, Allende-Vega N, et al. Human Leukemic Cells performing Oxidative Phosphorylation (OXPHOS) Generate an Antioxidant Response Independently of Reactive Oxygen species (ROS) Production. *EBioMedicine*. 2015;3:43-53. Published 2015 Nov 26. doi:10.1016/j.ebiom.2015.11.045
Khunamornpong S, Suprasert P, Pojchamarnwiputh S, Na Chiangmai W, Settakorn J, Siriaunkgul S. Primary and metastatic mucinous adenocarcinomas of the ovary: Evaluation of the diagnostic approach using tumor size and laterality. *Gynecol Oncol*. 2006;101(1):152-157. doi:10.1016/j.ygyno.2005.10.008
Kinderlerer AR, Ali F, Johns M, et al. KLF2-dependent, shear stress-induced expression of CD59: a novel cytoprotective mechanism against complement-mediated injury in the vasculature. *J Biol Chem*. 2008;283(21):14636-14644. doi:10.1074/jbc.M800362200
Kim J, Coffey DM, Creighton CJ, Yu Z, Hawkins SM, Matzuk MM. High-grade serous ovarian cancer arises from fallopian tube in a mouse model. *Proc Natl Acad Sci U S A*. 2012;109(10):3921-3926. doi:10.1073/pnas.1117135109
Kinross KM, Brown DV, Kleinschmidt M, et al. In vivo activity of combined PI3K/mTOR and MEK inhibition in a Kras(G12D);Pten deletion mouse model of ovarian cancer. *Mol Cancer Ther*. 2011;10(8):1440-1449. doi:10.1158/1535-7163.MCT-11-0240

Knight T, Irving JA. Ras/Raf/MEK/ERK Pathway Activation in Childhood Acute Lymphoblastic Leukemia and Its Therapeutic Targeting. *Front Oncol*. 2014;4:160. Published 2014 Jun 24. doi:10.3389/fonc.2014.00160
Köchl R, Thelen F, Vanes L, et al. WNK1 kinase balances T cell adhesion versus migration in vivo [published correction appears in Nat Immunol. 2017 Jan 19;18(2):246]. *Nat Immunol*. 2016;17(9):1075-1083. doi:10.1038/ni.3495
Komaravolu RK, Adam C, Moonen JR, Harmsen MC, Goebeler M, Schmidt M. Erk5 inhibits endothelial migration via KLF2-dependent down-regulation of PAK1. *Cardiovasc Res*. 2015;105(1):86-95. doi:10.1093/cvr/cvu236
Kondoh K, Terasawa K, Morimoto H, Nishida E. Regulation of nuclear translocation of extracellular signal-regulated kinase 5 by active nuclear import and export mechanisms. *Mol Cell Biol*. 2006;26(5):1679-1690. doi:10.1128/MCB.26.5.1679-1690.2006
Koneru M, Purdon TJ, Spriggs D, Koneru S, Brentjens RJ. IL-12 secreting tumor-targeted chimeric antigen receptor T cells eradicate ovarian tumors *in vivo*. *Oncoimmunology*. 2015;4(3):e994446. Published 2015 Jan 23. doi:10.4161/2162402X.2014.994446
Krishna M, Narang H. The complexity of mitogen-activated protein kinases (MAPKs) made simple. *Cell Mol Life Sci*. 2008;65(22):3525-3544. doi:10.1007/s00018-008-8170-7
Kurman RJ, Shih IeM. Molecular pathogenesis and extraovarian origin of epithelial ovarian cancer--shifting the paradigm. *Hum Pathol*. 2011;42(7):918-931. doi:10.1016/j.humpath.2011.03.003
Kurman RJ, Shih IeM. The Dualistic Model of Ovarian Carcinogenesis: Revisited, Revised, and Expanded. *Am J Pathol*. 2016;186(4):733-747. doi:10.1016/j.ajpath.2015.11.011
Kurnit KC, Fleming GF, Lengyel E. Updates and New Options in Advanced Epithelial Ovarian Cancer Treatment. Obstet Gynecol. 2021;137(1):108-121. doi:10.1097/AOG.0000000000004173
Kuroki L, Guntupalli SR. Treatment of epithelial ovarian cancer. *BMJ*. 2020;371:m3773. Published 2020 Nov 9. doi:10.1136/bmj.m3773
Kyriakis JM, Avruch J. Mammalian MAPK signal transduction pathways activated by stress and inflammation: a 10-year update. *Physiol Rev*. 2012;92(2):689-737. doi:10.1152/physrev.00028.2011
Labidi-Galy SI, Papp E, Hallberg D, et al. High grade serous ovarian carcinomas originate in the fallopian tube. *Nat Commun*. 2017;8(1):1093. Published 2017 Oct 23. doi:10.1038/s41467-017-00962-1
Ladanyi M, Pao W (2008) Lung adenocarcinoma: guiding EGFR-targeted therapy and beyond. Mod Pathol 21(Suppl 2):S16–S22
Lange-Carter CA, Pleiman CM, Gardner AM, Blumer KJ, Johnson GL. A divergence in the MAP kinase regulatory network defined by MEK kinase and Raf. *Science*. 1993;260(5106):315-319. doi:10.1126/science.8385802
Lee JD, Ulevitch RJ, Han J. Primary structure of BMK1: a new mammalian map kinase. *Biochem Biophys Res Commun*. 1995;213(2):715-724. doi:10.1006/bbrc.1995.2189
Lee Y, Miron A, Drapkin R, et al. A candidate precursor to serous carcinoma that originates in the distal fallopian tube [published correction appears in J Pathol. 2007 Sep;213(1):116]. *J Pathol*. 2007;211(1):26-35. doi:10.1002/path.2091
Lee BH, Chen W, Stippec S, Cobb MH. Biological cross-talk between WNK1 and the transforming growth factor beta-Smad signaling pathway. *J Biol Chem*. 2007;282(25):17985-17996. doi:10.1074/jbc.M702664200
Lee EK, Tan-Wasielewski Z, Aghajanian C, et al. Results of an abbreviated phase II study of AKT inhibitor MK-2206 in the treatment of recurrent platinum-resistant high grade serous ovarian, fallopian tube, or primary peritoneal carcinoma (NCT 01283035). *Gynecol Oncol Rep*. 2020;32:100546. Published 2020 Feb 3. doi:10.1016/j.gore.2020.100546
Lewis DR, Check DP, Caporaso NE, Travis WD, Devesa SS. US lung cancer trends by histologic type. *Cancer*. 2014;120(18):2883-2892. doi:10.1002/cncr.28749
Li CM, Chu WY, Wong DL, et al. Current and future molecular diagnostics in non-small-cell lung cancer. *Expert Rev Mol Diagn*. 2015;15(8):1061-1074. doi:10.1586/14737159.2015.1063420
Li L, Tatake RJ, Natarajan K, et al. Fluid shear stress inhibits TNF-mediated JNK activation via MEK5-BMK1 in endothelial cells. *Biochem Biophys Res Commun*. 2008;370(1):159-163. doi:10.1016/j.bbrc.2008.03.051
Liao BC, Griesing S, Yang JC. Second-line treatment of *EGFR* T790M-negative non-small cell lung cancer patients. *Ther Adv Med Oncol*. 2019;11:1758835919890286. Published 2019 Nov 25. doi:10.1177/1758835919890286
Lim SM, Hong MH, Kim HR. Immunotherapy for Non-small Cell Lung Cancer: Current Landscape and Future Perspectives. *Immune Netw*. 2020;20(1):e10. Published 2020 Jan 27. doi:10.4110/in.2020.20.e10
Lin EC, Amantea CM, Nomanbhoy TK, et al. ERK5 kinase activity is dispensable for cellular immune response and proliferation. *Proc Natl Acad Sci U S A*. 2016;113(42):11865-11870. doi:10.1073/pnas.1609019113
Lin SH, Zhao YS, Zhou DX, Zhou FC, Xu F. Coronavirus disease 2019 (COVID-19): cytokine storms, hyper-inflammatory phenotypes, and acute respiratory distress syndrome. *Genes Dis*. 2020;7(4):520-527. doi:10.1016/j.gendis.2020.06.009
Linnerth NM, Baldwin M, Campbell C, Brown M, McGowan H, Moorehead RA. IGF-II induces CREB phosphorylation and cell survival in human lung cancer cells. *Oncogene*. 2005;24(49):7310-7319. doi:10.1038/sj.onc.1208882
Lissowska J, Foretova L, Dabek J, et al. Family history and lung cancer risk: international multicentre case-control study in Eastern and Central Europe and meta-analyses. *Cancer Causes Control*. 2010;21(7):1091-1104. doi:10.1007/s10552-010-9537-2
Lisowska KM, Olbryt M, Dudaladava V, et al. Gene expression analysis in ovarian cancer - faults and hints from DNA microarray study. *Front Oncol*. 2014;4:6. Published 2014 Jan 28. doi:10.3389/fonc.2014.00006
Little AG. No nodes is good nodes. *Ann Thorac Surg*. 2006;82(1):4-5. doi:10.1016/j.athoracsur.2006.03.051
Litzky LA. Pulmonary Neuroendocrine Tumors. *Surg Pathol Clin*. 2010;3(1):27-59. doi:10.1016/j.path.2010.03.007
Liu L, Cavanaugh JE, Wang Y, Sakagami H, Mao Z, Xia Z. ERK5 activation of MEF2-mediated gene expression plays a critical role in BDNF-promoted survival of developing but not mature cortical neurons. *Proc Natl Acad Sci U S A*. 2003;100(14):8532-8537. doi:10.1073/pnas.1332804100
Liu D, Kang JS, Derynck R. TGF-beta-activated Smad3 represses MEF2-dependent transcription in myogenic differentiation. *EMBO J*. 2004;23(7):1557-1566. doi:10.1038/sj.emboj.7600179
Liu Z, Cao W. p38 mitogen-activated protein kinase: a critical node linking insulin resistance and cardiovascular diseases in type 2 diabetes mellitus. *Endocr Metab Immune Disord Drug Targets*. 2009;9(1):38-46. doi:10.2174/187153009787582397
Liu CJ, Liu HY, Zhu ZQ, Zhang YY, Wang KF, Xia WW. Roles of extra-cellular signal-regulated protein kinase 5 signaling pathway in the development of spinal cord injury. *Chin Med J (Engl)*. 2019;132(21):2601-2611. doi:10.1097/CM9.0000000000000362

Livak KJ, Schmittgen TD. Analysis of relative gene expression data using real-time quantitative PCR and the 2(-Delta Delta C(T)) Method. *Methods*. 2001;25(4):402-408. doi:10.1006/meth.2001.1262
Lochhead PA, Clark J, Wang LZ, et al. Tumor cells with KRAS or BRAF mutations or ERK5/MAPK7 amplification are not addicted to ERK5 activity for cell proliferation. *Cell Cycle*. 2016;15(4):506-518. doi:10.1080/15384101.2015.1120915
Lochhead PA, Tucker JA, Tatum NJ, et al. Paradoxical activation of the protein kinase-transcription factor ERK5 by ERK5 kinase inhibitors. *Nat Commun*. 2020;11(1):1383. Published 2020 Mar 13. doi:10.1038/s41467-020-15031-3
Lopez-Royuela N, Rathore MG, Allende-Vega N, et al. Extracellular-signal-regulated kinase 5 modulates the antioxidant response by transcriptionally controlling Sirtuin 1 expression in leukemic cells. *Int J Biochem Cell Biol*. 2014;53:253-261. doi:10.1016/j.biocel.2014.05.026
Luyckx M, Votino R, Squifflet JL, Baurain JF. Profile of vintafolide (EC145) and its use in the treatment of platinum-resistant ovarian cancer. *Int J Womens Health*. 2014;6:351-358. Published 2014 Mar 31. doi:10.2147/IJWH.S39696
Machado-Linde F, Sánchez-Ferrer ML, Cascales P, et al. Prevalence of endometriosis in epithelial ovarian cancer. Analysis of the associated clinical features and study on molecular mechanisms involved in the possible causality. *Eur J Gynaecol Oncol*. 2015;36(1):21-24.
Maemondo M, Inoue A, Kobayashi K, et al. Gefitinib or chemotherapy for nonsmall-cell lung cancer with mutated EGFR. N Engl J Med 2010;362(25):2380–8.
Maghfoor I, Perry MC. Lung cancer. *Ann Saudi Med*. 2005;25(1):1-12. doi:10.5144/0256-4947.2005.1
Maione P, Sacco PC, Sgambato A, Casaluce F, Rossi A, Gridelli C. Overcoming resistance to targeted therapies in NSCLC: current approaches and clinical application. *Ther Adv Med Oncol*. 2015;7(5):263-273. doi:10.1177/1758834015595048
Malvezzi M, Bosetti C, Rosso T, et al. Lung cancer mortality in European men: trends and predictions. *Lung Cancer*. 2013;80(2):138-145. doi:10.1016/j.lungcan.2013.01.020
Mangili G, Sigismondi C, Gadducci A, et al. Outcome and risk factors for recurrence in malignant ovarian germ cell tumors: a MITO-9 retrospective study. *Int J Gynecol Cancer*. 2011;21(8):1414-1421. doi:10.1097/IGC.0b013e3182236582
Marx J. Hypertension. Possible new path for blood pressure control. *Science*. 2001;293(5532):1030. doi:10.1126/science.293.5532.1030a
McCaw BJ, Chow SY, Wong ES, Tan KL, Guo H, Guy GR. Identification and characterization of mErk5-T, a novel Erk5/Bmk1 splice variant. *Gene*. 2005;345(2):183-190. doi:10.1016/j.gene.2004.11.011
McConechy MK, Ding J, Senz J, et al. Ovarian and endometrial endometrioid carcinomas have distinct CTNNB1 and PTEN mutation profiles. *Mod Pathol*. 2014;27(1):128-134. doi:10.1038/modpathol.2013.107
McCracken SR, Ramsay A, Heer R, et al. Aberrant expression of extracellular signal-regulated kinase 5 in human prostate cancer. *Oncogene*. 2008;27(21):2978-2988. doi:10.1038/sj.onc.1210963
McKenna RJ Jr, Houck W, Fuller CB. Video-assisted thoracic surgery lobectomy: experience with 1,100 cases. *Ann Thorac Surg*. 2006;81(2):421-426. doi:10.1016/j.athoracsur.2005.07.078
Mehta PB, Jenkins BL, McCarthy L, et al. MEK5 overexpression is associated with metastatic prostate cancer, and stimulates proliferation, MMP-9 expression and invasion. *Oncogene*. 2003;22(9):1381-1389. doi:10.1038/sj.onc.1206154
Miranda M, Rozali E, Khanna KK, Al-Ejeh F. MEK5-ERK5 pathway associates with poor survival of breast cancer patients after systemic treatments. *Oncoscience*. 2015;2(2):99-101. Published 2015 Feb 20. doi:10.18632/oncoscience.135
Mirza MR, Monk BJ, Herrstedt J, et al. Niraparib Maintenance Therapy in Platinum-Sensitive, Recurrent Ovarian Cancer. *N Engl J Med*. 2016;375(22):2154-2164. doi:10.1056/NEJMoa1611310
Mody N, Campbell DG, Morrice N, Peggie M, Cohen P. An analysis of the phosphorylation and activation of extracellular-signal-regulated protein kinase 5 (ERK5) by mitogen-activated protein kinase kinase 5 (MKK5) in vitro. *Biochem J*. 2003;372(Pt 2):567-575. doi:10.1042/BJ20030193
Molina JR, Yang P, Cassivi SD, Schild SE, Adjei AA. Non-small cell lung cancer: epidemiology, risk factors, treatment, and survivorship. *Mayo Clin Proc*. 2008;83(5):584-594. doi:10.4065/83.5.584
Moncho-Amor V, Pintado-Berninches L, Ibañez de Cáceres I, et al. Role of Dusp6 Phosphatase as a Tumor Suppressor in Non-Small Cell Lung Cancer. *Int J Mol Sci*. 2019;20(8):2036. Published 2019 Apr 25. doi:10.3390/ijms20082036
Montero JC, Ocaña A, Abad M, Ortiz-Ruiz MJ, Pandiella A, Esparís-Ogando A. Expression of Erk5 in early stage breast cancer and association with disease free survival identifies this kinase as a potential therapeutic target. *PLoS One*. 2009;4(5):e5565. doi:10.1371/journal.pone.0005565
Montero JC, Chen X, Ocaña A, Pandiella A. Predominance of mTORC1 over mTORC2 in the regulation of proliferation of ovarian cancer cells: therapeutic implications. *Mol Cancer Ther*. 2012;11(6):1342-1352. doi:10.1158/1535-7163.MCT-11-0723
Mordant P, Grand B, Cazes A, et al. Adenosquamous carcinoma of the lung: surgical management, pathologic characteristics, and prognostic implications. *Ann Thorac Surg*. 2013;95(4):1189-1195. doi:10.1016/j.athoracsur.2012.12.037
Moreno-Bueno G, Gamallo C, Pérez-Gallego L, de Mora JC, Suárez A, Palacios J. beta-Catenin expression pattern, beta-catenin gene mutations, and microsatellite instability in endometrioid ovarian carcinomas and synchronous endometrial carcinomas. *Diagn Mol Pathol*. 2001;10(2):116-122. doi:10.1097/00019606-200106000-00008
Morice P, Gouy S, Leary A. Mucinous Ovarian Carcinoma. *N Engl J Med*. 2019;380(13):1256-1266. doi:10.1056/NEJMra1813254
Morimoto H, Kondoh K, Nishimoto S, Terasawa K, Nishida E. Activation of a C-terminal transcriptional activation domain of ERK5 by autophosphorylation. *J Biol Chem*. 2007;282(49):35449-35456. doi:10.1074/jbc.M704079200
Mosmann T. Rapid colorimetric assay for cellular growth and survival: application to proliferation and cytotoxicity assays. *J Immunol Methods*. 1983;65(1-2):55-63. doi:10.1016/0022-1759(83)90303-4
Murai J, Huang SY, Das BB, et al. Trapping of PARP1 and PARP2 by Clinical PARP Inhibitors. *Cancer Res*. 2012;72(21):5588-5599. doi:10.1158/0008-5472.CAN-12-2753
Murali R, Selenica P, Brown DN, et al. Somatic genetic alterations in synchronous and metachronous low-grade serous tumours and high-grade carcinomas of the adnexa. *Histopathology*. 2019;74(4):638-650. doi:10.1111/his.13796
Myers SM, Bawn RH, Bisset LC, et al. High-Throughput Screening and Hit Validation of Extracellular-Related Kinase 5 (ERK5) Inhibitors. *ACS Comb Sci*. 2016;18(8):444-455. doi:10.1021/acscombsci.5b00155
Myers SM, Miller DC, Molyneux L, et al. Identification of a novel orally bioavailable ERK5 inhibitor with selectivity over p38α and BRD4. *Eur J Med Chem*. 2019;178:530-543. doi:10.1016/j.ejmech.2019.05.057
Nakamura K, Johnson GL. PB1 domains of MEKK2 and MEKK3 interact with the MEK5 PB1 domain for activation of the ERK5 pathway. *J Biol Chem*. 2003;278(39):36989-36992. doi:10.1074/jbc.C300313200

Nakamura K, Johnson GL. Noncanonical function of MEKK2 and MEK5 PB1 domains for coordinated extracellular signal-regulated kinase 5 and c-Jun N-terminal kinase signaling. *Mol Cell Biol*. 2007;27(12):4566-4577. doi:10.1128/MCB.00125-07
Nakaoka Y, Nishida K, Fujio Y, et al. Activation of gp130 transduces hypertrophic signal through interaction of scaffolding/docking protein Gab1 with tyrosine phosphatase SHP2 in cardiomyocytes. *Circ Res*. 2003;93(3):221-229. doi:10.1161/01.RES.0000085562.48906.4A
Naor Z, Benard O, Seger R. Activation of MAPK cascades by G-protein-coupled receptors: the case of gonadotropin-releasing hormone receptor. *Trends Endocrinol Metab*. 2000;11(3):91-99. doi:10.1016/s1043-2760(99)00232-5
National Cancer Institute: SEER Stat Fact Sheets: Ovarian Cancer. Bethesda, Md: National Institutes of Health. Available online. Last accessed March 26, 2021.
Nguyen D, Lemos C, Wortmann L, et al. Discovery and Characterization of the Potent and Highly Selective (Piperidin-4-yl)pyrido[3,2- d]pyrimidine Based in Vitro Probe BAY-885 for the Kinase ERK5. *J Med Chem*. 2019;62(2):928-940. doi:10.1021/acs.jmedchem.8b01606
Nickles Fader A, Java J, Ueda S, et al. Survival in women with grade 1 serous ovarian carcinoma. *Obstet Gynecol*. 2013;122(2 Pt 1):225-232. doi:10.1097/AOG.0b013e31829ce7ec
Nicol RL, Frey N, Pearson G, Cobb M, Richardson J, Olson EN. Activated MEK5 induces serial assembly of sarcomeres and eccentric cardiac hypertrophy. *EMBO J*. 2001;20(11):2757-2767. doi:10.1093/emboj/20.11.2757
Nishimoto S, Nishida E. MAPK signalling: ERK5 versus ERK1/2. *EMBO Rep*. 2006;7(8):782-786. doi:10.1038/sj.embor.7400755
Nithianandarajah-Jones GN, Wilm B, Goldring CE, Müller J, Cross MJ. ERK5: structure, regulation and function. *Cell Signal*. 2012;24(11):2187-2196. doi:10.1016/j.cellsig.2012.07.007
Oaknin A, Guarch R, Barretina P, et al. Recommendations for biomarker testing in epithelial ovarian cancer: a National Consensus Statement by the Spanish Society of Pathology and the Spanish Society of Medical Oncology [published correction appears in Clin Transl Oncol. 2017 Sep 20;:]. *Clin Transl Oncol*. 2018;20(3):274-285. doi:10.1007/s12094-017-1719-x
Obara Y, Yamauchi A, Takehara S, et al. ERK5 activity is required for nerve growth factor-induced neurite outgrowth and stabilization of tyrosine hydroxylase in PC12 cells. *J Biol Chem*. 2009;284(35):23564-23573. doi:10.1074/jbc.M109.027821
Ogawa S, Kaku T, Amada S, et al. Ovarian endometriosis associated with ovarian carcinoma: a clinicopathological and immunohistochemical study. *Gynecol Oncol*. 2000;77(2):298-304. doi:10.1006/gyno.2000.5765
Ohashi K, Sequist LV, Arcila ME, et al. Characteristics of lung cancers harboring NRAS mutations. *Clin Cancer Res*. 2013;19(9):2584-2591. doi:10.1158/1078-0432.CCR-12-3173
Ohnesorge N, Viemann D, Schmidt N, et al. Erk5 activation elicits a vasoprotective endothelial phenotype via induction of Kruppel-like factor 4 (KLF4). *J Biol Chem*. 2010;285(34):26199-26210. doi:10.1074/jbc.M110.103127
Ornatsky OI, Cox DM, Tangirala P, et al. Post-translational control of the MEF2A transcriptional regulatory protein. *Nucleic Acids Res*. 1999;27(13):2646-2654. doi:10.1093/nar/27.13.2646
Ortiz-Ruiz MJ, Álvarez-Fernández S, Parrott T, et al. Therapeutic potential of ERK5 targeting in triple negative breast cancer. *Oncotarget*. 2014;5(22):11308-11318. doi:10.18632/oncotarget.2324
Paik PK, Arcila ME, Fara M, et al. Clinical characteristics of patients with lung adenocarcinomas harboring BRAF mutations. *J Clin Oncol*. 2011;29(15):2046-2051. doi:10.1200/JCO.2010.33.1280
Patch AM, Christie EL, Etemadmoghadam D, et al. Whole-genome characterization of chemoresistant ovarian cancer [published correction appears in Nature. 2015 Nov 19;527(7578):398]. *Nature*. 2015;521(7553):489-494. doi:10.1038/nature14410
Payne DM, Rossomando AJ, Martino P, et al. Identification of the regulatory phosphorylation sites in pp42/mitogen-activated protein kinase (MAP kinase). *EMBO J*. 1991;10(4):885-892.
Pearson G, Robinson F, Beers Gibson T, et al. Mitogen-activated protein (MAP) kinase pathways: regulation and physiological functions. *Endocr Rev*. 2001;22(2):153-183. doi:10.1210/edrv.22.2.0428
Pennington KP, Walsh T, Harrell MI, et al. Germline and somatic mutations in homologous recombination genes predict platinum response and survival in ovarian, fallopian tube, and peritoneal carcinomas. *Clin Cancer Res*. 2014;20(3):764-775. doi:10.1158/1078-0432.CCR-13-2287
Pereira DM, Simões AE, Gomes SE, et al. MEK5/ERK5 signaling inhibition increases colon cancer cell sensitivity to 5-fluorouracil through a p53-dependent mechanism. *Oncotarget*. 2016;7(23):34322-34340. doi:10.18632/oncotarget.9107
Peres LC, Cushing-Haugen KL, Köbel M, et al. Invasive Epithelial Ovarian Cancer Survival by Histotype and Disease Stage. *J Natl Cancer Inst*. 2019;111(1):60-68. doi:10.1093/jnci/djy071
Pfister DG, Johnson DH, Azzoli CG, et al. American Society of Clinical Oncology treatment of unresectable non-small-cell lung cancer guideline: update 2003. *J Clin Oncol*. 2004;22(2):330-353. doi:10.1200/JCO.2004.09.053
Pi X, Yan C, Berk BC. Big mitogen-activated protein kinase (BMK1)/ERK5 protects endothelial cells from apoptosis. *Circ Res*. 2004;94(3):362-369. doi:10.1161/01.RES.0000112406.27800.6F
Pi X, Garin G, Xie L, et al. BMK1/ERK5 is a novel regulator of angiogenesis by destabilizing hypoxia inducible factor 1alpha. *Circ Res*. 2005;96(11):1145-1151. doi:10.1161/01.RES.0000168802.43528.e1
Pignata S, Lorusso D, Scambia G, et al. Pazopanib plus weekly paclitaxel versus weekly paclitaxel alone for platinum-resistant or platinum-refractory advanced ovarian cancer (MITO 11): a randomised, open-label, phase 2 trial. Lancet Oncol. 2015;16(5):561-568. doi:10.1016/S1470-2045(15)70115-4
Pines G, Köstler WJ, Yarden Y. Oncogenic mutant forms of EGFR: lessons in signal transduction and targets for cancer therapy. *FEBS Lett*. 2010;584(12):2699-2706. doi:10.1016/j.febslet.2010.04.019
Planchard D, Le Péchoux C. Small cell lung cancer: new clinical recommendations and current status of biomarker assessment. *Eur J Cancer*. 2011;47 Suppl 3:S272-S283. doi:10.1016/S0959-8049(11)70173-3
Plotnikov A, Zehorai E, Procaccia S, Seger R. The MAPK cascades: signaling components, nuclear roles and mechanisms of nuclear translocation. *Biochim Biophys Acta*. 2011;1813(9):1619-1633. doi:10.1016/j.bbamcr.2010.12.012
Pouysségur J, Volmat V, Lenormand P. Fidelity and spatio-temporal control in MAP kinase (ERKs) signalling. *Biochem Pharmacol*. 2002;64(5-6):755-763. doi:10.1016/s0006-2952(02)01135-8
Pradeep S, Kim SW, Wu SY, et al. Hematogenous metastasis of ovarian cancer: rethinking mode of spread. *Cancer Cell*. 2014;26(1):77-91. doi:10.1016/j.ccr.2014.05.002

Prat J. Ovarian carcinomas: five distinct diseases with different origins, genetic alterations, and clinicopathological features. *Virchows Arch.* 2012;460(3):237-249. doi:10.1007/s00428-012-1203-5Prat J, FIGO Committee on Gynecologic Oncology. Staging classification for cancer of the ovary, fallopian tube, and peritoneum. Int J Gynaecol Oncol. 2014;124:1–5.
Qiu F, Yang L, Fang W, et al. A functional polymorphism in the promoter of ERK5 gene interacts with tobacco smoking to increase the risk of lung cancer in Chinese populations. *Mutagenesis*. 2013;28(5):561-567. doi:10.1093/mutage/get033
Raman M, Chen W, Cobb MH. Differential regulation and properties of MAPKs. *Oncogene*. 2007;26(22):3100-3112. doi:10.1038/sj.onc.1210392
Raviv Z, Kalie E, Seger R. MEK5 and ERK5 are localized in the nuclei of resting as well as stimulated cells, while MEKK2 translocates from the cytosol to the nucleus upon stimulation. *J Cell Sci*. 2004;117(Pt 9):1773-1784. doi:10.1242/jcs.01040
Razmara M, Eger G, Rorsman C, Heldin CH, Lennartsson J. MKP3 negatively modulates PDGF-induced Akt and Erk5 phosphorylation as well as chemotaxis. *Cell Signal*. 2012;24(3):635-640. doi:10.1016/j.cellsig.2011.11.001
Razumovskaya E, Sun J, Rönnstrand L. Inhibition of MEK5 by BIX02188 induces apoptosis in cells expressing the oncogenic mutant FLT3-ITD [published correction appears in Biochem Biophys Res Commun. 2011 Nov 11;415(1):214]. *Biochem Biophys Res Commun*. 2011;412(2):307-312. doi:10.1016/j.bbrc.2011.07.089
Redondo A, Guerra E, Manso L, et al. SEOM clinical guideline in ovarian cancer (2020). *Clin Transl Oncol*. 2021;23(5):961-968. doi:10.1007/s12094-020-02545-x
Rekhtman N, Ang DC, Sima CS, Travis WD, Moreira AL. Immunohistochemical algorithm for differentiation of lung adenocarcinoma and squamous cell carcinoma based on large series of whole-tissue sections with validation in small specimens. *Mod Pathol*. 2011;24(10):1348-1359. doi:10.1038/modpathol.2011.92
Rekhtman N, Tafe LJ, Chaft JE, et al. Distinct profile of driver mutations and clinical features in immunomarker-defined subsets of pulmonary large-cell carcinoma [published correction appears in Mod Pathol. 2014 Jan;27(1):163]. *Mod Pathol*. 2013;26(4):511-522. doi:10.1038/modpathol.2012.195
Ren S, Rollins BJ. Cyclin C/cdk3 promotes Rb-dependent G0 exit. *Cell*. 2004;117(2):239-251. doi:10.1016/s0092-8674(04)00300-9
Repapi E, Sayers I, Wain LV, et al. Genome-wide association study identifies five loci associated with lung function. *Nat Genet*. 2010;42(1):36-44. doi:10.1038/ng.501
Rittmeyer A, Barlesi F, Waterkamp D, et al. Atezolizumab versus docetaxel in patients with previously treated non-small-cell lung cancer (OAK): a phase 3, open-label, multicentre randomised controlled trial [published correction appears in Lancet. 2017 Apr 8;389(10077):e5]. *Lancet*. 2017;389(10066):255-265. doi:10.1016/S0140-6736(16)32517-X
Roberts OL, Holmes K, Müller J, Cross DA, Cross MJ. ERK5 is required for VEGF-mediated survival and tubular morphogenesis of primary human microvascular endothelial cells [published correction appears in J Cell Sci. 2010 Oct 1;123(Pt 19):3413]. *J Cell Sci*. 2010;123(Pt 18):3189-3200. doi:10.1242/jcs.072801
Rodriguez-Canales J, Parra-Cuentas E, Wistuba II. Diagnosis and Molecular Classification of Lung Cancer. *Cancer Treat Res*. 2016;170:25-46. doi:10.1007/978-3-319-40389-2_2
Rosell R, Gómez-Codina J, Camps C, et al. Preresectional chemotherapy in stage IIIA non-small-cell lung cancer: a 7-year assessment of a randomized controlled trial. *Lung Cancer*. 1999;26(1):7-14. doi:10.1016/s0169-5002(99)00045-8
Rovida E, Navari N, Caligiuri A, Dello Sbarba P, Marra F. ERK5 differentially regulates PDGF-induced proliferation and migration of hepatic stellate cells. *J Hepatol*. 2008;48(1):107-115. doi:10.1016/j.jhep.2007.08.010
Rovida E, Di Maira G, Tusa I, et al. The mitogen-activated protein kinase ERK5 regulates the development and growth of hepatocellular carcinoma. *Gut*. 2015;64(9):1454-1465. doi:10.1136/gutjnl-2014-306761
Russo AE, Priolo D, Antonelli G, Libra M, McCubrey JA, Ferraù F. Bevacizumab in the treatment of NSCLC: patient selection and perspectives. *Lung Cancer (Auckl)*. 2017;8:259-269. Published 2017 Dec 14. doi:10.2147/LCTT.S110306
Sánchez-Fdez A, Ortiz-Ruiz MJ, Re-Louhau MF, et al. MEK5 promotes lung adenocarcinoma. *Eur Respir J*. 2019;53(2):1801327. Published 2019 Feb 28. doi:10.1183/13993003.01327-2018
Sandler A, Gray R, Perry MC, et al. Paclitaxel-carboplatin alone or with bevacizumab for non-small-cell lung cancer [published correction appears in N Engl J Med. 2007 Jan 18;356(3):318]. *N Engl J Med*. 2006;355(24):2542-2550. doi:10.1056/NEJMoa061884
Santaballa A, Barretina P, Casado A, et al. SEOM Clinical Guideline in ovarian cancer (2016). *Clin Transl Oncol*. 2016;18(12):1206-1212. doi:10.1007/s12094-016-1588-8
Sarközi R, Miller B, Pollack V, et al. ERK1/2-driven and MKP-mediated inhibition of EGF-induced ERK5 signaling in human proximal tubular cells. *J Cell Physiol*. 2007;211(1):88-100. doi:10.1002/jcp.20909
Sato MS, Shames DS, Girard L, Gazdar AF, Minna JD: Molecular basis of lung cancer; in Meloni D (ed): The Molecular Basis of Cancer, ed 3. Philadelphia, Saunders, 2008, pp 397–407.
Sattler M, Reddy MM, Hasina R, Gangadhar T, Salgia R. The role of the c-Met pathway in lung cancer and the potential for targeted therapy. *Ther Adv Med Oncol*. 2011;3(4):171-184. doi:10.1177/1758834011408636
Scagliotti GV, Selvaggi G, Novello S, Hirsch FR. The biology of epidermal growth factor receptor in lung cancer. *Clin Cancer Res*. 2004;10(12 Pt 2):4227s-4232s. doi:10.1158/1078-0432.CCR-040007
Schaeffer HJ, Weber MJ. Mitogen-activated protein kinases: specific messages from ubiquitous messengers. *Mol Cell Biol*. 1999;19(4):2435-2444. doi:10.1128/MCB.19.4.2435
Schweppe RE, Cheung TH, Ahn NG. Global gene expression analysis of ERK5 and ERK1/2 signaling reveals a role for HIF-1 in ERK5-mediated responses. *J Biol Chem*. 2006;281(30):20993-21003. doi:10.1074/jbc.M604208200
Sears R, Nuckolls F, Haura E, Taya Y, Tamai K, Nevins JR. Multiple Ras-dependent phosphorylation pathways regulate Myc protein stability. *Genes Dev*. 2000;14(19):2501-2514. doi:10.1101/gad.836800
Seidman JD, Savage J, Krishnan J, Vang R, Kurman RJ. Intratumoral Heterogeneity Accounts for Apparent Progression of Noninvasive Serous Tumors to Invasive Low-grade Serous Carcinoma: A Study of 30 Low-grade Serous Tumors of the Ovary in 18 Patients With Peritoneal Carcinomatosis. *Int J Gynecol Pathol*. 2020;39(1):43-54. doi:10.1097/PGP.0000000000000566
Selvan LDN, Danda R, Madugundu AK, et al. Phosphoproteomics of Retinoblastoma: A Pilot Study Identifies Aberrant Kinases. *Molecules*. 2018;23(6):1454. Published 2018 Jun 15. doi:10.3390/molecules23061454
Serysheva E, Berhane H, Grumolato L, et al. Wnk kinases are positive regulators of canonical Wnt/β-catenin signalling [published correction appears in EMBO Rep. 2013 Sep;14(9):845]. *EMBO Rep*. 2013;14(8):718-725. doi:10.1038/embor.2013.88

Seyfried J, Wang X, Kharebava G, Tournier C. A novel mitogen-activated protein kinase docking site in the N terminus of MEK5alpha organizes the components of the extracellular signal-regulated kinase 5 signaling pathway. *Mol Cell Biol*. 2005;25(22):9820-9828. doi:10.1128/MCB.25.22.9820-9828.2005
Sheng Q, Liu X, Fleming E, et al. An activated ErbB3/NRG1 autocrine loop supports in vivo proliferation in ovarian cancer cells [published correction appears in Cancer Cell. 2010 Apr 13;17(4):412]. *Cancer Cell*. 2010;17(3):298-310. doi:10.1016/j.ccr.2009.12.047
Shigematsu H, Takahashi T, Nomura M, et al. Somatic mutations of the HER2 kinase domain in lung adenocarcinomas. *Cancer Res*. 2005;65(5):1642-1646. doi:10.1158/0008-5472.CAN-04-4235
Shukla A, Miller JM, Cason C, et al. Extracellular signal-regulated kinase 5: a potential therapeutic target for malignant mesotheliomas. *Clin Cancer Res*. 2013;19(8):2071-2083. doi:10.1158/1078-0432.CCR-12-3202
Simões AE, Pereira DM, Gomes SE, et al. Aberrant MEK5/ERK5 signalling contributes to human colon cancer progression via NF-κB activation. *Cell Death Dis*. 2015;6(4):e1718. Published 2015 Apr 9. doi:10.1038/cddis.2015.83
Simões AE, Rodrigues CM, Borralho PM. The MEK5/ERK5 signalling pathway in cancer: a promising novel therapeutic target. *Drug Discov Today*. 2016;21(10):1654-1663. doi:10.1016/j.drudis.2016.06.010
Sie ZL, Li RY, Sampurna BP, et al. WNK1 Kinase Stimulates Angiogenesis to Promote Tumor Growth and Metastasis. *Cancers (Basel)*. 2020;12(3):575. Published 2020 Mar 2. doi:10.3390/cancers12030575
Siwak DR, Carey M, Hennessy BT, et al. Targeting the epidermal growth factor receptor in epithelial ovarian cancer: current knowledge and future challenges. *J Oncol*. 2010;2010:568938. doi:10.1155/2010/568938
Skoulidis F, Li BT, Dy GK, et al. Sotorasib for Lung Cancers with *KRAS* p.G12C Mutation [published online ahead of print, 2021 Jun 4]. *N Engl J Med*. 2021;10.1056/NEJMoa2103695. doi:10.1056/NEJMoa2103695
Soh J, Okumura N, Lockwood WW, et al. Oncogene mutations, copy number gains and mutant allele specific imbalance (MASI) frequently occur together in tumor cells. *PLoS One*. 2009;4(10):e7464. Published 2009 Oct 14. doi:10.1371/journal.pone.0007464
Sohn SJ, Sarvis BK, Cado D, Winoto A. ERK5 MAPK regulates embryonic angiogenesis and acts as a hypoxia-sensitive repressor of vascular endothelial growth factor expression. *J Biol Chem*. 2002;277(45):43344-43351. doi:10.1074/jbc.M207573200
Song H, Jin X, Lin J. Stat3 upregulates MEK5 expression in human breast cancer cells. *Oncogene*. 2004;23(50):8301-8309. doi:10.1038/sj.onc.1208026
Stella GM, Scabini R, Inghilleri S, et al. EGFR and KRAS mutational profiling in fresh non-small cell lung cancer (NSCLC) cells. *J Cancer Res Clin Oncol*. 2013;139(8):1327-1335. doi:10.1007/s00432-013-1444-y
Stewart B, Wild C. Cancer by Organ Site: Cancers of the female genital Organs. Lyon: International Agency for Research on Cancer; 2014. Cancer by organ site: Cancers of the female genital organs. World Cancer Report 2014; pp. 465–481.
Stewart EL, Tan SZ, Liu G, Tsao MS. Known and putative mechanisms of resistance to EGFR targeted therapies in NSCLC patients with EGFR mutations-a review. *Transl Lung Cancer Res*. 2015;4(1):67-81. doi:10.3978/j.issn.2218-6751.2014.11.06
Sun W, Kesavan K, Schaefer BC, et al. MEKK2 associates with the adapter protein Lad/RIBP and regulates the MEK5-BMK1/ERK5 pathway. *J Biol Chem*. 2001;276(7):5093-5100. doi:10.1074/jbc.M003719200
Sun W, Wei X, Kesavan K, et al. MEK kinase 2 and the adaptor protein Lad regulate extracellular signal-regulated kinase 5 activation by epidermal growth factor via Src. *Mol Cell Biol*. 2003;23(7):2298-2308. doi:10.1128/MCB.23.7.2298-2308.2003
Sunadome K, Yamamoto T, Ebisuya M, Kondoh K, Sehara-Fujisawa A, Nishida E. ERK5 regulates muscle cell fusion through Klf transcription factors. *Dev Cell*. 2011;20(2):192-205. doi:10.1016/j.devcel.2010.12.005
Sureban SM, May R, Weygant N, et al. XMD8-92 inhibits pancreatic tumor xenograft growth via a DCLK1-dependent mechanism. *Cancer Lett*. 2014;351(1):151-161. doi:10.1016/j.canlet.2014.05.011
Stecca B, Rovida E. Impact of ERK5 on the Hallmarks of Cancer. *Int J Mol Sci*. 2019;20(6):1426. Published 2019 Mar 21. doi:10.3390/ijms20061426
Takeishi Y, Abe Ji, Lee JD, Kawakatsu H, Walsh RA, Berk BC. Differential regulation of p90 ribosomal S6 kinase and big mitogen-activated protein kinase 1 by ischemia/reperfusion and oxidative stress in perfused guinea pig hearts. *Circ Res*. 1999;85(12):1164-1172. doi:10.1161/01.res.85.12.1164
Takeuchi K, Choi YL, Togashi Y, et al. KIF5B-ALK, a novel fusion oncokinase identified by an immunohistochemistry-based diagnostic system for ALK-positive lung cancer. *Clin Cancer Res*. 2009;15(9):3143-3149. doi:10.1158/1078-0432.CCR-08-3248
Tam IY, Chung LP, Suen WS, et al. Distinct epidermal growth factor receptor and KRAS mutation patterns in non-small cell lung cancer patients with different tobacco exposure and clinicopathologic features. *Clin Cancer Res*. 2006;12(5):1647-1653. doi:10.1158/1078-0432.CCR-05-1981
Tanoue T, Nishida E. Molecular recognitions in the MAP kinase cascades. *Cell Signal*. 2003;15(5):455-462. doi:10.1016/s0898-6568(02)00112-2
Tatake RJ, O'Neill MM, Kennedy CA, et al. Identification of pharmacological inhibitors of the MEK5/ERK5 pathway. *Biochem Biophys Res Commun*. 2008;377(1):120-125. doi:10.1016/j.bbrc.2008.09.087
Terasawa K, Okazaki K, Nishida E. Regulation of c-Fos and Fra-1 by the MEK5-ERK5 pathway. *Genes Cells*. 2003;8(3):263-273. doi:10.1046/j.1365-2443.2003.00631.x
Thandra KC, Barsouk A, Saginala K, Aluru JS, Barsouk A. Epidemiology of lung cancer. *Contemp Oncol (Pozn)*. 2021;25(1):45-52. doi:10.5114/wo.2021.103829
Thein KZ, Biter AB, Hong DS. Therapeutics Targeting Mutant KRAS. *Annu Rev Med*. 2021;72:349-364. doi:10.1146/annurev-med-080819-033145
Thomas GM, Huganir RL. MAPK cascade signalling and synaptic plasticity. *Nat Rev Neurosci*. 2004;5(3):173-183. doi:10.1038/nrn1346
Thompson JK, Shukla A, Leggett AL, et al. Extracellular signal regulated kinase 5 and inflammasome in progression of mesothelioma. *Oncotarget*. 2017;9(1):293-305. Published 2017 Dec 6. doi:10.18632/oncotarget.22968
Thun MJ, Carter BD, Feskanich D, et al. 50-year trends in smoking-related mortality in the United States. *N Engl J Med*. 2013;368(4):351-364. doi:10.1056/NEJMsa1211127
Togashi Y, Soda M, Sakata S, Sugawara E, Hatano S, Asaka R, Nakajima T, Mano H, Takeuchi K. KLC1-ALK: A novel fusion in lung cancer identified using a formalin-fixed paraffin-embedded tissue only. PLoS One. 2012;7:e31323. doi: 10.1371/journal.pone.0031323.
Torre LA, Siegel RL, Ward EM, Jemal A. International variation in lung cancer mortality rates and trends among women. *Cancer Epidemiol Biomarkers Prev*. 2014;23(6):1025-1036. doi:10.1158/1055-9965.EPI-13-1220

Torre LA, Siegel RL, Jemal A. Lung Cancer Statistics. *Adv Exp Med Biol*. 2016;893:1-19. doi:10.1007/978-3-319-24223-1_1
Torre LA, Trabert B, DeSantis CE, et al. Ovarian cancer statistics, 2018. *CA Cancer J Clin*. 2018;68(4):284-296. doi:10.3322/caac.21456
Tran PT, Shroff EH, Burns TF, et al. Twist1 suppresses senescence programs and thereby accelerates and maintains mutant Kras-induced lung tumorigenesis. *PLoS Genet*. 2012;8(5):e1002650. doi:10.1371/journal.pgen.1002650
Travis WD. Sarcomatoid neoplasms of the lung and pleura. *Arch Pathol Lab Med*. 2010;134(11):1645-1658. doi:10.5858/2010-0086-RAR.1
Travis WD, Brambilla E, Noguchi M, et al. Diagnosis of lung adenocarcinoma in resected specimens: implications of the 2011 International Association for the Study of Lung Cancer/American Thoracic Society/European Respiratory Society classification. *Arch Pathol Lab Med*. 2013;137(5):685-705. doi:10.5858/arpa.2012-0264-RA
Travis WD, Brambilla E, Nicholson AG, Yatabe Y, Austin JHM, Beasley MB, Chirieac LR, Dacic S, Duhig E, Flieder DB, Geisinger K, Hirsch FR, Ishikawa Y, Kerr KM, Noguchi M, Pelosi G, Powell CA, Tsao MS, Wistuba I; WHO Panel. The 2015 World Health Organization Classification of Lung Tumors: Impact of Genetic, Clinical and Radiologic Advances Since the 2004 Classification. J Thorac Oncol. 2015 Sep;10(9):1243-1260. doi: 10.1097/JTO.0000000000000630. PMID: 26291008.
Trimbos JB, Vergote I, Bolis G, et al. Impact of adjuvant chemotherapy and surgical staging in early-stage ovarian carcinoma: European Organisation for Research and Treatment of Cancer-Adjuvant ChemoTherapy in Ovarian Neoplasm trial. *J Natl Cancer Inst*. 2003;95(2):113-125.
Tubita A, Lombardi Z, Tusa I, Dello Sbarba P, Rovida E. Beyond Kinase Activity: ERK5 Nucleo-Cytoplasmic Shuttling as a Novel Target for Anticancer Therapy. *Int J Mol Sci*. 2020;21(3):938. Published 2020 Jan 31. doi:10.3390/ijms21030938
Tubita A, Tusa I, Rovida E. Playing the Whack-A-Mole Game: ERK5 Activation Emerges Among the Resistance Mechanisms to RAF-MEK1/2-ERK1/2- Targeted Therapy. *Front Cell Dev Biol*. 2021;9:647311. Published 2021 Mar 11. doi:10.3389/fcell.2021.647311
Umapathy G, El Wakil A, Witek B, et al. The kinase ALK stimulates the kinase ERK5 to promote the expression of the oncogene MYCN in neuroblastoma. *Sci Signal*. 2014;7(349):ra102. Published 2014 Oct 28. doi:10.1126/scisignal.2005470
Vang R, Shih IeM, Kurman RJ. Ovarian low-grade and high-grade serous carcinoma: pathogenesis, clinicopathologic and molecular biologic features, and diagnostic problems. *Adv Anat Pathol*. 2009;16(5):267-282. doi:10.1097/PAP.0b013e3181b4fffa
Varga A, Piha-Paul S, Ott PA, et al. Pembrolizumab in patients with programmed death ligand 1-positive advanced ovarian cancer: Analysis of KEYNOTE-028. *Gynecol Oncol*. 2019;152(2):243-250. doi:10.1016/j.ygyno.2018.11.017
Vargo-Gogola T, Rosen JM. Modelling breast cancer: one size does not fit all. *Nat Rev Cancer*. 2007;7(9):659-672. doi:10.1038/nrc2193
Vaseva AV, Blake DR, Gilbert TSK, et al. KRAS Suppression-Induced Degradation of MYC Is Antagonized by a MEK5-ERK5 Compensatory Mechanism. *Cancer Cell*. 2018;34(5):807-822.e7. doi:10.1016/j.ccell.2018.10.001
Vicent S, Garayoa M, López-Picazo JM, et al. Mitogen-activated protein kinase phosphatase-1 is overexpressed in non-small cell lung cancer and is an independent predictor of outcome in patients. *Clin Cancer Res*. 2004;10(11):3639-3649. doi:10.1158/1078-0432.CCR-03-0771
Villa-Moruzzi E. Tyrosine phosphatases in the HER2-directed motility of ovarian cancer cells: Involvement of PTPN12, ERK5 and FAK. *Anal Cell Pathol (Amst)*. 2011;34(3):101-112. doi:10.3233/ACP-2011-0008
Wang X, Tournier C. Regulation of cellular functions by the ERK5 signalling pathway. *Cell Signal*. 2006;18(6):753-760. doi:10.1016/j.cellsig.2005.11.003
Wang CG, Lu XF, Wei JQ, et al. Activation of the spinal extracellular signal-regulated kinase 5 signaling pathway contributes to morphine physical dependence in rats. *Neurosci Lett*. 2011;494(1):38-43. doi:10.1016/j.neulet.2011.02.049
Wang R, Hu H, Pan Y, et al. RET fusions define a unique molecular and clinicopathologic subtype of non-small-cell lung cancer. *J Clin Oncol*. 2012;30(35):4352-4359. doi:10.1200/JCO.2012.44.1477
Wang J, Erazo T, Ferguson FM, et al. Structural and Atropisomeric Factors Governing the Selectivity of Pyrimido-benzodiazipinones as Inhibitors of Kinases and Bromodomains. *ACS Chem Biol*. 2018;13(9):2438-2448. doi:10.1021/acschembio.7b00638
Wang Z, Sun K, Xiao Y, et al. Niraparib activates interferon signaling and potentiates anti-PD-1 antibody efficacy in tumor models. *Sci Rep*. 2019;9(1):1853. Published 2019 Feb 12. doi:10.1038/s41598-019-38534-6
Watson FL, Heerssen HM, Bhattacharyya A, Klesse L, Lin MZ, Segal RA. Neurotrophins use the Erk5 pathway to mediate a retrograde survival response [published correction appears in Nat Neurosci 2002 Oct;5(10):1017]. *Nat Neurosci*. 2001;4(10):981-988. doi:10.1038/nn720
Way GP, Rudd J, Wang C, et al. Comprehensive Cross-Population Analysis of High-Grade Serous Ovarian Cancer Supports No More Than Three Subtypes. *G3 (Bethesda)*. 2016;6(12):4097-4103. Published 2016 Dec 7. doi:10.1534/g3.116.033514
Weldon CB, Scandurro AB, Rolfe KW, et al. Identification of mitogen-activated protein kinase kinase as a chemoresistant pathway in MCF-7 cells by using gene expression microarray. *Surgery*. 2002;132(2):293-301. doi:10.1067/msy.2002.125389
Wentzensen N, Poole EM, Trabert B, et al. Ovarian Cancer Risk Factors by Histologic Subtype: An Analysis From the Ovarian Cancer Cohort Consortium. *J Clin Oncol*. 2016;34(24):2888-2898. doi:10.1200/JCO.2016.66.8178
Widmann C, Gibson S, Jarpe MB, Johnson GL. Mitogen-activated protein kinase: conservation of a three-kinase module from yeast to human. *Physiol Rev*. 1999;79(1):143-180. doi:10.1152/physrev.1999.79.1.143
William AD, Lee AC, Goh KC, et al. Discovery of kinase spectrum selective macrocycle (16E)-14-methyl-20-oxa-5,7,14,26-tetraazatetracyclo[19.3.1.1(2,6).1(8,12)]heptacosa-1(25),2(26),3,5,8(27),9,11,16,21,23-decaene (SB1317/TG02), a potent inhibitor of cyclin dependent kinases (CDKs), Janus kinase 2 (JAK2), and fms-like tyrosine kinase-3 (FLT3) for the treatment of cancer. *J Med Chem*. 2012;55(1):169-196. doi:10.1021/jm201112g
Wilson FH, Disse-Nicodème S, Choate KA, et al. Human hypertension caused by mutations in WNK kinases. *Science*. 2001;293(5532):1107-1112. doi:10.1126/science.1062844
Woo CH, Shishido T, McClain C, et al. Extracellular signal-regulated kinase 5 SUMOylation antagonizes shear stress-induced antiinflammatory response and endothelial nitric oxide synthase expression in endothelial cells. *Circ Res*. 2008;102(5):538-545. doi:10.1161/CIRCRESAHA.107.156877

Wright TD, Raybuck C, Bhatt A, et al. Pharmacological inhibition of the MEK5/ERK5 and PI3K/Akt signaling pathways synergistically reduces viability in triple-negative breast cancer. *J Cell Biochem*. 2020;121(2):1156-1168. doi:10.1002/jcb.29350

Wu K, Nie B, Zhou Q, et al. [Effects of WNK1 on Human Chronic Myeloid Leukemia K562 Cells via MAPK7 Phosphorylation and Its Relative Mechanism]. *Zhongguo Shi Yan Xue Ye Xue Za Zhi*. 2020;28(2):365-370. doi:10.19746/j.cnki.issn.1009-2137.2020.02.002

Xu B, English JM, Wilsbacher JL, Stippec S, Goldsmith EJ, Cobb MH. WNK1, a novel mammalian serine/threonine protein kinase lacking the catalytic lysine in subdomain II. *J Biol Chem*. 2000;275(22):16795-16801. doi:10.1074/jbc.275.22.16795

Xu BE, Stippec S, Lenertz L, et al. WNK1 activates ERK5 by an MEKK2/3-dependent mechanism. *J Biol Chem*. 2004;279(9):7826-7831. doi:10.1074/jbc.M313465200

Yan C, Takahashi M, Okuda M, Lee JD, Berk BC. Fluid shear stress stimulates big mitogen-activated protein kinase 1 (BMK1) activity in endothelial cells. Dependence on tyrosine kinases and intracellular calcium. *J Biol Chem*. 1999;274(1):143-150. doi:10.1074/jbc.274.1.143

Yan C, Luo H, Lee JD, Abe J, Berk BC. Molecular cloning of mouse ERK5/BMK1 splice variants and characterization of ERK5 functional domains. *J Biol Chem*. 2001;276(14):10870-10878. doi:10.1074/jbc.M009286200

Yan C, Ding B, Shishido T, et al. Activation of extracellular signal-regulated kinase 5 reduces cardiac apoptosis and dysfunction via inhibition of a phosphodiesterase 3A/inducible cAMP early repressor feedback loop. *Circ Res*. 2007;100(4):510-519. doi:10.1161/01.RES.0000259045.49371.9c

Yanagawa N, Shiono S, Abiko M, Ogata SY, Sato T, Tamura G. New IASLC/ATS/ERS classification and invasive tumor size are predictive of disease recurrence in stage I lung adenocarcinoma. *J Thorac Oncol*. 2013;8(5):612-618. doi:10.1097/JTO.0b013e318287c3eb

Yang Q, Deng X, Lu B, et al. Pharmacological inhibition of BMK1 suppresses tumor growth through promyelocytic leukemia protein [published correction appears in Cancer Cell. 2010 Oct 19;18(4):396]. *Cancer Cell*. 2010;18(3):258-267. doi:10.1016/j.ccr.2010.08.008

Yang Q, Lee JD. Targeting the BMK1 MAP kinase pathway in cancer therapy. *Clin Cancer Res*. 2011;17(11):3527-3532. doi:10.1158/1078-0432.CCR-10-2504

Yap TA, Carden CP, Kaye SB. Beyond chemotherapy: targeted therapies in ovarian cancer. *Nat Rev Cancer*. 2009;9(3):167-181. doi:10.1038/nrc2583

Yoon, S. & Seger, R. 2006. The extracellular signal-regulated kinase: multiple substrates regulate diverse cellular functions. Growth Factors, 24, 21-44.

Young RP, Hopkins RJ, Christmas T, Black PN, Metcalf P, Gamble GD. COPD prevalence is increased in lung cancer, independent of age, sex and smoking history. *Eur Respir J*. 2009;34(2):380-386. doi:10.1183/09031936.00144208

Zanetta G, Chiari S, Rota S, et al. Conservative surgery for stage I ovarian carcinoma in women of childbearing age. *Br J Obstet Gynaecol*. 1997;104(9):1030-1035. doi:10.1111/j.1471-0528.1997.tb12062.x

Zarkowska, T., & Mittnacht, S. (1997). Differential phosphorylation of the retinoblastoma protein by G1/S cyclin-dependent kinases. *The Journal of biological chemistry*, *272*(19), 12738–12746. https://doi.org/10.1074/jbc.272.19.12738

Zen K, Yasui K, Nakajima T, et al. ERK5 is a target for gene amplification at 17p11 and promotes cell growth in hepatocellular carcinoma by regulating mitotic entry. *Genes Chromosomes Cancer*. 2009;48(2):109-120. doi:10.1002/gcc.20624

Zhang Y, Dong C. Regulatory mechanisms of mitogen-activated kinase signaling. *Cell Mol Life Sci*. 2007;64(21):2771-2789. doi:10.1007/s00018-007-7012-3

Zhong CY, Zhou YM, Douglas GC, Witschi H, Pinkerton KE. MAPK/AP-1 signal pathway in tobacco smoke-induced cell proliferation and squamous metaplasia in the lungs of rats. *Carcinogenesis*. 2005;26(12):2187-2195. doi:10.1093/carcin/bgi189

Zhou G, Bao ZQ, Dixon JE. Components of a new human protein kinase signal transduction pathway. *J Biol Chem*. 1995;270(21):12665-12669. doi:10.1074/jbc.270.21.12665

Zhou LL, Dong JL, Huang G, Sun ZL, Wu J. MicroRNA-143 inhibits cell growth by targeting ERK5 and MAP3K7 in breast cancer. *Braz J Med Biol Res*. 2017;50(8):e5891. Published 2017 Jul 20. doi:10.1590/1414-431X20175891

Zheng M. Classification and Pathology of Lung Cancer. *Surg Oncol Clin N Am*. 2016;25(3):447-468. doi:10.1016/j.soc.2016.02.003

Zyla RE, Olkhov-Mitsel E, Amemiya Y, et al. CTNNB1 Mutations and Aberrant β-Catenin Expression in Ovarian Endometrioid Carcinoma: Correlation With Patient Outcome. *Am J Surg Pathol*. 2021;45(1):68-76. doi:10.1097/PAS.0000000000001553

# *ACKNOWLEDGEMENTS*

En primer lugar y como no puede ser de otra forma, quiero mostrar mi más profunda gratitud hacia **mi Directora**, la Dra. Azucena Esparís y también al Dr. Atanasio Pandiella. Esta tesis es la culminación de un largo viaje del que ellos me abrieron las puertas y me guiaron de principio a fin. Gracias por vuestro apoyo, vuestra confianza y por compartir vuestro tiempo, esfuerzo y conocimientos conmigo.

Por otra parte, no puedo sino estar inmensamente agradecido por los maravillosos **compañeros de laboratorio** que he tenido durante todos estos años. A los que siempre estuvieron y de los que más pude aprender: Juan Carlos, por tu admirable sentido del esfuerzo, tu sencillez, amabilidad y pasión por la ciencia. Y Elena, por tu tesón, tu paciencia y tu papel esencial en el día a día de todos nosotros, eres nuestra guardiana, nuestra p53, gracias por tus sacrificios para que el lab 15 funcione como un reloj. A los compañeros de la primera etapa, sobre todo a Flor, Anita, Carla, Sara y Ariana. Os guardaré eternamente cariño. A todos aquellos a los que tuve el honor de "tutorizar": María José, Jorge, Pilar y especialmente a Sofía. Gracias por permitirme aprender a enseñar, espero no haberlo hecho muy mal. Gracias por supuesto a Yolanda por haber compartido, pese a la distancia que marcan nuestros proyectos, todo este viaje. Eres un ejemplo de honestidad y trabajo duro. Gracias a todos los compañeros de la segunda etapa, especialmente a Lucía, Laura e Inés por tener siempre una sonrisa y permitir que el día a día sea mucho más agradable. Y a todos aquellos que pasasteis temporalmente por el laboratorio, igualmente, mi más sincero agradecimiento. Calculo que habréis sido más de 30 personas y lamento no poder mencionaros uno a uno… pero daros todos por aludidos. A todos os deseo de corazón muchísima suerte y felicidad.

No me olvido de toda la gente que, con su trabajo, ha hecho posible que el mío fuera posible y más sencillo. Al **personal del CiC**: Eugenio Santos por el apoyo que siempre me ha brindado tanto primero como profesor y tutor universitario como posteriormente como director del centro; pasando por Celso y Carlos en mantenimiento; Sonia y Pablo en informática; Marga y Almudena en secretaría; Ángel y Ana en microscopía; al servicio de Patología Molecular, al de Genómica, a la gente de cocina y almacén, la gente de conserjería; las personas de administración del IBSAL; el personal del animalario y un largo etcétera de

personas con las que da gusto trabajar y que directa o indirectamente me han facilitado mucho las cosas.

Quiero también hacer una mención especial a las **instituciones y agrupaciones** que me han apoyado científica, curricular o económicamente para poder desarrollar esta tesis y mi carrera como investigador. Al IBSAL, la Fundación Inés Luna Terrero, eCOST, Escuela de Doctorado y CIBERONC por sus becas y premios. A la Asociación de Vecinos de Fuenterrico, por su generosidad y su apoyo en la lucha contra el cáncer. Y por supuesto a la Asociación Española Contra el Cáncer: por depositar su confianza en mí y ser los responsables últimos y directos de que yo haya podido realizar este proyecto, financiar este trabajo y darme la oportunidad de cumplir esta meta de mi vida que es ser Doctor.

De forma generalizada y personificada, gracias a la **Universidad de Salamanca.** Espero que, como me dijo mi abuela al comenzar, hayas pasado por mí y no simplemente yo por tí. Creo que así ha sido. He pasado contigo los últimos 14 años, literalmente la mitad de mi vida. Siempre serás parte de mí y una parte de mí se quedará contigo. Gracias Salamanca por tus maravillosos atardeceres y tu piedra mágica.

Por último y por encima de todo, gracias a mi **familia**: a mamá, papá, Laura, Blanca, a mi esposa Maritza, mis abuelos, tíos, primos, sobrinos, amigos…. El mayor valor de esta tesis reside en el tiempo que nos ha impedido estar juntos. Necesitaría 100 folios para llenarlos de gracias y aun así no sería suficiente.  GRACIAS.